THE UNIVERSITY *of* EDINBURGH

The University of Edinburgh

College of Science and Engineering
School of Chemistry

Polymer Microarrays for Microbial High-Content Screening

Mei Wu

Doctor of Philosophy

July 2012

Abstract

Research on the interactions between microbes and polymeric materials constitutes an important part in antimicrobial identification and provides an insight into microbial response on the polymer surfaces. Herein, a high-content screening method with polymer microarray technology was developed to investigate microbe-polymer interactions, especially in studying adhesion/repellence of microbes (bacteria and parasites). Firstly, the polymer microarray approach was used to successfully identify polymers which either selectively captured or prevented the binding of major food-borne pathogen, *Salmonella* Typhimurium. A parallel study with a lab strain of *Escherichia coli* was also carried out, revealing polymers which either displayed a common binding activity or which exhibited species discrimination. Likewise, this polymer microarray technology was applied to more bacterial strains, such as *Campylobacter*, *Clostridium*, *Streptococcus*, *Klebsiella* and their cocktails to discover families of substrates that displayed strong broad-spectrum bacterial non-binding activity. These synthetic polymers represented a novel class of coating materials which can be used to prevent surface colonisation and subsequent formation of bacterial biofilms. The study of protozoan-polymer interactions was also explored in this thesis. Polymers were identified which either bound or prevented parasites (*Crysporidium parvum* and *Giardia lamblia*) binding. Material properties, including wettability, surface roughness and polymer composition were analysed to study correlation of parasite binding and the generation of polymer structure function relationships.

Declaration of authorship

The research described in this thesis was carried out by the author under the supervision of Prof. Mark Bradley at the University of Edinburgh between October 2008 and October 2011. No part of this thesis has been previously submitted for any other degree or professional qualification. Part of this work has been published.

Patents:

Binding and non-binding polymer (PCT/GB2011001354 and GB1015492.0)
Wu M., Pernagallo S., Gallagher M.P. and Bradley M.

Water treatment and monitoring (GB 50893728.1)
Wu M., Bridle H. and Bradley M.

Articles:

Pernagallo S., Wu M., Gallagher M.P. and Bradley M. *Journal of Materials Chemistry* **2011**, 21(1), 96-101

Wu M., Bridle H. and Bradley M. *Water Research* **2012**, 46(6), 1715-1722

Pickering H., Wu M., Bradley M. and Bridle H. *Environmental Science & Technology* **2012**, 46(4), 2179-86

Signed: ……

Date: ……

Acknowledgement

First of all I would like to thank my supervisor, Professor Mark Bradley for the invaluable support and encouragement he has provided during my PhD. I am eternally grateful for everything he has done to help me complete this thesis.

I hugely acknowledge the Chinese Scholarship Council and the University of Edinburgh for sponsoring my study here. I would thank all the previous PhD students (Hitoshi, Jeff and Jasmine) in the Bradley group, who synthesised the polymers I have used. I would also thank Guilhem for developing the polymer microarray technology and working with me on the Altrika project.

I would like to thank all members in the Bradley group. Particularly, a big thanks goes to Salvo for working with me on the *S.* Typhimurium project and his fun-filled talks. A big hug goes to Rong for his every little help in lab and life, thank you so much. I am hugely grateful to Jeff, Liz and Frank B. for proof reading this thesis. I must acknowledge all my friends, Martin, Frank T., Anne, Thingsoon, Rahimi, Aurelie, Neil, Martha, Gege, Juanjo, Rosario, Asier, Adam, Mazen, Nicos, Effie, Juanma, Gouher, Tash, Emma and Ferdous for their daily casual jokes, without you, the hard work in the Joseph Black building would not be so enjoyable. I will be deeply grateful to all staff in the School of Chemistry and other schools who helped and supported me in my studies; particular thanks goes to Nicola for her help during my use of SEM and Oleg for my AFM enquiries.

I gratefully thank my collaborators who helped to develop the microarray technology into biological applications: Dr. Maurice Gallagher for working with me on the bacterium projects, kindly teaching me microbiological skills and providing me invaluable advice both in research and life; Dr. Helen Bridle for working with me on the parasite projects, taking time to chat with me and giving me invaluable advice. I also thank the kind assistance from their students, especially Harry, Pete and Ailsa.

Finally I would eternally thank my family (mum and dad) and Wenduan for their endless love and support over the years, this thesis is dedicated to you all.

Abbreviations

Abbreviations	Full name
AAG-H	2-acrylaminoglycolic acid
AATBTB	*m*-acryloylamino-(tri-*n*-butyltin benzoate)
AES-H	*mono*-2-(acryloyoxy)ethyl succinate
AFM	atomic force microscopy
A-H	acrylic acid
Alb	albumin
APTES	3-aminopropyltriethoxysilane
au	arbitrary units
AVG	average
BACOEA	a-[[(butylamino)carbonyl]oxy]ethyl acrylate
BAEMA	2-(*tert*-butylamino)ethyl methacrylate
BD	1,4-butanediol
BICH	1,3-bis(isocyanatomethyl)cyclohaxane
BHI	brain-heart infusion
BMA	*N*-butyl methacrylate
BMDCs	bone marrow dendritic cells
BnMA	benzylmethylamine
C. difficile	*Clostridium difficile*
CFU	colony-forming unit
cHMA	cyclohexane methylamine
C. jejuni	*Campylobacter jejuni*
C. parvum	*Cryptosporidium parvum*
C. perfringers	*Clostridium perfringens*
Ctrl	control
Da	Dalton
DAAA	diacetone acrylamide (*N*-1,1-dimethyl-3-oxobutyl)-acrylamide)
DAPI	4’,6-diamidino-2-phenylindole
DBnA	dibenzylamine
DcHA	dicyclohexylamine
DEAA	*N*,*N*-diethyl acrylate
DEAEA	2-(diethylamino)ethyl acrylate
DEAEMA	2-(diethylamino)ethyl methacrylate
DEAPD	3-(diethylamino)-1,2-propanediol
DEGMEMA	di(ethylene glycol)methyl ether methacrylate
DEMEDA	*N*,*N*-dimethyl-*N’*-methylethylenediamine
DHM	diethyl bis(hydroxymethyl)malonate
Dis	diisocryanate
DLVO	theory developed by Derjaguin, Landau, Verwey and Overbeek
DMAA	*N*,*N*-dimethyl acrylamide
DMF	dimethylformamide
DMAEA	2-(dimethylamino)ethyl acrylate

Abbreviations	Full name
DMAEMA	2-(dimethylamino)ethyl methacrylate
DMAPD	3-(dimethylamino)-1,2-propanediol
DMAPMAA	*N*-[3-(dimethylamino)propyl]methacrylate
DMVBA	*N*,*N*-dimethylvinylbenzylamine
DNA	deoxyribonucleic acid
DnBA	di-*n*-butylamine
DnHA	di-*n*-hexylamine
DSC	differential scanning calorimetry
E. coli	*Escherichia coli*
ECM	extracellular matrix
ED	ethylene diamine
E. faecalis	*Enterococcus faecalis*
EG	ethylene glycol
e.g.	for exmaple
EGMP-H	ethylene glycol methacrylate phosphate
EMA	ethyl methacrylate
EPCs	endothelial progenitor cells
EPS	extracellular polymeric substance
ESCs	embryonic stem cells
Ext	chain extender
FBS	fetal bovine serum
FBP	*Campylobacter* growth supplement
Fib	fibronectin
FITC	fluorescein isothiocyanate
FT-IR	fourier transform infra-red
GFP	green fluorescent protein
G. lamblia	*Giardia lamblia*
GMA	glycidyl methacrylate
GPC	gel permeation chromatography
HBMA	hydroxybutyl methacrylate
HCS	high-content screening
HDI	hexamethylene diisocyanate
HEA	2-hydroxyethyl acrylate
HEMA	2-hydroxyethyl methacrylate
HEK	human embryonic kidney cells
HeLa	human cervical cancer cells
HEMA	2-hydroxyethylmethacrylate
hESCs	human embryonic stem cells
hMSCs	human mesenchymal stem cells
HMDI	4,4’-methylenebis(cyclohexyl isocyanate)
HPMA	hydroxypropyl methacrylate
HT	high-throughput
HUVECs	human umbilical vein endothelial cells
IgG	immunoglobulin-G
K. pneumoniae	*Klebsiella pneumoniae*
LB	Luria-Bertani

Abbreviations	Full name
MA	methacrylate
MAEPy	2-(2-methylaminoethyl)pyridine
MA-H	methacrylic acid
MALDI	matrix assisted laser desorption/ionization-mass spectrometry
MAn	*N*-methylaniline
mbar	millibar
MDI	methylenebis(phenyl isocyanate)
MEA	2-methoxyethy acrylate
MEMA	2-methoxyethy methacrylate
mESCs	mouse embryonic stem cells
ml	millilitre
MMA	methyl methacrylate
MnHA	*N*-methylhexylamine
Mn	molecular weight
MNPMA	2-methyl-2-nitropropyl methacrylate
Mpi	1-methylpiperazine
MRSA	methicillin-resistant *Staphylococcus aureus*
MS	mass spectrometry
MTEMA	2-(methylthio)ethyl methacrylate
ms	millisecond
NF	necrotizing fasciitis
NiPAA	*N*-isopropyl acrylamide
NMP	1-methyl-2-pyrrolidinone
NMPD	2-nitro-2-methyl-1,3-propanediol
OFHD	2,2,3,3,4,4,5,5-octafluoro-1,6-hexanediol
PA	poly(acrylate)
pAAm	poly(acrylamide)
PBS	phosphate buffered saline
PCR	polymerase chain reaction
PEG	poly(ethylene glycol)
1.4-PDC	1,4-phenylenedioxy diacetylchloride
PDI	1,4-phenylene diisocyanate (1,4-diisocyanobenzene)
PG	propylene glycol
pHEMA	poly(2-hydroxyethyl methacrylate)
pHMAAm	poly(*N*-(hydroxymethyl) acrylate)
PHNAD	poly[1,6-hexanediol/neopentyl glycol-*alt*-adipic acid] diol
PHNGAD	poly[1,6-hexanediol/neopentyl glycol/di(ethylene glycol)-*alt*-adipic acid] diol
PI	propidium iodide
PLS	partial least-squares
pMMA	poly(methyl methacrylate)
poly(TBAM-co-EGDMA)	poly(2-(tert-butylamino)ethyl methacrylate-co-ethylene glycol dimethacrylate)
PPG	poly(propylene glycol)

Abbreviations	**Full name**
PPG-PEG	poly(propylene/ethylene glycol)
PTMG	poly(butylene glycol)
PU	poly(urethane)
Pyrle	pyrrole
RBCs	red blood cells
RMS	root mean square
RNA	ribonucleic acid
ROMP	ring-opening metathesis polymerisation
rpm	revolutions per minute
RT	room temperature
S. aureus	*Staphylococcus aureus*
SD	standard deviation
SEM	scanning electron microscopy
S. epidermidis	*Staphylococcus epidermidis*
S. mutans	*Streptococcus mutans*
S. saprophyticus	*Staphylococcus saprophyticus*
SSD	silver sulphadiazine
St	styrene
S. Typhimurium	*Salmonella enterica* serovar Typhimurium
TBTM	(*N*-tri-*n*-butyltin)maleimide
TDI	tolylene 2,4-diisocyanate (4-methyl-1,3-phenylene diisocyanate)
TFA	trifluoroacetic acid
TMEDA	*N,N,N'*-trimethylethylenediamine
TMPDA	*N,N,N'*-trimethyl-1,3-proanediamine
THF	tetrahydrofuran
THFFA	tetrahydrofurfuryl acrylate
THFFMA	tetrahydrofurfuryl methacrylate
ToF-SIMS	time-of-flight secondary ion mass spectrometry
UV	ultraviolet
VAA	*N*-vinylacetamide
VI	1-vinylimidazol
VP-2	2-vinylpyridine
VP-4	4-vinylpyridine
VPNO	1-vinyl-2-prrolidinone
WCA	water contact angle
XPS	x-ray photoelectron spectroscopy

Table of Contents

Chapter 1

Introduction

1.1 Antimicrobials and Antimicrobial Polymeric materials

1.1.1 A Brief Historical Sketch of Antimicrobials

Antimicrobials are classes of compounds that are used to kill or slow the growth of microorganisms, particularly pathogens. The term, antimicrobial refers to all natural, synthetic and semi-synthetic compounds, such as host defense peptides or β-lactams, which are able to inhibit pathogenic microorganisms.

The history of antimicrobial research is the history of mankind fighting against microbial infection over the centuries. Antimicrobials and antimicrobial materials still receive great attention while antimicrobial materials play an important role in almost every area of people's daily lives, such as food packaging and storage, water purification, personal and public hygiene, and of course hospital and surgical equipment. This includes silver and silver salts that have been used medically for the treatments of wounds for over 2000 years and which today are widely used in a variety of applications. For example, silver sulfadiazine (SSD) is still one of the most widely used compounds for the topical treatment of burns[1-3].

In the middle of the nineteenth century, Pasteur demonstrated that "invisible organisms" (e.g. bacteria) were responsible for spoiling wine, beer and milk, and later introduced pasteurisation which could effectively kill bacteria in a liquid[4]. In the late 1880s, he accidentally found that one microorganism could inhibit the growth of another; although at that time it was not clear that an antibiotic was

produced[4]. Based on Pasteur's germ theory, Lister proved that wounds were infected by microorganisms, and hence promoted the method of sterile surgery to prevent infectious diseases during surgical operations. He thus used phenol solutions to clean wounds and surgical instruments, which enormously reduced surgical infections for patients[5].

After the appearance of antibiotics in the 1940s, many infectious diseases seemed to be controlled and prevented by antibiotic treatment. In particular, therapeutic uses of antibiotics such as gramicidin[6] and penicillin[6-8] for wound treatment extensively saved soldiers' lives in the allied military during World War II. Between the 1940s and 1960s, people became over-optimistic about defeating and controlling infectious diseases, and believed they were under control due to the great development and success of antibiotics and immunisation treatments[9]. In the 1980s, many pharmaceutical companies significantly reduced new antimicrobial drug research efforts[10]. However, this optimism was soon broken by the emergence of new antimicrobial-resistant infections. Legionarie's disease, flesh-eating bacteria syndrome (necrotizing fasciitis (NF)), toxic shock syndrome (TSS) and many infections began to appear both in developing and developed countries[11]. Of these, methicillin-resistant *Staphylococcus aureus* (MRSA) is now the most common cause for skin and soft-tissue infections among patients in hospitals in the US[12] and in Asia[13].

Moreover, infectious diseases are still serious in most developing countries, and are a major cause of morbidity and mortality. According to a report of the World Health Organization (WHO) in 2010[14], the coverage of interventions such as oral rehydration therapy (ORT) for diarrhoea and case management of antibiotics for acute respiratory infections (ARIs) are still insufficient. As a result, three million children under five years old are killed by diarrhoea and pneumonia every year, and this phenomenon is more obvious in low-income countries.

As a result of the rapid propagation and proliferation of microorganisms, new infectious diseases and microbial species have been emerging, and even in some developed countries, mortality caused by microbial infection is increasing[11]. The haemolytic uraemic syndrome (HUS) epidemic in northern Germany in 2011 is a

recent example of a large scale microbial infection, which led to serious human mortality as a result of *Escherichia coli* contamination in the human food chain[15].

We have learnt from the battle against microbial infections that we need to continue antimicrobial research, prevent disease transmission, and increase the hygiene levels for the general public (e.g. water treatment) and in particular for young children and patients in hospitals. To this end, the development of new antimicrobial materials is of fundamental importance for human health.

1.1.2 Antimicrobial Polymers

Antimicrobial polymers can be divided into two classes: natural and synthetic. Natural antimicrobial polymers are widely applied in the antimicrobial field, because of their biocompatibility, good bioactivities and the lack of allergenicity. Chitosan, a deacetylated polymer of chitin (acetyl glucosamine), is a good example of a natural antimicrobial polymer which is widely distributed in nature. Chitosan and its oligomers have shown high antimicrobial activity[16], and have been widely used as antimicrobial materials in waste and water treatment, food processing and biomedical materials[17].

For synthetic antimicrobial polymers, numerous approaches have been applied to prepare polymeric materials with antimicrobial activity. Here, a brief survey of synthetic polymers displaying antimicrobial properties is given. An ideal synthetic antimicrobial polymer should have the following characteristics[18]:

- Easy and inexpensive synthesis;
- Stability and long term durability;
- Broad spectrum against pathogenic microorganisms;
- Does not decompose or produce toxic residues;
- Should not be toxic or irritating to those people who are handling/using it;
- Insoluble in water, water disinfection systems, and food packing.

Polymers with antimicrobial derivatives:

Cationic amphiphilic polymers with alkyl substituents, or hydrophobic alkyl side tails, have gained great attention in many different fields[19]. Several amphiphilic polymers (Figure 1.1) with different alkyl side chains (methyl to hexyl) have been synthesised by ring-opening metathesis polymerisation (ROMP) by the Tew group[20]. The antimicrobial and haemolytic properties of polymers were studied against *S. aureus*, *E. coli* and human red blood cells (RBCs), respectively. They concluded that the hydrophobic nature of the polymers plays a very important role in both the antimicrobial activity and toxicity of polymers[20]. For example, the long alkyl polymers (propyl onward) showed strong antimicrobial activity but caused significant haemolysis. In contrast, the methyl-polymer was neither pathogen-active nor toxic. Moreover, they copolymerised an active/toxic monomer with another inactive/non-toxic monomer, and generated a copolymer series (e.g. methyl-propyl copolymer) that presented low toxicity to RBCs but selectively killed *S. aureus* and remained totally inactive against *E. coli*.

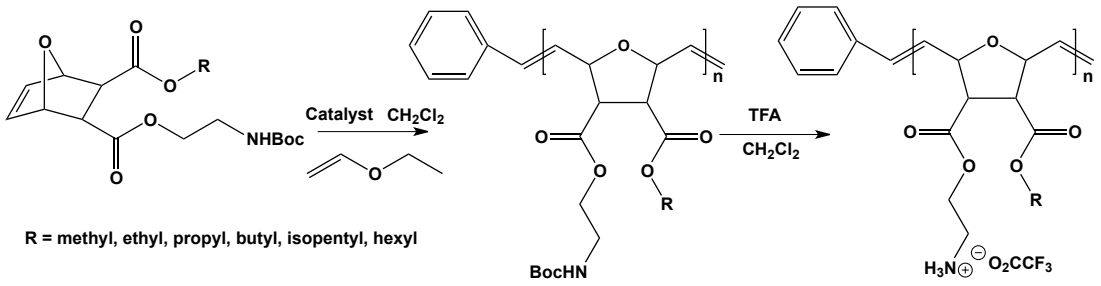

Figure 1.1 ROMP polymerisation and hydrolysis with trifluoroacetic acid to obtain amphiphilic polymers.

Kuroda used radial polymerisation to synthesise a library of amphiphilic copolymers with side chains containing primary, tertiary or quaternary ammonium groups (Figure 1.2)[21-23], and tested their antimicrobial and haemolytic activities. This work concluded that the antimicrobial activity of polymers strongly depended on the chemical structure of the amine, because the copolymers with primary or tertiary

amine side chains were generally much more effective at inhibiting bacteria than those with quaternary ammonium groups. Furthermore, they reported that the increase of hydrophobicity of the primary or tertiary amine copolymers (e.g. longer alkyl chain) might enhance their antimicrobial potency. However, excessive hydrophobicity of the polymers might also lead to decrease antimicrobial activity. Hydrophobicity of the side chains influenced the haemolytic activity of the polymers, with a decrease of RBC lysis observed when the hydrophobicity of the primary or tertiary amine copolymers was increased.

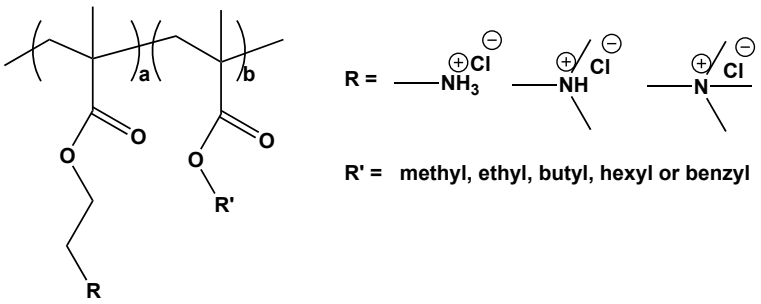

Figure 1.2 Chemical structures of the copolymers showing antimicrobial property with different side chains.

Polymers with organometallic derivatives attached through side chains have been shown to have potent antimicrobial activities[24]. Al-Muaikel synthesised two organotin monomers, (*N*-tri-*n*-butyltin)maleimide (TBTM) and *m*-acryloylamino-(tri-*n*-butyltin benzoate) (AATBTB) (Figure 1.3), and copolymerised the two monomers with styrene[25]. Antimicrobial activities of the copolymers were analysed with a wide range of Gram-positive and Gram-negative bacteria. Results demonstrated that the polymer with TBTM displayed stronger antimicrobial activity than those with AATBTB, and Gram-positive bacteria were much more sensitive to these copolymers than were Gram-negative.

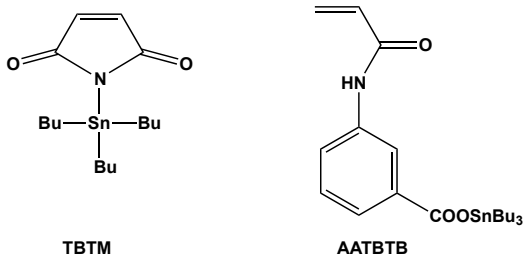

Figure 1.3 TBTM and AATBTB monomers.

Other polymers with antimicrobial derivatives include those containing sulfo derivatives. Kanazawa reported the synthesis and antimicrobial activity of polymers with sulfonium salts[26]. The polymeric sulfonium salt (Figure 1.4) exhibited strong antimicrobial activity against Gram-positive bacteria (*S. aureus*), but was less effective against Gram-negative bacteria (*E. coli*). It also displayed much higher activity than that of its corresponding model compound. However, due to low thermal stability, there might be some limits for polymeric sulfonium salts used as disinfectants[27, 28].

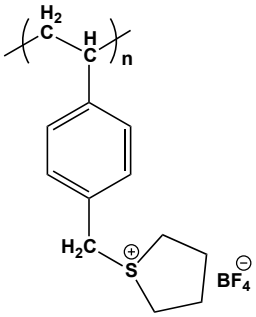

Figure 1.4 Chemical structure of polymeric sulfonium salt.

Polymers with antimicrobial agents in the main chain:

Polymers with antimicrobial moieties incorporated into the polymer backbone are often employed as antimicrobial polymers, with the biologically active groups on the main chains hydrolysed to give the active antimicrobial agent. Drug-polymer models consisting of polyurethanes and a fluoroquinolone antibiotic (ciprofloxacin or norfloxacin) were synthesised by Santerre (Figure 1.5)[29-31]. In this case, the antibiotic was polymerised into a polyurethane backbone to form a copolymer, with slow biodegradation providing the antibiotic. In their studies, the degradation products included fragments with antibiotic coupled with diol or diisocyanate which did not show antimicrobial activity. However, free ciprofloxacin was also detected in the solutions and effectively inhibited the growth of Gram-negative bacteria.

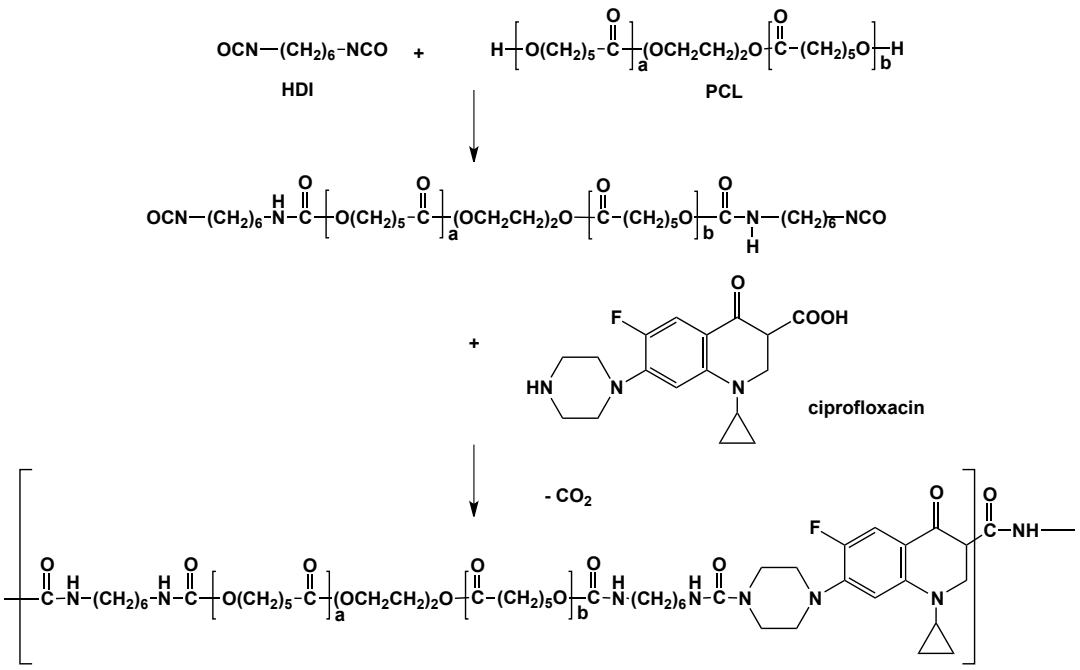

Figure 1.5 Incorporation of ciprofloxacin into a polyurethane backbone.

Patel prepared poly(ether ketone) systems (Figure 1.6) by reacting phenol, 1,4-phenylenedioxy diacetylchloride (1,4-PDC), or dicholomethane/dicholoethane in solvent carbon disulfide with anhydrous aluminum chloride as a catalyst[32], and tested for their antimicrobial activity against bacteria, fungi and yeast. It was demonstrated that all synthesised samples of the poly(ether ketone)s generally inhibited microbial growth during 48 hour incubation. P2 exhibited the strongest antimicrobial effect preventing over 80% growth of bacteria, 80% growth of fungi and 95% growth of yeast.

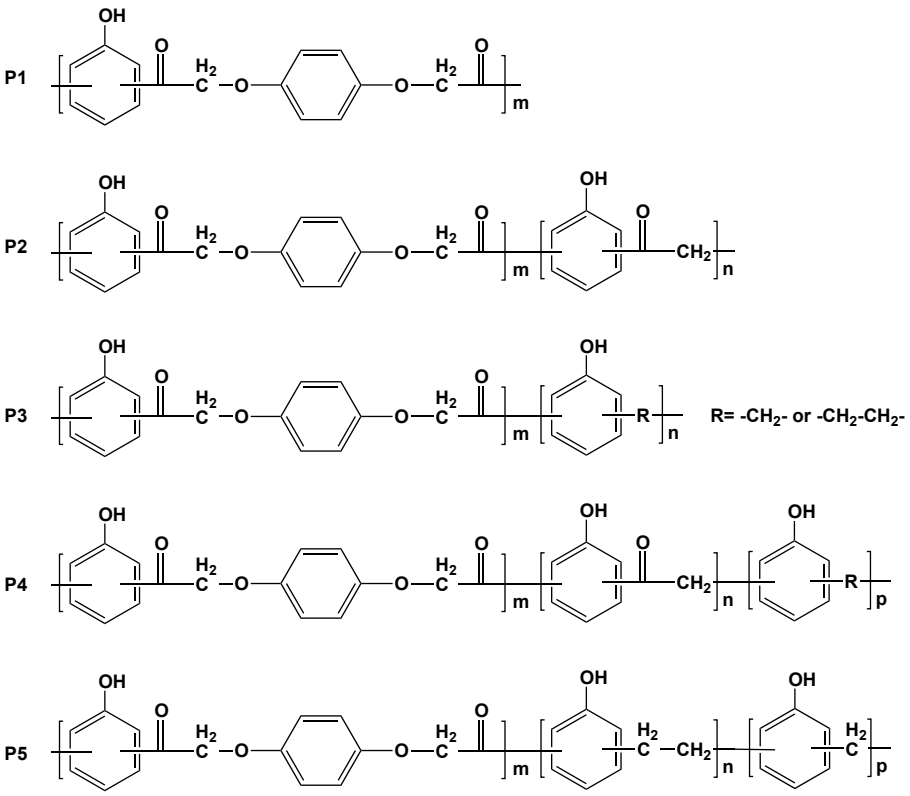

Figure 1.6 Chemical structures of antimicrobial poly(ether ketone)s.

Polymers with inorganic conjugates:

Silver nanoparticles are possibly the most widely used nanocomposites and potent antimicrobial agents. In general, silver/polymeric composites are generated *via in situ* Ag (I) reduction, embedding metallic nanoparticles into a polymer matrix. However, many different strategies for preparing antimicrobial polymer silver nanocomposites have been reported, and the size and shape of the silver nanoparticles in the matrix greatly influence the antimicrobial activities[33].

Kong synthesised a poly(methyl methacrylate) (pMMA) nanofibre containing silver nanoparticles using radical-mediated dispersion polymerisation, and compared its antimicrobial activity to silver sulfadiazine and $AgNO_3$ at the same silver concentration against *E. coli* and *S. aureus*[34]. The silver/pMMA conjugates had a quicker killing rate than both silver sulfadiazine and $AgNO_3$, significantly enhancing its antimicrobial efficacy. Polymeric gels containing silver nanoparticles have also been developed with silver nanoparticles embedded into a crosslinked poly(acrylamide)/poly(*N*-(hydroxymethyl)acrylamide)(pAAm-pHMAAm) network[35].

Other metals have been used as antimicrobial agents. For example, Kamrupi prepared nanocomposties of copper and polystyrene *via in situ* synthesis, adding copper nanoparticles into a solution of monomers during polymerisation[36]. The copper/polystyrene composites strongly inhibited the growth of *Pseudomonas fluorescens*, *Bacillus circulans, E. coli* and *S. aureus*. Furthermore, Kong synthesised TiO_2/poly(2-(tert-butylamino)ethyl methacrylate-co-ethylene glycol dimethacrylate) (poly(TBAM-co-EGDMA)) nanoparticles by photopolymerisation and tested their antimicrobial activity against *E. coli* and *S. aureus*[37]. The TiO_2/poly(TBAM-co-EGDMA) nanoparticles displayed significantly higher antimicrobial efficiency compared with TiO_2 nanoparticles and bulk poly(TBAM-co-EGDMA).

1.2 Microbial Adhesion and Antimicrobial Surface Design

1.2.1 Biofilm Formation on Substrates

A biofilm is an accumulation of microorganisms (bacteria, fungi, and/or protozoans, with associated bacteriophages) embedded in a polysaccharide matrix and adhered to a surface. Biofilm formation is medically important, leading to over eighty percent of microbial infections in the human body, such as infections in oral soft tissue, middle ear, lung, eye, gastrointestinal tract as well as in cardiac implants[38].

The first reported observation of biofilms was by Henrici in 1933, who discovered that most water microbes were not free swimming organisms, but grew upon surfaces[39]. Although biofilms have been known for over eighty years, the adhesion process is only partially understood[40, 41]. Previous studies have shown that the rates of the biofilm adhesion process are variable, and dependent on diverse conditions, such as differences in microorganisms and variation in environment, which are crucial factors for initial biofilm formation[42, 43].

Biofilms can be formed from single or multiple species, and can form on biotic or abiotic surfaces[43]. The formation of a biofilm may be initiated by the direct contact of microbes with a solid surface, or microbe-microbe adhesion in the aqueous system. Microbial adhesion onto substrates may first lead to microbial proliferation, which produces microbial colonies; subsequently, biofilms are formed by the generation of a polysaccharide matrix by the attached microbes[43, 44]. Once a biofilm is formed, the microorganisms within it begin to undergo a series of changes adapting themselves onto the surface[43], and become much more resistant to both antimicrobials and the action of the host immune system[38].

The formation of biofilm can be considered to occur in three phases (shown in Figure 1.7)[43-45]. The first phase consists of rapid reversible interactions among microbes and material surfaces, and this phase occurs over 1 to 2 hours. The second phase involves specific and non-specific interactions between adhesion proteins expressed on the microbial cell wall and binding sites of the materials. This phase is relatively slow and induces irreversible formation of the microbial monolayer, with microbial autoaggregation on the surface leading to the formation of micro-colonies.

With time, micro-colonies develop into three dimensional (3D) mature biofilms, which are normally associated with a self-produced matrix[44], such as an extracellular polymeric substance (EPS, also known as exopolysaccharide), which protects the biofilm and leads to biocide resistance. This is normally considered as the final phase of the process.

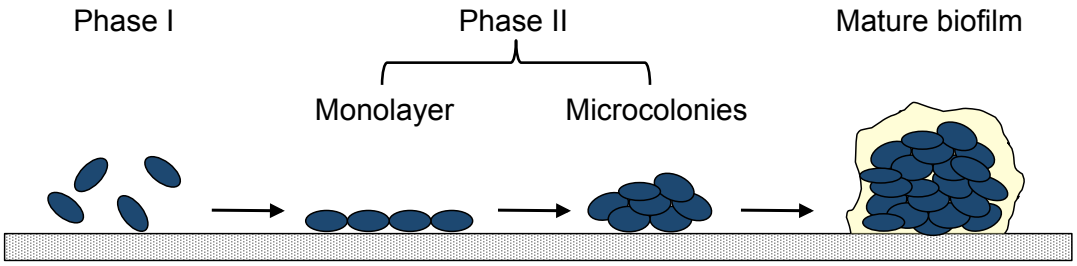

Figure 1.7 Principal mechanism of microbial adhesion to material surfaces.

1.2.2 Antimicrobial Polymeric Surface Design

Studies of microbial adhesion onto substrates has been carried out at different levels of complexity in various experimental systems, looking at the balance between repulsive and attractive interactions of the involved microorganisms, and various experimental conditions, including rinsing, dipping and other hydrodynamic forces[46]. The design of the methods used to study microbial adhesion may be of importance as well, which occasionally leads to uninterpretable and incomparable results from different laboratories[46].

Apart from the complexity in microorganism populations and the variation of polymer surface characteristics, three general strategies have been determined for the development of antimicrobial polymeric surfaces: (I) adhesion resistance, (II) contact killing and (III) biocide leaching (Figure 1.8)[47, 48].

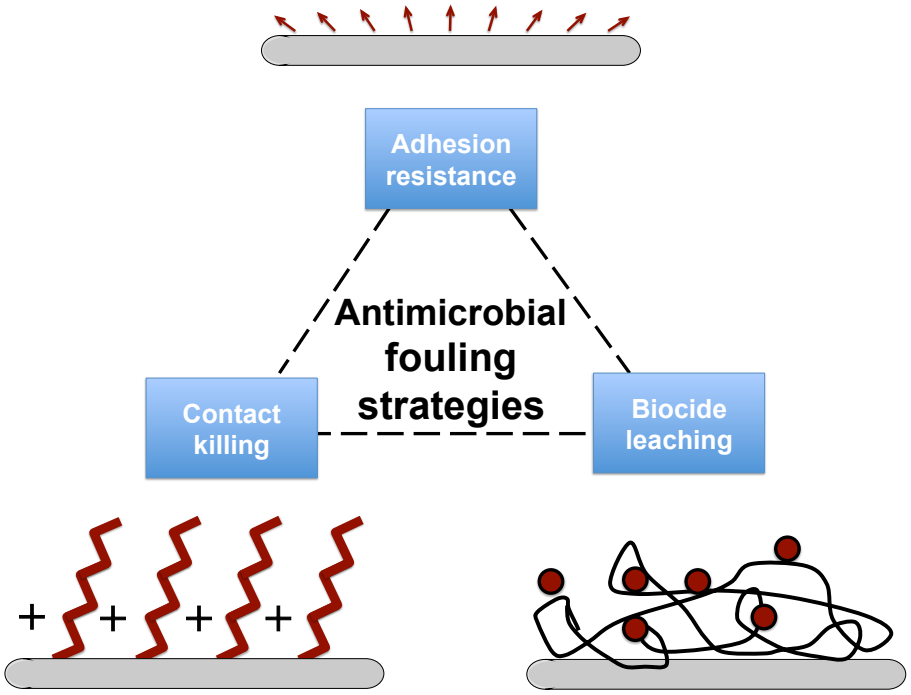

Figure 1.8 Strategies of antimicrobial polymeric surface design[47]. Plus sign in left corner indicates charges on the surface; red dots in the right corner indicate immobilised antimicrobial agents.

Adhesion resistance:

In this strategy, polymers prevent microbial adhesion and minimise their contact with the surface. These polymers may or may not contain microbial killing components[47]. In practice, the physical and chemical properties of the polymer surfaces, such as roughness, hydrophobicity/hydrophilicity, and steric effects, are all important for the design of microbial resistance polymers[49]. Previous studies noted that the extent of microbial colonisation might decrease as the surface roughness decreases[50, 51], because the rougher surfaces have higher surface areas, and diminish shear forces between the cell surface and the substrates[50]. While the rate and extent of microbial attachment appears to be influenced by other factors, hydrophilic surfaces appear to be more microorganism adhesion resistant than hydrophobic, nonpolar surfaces[52-54]. An excellent example is poly(ethylene glycol) (PEG) which coated or grafted on to a

surface significantly reduces the adhesion of microorganisms[42, 55, 56]. Park investigated the microbial adhesion on both PEG and poly(propylene glycol) (PPG) modified surfaces, and PEG modified surfaces demonstrated consistently lower microbial adhesion[55]. In contrast, no reduction in microbial adhesion was observed on PPG modified surfaces.

Contact killing:

This strategy focuses on contact killing, which induces the death of microbes that have stably attached to the polymer surfaces. It is a non-release strategy[57], and is generally approached *via* direct polymerisation of antimicrobial monomers or post polymer modification. This approach can also involve conjugation of the polymers with antimicrobials, such as antimicrobial peptides, or compounds that display positive charges to penetrate the cell membrane[50], or cationic sites that can disrupt the cell membrane and cause cell lysis[47]. These compounds include ammonium polymeric salts[58, 59] and quaternary phosphonium salts[60, 61]. For example, Russell described a simple method to make a permanent non-leaching antibacterial polymer surface by treatment of a tertiary amine polymer with a alkyl halide (Figure 1.9)[62]. These polymer surfaces killed over 99% of bacteria (*E. coli* and *Bacillus subtilis*) within one hour.

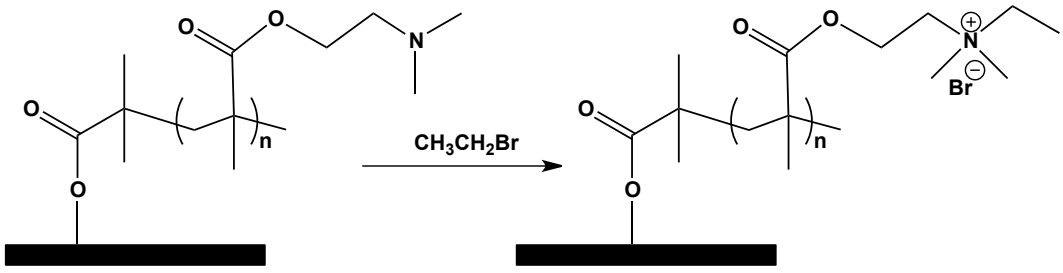

Figure 1.9 Chemical structure of polymer surface before (left) and after (right) alkyl halide modification.

Biocide leaching:

This strategy mainly focuses on leaching biocides/cytotoxic compounds from the polymer substrates, causing death of microbes attached or in close contact. In this strategy, polymer surfaces hold and release antimicrobials (e.g. antibiotics, silver), biomolecules (e.g. antibodies) or gaseous antimicrobial agents (e.g. nitric oxide, NO) at a preset rate[63]. Immobilisation of antimicrobial agents onto natural or synthetic polymer surfaces varies and includes absorption, grafting and ligand coordination. The controlled release system can effectively avoid the toxicity of some drugs. Nevertheless, the efficiency of a drug-polymer release system is strongly dependent on the rate and manner that the drug is released, and also on the polymer matrix that the drug is loaded onto. Schierholz dispersed antibiotics homogenously within a polyurethane substrate by using polymer and antibiotics with similar lipophilicity[64, 65], and the uniformity of the "antibiotics" distribution significantly controled the release of drug and the effectiveness of the coating in this case. For example, hydrophilic ciprofloxacin showed fast release (~100 μg cm^{-2} day^{-1}, weight per matrix area per day) for the first 24 hours from hydrophobic polyurethane, but at a much lower flux over 48 hours (~1 μg cm^{-2} day^{-1})[64]. In contrast, lipophilic flucloxacillin dispersed in an identical hydrophobic polyurethane matrix and showed reduced initial burst of release (~25 μg cm^{-2} day^{-1}) compared to that of ciprofloxacin, but greater overall flux over five days (10-20 μg cm^{-2} day^{-1}), which allowed almost 100% killing of *S. epidermidis*[64].

1.3 Polymer Microarrays

1.3.1 A Brief Historical Sketch of Microarrays

Microarrays are a tool developed for the parallel addressing of molecules arrayed on a planar substrate (typically a slide), which allows a large number of materials to be analysed in parallel.

The first generations of microarrays were developed in the late 1980s and the early 1990s[66, 67]. Hoheisel promoted an idea of using multiple libraries of *Drosophila* genomic DNAs arrayed on filters at a high density as tools for genome sequencing[68], and shortly after, Saiki introduced the reverse dot blot, in which multiple nucleic acids of known sequence were patterned onto membranes and used for the analysis of unknown sequences[69]. Southern revealed the concept of analysing and comparing nucleic acid sequencing by hybridisation of oligonucleotides onto arrays[70]. The first arrays, which were made with short oligonucleotides (19-mer), were made on glass supports by Maskos[71, 72], and marked the foundation of current microarray technology. At nearly the same time, Fodor synthesised a peptide microarray, and studied its interaction with a fluorescence labeled monoclonal antibody[73]. Fodor also developed DNA microarrays[74]. As a rapid complement to Southern's approach, Frank presented the facile and rapid "spot-synthesis" of large numbers of peptides on cellulose sheets[75], and this spot-synthesis method provided opportunities to synthesise and screen a large number of synthetic peptides arrayed on a cellulose support[76]. Since then, microarray methodology has blossomed with commercial development of microarray technologies and industries[77, 78], and DNA microarrays have become a fundamental tool for genetic analysis.

Later on, other materials, including, carbohydrates[79-81], small molecules[82] and biomaterials[83-85], have been immobilised onto surfaces, allowing their applications in a broad range of biological, chemical, physical and medicinal applications. Over the last decade, cell-based microarray technologies have emerged for a variety of applications, for example for investigation of cell and extracellular matrix (ECM) interactions, between cells and specific receptors[86, 87], analysis of the phenotypic consequences of perturbing cells with functionalised genes and interfering RNA[88],

and evaluation of potential drug targets by functionally characterising their effect in cells[89].

1.3.2 A Brief Historical Sketch of Polymer Microarrays

Polymer microarrays can be generated with hundreds to thousands of polymer spots on one slide and have been employed as a high-throughput (HT) method for the screening of polymeric biomaterials, which can bind/control specific kinds of cells and proteins[90, 91]. Two research groups, the Bradley group and the Langer group, independently developed polymer microarray technology to study the interactions between cells and biomaterials[91-94].

In 2004, the Bradley group completed the synthesis of a polymer library, and screened the polymers for the absorption of proteins (human albumin (Alb), immunoglobulin G (IgG) and fibronectin (Fib)) and for the depletion of leucocytes[91, 95]. The Bradley group also printed polymers and looked at cellular transfections with a broad range of cell lines in 2004[92]. Furthermore, the analyses of the chemical and physical properties of the synthesised polymers (wettability, functional group and thermal properties) were also completed in a high-throughput manner using time-of-flight secondary ion mass spectrometry (ToF-SIMS) and fourier transform infra-red spectroscopy (FT-IR)[91, 96, 97]. In the same year, Anderson published a polymer microarray made on a glass slide, using poly(2-hydroxyethyl methacrylate) (pHEMA) as a slide coating, and screening human embryonic stem cells (hESCs) to test polymers' effects on the growth and differentiation of hESCs[93]. Shortly afterwards, Anderson fabricated microarrays with biodegradable polymers, and studied the ability of the polymers to support the attachment and spreading of human mesenchymal stem cells (hMSCs), murine neural stem cells (clone C17.2), and ovine articular chondrocytes[98].

In 2006, Tourniaire fabricated polymer microarrays with a library of polyurethanes, and demonstrated agarose was a cytophobic coating which could effectively prevent cellular attachment to avoid non-specific cell binding, and could be used as a coating surface for polymer microarrays[94]. Tourniaire also investigated protein deposition (including fibronectin, glycoprotein Y and glycophorin A) onto

polymer microarrays[90]. Shortly after, a polymer library with 120 polyurethane members was arrayed and used to identify the polymers which promoted immobilisation of bone marrow dendritic cells (BMDCs)[99]. In 2007, Urquhart reported a high-throughput characterisation of surface chemistry on microarrayed polymers[100], allowing fast automated X-ray photoelectron spectroscopy (XPS) and ToF-SIMS analysis of arrayed polymer libraries, and later in 2008, he demonstrated a partial least-squares regression (PLS) model which can be used to correlate wettability and surface chemistry for a large number of materials[97].

In 2008, the Bradley group studied polymers for their effects on the transfections of cells using an ultrasonic nebulizer to dispense lipoplexes onto cell-based microarrays[101]. In the same year, a polymer microarray was used to study the attachment of mouse fibroblast cells (L929), and a comparison between the wettability of the materials and cell attachment was characterised in this work[84]. Also in 2008, Tare identified polyurethanes for the isolation of human skeletal progenitor cells and augmentation of skeletal cell growth[102]. Subsequently, Zhang published work on the fabrication of hydrogel microarrays *via in situ* polymerisation with ink-jet printing of the monomers[103]. This approach was used to identify and study a series of thermo-sensitive hydrogels for culturing human cervical cancer cells (HeLa), mouse fibroblast cells (L929), human embryonic kidney cells (HEK-293T), and mouse embryonic stem cells (mESCs)[104]. In 2009, Liberski published his work on the fabrication of polymer microarrays and inter-crossed gradient lines by ink-jet printing individual monomers and initiator solutions in organic solvents through a thin film of oil, and polymerisation *in situ*[105]. A cooperative polymer-DNA microarray approach was investigated to study the cellular adhesion and proliferation of suspension human erythroleukemic cells (K562), and demonstrated that interactions between cells and the identified materials induce a number of changes in the transcriptom by gene expression profiling[85].

In 2009, Mei used a polymer microarray approach to study the correlation of cell attachment, the chemical structure of monomers and fibronectin absorption[106]. In 2010, Khan illustrated blend hydrogels in a microarray formulation, and these blend microarrays were used to identify cell-compatible materials for human skeletal stem

cell growth in both *in vitro* and *in vivo* applications[107]. In 2010, Mei evaluated a fetal bovine serum (FBS) coated polyacrylate microarrays in human embryonic stem cells (hESCs) and human induced pluripotent stem cells (hiPSCs), which maintained their pluripotent properties after ten passages[108]. In 2011, Hay screened a library of polyurethanes for long-term hepatocyte function and growth using polymer microarrays, and identified a polyurethane as a liver matrix[109]. In 2011, Hansen demonstrated that specific polyacrylates could rapidly bind and activate platelets and control their activity[110]. Furthermore, polymer microarrays were developed to identify a cardiovascular matrix that specifically supported the attachment of endothelial progenitor cells (EPCs) and human umbilical vein endothelial cells (HUVECs), potentially providing new strategies to enhance vascular repair *in vivo*[111].

1.3.3 Fabrications of Polymer Microarrays

Polymer microarrays have been made in a number of ways with either a pre-synthesised polymer library or *via in situ* synthesis, and fabricated either by a contact printer or *via* ink-jet printing. Contact printing is often preferred to generate polymer microarrays when resynthesised polymers are available, while ink-jet printing is usually chosen to fabricate *in situ* polymer microarray synthesis. Contact printing is well defined in the Langer group to produce polymer microarrays[93, 98], whereas both contact printing and ink-jet printing approaches for the polymer microarray fabrications are well developed in the Bradley group[92, 94, 103, 104].

1.3.3.1 The Langer Approach

In this approach, the deposition of diverse acrylate monomers onto substrates to fabricate polymer microarrays is achieved by contact printing. Various monomers are diluted and then well premixed with initiator at a set ratio using a robotic fluid handling system, and the different combinations of these monomer mixtures are transferred from their reservoirs and arrayed using robotic pins onto epoxy monolayer-coated glass slides, which are typically treated with a thin layer of pHEMA[93]. After each round of printing, monomers on the slides are polymerised by exposure to long-wave UV for at least 10 minutes[112]. The solvent is removed by drying the slides under vacuum for over a week. However, Langer also discussed

some difficulties for this approach[93]. First of all, difference in monomers' viscosity affects all aspects of monomer printing and pin washing. Secondly, as radical polymerisation is sensitive to oxygen, the printings have to be done under an atmosphere of humid argon. Likewise, humidity is also an essential part of avoiding failed printing. Finally, irregular polymer spots often form because of the fast spread of some monomers after deposition.

Consequently, a microarray with commercial biodegradable polymers has been fabricated using a method similar to that described above[98]. Polymers are dissolved and spotted. In this case, deposited polymers are interpenetrated and blended with the layer of pHEMA surface[98].

1.3.3.2 The Bradley Approach

Contact printing approach for pre-synthesised polymers:

The contact printing of pre-synthesised polymers on a microscope slide is very similar to the original methods of DNA microarray generation. In this approach, numerous polymers, such as polyacrylates, polyurethanes, polyesters, polyamides and so on, need to be synthesised and purified prior to microarray fabrication[91, 95, 96]. Polymer members can then be dissolved in a suitable solvent with low volatility that allows good solubility of the polymers in the library but avoids rapid evaporation during printing. Contact printing involves the use of moving metallic solid pins, which are dipped into polymer solutions, and then "stamped" onto the microscope slide (Figure 1.10)[94]. Printing parameters, such as inking and stamping time, properties of the pin, can be adjusted according to requirements of the size, density and layout of the microarray. Polymer spots on the microarray have been studied *via* FT-IR[90, 95], ToF-SIMS[91, 113] for chemical composition analysis, scanning electron microscopy (SEM)[90] for morphology analysis and atomic force microscopy (AFM) for surface roughness analysis[95, 114]. The evaporation of solvent can also affect the morphology of the spots in contact printing, for example, giving rise to the "coffee ring" effect[115]. Nevertheless, it can be controlled or diminished if external factors are well controlled, such as humidity and temperature.

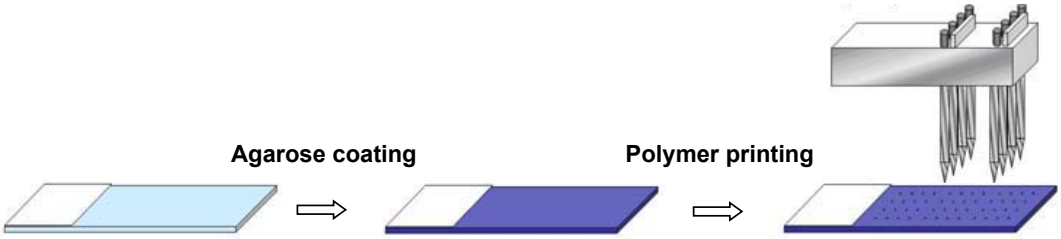

Figure 1.10 Contact printing approach[99]. Polymer spots printed by "placing" of the solid pins loaded with a solution of polymer onto the agarose precoated microscope slide.

Ink-jet printing approach[103, 104]:

In this approach, a nozzle is used to suck in and then dispense defined droplets of the polymer/monomer solution onto the substrates. This method can effectively control the amount of material deposited and avoids contact with the surface. High-density DNA microarrays are also made *via* ink-jet printing. The ink-jet printing approach also allows high-throughput *in situ* polymerisation on a microscope glass slide, and can rapidly synthesise new polymers at a pico-nano litre scale. Many acrylamide and acrylate monomers and various crosslinkers with different chain lengths have been used to generate polymer microarrays with thousands of different polymer spots per microarray. In this approach, monomers are well mixed using the drop-by-drop dispensing method, and the range of monomer combinations enhanced significantly.

1.4 Summary

In conclusion, research for new antimicrobial materials is of importance in a great number of applications, including food packaging and storage, health care products, water treatment and hospital equipment, and will improve the health and well-being of mankind. The development of antimicrobial polymers has been progressing steadily over the past decades[18].

Polymer microarrays allow thousands of microbe-polymer interactions to be studied in a single experiment. Polymer microarrays would provide a high-throughput method for the identification of antimicrobial polymers by screening many different polymers. This would considerably speed up the progress of new antimicrobial polymer hunting, whilst requiring only tiny amounts of polymer and microbes. In this thesis, polymers with very strong affinity/repellence for microbes are described, and an understanding of their interactions is discussed.

1.5 Aims for this Thesis

The aims of this thesis were to identify and develop polymeric materials that either selectively bind or strongly repel food-borne and water-borne pathogens using a polymer microarray platform. The identified polymers would then be explored on a large-scale, and analysed to understand their microbial adhesion or repellence properties.

Four main objectives of the research presented in this thesis are:

(i) The discovery of polymers for the binding and the prevention of binding of food-borne pathogens (*S.* Typhimurium);

(ii) Screening polymer libraries with Gram-positive and Gram-negative bacteria for the identification of multi-bacteria non-adhesion substrates;

(iii) Identification of polymers that promote or limit *Cryptosporidium parvum* (*C. parvum*) attachment using a polymer microarray approach;

(iv) Analysis of the interactions between *Giardia lambia* (*G. lambia*) and polymer substrates.

It was hoped that these results would have practical applications, in particular that these polymers could help prevent pathogenic bacterial contamination or be used to remove water-borne parasites from water supplies.

.

Chapter 2

Colonising New Frontiers - Microarrays Reveal Biofilm Modulating Polymers

Published as: Salvatore Pernagallo, Mei Wu, Maurice P. Gallagher and Mark Bradley. Colonising new frontiers - microarrays reveal biofilm modulating polymers. *Journal of Materials Chemistry* **2011**, 21, 96–101

Patent: Mei Wu, Salvatore Pernagallo, Maurice P. Gallagher and Mark Bradley. Binding and non-binding polymers (PCT/GB2011001354 and GB1015492.0).

The work reported in this chapter was undertaken by Dr. Salvatore Pernagallo and myself.

2.1 Introduction

It is well known that bacterial cell surface charge, cell density, and the presence of a variety of microbially produced compounds such as exopolysaccharides, are determinant factors in the adhesion process. However, other physicochemical features such as pH, temperature, composition of growth media and surface conditioning factors are also known to affect surface attachment[116]. In order to control bacterial attachment, there is a need for materials which result in specific bacterial sequestration or repulsion. These materials when discovered could underpin wide-ranging applications in hygiene and avoidance of bio-fouling, offering for example a means for the rapid isolation of hospital pathogens, or minimisation of surface contamination through the development of microbe repelling surfaces. They

could also provide opportunities for innovative intervention approaches, such as the selective reduction of pathogen loads *via* animal feeds. Other possible applications could be the selective capture of bacteria, spores or viruses on cleaning materials used in clinical, industrial and domestic environments. Minimising attachment and colonisation could be beneficial in areas ranging from artificial implants to packaging for food preparation.

In the present study, we assessed the value of the polymer-based microarray platform to identify novel materials which could be used for the rapid and selective capture of major food-borne pathogens or materials capable of limiting or preventing bacterial adhesion onto surfaces.

For the purposes of this study, work in this chapter focused on the adhesion of the food-borne pathogenic bacterium *Salmonella enterica* serovar Typhimurium (*S.* Typhimurium, strain SL1344)[117], a serious pathogen of clinical and veterinary importance[118] globally and also a substantial problem in the food industry, and the commensal bacterium *Escherichia coli* (*E. coli,* strain W3110)[119].

2.2 *S.* Typhimurium

S. Typhimurium is a Gram-negative facultative intracellular anaerobic bacterium, and does not require strict conditions for its growth[120]. *S.* Typhimurium can be found in water, soil, animal faeces, raw meats, and eggs, and can be transmitted into the food chain *via* some animals. After infection with *S.* Typhimurium, different hosts display different disease symptoms and host responses. *S.* Typhimurium can cause diseases, such as gastroenteritis both in humans and animals, while in mice, it can cause symptoms resembling typhoid fever in humans[118]. In the United States, the most frequent cause of diarrhoea is *S.* Typhimurium, with 15 to 20 outbreaks each year[121]. In contrast, although *S.* Typhimurium is very closely related to *S.* Typhi, with > 96% DNA sequence identity with shared genes, *S.* Typhi uniquely infects humans and causes serious, often fatal diseases[122].

The *S.* Typhimurium strain used in this work is SL1344, which is virulent to susceptible mice and tetracycline-sensitive[117]. This *S.* Typhimurium was transformed with plasmid pHC60 that constitutively expresses green fluorescent protein (GFP)

and carries tetracycline resistance genes[123]. Additionally, for the commensal bacterium, *E. coli* (strain W3110), it is widely used as a wild-type strain and also transformed with plasmid pHC60 for expressing GFP.

2.3 Polymer Microarray Screening of Bacteria Attachment

2.3.1 Analysis of Bacteria Attachment

In this study, analysis was enabled by the expression of Green Fluorescent Protein (GFP)[124] within the bacteria, allowing detection of bacterial binding onto polymer features of a microarray with quadruplicates of 370 polyurethanes (PUs) and polyacrylates (PAs)[85, 91, 96, 101].

This work focused on the adhesion of *S.* Typhimurium in comparison with *E. coli* as a commensal strain. These two bacteria both expressing GFP were plated into polymer microarrays containing 1480 spots (four for each polymer), and incubated overnight at room temperature. Subsequently the polymer microarrays were washed and measured by a BioAnalyzer 4F/4S LaVition BioTech scanner with a fluorescein (FITC) filter. The bacterial adhesion on the microarrays was evaluated *via* the integrated fluorescence intensity for each polymer spot after background correction (Figure 2.1). The mean fluorescence intensity and standard deviation (SD) from 8 spots (four polymer spots per microarray, and two microarrays per bacterium strain) were calculated assuming a spot diameter of 300 μm.

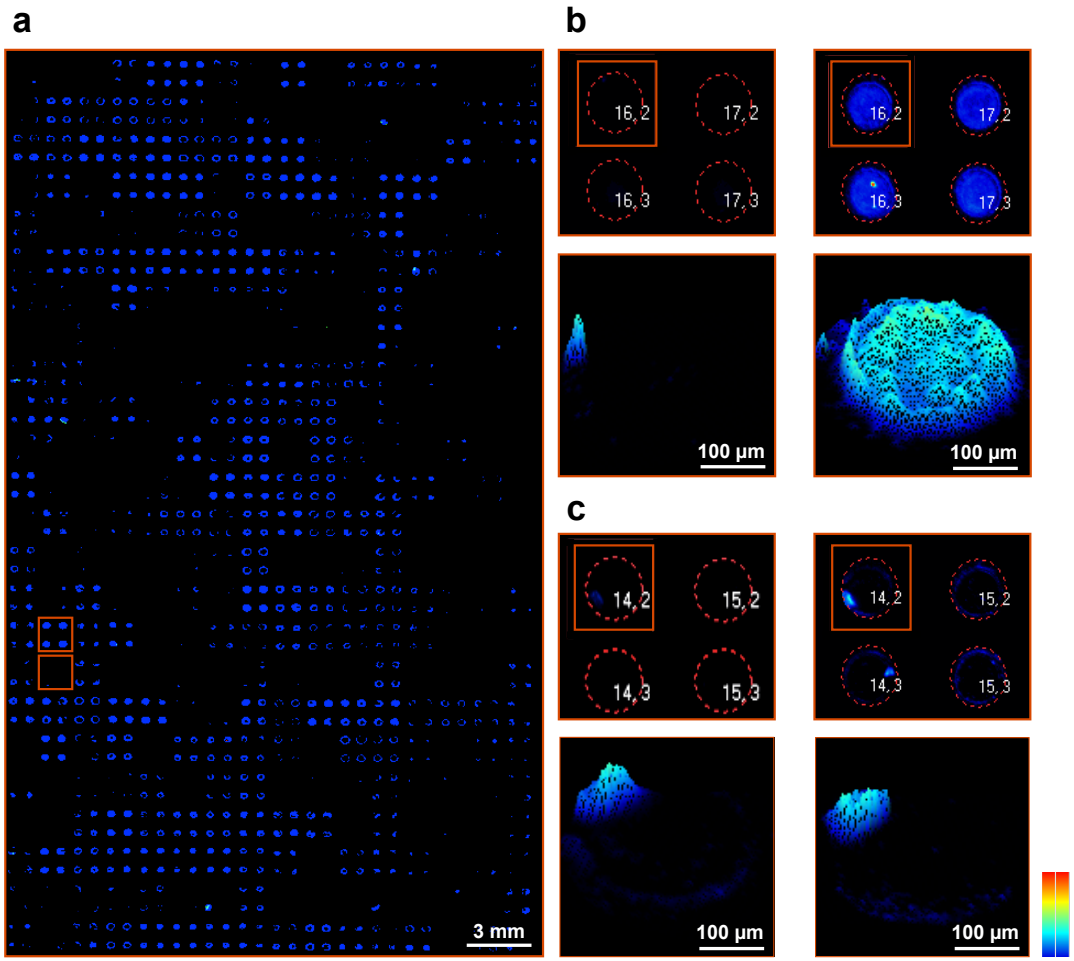

Figure 2.1 LaVision Bio Analyzer 4F/4S BioTech quantification. (a) Fluorescence associated with the binding of bacteria (expressing GFP) on a library of 370 polyurethanes and polyacrylates (each polymer was printed in quadruplicate). The two highlighted squares of the 4 polymer spots are shown in b and c. (b) Strong binding polymer (PA155). Upper left: Background polymer auto-fluorescence prior to bacterial binding. Upper right: Fluorescence intensity in the presence of bacteria. A 3D image of the spot in the selected area is shown in the lower panels, respectively. (c) Poor binding polymer (PA325). Upper-left: Background polymer auto-fluorescence prior to bacterial binding. Upper right: Fluorescence intensity in the presence of bacteria. A 3D image of the spot in the selected area is shown in the lower panels, respectively. In b and c: the number in the square is the position of the polymer spot in the array, which was allocated automatically by the software. An intensity scale bar is shown (bottom right).

Analysis revealed six PAs (PA55, PA155, PA172, PA181, PA182 and Pg17) and thirteen PUs (PU39, PU92, PU104, PU116, PU119, PU120, PU126, PU138, PU159, PU178, PU208, PU219 and PU222) which showed strong binding of *S.* Typhimurium. *E. coli* affinity was weaker in general, but varied with the particular polymers (Figure 2.2).

In the study of *S.* Typhimurium adhesion, four of the six high binding PAs (PA155, PA172, PA181 and PA182) (Figure 2.2) contained the monomer 2-hydroxyethylmethacrylate (HEMA) (see Table 2.1 and Figure 2.3) and of those four, two (PA181 and PA182) contained the monomer 1-vinylimidazole (VI) with the monomer ratios: 70/30 and 50/50, respectively (Figure 2.3 for structures). Polymer structure analysis of the PUs revealed that the diols polybutylene glycol (PTMG) and polypropylene glycol (PPG) were common in ten of the thirteen hit polymers (see Table 2.2 and Figure 2.3). Thus for example, polymer PU222 showed good binding of *S.* Typhimurium and *E. coli*, whereas there was a substantial difference between the binding of *S.* Typhimurium and *E. coli* on polymer PU178 (see Figure 2.3 for structures).

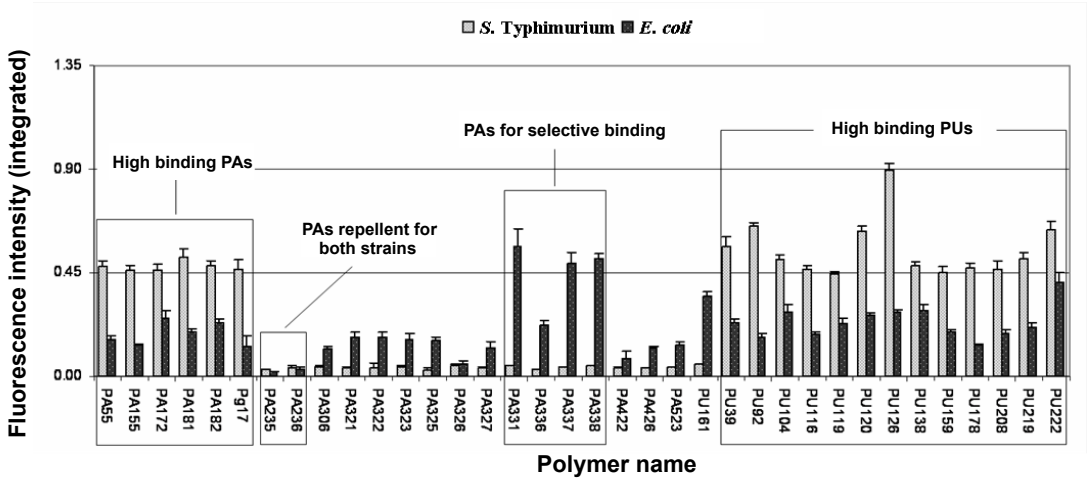

Figure 2.2 Analysis of *S.* Typhimurium and *E. coli* binding on the polymer microarrays. PA and PU library members showing strong/poor *S.* Typhimurium and/or *E. coli* binding. Binding is expressed as background corrected mean fluorescence intensity with error bars representing the standard deviation in arbitrary units (au).

Table 2.1 Polyacrylates showing strong/poor binding of *S.* Typhimurium. Monomer ratios were Monomer (1)/Monomer (2)/Monomer (3): PA155 and PA182 (50/50/0); PA172 and PA 181 (70/30/0); PA155 (90/10/0); PA422 and PA426 (40/30/30); Pg17 (50/15/35); PA523 (60/10/30); PA235 (70/25/5); PA236 (70/10/20).

		Polymer			*S.* Typhimurium		*E. coli*	
		Monomer (1)	Monomer (2)	Monomer (3)	Mean	SD	Mean	SD
PA with strong binding	PA55	HBMA	DEAA	-	0.48	0.024	0.16	0.016
	PA155	HEMA	DMAEMA	-	0.46	0.021	0.13	0.005
	PA172	HEMA	BACOEA	-	0.46	0.027	0.25	0.030
	PA181	HEMA	VI	-	0.52	0.035	0.19	0.014
	PA182	HEMA	VI	-	0.48	0.024	0.24	0.014
	Pg17	MEMA	A-H	DEAEA	0.46	0.041	0.13	0.045
PA with poor binding	PA235	MMA	MA-H	DEAEMA	0.03	0.001	0.02	0.002
	PA236	MMA	MA-H	DEAEMA	0.04	0.008	0.03	0.008
	PA422	MEMA	DEAEMA	BMA	0.04	0.005	0.08	0.027
	PA426	MEMA	DEAEA	BMA	0.04	0.003	0.12	0.008
	PA523	MEMA	DEAEA	St	0.04	0.003	0.13	0.018

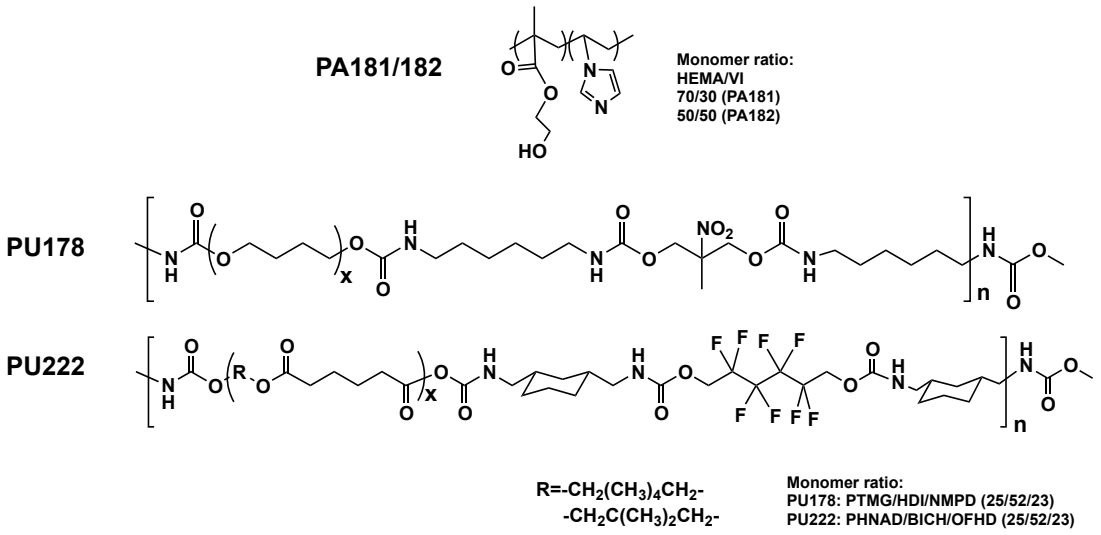

Figure 2.3 Structures of the strong *S.* Typhimurium binding PAs and PUs.

Table 2.2 Polyurethanes showing *S.* Typhimurium binding. Monomer ratios: Diol/Dis/Ext (25/5/25) except 92 and 116 (Diol/Dis: 50/50). Mn = average molecular weight of diol. Dis = Diisocyanate. Ext = chain extender.

	Polymer				*S.* Typhimurium		*E. coli*	
	Diol	Mn	Dis	Ext	Mean	SD	Mean	SD
PU39	PTMG	2000	HDI	BD	0.56	0.042	0.23	0.017
PU92	PTMG	1000	HDI	-	0.65	0.015	0.17	0.014
PU104	PHNGAD	1800	MDI	DEAPD	0.51	0.018	0.28	0.032
PU116	PPG	425	BICH	-	0.47	0.018	0.18	0.009
PU119	PPG	1000	MDI	DMAPD	0.45	0.009	0.23	0.026
PU120	PPG	425	BICH	DEAPD	0.63	0.020	0.27	0.009
PU126	PPG	425	TDI	DMAPD	0.90	0.030	0.28	0.013
PU138	PTMG	250	BICH	EG	0.48	0.018	0.29	0.022
PU159	PTMG	250	MDI	BD	0.45	0.026	0.19	0.007
PU178	PTMG	1000	HDI	NMPD	0.47	0.022	0.13	0.007
PU208	PPG	1000	MDI	OFHD	0.47	0.032	0.18	0.017
PU219	PHNAD	900	BICH	DMAPD	0.51	0.027	0.21	0.018
PU222	PHNAD	900	BICH	OFHD	0.64	0.035	0.41	0.041

Sixteen PAs showed substantial inhibition of *S.* Typhimurium adhesion (Figure 2.2), with thirteen containing the monomer methyl methacrylate (MMA), with eleven of these also containing the derivatisable monomer glycidyl methacrylate (GMA) (Table 2.1 (poor binding polymers), Table 2.3 (different functionalisation) and Figure 2.4 (functional scheme)). PA235 and PA236, which were composed of methyl methacrylate (MMA), methacrylic acid (MA-H) and 2-(diethylamino)ethyl methacrylate (DEAEMA), were highly successful in preventing adhesion of both *S.* Typhimurium and *E. coli* (Figure 2.4). Polymers PA331, PA337 and PA338 selectively bound *E. coli*, but did not bind *S.* Typhimurium, with PA337 and PA338 differing only in the molar ratios of the relevant monomers (MMA and GMA): 70/30 (PA337) and 50/50 (PA338) (Figure 2.4).

The related polymer PA336 (90/10) showed a similar trend, but with slightly less selectivity (Figure 2.4). This suggested the importance of GMA functionalisation with *N*-methylaniline (MAn) in making this group of polymers selective for *E. coli* binding (Table 2.3 and Figure 2.4).

Table 2.3 Polyacrylate series with poor *S.* Typhimurium binding. These polyacrylates had similar polymer backbones (MMA and GMA) but different functionalisation. Monomer ratios of MMA and GMA were: PA306, PA321, PA327 and PA336 (90/10), PA322, PA325, PA331, and PA337 (70/30); PA323, PA326 and PA338 (50/50).

Polymer	Functionalisation Amines	*S.* Typhimurium		*E. coli*	
		Mean	SD	Mean	SD
PA306	di-*n*-butylamine	0.04	0.005	0.12	0.013
PA321	cyclohexane methylamine	0.04	0.002	0.17	0.020
PA322	cyclohexane methylamine	0.04	0.017	0.17	0.019
PA323	cyclohexane methylamine	0.04	0.005	0.16	0.021
PA325	benzyl methylamine	0.03	0.006	0.15	0.018
PA326	benzyl methylamine	0.04	0.006	0.05	0.016
PA327	2-(2-methylaminoethyl)pyridine	0.04	0.004	0.12	0.025
PA331	pyrrole	0.04	0.003	0.56	0.080
PA336	*N*-methylaniline	0.03	0.002	0.22	0.021
PA337	*N*-methylaniline	0.04	0.002	0.49	0.021
PA338	*N*-methylaniline	0.04	0.002	0.51	0.021

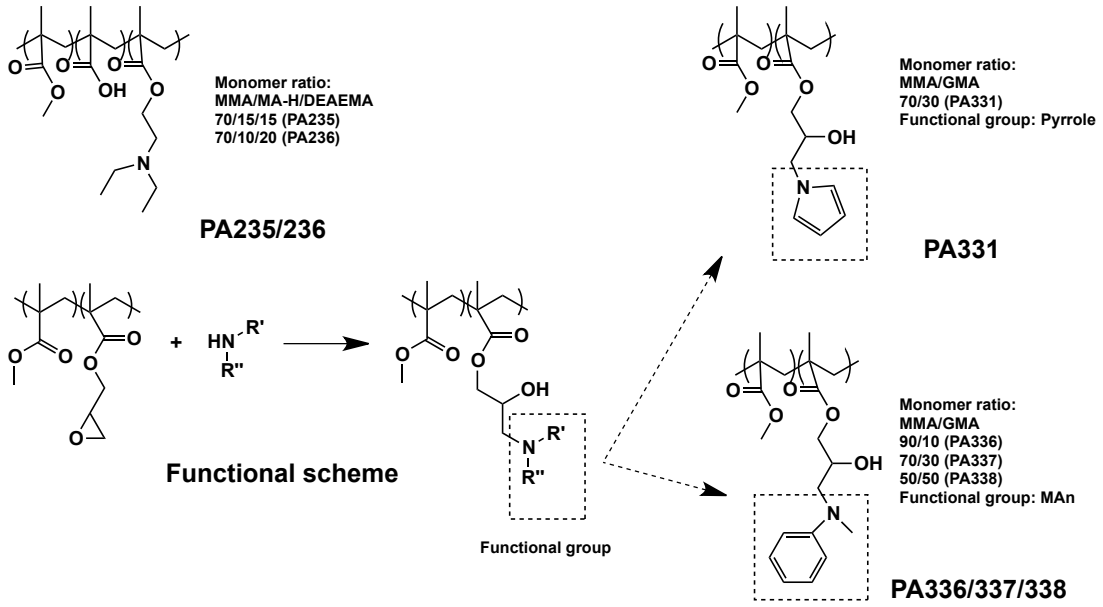

Figure 2.4 Structure of the selected poor binding PAs (top left) and scheme of the poor binding polymer functionalisation (bottom).

2.3.2 Reproducibility

Following the initial analysis of the library (in duplicate and with eight copies of each polymer), several polymers which resulted in the strongest or poorest binding of *S.* Typhimurium were re-printed and re-examined with each polymer printed in a 5 × 5 pattern. Of the four good binding polymers examined (PU104, PA155, PU120 and PU126), each showed consistent cellular attachment, whilst the four poor binding polymers (PA325, PA422, PA426 and PA235) confirmed their "poor bacterial" binding properties (Figure 2.5).

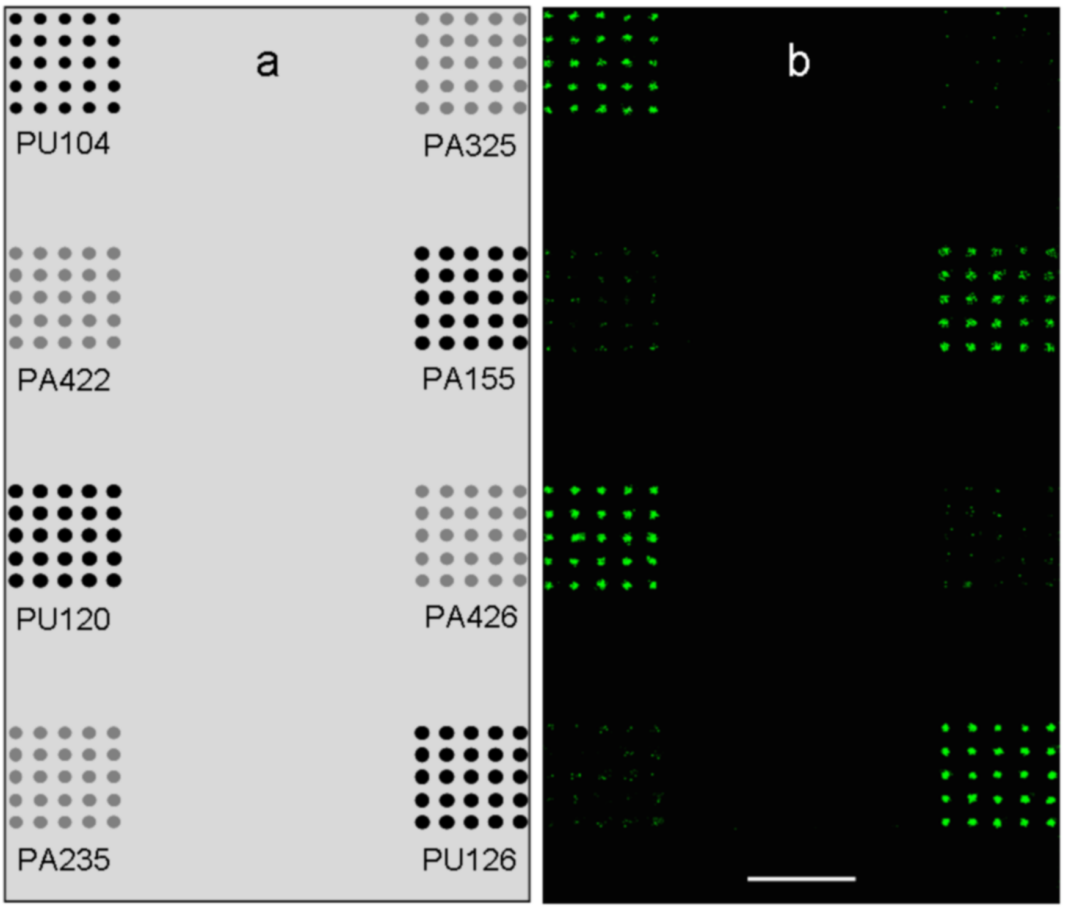

Figure 2.5 (a) Slide template with 8 fields of 25 polymer spots (PU104, PA325, PA422, PA155, PU120, PA426, PA235 and PU126, respectively), and array design with the binding polymers (in black) and the poor binding polymers (in grey). (b) Fluorescence microscopy image of *S.* Typhimurium (fluorescein channel) binding. Scale bar = 3 mm.

2.3.3 Effect of Time on Attachment

It would clearly be advantageous for a polymer to be able to bind bacteria in a rapid time frame. Therefore, to test the rapidity of *S.* Typhimurium binding, an array with the letters 'UK' was fabricated using high and low binding polymers (PU104 and PA325, respectively), and *S.* Typhimurium incubated on the array for four hours, considerably less time than the previous overnight incubation period. As can be seen (Figure 2.6), a uniform binding pattern was observed with PU104, with little binding observed on polymer PA325.

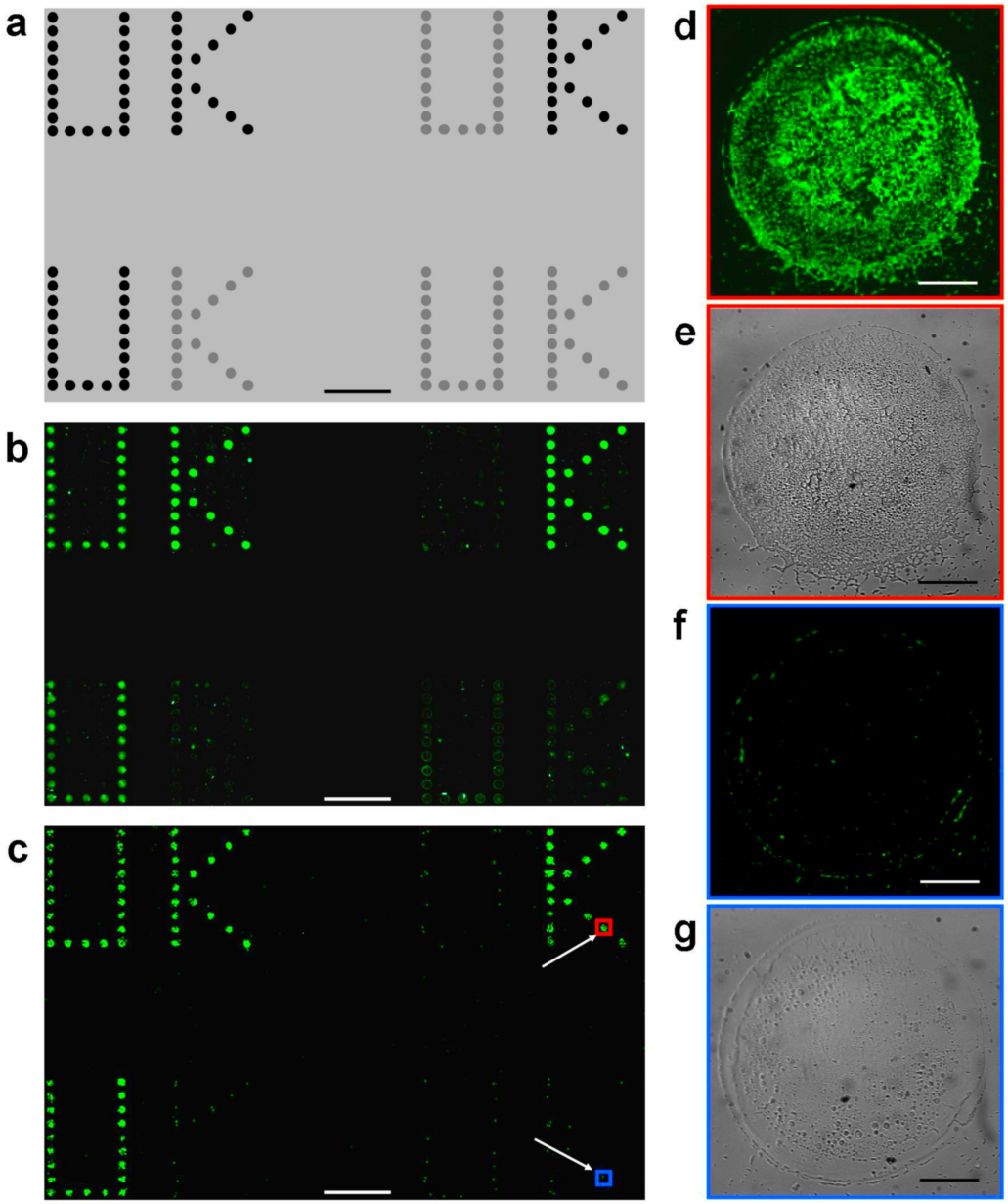

Figure 2.6 *S.* Typhimurium attachment/repulsion: (a) Array design with the binding polymer PU104 (in black) and the poor binding polymer PA325 (in grey); (b) Bio Analyzer scanning of the array using a fluorescein filter; (c) integration of high-content screening fluorescence microscopy (IMSTAR) images (20× objective). Scale bar = 4 mm. Arrows indicate fluorescent and brightfield microscopy images of *S.* Typhimurium grown on representative polymer spots: (d) fluorescein channel and (e) brightfield of PU104; (f) fluorescein channel and (g) brightfield of PA325. Scale bar = 100 µm.

2.4. Scanning Electron Microscopy (SEM) Analysis

SEM uses finely focused electron beams to scan across a sample to produce high-resolution images. Typically, signals that contain information about the sample's surface are captured from interactions of the electron beam with atoms at or near the surface of the sample. Firstly, after incubation with bacteria, polymer microarrays or coated coverslips are fixed. They then need to be sputter-coated with a very thin conductive metallic layer, such as gold or platinum, which is used to induce electrons and produce high topographic contrast and resolution. Next, samples are inserted into a high vacuum chamber for SEM measurement. This allows the study of bacterial morphologies on polymer spots in the microarrays and also on large-scale polymer surfaces.

2.4.1 Polymer Spot Analysis

SEM images of polymer microarrays with *S.* Typhimurium binding on some of the selected strong binding polyurethanes (PU104, PU120, PU126) and polyacrylate 155 as well as poor binding polyacrylates (PA325, PA422, PA426 and PA235), were analysed with particular attention paid to the binding characteristics and bacterial morphology on each polymer spot (Figure 2.7).

Bacteria appeared firmly attached and closely packed on PA155, aligning along their longitudinal axes. Small micro-colonies were observed on the strong-binding polymer surface (Figure 2.7a). In contrast, non-binding polymers (PA325) showed little attachment and no evidence for early biofilm formation, indicating that these polymers show potential as new materials for poor bacterial adhesion surface coatings (Figure 2.7b).

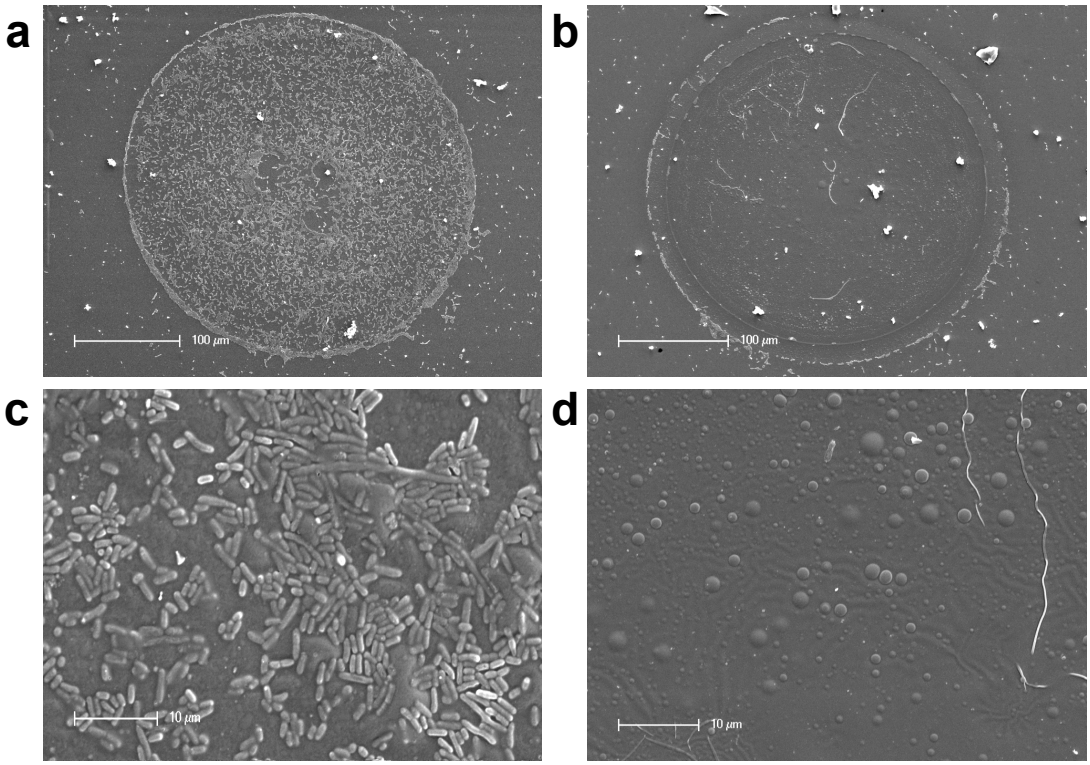

Figure 2.7 SEM images of *S.* Typhimurium binding on selected polymer spots: (a) PA155 (strong binding); (b) PA325 (poor binding). High magnification SEM images of *S.* Typhimurium binding on selected polymers are also shown: (c) PA155 (strong binding); (d) PA325 (poor binding). Scale bar is shown.

2.4.2 Scale-up Analysis

In order to test whether the selected polymers could be scaled up and to assess the feasibility of their applications in a practical context, PA155 and PA325 were spin-coated onto glass coverslips, which contained a central square (1 × 1 mm) subdivided in one hundred squares (100 × 100 µm). These coated coverslips, and uncoated coverslips (as a control), were incubated with *S.* Typhimurium and imaged *via* SEM (Figure 2.8a-c). For each coverslip, SEM image files of four randomly chosen subsquares out of the 100 squares were then transferred into Image-Pro Plus 4.5 software (©2001 Media Cybernetics) for analysis[125]. This software was used to automatically count the number of particles in the image, in this case, the number of bacteria. It identified bacteria within the images by analysing the differences in pixel

intensity between the lighter coloured particles and the dark background. The average number of bacteria on randomly selected subsquares on the coverslips was counted to give the number of bacteria per mm^2 (Figure 2.8d). The analysis of binding on both coated and uncoated coverslips showed that *S.* Typhimurium attached onto polymer PA155 with a 7-fold increase in binding compared to an uncoated coverslip, whereas the number of *S.* Typhimurium on the poor-binding polymer PA325 was twenty times less than the glass control (Figure 2.8d).

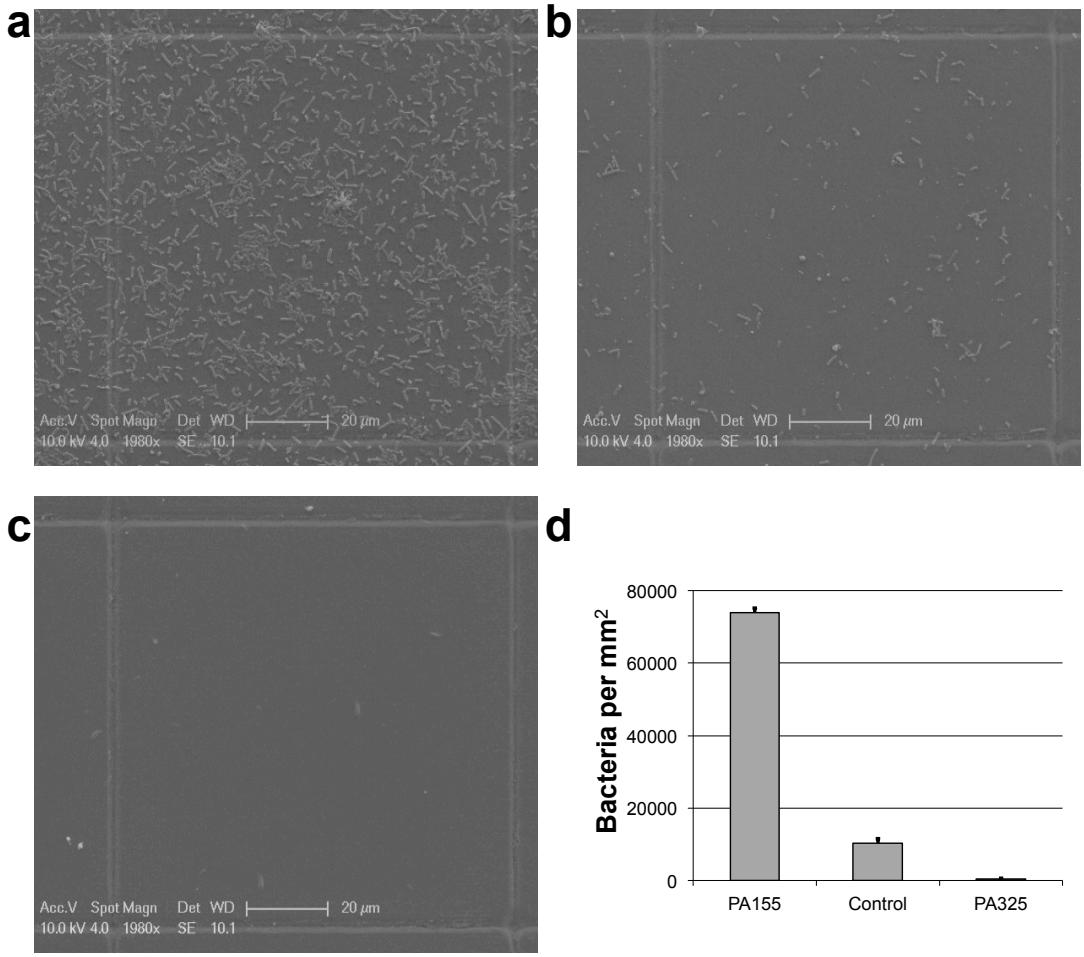

Figure 2.8 SEM images and analysis of the *S.* Typhimurium binding on the selected polymer coated coverslips. (a) PA155 (strong binding); (b) control (no-polymer coating). (c) PA325 (non-binding). Scale bar: 20 µm. (d) The average number of bacteria (*S.* Typhimurium) per square millimeter on PA155 (strong binding) and PA325 (poor-binding) coated coverslips (n = 4).

2.5 Conclusion

In summary, polymer microarrays were successfully used for the identification of polymers which bound either *S.* Typhimurium and/or *E. coli* or prevented their colonisation of surfaces, with fluorescence imaging allowing the rapid, parallel, and comprehensive evaluation of bacterial adhesion on 370 polymers. The binding or poor-binding properties of the surfaces were shown to be highly dependent on both the chemical structures and properties of the polymers, and were sufficient to enable discrimination between adhesive properties of different bacterial genera. For the strongest binding polymers SEM revealed the formation of early biofilm-like micro-colonies, where cells were longitudinally aligned and closely packed. Additionally a number of polymers were also identified which clearly prevented bacterial attachment, even at very high cell densities over a long period.

Chapter 3

Polymer Libraries and the Discovery of Broad-Spectrum Bacterial Repellent Coatings

A polymer library was screened against a broad spectrum of both Gram-negative and Gram-positive bacterial pathogens of clinical origin. This resulted in the discovery of materials that facilitated or prevented bacterial adherence; of particular interest was the discovery of a family of polymers that displayed strong broad-spectrum repellent properties. These readily synthesised polymers represent a novel class of coating materials which could be used to prevent surface colonisation and subsequent formation of bacterial biofilms.

3.1 Introduction

Bacteria are capable of colonising a wide range of surfaces, eventually forming biofilms which can lead to beneficial bacterial interactions, such as occurs with rhizobial species which interact with leguminous plants facilitating nitrogen fixation; or alternatively they may result in unwanted outcomes, such as occurs during colonisation of food preparation surfaces or medical implants, or biofouling of pipes in engineering systems or machines (*e.g.* heating and cooling systems)[126]. Once formed, biofilms can be extremely difficult to eliminate due to their inherent resistance to antimicrobial agents and physical stresses[127]. It has been estimated that approximately 60% of hospital-acquired infections can be attributed to bacterial biofilm formation on medical devices and implants[47].

Traditional chemical methods for preventing bacterial growth utilise antibiotics (such as fluoroquinolones, tetracyclines or *β*-lactams) or disinfectants (such as hypochlorites, quaternary ammonium compounds or low molecular weight organic acids)[126]. Whilst disinfectants act against a broad spectrum of cellular targets, antibiotics exhibit specificity for defined molecular targets, such as DNA gyrase (*e.g.* Ofloxacin), RNA polymerase (*e.g.* Rifamycin) or enzymes involved in peptidoglycan synthesis (*e.g.* Carbenicillin)[128]. Studies on the use of peptides for bacterial prevention have also increased significantly in recent decades.

Numerous factors influence bacterial interactions with their substrates, including the nature of the bacteria (*e.g.* whether they are Gram-positive or Gram-negative), and the physical or chemical composition of the surface undergoing colonisation (*e.g.* roughness, hydrophobicity or charge) and the surrounding environment (*e.g.* time of interaction, pH and nutrients available for growth)[129].

This chapter reports the screening of a library of 381 synthetic polymers (including polyacrylates and polyurethanes) produced by combinatorial chemistry for their ability to reduce or prevent attachment of a wide range of Gram-positive and Gram-negative bacteria of clinical or veterinary importance (Figure 3.1). This study included analysis with a number of major enteric pathogens, including *Campylobacter jejuni* (*C. jejuni*, strain CH4[130] and NCTC 11168[131]), *Clostridium difficile* (*C. difficile*, strain 630[132]), *Clostridium perfringens* (*C. perfringens*, strain NCTC 8257) and *Streptococcus mutans* (*S. mutans*, strain NCTC 10923[133]) as well as cocktails of clinical isolates obtained from endotracheal tubes taken from intensive care unit patients[134] or from patients who exhibited infectious endocarditis[135, 136], such as that associated with cardiovascular implants. Two clinical cocktails were used: clinical cocktail 1 (clinical 1) included *Klebsiella pneumoniae* (*K. pneumoniae*), *Staphylococcus saprophyticus* (*S. saprophyticus*) and *Staphylococcus aureus* (*S. aureus*); clinical cocktail 2 (clinical 2) contained *K. pneumoniae*, *S. mutans*, *S. aureus* and *Enterococcus faecalis* (*E. faecalis*).

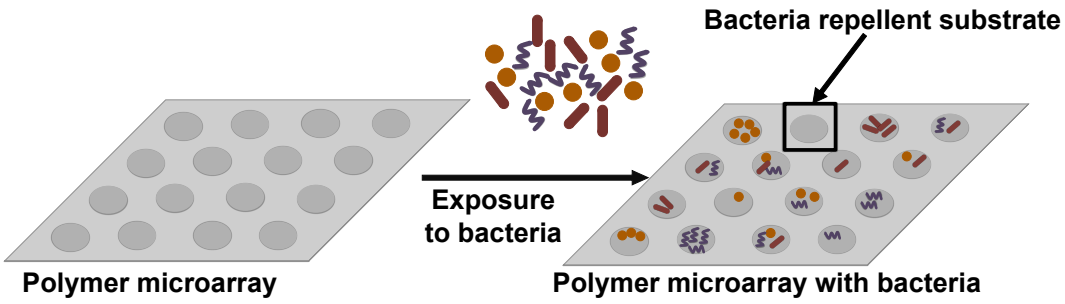

Figure 3.1 Bacterial mixtures incubated on a polymer microarray.

3.2 Background Information on the Bacteria in this Study

To screen the repellent activity of the polymer libraries, various strains of Gram-positive and Gram-negative pathogenic bacteria (listed in Table 3.1) were exposed to the polymer microarrays either as a single culture or mixed cultures (clinical cocktails 1 and 2). A summary of the properties and pathological significance of these bacteria is presented.

Table 3.1 Basic characterisation of the bacteria used in this study.

Bacterial species	Gram stain (+/−)	Cell shape	Oxygen tolerance (+/−)
C. jejuni	−	spiral	−
C. difficile	+	rod	−
C. perfringens	+	rod	−
S. mutans	+	sphere	+
K. pneumoniae	−	rod	+
S. saprophyticus	+	sphere	+
S. aureus	+	sphere	+
E. faecalis	+	sphere	+

C. jejuni

C. jejuni is the most common food-borne enteric pathogen in the developed world[137]. Animals provide the major source of *C. jejuni* causing human infections. *C. jejuni* pathogens have been isolated from many species of birds, such as chickens, pigeons, quails, turkeys, ducks, geese and ostriches[130, 137]. *C. jejuni* can cause human gastroenteritis (normally Campylobacteriosis), with an incubation period typically from one to three days, but sometimes lasting up to a week[130]. *C. jejuni* has a wide range of infectious doses, from 500 to 10^6 cells, depending on the strain and transmission route. The symptoms of *C. jejuni* infection include abdominal pain, diarrhoea, and fever. In the US, 2 to 3 million people are infected by *C. jejuni* each year, with a cost to the economy in excess of 4 billion dollars[138].

C. difficile and *C. perfringens*

Clostridia are endospore forming, and strictly anaerobic bacteria, which can be easily killed in the presence of oxygen. *C. difficile* is one of the most common *Clostridium* species that infect humans, and has surpassed methicillin-resistant *S. aureus* (MRSA) to become the premier cause of hospital-acquired infections in some areas of the US[139]. Human infection occurs by accidental ingestion of spores of *C. difficile*, which is distributed throughout hospitals and nursing homes[140]. Antibiotic therapy is widely recognised as a high risk factor for *C. difficile* infection, because the resulting disruption of the gut micro-flora destroys any normal protection that the flora provide against enteric pathogens[140]. *C. difficile* infection results in flu-like symptoms, sometimes with abdominal pain and severe diarrhoea[141], but the most severe cases can lead to pseudomembranous colitis[142]. *C. perfringens* exists almost everywhere in nature, because it is spore-forming and the spores are persistent and able to survive in a variety of environments, such as high or low temperatures[143]. *C. perfringens* regularly causes food poisoning, which often leads to diarrhoea, abdominal pain and enteritis[141, 144]. Additionally, this bacterium can penetrate broken skin, subsequently proliferating and secreting toxins (*e.g.* alpha-toxin), which can result in severe tissue decay and generate gas (often known as deadly gas gangrene)[145, 146].

S. mutans

Streptococci are lactic acid bacteria. Most species can grow in the presence of oxygen, but they do not use oxygen for respiration. *S. mutans* is the dominant microorganism in the human mouth[147], where it metabolises sugars to produce dextran, which promotes bacterial adhesion onto the tooth surface and results in biofilm formation[148]. Consequently, it rapidly produces lactic acid lowering the pH in the mouth and promoting loss of minerals from the tooth surface[149]. It is not fatal, but tooth decay is one of the most infectious diseases in humans. In some hospitals, salivary *S. mutans* counts are recommended as a means of monitoring patients at risk[150].

K. pneumoniae

K. pneumoniae is ubiquitous in the natural environment and mammal carriers, and the reservoirs for the transmission of *K. pneumoniae* are the gastrointestinal tract and the hands of hospital personnel[151]. It is a very common community-acquired and hospital-acquired pathogen. 8% of all nosocomial bacterial infections in the US and in Europe are caused by *K. pneumoniae*, which typically leads to pneumonia and often causes diarrhoea, urinary tract infections, biliary tract infections, bacteremia, septicemia and purulent meningitis[152]. In Asia, *K. pneumoniae* has been the major cause of pyogenic liver abscesses, and is particularly dangerous among diabetic patients in Taiwan[153].

S. saprophyticus* and *S. aureus

Staphylococci are facultative anaerobes, which are widely present on the skin and in the nasal membranes. Among *Staphylococci*, *S. saprophyticus* is rarely found in healthy humans. It is usually associated with urinary tract infections in humans[154], but it appears more frequently in female urinary tract infections, and is the most common reason for cystitis among young women[155]. Humans often acquire *S. saprophyticus* though sexual intercourse, direct contact with domestic animals, inadequately cooked meat or outdoor swimming pools[154]. *S. aureus* is the most common species of *Staphylococci*. It infects both humans and animals, and is a main cause of hospital-acquired infections, leading to sepsis, osteomyelitis, endocarditis,

wound infection, pneumonia and toxic shock syndrome[156-158]. It also causes food poisoning. *S. aureus* has quickly developed resistance to penicillin and methicillin, and the prevalence of MRSA infection has become an important problem for the treatment of severe *S. aureus* diseases[156].

E. faecalis

E. faecalis is a Gram-positive and anaerobic bacterium that can be found in soil, water, sewage and food. It is tolerant of tough conditions and can grow at extremely low or high pH values, at a broad range of temperatures and in high salt concentrations[159, 160]. It is the major species of the clinically isolated *Enterococci*. *E. faecalis* infection is both community-acquired and hospital-acquired[160]. Insects often transmit *E. faecalis* from animal faeces or other decaying organic substrates to residential settings, causing infection[161]. While in nosocomial environments, *E. faecalis* can be simply transmitted within patients, and can also be transferred by the hospital personnel who touch contaminated items. Once infected, *E. faecalis* mainly causes enterococcal infections, urinary tract infections, bacteraemia and endocarditis in humans[162, 163].

3.3 Results and Discussion

3.3.1 Analysis of Bacterial Repellence *via* High-throughput Screening

Polymer microarrays with 381 polymer members (printed in quadruplicate) were fabricated as previously reported[164] on agarose-coated slides[94]. Bacteria or bacterial cocktails (~2 × 10^8 CFU/ml, 6ml) were incubated overnight directly on the arrays. Loosely bound bacteria were removed by gentle washing and bacterial DNA was then stained by the addition of 4',6-diamidino-2-phenylindole (DAPI). Subsequently the polymer microarrays were analysed on a BioAnalyzer 4F/4S LaVition BioTech scanner using a DAPI filter. This scanner allows the imaging of one whole microarray in minutes and measures the fluorescence intensity of each polymer feature. Bacterial adhesion on the microarrays was evaluated *via* the integrated fluorescence intensity for each polymer spot (background corrected). The mean fluorescence intensity and standard deviation from 8 spots (four polymer spots on each microarray with two microarrays analysed for each bacterial strain/cocktail) were calculated assuming a spot diameter of 300 μm.

To locate the polymers with greatest binding or non-binding for each bacterial strain, the fluorescence intensity of each polymer was normalised using an arbitrary scale (by setting the strongest fluorescence of the polymer on the microarray intensity to 1 and the others scaling accordingly, from 1 to 0). This allowed the optimal binding or non-binding polymers for each single bacterial strain to be determined. This also allowed polymers with the lowest fluorescence intensity (lowest number of bacteria binding) to be rapidly identified as bacteria "repellent" substrates (Table 3.2).

Analysis revealed that there were differences in the inhibitory behaviour of polymers among different bacterial strains/cocktails (Table 3.2). Eleven polyacrylates (PA13, PA465, PA475, PA513, PA515 and a family of related polymers PA309, PA315, PA316, PA336, PA337 and PA338) and eleven polyurethanes (PU1, PU5, PU7, PU10, PU16, PU20, PU61, PU83, PU129, PU179

and PU227) showed strong repellence against all bacterial strains/cocktails (Table 3.2).

Table 3.2 Analysis of bacterial attachment on hit polymers. Normalised fluorescence intensity of each polymer with seven different bacteria. Unit = arbitrary units (au)

Polymer	*C. jejuni* 11168	*C. jejuni* CH4	*C. perfringens*	*C. difficile*	*S. mutans*	Clinical 1	Clinical 2
Agarose	1.9×10^{-4}	1.0×10^{-3}	1.5×10^{-3}	2.5×10^{-4}	2.0×10^{-3}	4.2×10^{-3}	3.1×10^{-3}
PA13	9.0×10^{-3}	1.7×10^{-2}	1.4×10^{-3}	2.6×10^{-3}	1.5×10^{-2}	7.9×10^{-3}	3.5×10^{-2}
PA309	8.9×10^{-3}	5.6×10^{-3}	1.9×10^{-2}	1.2×10^{-3}	1.7×10^{-2}	6.7×10^{-3}	5.0×10^{-3}
PA315	4.1×10^{-2}	1.2×10^{-2}	2.6×10^{-2}	1.6×10^{-4}	2.7×10^{-2}	1.0×10^{-3}	2.1×10^{-2}
PA316	2.4×10^{-2}	7.1×10^{-3}	1.2×10^{-2}	3.2×10^{-3}	2.6×10^{-2}	1.2×10^{-2}	1.3×10^{-2}
PA336	2.3×10^{-2}	3.5×10^{-3}	1.1×10^{-2}	3.0×10^{-3}	5.6×10^{-2}	3.0×10^{-3}	3.2×10^{-2}
PA337	6.1×10^{-3}	2.4×10^{-3}	1.6×10^{-2}	3.0×10^{-4}	2.2×10^{-2}	6.0×10^{-6}	1.7×10^{-2}
PA338	1.1×10^{-2}	1.3×10^{-3}	4.0×10^{-2}	1.1×10^{-4}	3.1×10^{-2}	2.4×10^{-2}	3.3×10^{-2}
PA465	1.5×10^{-2}	1.5×10^{-2}	1.9×10^{-2}	2.9×10^{-4}	2.0×10^{-2}	1.0×10^{-2}	3.5×10^{-2}
PA475	1.6×10^{-2}	2.7×10^{-3}	2.6×10^{-2}	1.3×10^{-3}	1.7×10^{-2}	1.4×10^{-3}	1.0×10^{-2}
PA513	1.6×10^{-2}	4.8×10^{-3}	2.6×10^{-2}	1.9×10^{-3}	1.6×10^{-2}	7.0×10^{-3}	2.6×10^{-2}
PA515	2.8×10^{-2}	5.4×10^{-3}	1.5×10^{-2}	2.1×10^{-3}	1.2×10^{-2}	9.5×10^{-3}	2.6×10^{-2}
PU1	4.4×10^{-2}	4.4×10^{-2}	3.0×10^{-2}	2.8×10^{-4}	6.7×10^{-3}	2.7×10^{-3}	1.1×10^{-2}
PU5	8.3×10^{-3}	8.0×10^{-2}	8.1×10^{-3}	9.6×10^{-4}	1.2×10^{-2}	1.8×10^{-3}	9.8×10^{-3}
PU7	5.2×10^{-2}	1.6×10^{-2}	3.4×10^{-2}	6.3×10^{-4}	9.9×10^{-3}	2.1×10^{-3}	4.5×10^{-3}
PU10	3.4×10^{-2}	7.7×10^{-4}	1.4×10^{-2}	2.8×10^{-3}	2.0×10^{-2}	1.4×10^{-2}	2.0×10^{-3}
PU16	8.4×10^{-3}	3.5×10^{-3}	1.3×10^{-2}	6.3×10^{-3}	1.2×10^{-2}	1.9×10^{-2}	2.7×10^{-3}
PU20	3.7×10^{-2}	1.5×10^{-3}	1.4×10^{-2}	1.3×10^{-3}	2.6×10^{-2}	4.5×10^{-3}	1.3×10^{-2}
PU61	7.2×10^{-4}	1.1×10^{-3}	1.2×10^{-2}	1.4×10^{-5}	3.4×10^{-2}	2.2×10^{-3}	3.8×10^{-2}
PU83	1.2×10^{-3}	1.1×10^{-3}	3.3×10^{-2}	2.9×10^{-3}	2.2×10^{-2}	2.3×10^{-3}	1.3×10^{-2}
PU129	2.9×10^{-2}	2.7×10^{-2}	3.1×10^{-2}	3.8×10^{-4}	1.3×10^{-2}	7.3×10^{-3}	1.8×10^{-2}
PU179	5.5×10^{-3}	7.7×10^{-3}	1.1×10^{-2}	1.2×10^{-3}	2.7×10^{-2}	1.2×10^{-3}	7.6×10^{-3}
PU227	7.1×10^{-2}	5.1×10^{-2}	4.4×10^{-2}	1.9×10^{-4}	2.4×10^{-2}	5.5×10^{-3}	1.2×10^{-2}

3.3.1.1 Polyacrylates

Analysis revealed that the repellent property of those polyacrylates varied with the different bacterial cultures (Figure 3.2). *C. difficile* binding on these hit polymers was weaker in general than all other bacterial cultures. Comparing the binding properties within the two *C. jejuni* strains (CH4 and 11168), PA315, PA316, PA336-338, PA475, PA513 and PA515 exhibited significantly poor binding for *C. jejuni* CH4 and less poor binding for *C. jejuni* 11168, while only PA13 bound slightly more *C. jejuni* CH4 than *C. jejuni* 11168. Subsequently, it appeared that all these hit polyacrylates displayed very similar repellence for *S. mutans* (fluorescence intensities are around 0.02) apart from PA336 showing a fluorescence intensity of 0.056. Most hit polyacrylates showed much stronger repellent activity for clinical cocktail 1 than for clinical cocktail 2, except for PA309 and PA316, which displayed almost equal binding for both clinical cocktails.

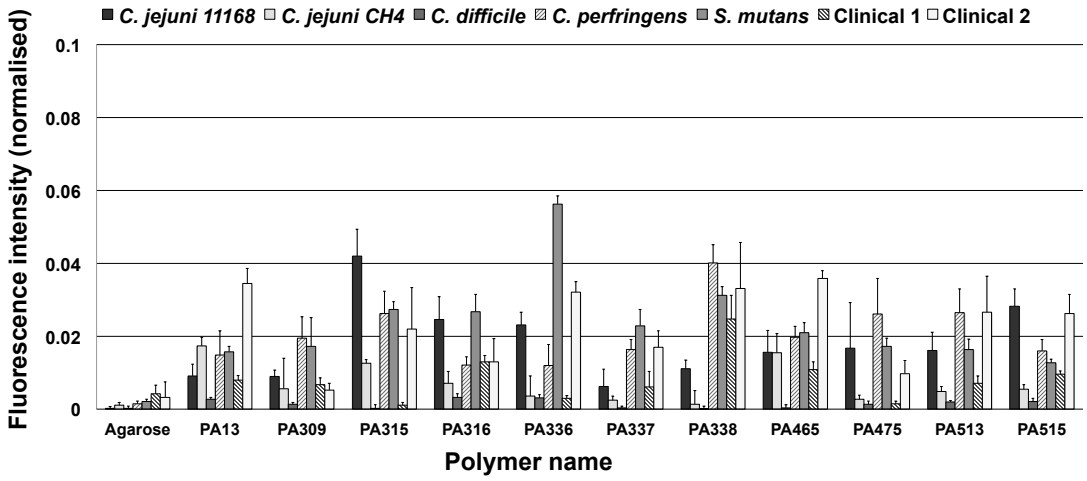

Figure 3.2 Analysis of bacterial repellence: Polyacrylate members showing poor binding of bacteria strains (*C. jejuni*, *C. difficile*, *C. perfringens*, *S. mutans* and two clinical cocktails). Binding is expressed as background corrected mean fluorescence intensity (normalised in au).

The bacterial repellent polyacrylates, PA465, PA475, PA513 and PA515 (Figure 3.3 and Table 3.3) consisted of three monomers with methyl ethylene methacrylate (MEMA) and methyl methacrylate (MMA) being the main monomer components. The minor monomer moiety was either 2-(diethylamino)ethyl methacrylate (DEAEMA) or 2-(diethylamino)ethyl acrylate (DEAEA), making up just 10% of the monomers in the four polymers. In addition, another repellent acrylate, PA13 (Figure 3.3 for structure) contained MMA and *N*,*N*-dimethyl acrylamide (DMAA).

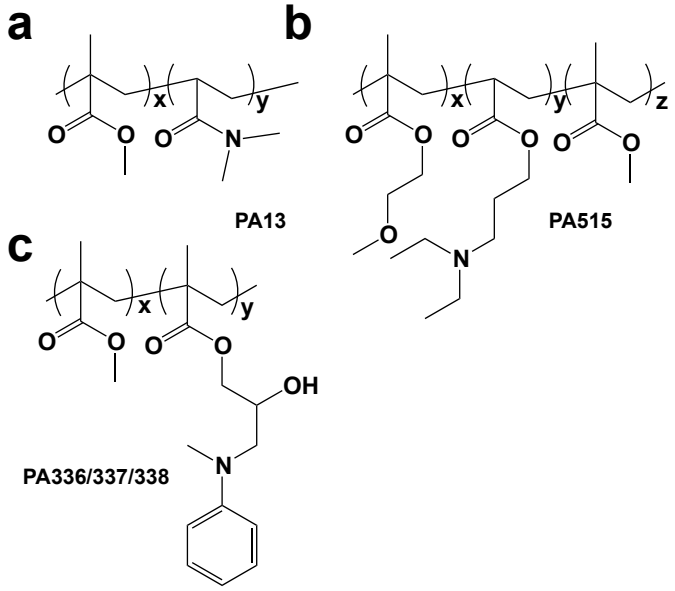

Figure 3.3 Structures of the selected bacterial repellent polyacrylates. (a) PA13; (b) PA515; (c) PA336/337/338.

Table 3.3 Composition of polyacrylates showing bacterial repellence. Monomer ratios were Monomer (1)/Monomer (2)/Monomer (3): PA13 (90/10/0); PA465 and PA513 (80/10/10); PA475 and PA515 (60/10/30).

Polymer	Monomer (1)	Monomer (2)	Monomer (3)
PA13	MMA	DMAA	-
PA465	MEMA	DEAEMA	HEA
PA475	MEMA	DEAEA	HEMA
PA513	MEMA	DEAEMA	MMA
PA515	MEMA	DEAEA	MMA

PA309, PA315-316, and PA336-338 were all based on MMA and glycidyl methacrylate (GMA) in the ratios (90/10, 70/30 and 50/50) (Table 3.4), functionalised with amines. PA309 was functionalised with di-*n*-hexylamine (DnHA), while PA315 and PA316 with dibenzylamine (DBnA), and PA336-338 with *N*-methylaniline (MAn) (Figure 3.3 and Table 3.4).

Table 3.4 Functionalisation of polyacrylates showing bacterial repellence. These polyacrylates had similar polymer backbones (MMA and GMA) but different amine functionalisation. Monomer ratios between MMA and GMA were: PA309, PA315 and PA336 (90/10); PA316 and PA337 (70/30); PA338 (50/50). MMA: methyl methacrylate; GMA: glycidyl methacrylate.

Polymer	Amine fuctionalisation
PA309	di-*n*-hexylamine
PA315	dibenzylamine
PA316	dibenzylamine
PA336	*N*-methylaniline
PA337	*N*-methylaniline
PA338	*N*-methylaniline

3.3.1.2 Polyurethanes

Eleven polyurethanes showed strong inhibition of bacterial attachment (Figure 3.4 and Table 3.5). The best repelling polyurethanes contained some common features: poly(butylene glycol) 2000 (PTMG2000) was present in PU5 (Figure 3.5), PU10, PU20 and PU179. Likewise, another monomer, poly(ethylene glycol) 2000 (PEG2000) was the main component of PU1, PU16 and PU61 (Table 3.1 and Table 3.4). Only four of the eleven polyurethanes had a chain extender: PU61, PU83, PU129 and PU179 (Table 3.5). PU61 and PU83 (Figure 3.5) showed much less binding for *C. jejuni* strains than for all other strains, while PU10 and PU16 showed very strong repellence of the isolates in clinical cocktail 2 over all the bacteria tested.

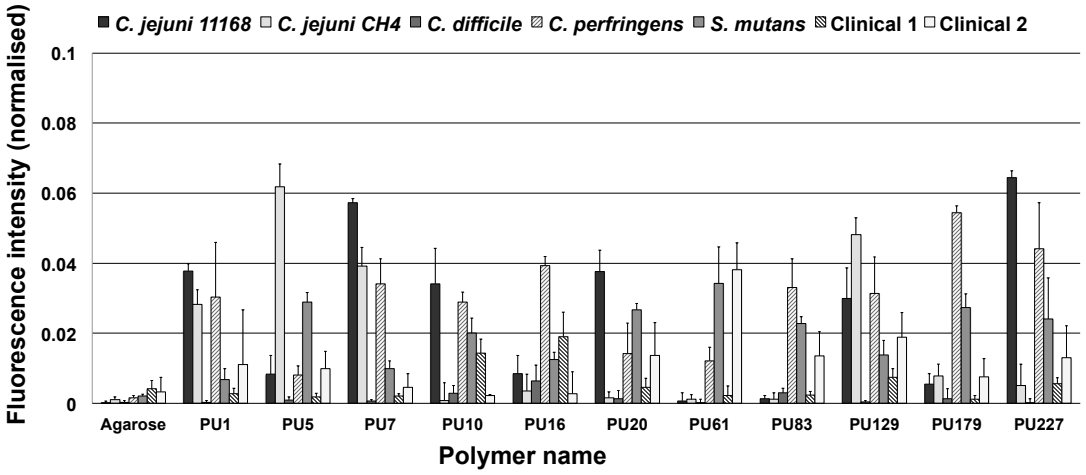

Figure 3.4 Analysis of bacterial repellence: Polyurethane members showing poor binding of bacteria strains (*C. jejuni*, *C. difficile*, *C. perfringens*, *S. mutans* and two clinical cocktails), binding is expressed as background corrected mean fluorescence intensity (normalised in au).

Table 3.5 Composition of polyurethanes showing bacterial repellence. Monomer ratios were: Diol/Dis/Ext (48.5/51.5/0) except PU61, PU83, PU129 and PU179 (Diol/Dis/Ext: 25/52/23). Mn = molecular weight of diol. Dis = Diisocyanate. Ext = chain extender.

Polymer	Diol	Mn	Dis	Ext
PU1	PEG	2000	HDI	-
PU5	PTMG	2000	HDI	-
PU7	PEG	900	BICH	-
PU10	PTMG	2000	BICH	-
PU16	PEG	2000	MDI	-
PU20	PTMG	2000	MDI	-
PU61	PEG	2000	MDI	BD
PU83	PEG	900	HMDI	BD
PU129	PPG	445	BICH	DMAPD
PU179	PTMG	2000	HDI	NMPD
PU227	PPG-PEG	1900	HDI	-

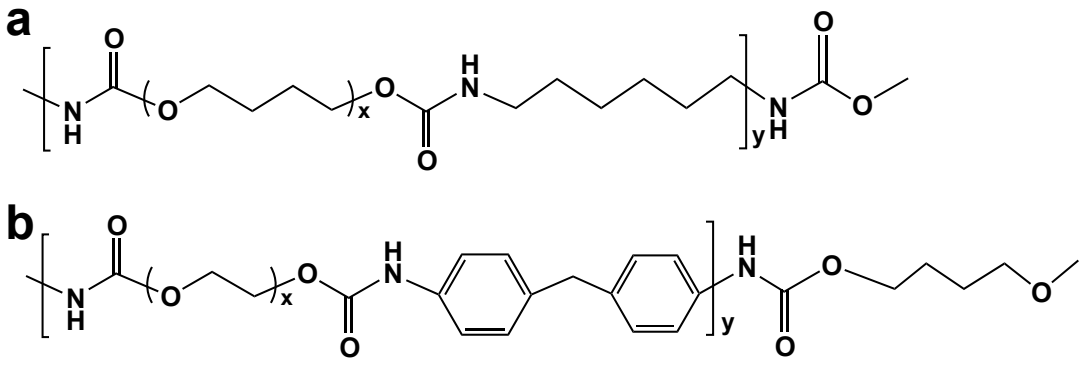

Figure 3.5 Structure of the selected bacterial repellent polyurethanes. (a) PU5; (b) PU83.

3.3.2 Analysis of Bacterial Repellence *via* High-Content Screening

To validate the results obtained from the high-throughput scanner, each polymer microarray was also imaged using an automated fluorescent microscope (with an X-Y-Z stage running Pathfinder^{TM}, IMSTAR), allowing analysis of each single polymer spot on the microarray to be captured by both brightfield and fluorescence (DAPI) channels. As can be seen (Figure 3.6), there was a significant reduction in the

binding of clinical cocktail isolates to the selected repellent polymers (*e.g.* PU 179 and PA336) compared to one of the strong binding polymers.

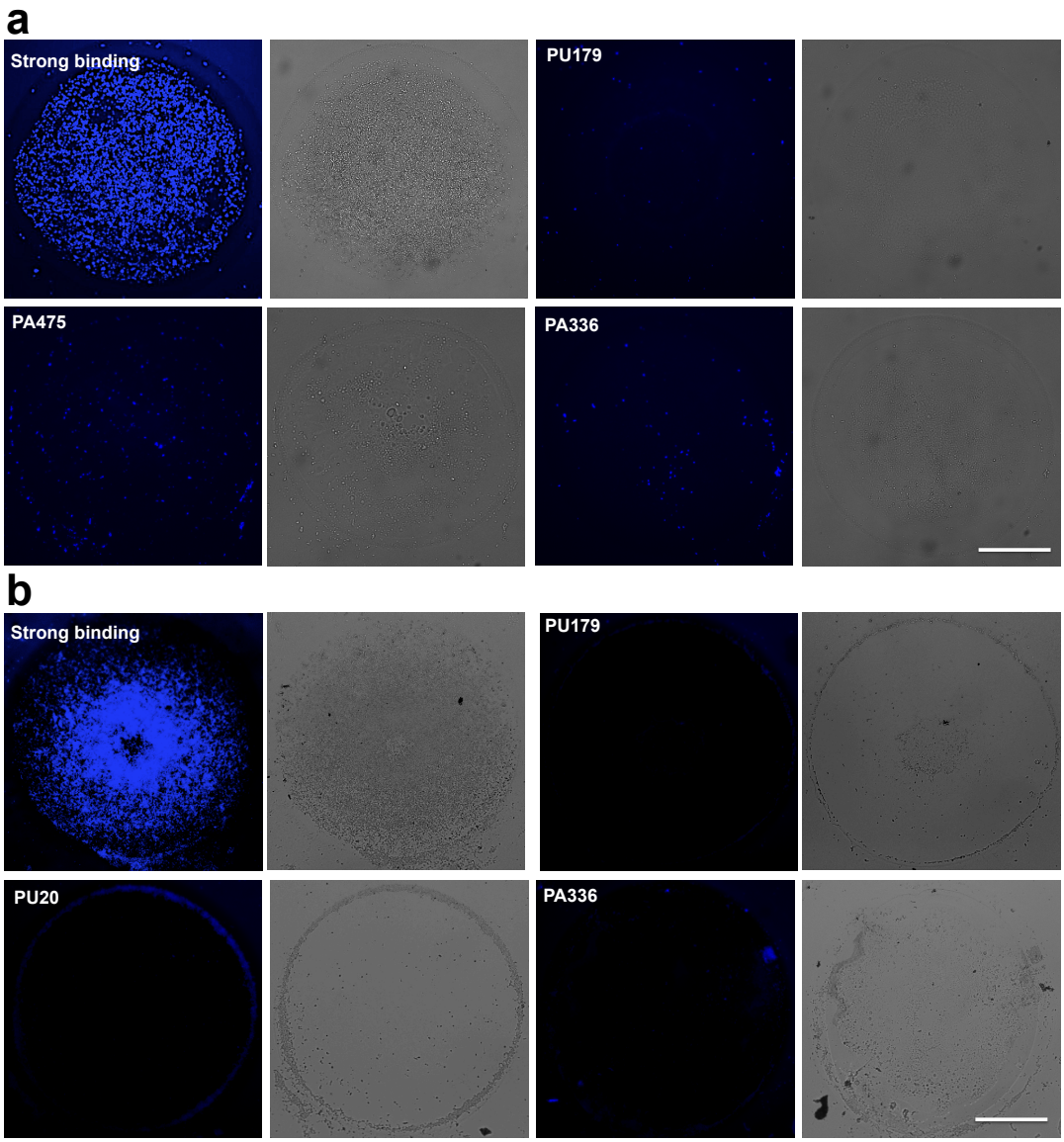

Figure 3.6 Fluorescent and Brightfield microscopy images (Pathfinder^{TM}, IMSTAR) of clinical cocktail isolates attachment on strong binding polymer spots and the clinical cocktail repellent polymers. From left to right: fluorescein channel and brightfield, respectively. (a) Clinical cocktail 1; (b) clinical cocktail 2. Scale bar = 100 µm.

3.3.2 Scale-up

In order to analyse the bacteria repelling activity of the polymers on a larger scale, polyacrylates (PA13, PA338 and PA515) and polyurethanes (PU5, PU20, PU83 and PU179) were resynthesised and spin-coated onto glass coverslips and analysed with clinical cocktails 1 and 2. Scanning Electron Microscopy (SEM) was used to measure the repelling ability of the polymers (Figure 3.7) by determining the number of bacteria attached to each test polymer surface (Figure 3.8).

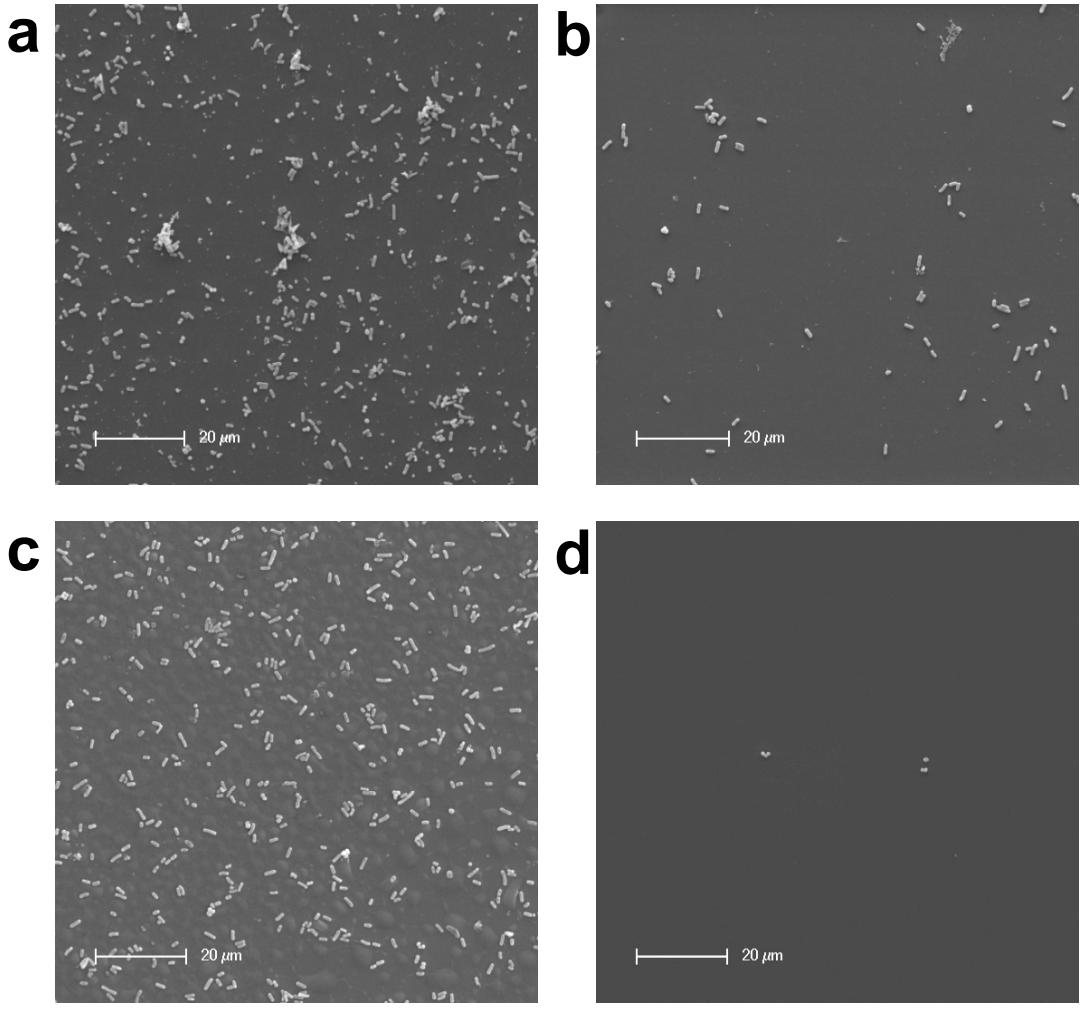

Figure 3.7 Scale-up and analysis *via* SEM of selected polymers and controls (glass and agarose). (a) Clinical 1 on a glass coverslip without coating; (b) clinical 1 on agarose-coated surface; (c) clinical cocktail 1 on PU20 coated surface; (d) clinical cocktail 2 on PU83 coated surface. Scale bar = 20 µm.

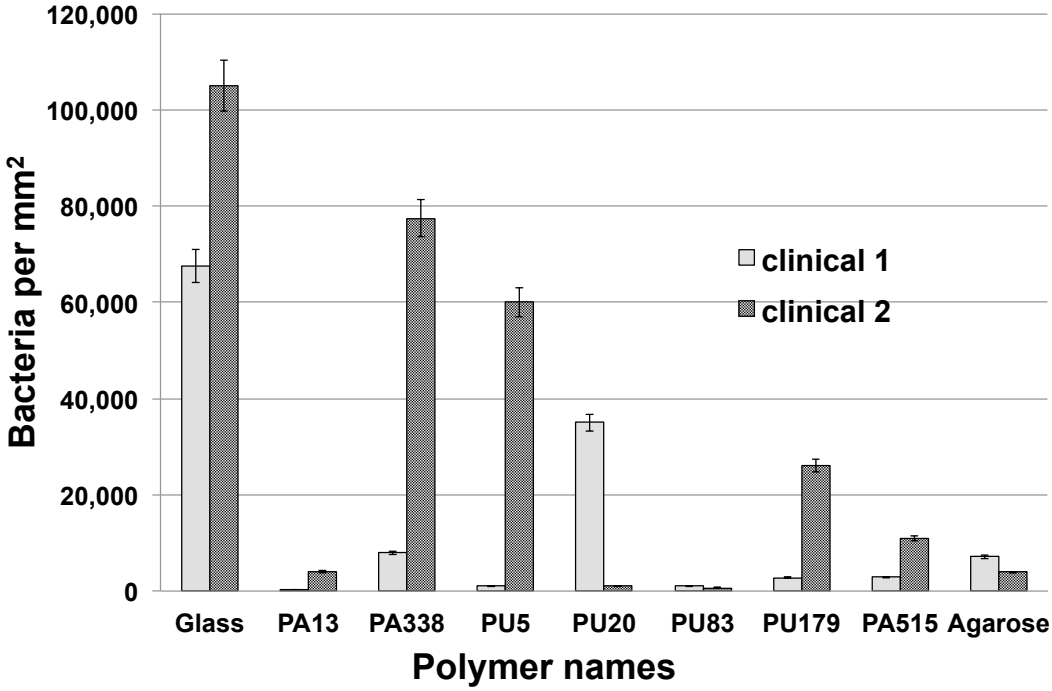

Figure 3.8 The average number of bacteria per square millimeter on polymer/agarose surfaces or glass surfaces (n=4).

Analysis demonstrated that PA13 and PU83 (Figure 3.7d) prevented attachment of both clinical cocktail 1 and 2 (Figure 3.8). PA338, PU5 and PU179 showed almost no binding of bacteria from clinical cocktail 1, but bound relatively high number of bacteria from clinical cocktail 2. However, PU20 coated coverslips bound considerably fewer bacteria from clinical cocktail 2 than clinical cocktail 1 (Figure 3.7c, 3.8). As expected, the numbers of bacteria on all of the strongly repellent polymer surfaces were much lower than on glass.

3.4 Conclusion

In summary, a 381 member polymer library was screened with different bacterial strains, and substrates were identified that allow the broad prevention of binding of both Gram-negative and Gram-positive bacteria. The non-binding properties of the surfaces were dependent on the chemical structures of the polymers and the nature of the bacteria. Comparison of polymer compositions with bacteria binding ability demonstrated that the presence of certain components, PEG and PTMG, and hexamethylene diisocyanate appeared to prevent adhesion. Studies with two clinical cocktails and the polymer surfaces demonstrated very poor binding of the two cocktails. Compared to uncoated glass surfaces, several polymers showed poor binding of only one cocktail, such as PA338 and PU5, repelling more bacteria from clinical cocktail 1 than clinical cocktail 2.

This approach establishes a strategy for the high-throughput screening of polymers with strongly bacteria repelling properties. Broad-spectrum repellent polymers may have hygiene applications, such as use in “clean” areas and in packaging as a means to minimise biofilm formation, consequently reducing the risk of infection. Potentially, because of their broad repellent action, these polymers could be useful coating materials for medical implants, such as cardiovascular stents or endotracheal tubes. Future work would be focused on the exploration of such polymer materials in medical devices and the repellent ability of the polymers for use in a clinical setting.

Chapter 4

Polymeric Materials for Promoting or Limiting *Cryptosporidium parvum* Attachment

Published as: Mei Wu, Helen Bridle and Mark Bradley. Targeting *Cryptosporidium parvum* capture, *Water Research* **2012**, 46, 1715-1722

Patent: Mei Wu, Helen Bridle and Mark Bradley. Water treatment and monitoring (GB 50893728.1).

4.1 Introduction

Contamination of water by *C. parvum* protozoa is a serious global issue. *C. parvum* is ubiquitous in the environment, resistant to standard chlorination disinfection procedures and has a low infectious dose[165-167]. Likewise, *C. parvum* oocysts can stay and survive in water supplies for up to sixteen months. Ingestion of *C. parvum* oocysts causes cryptosporidiosis (a gastrointestinal illness associated with nausea, diarrhoea, headache, vomiting and fever), for which there is no safe and effective treatment[168]. In developing countries, it is estimated that 250-500 million cases occur each year, playing a significant role in high childhood mortality and morbidity. In developed countries, numerous outbreaks associated with contamination of drinking water have been reported, one of the most serious being in 1993 in Milawaukee in the US[169], where more than 400,000 people were estimated to be affected during this massive outbreak of *Cryptosporidium* infection. Of these, 4400 people were

clinically treated in hospital, and 100 people died. There have been several recent cases in the UK[168] with 3000-6000 cases of *Cryptosporidium*, which causes acute gastroenteritis confirmed each year. 476 cryptosporidiosis cases were reported in Western Australia, and 393 cases in South Australia in 2007[170]. The most recent outbreak was in 2010 in Sweden[171] with 4000 cases of cryptosporidiosis reported.

As spore-forming parasites, over twenty *Cryptosporidium* species have been recognised in the laboratory so far, but only a few of them infect humans, including *C. hominis*, *C. parvum*, *C. meleagridis*, *C. felis*, *C. canis*, *C. suis* and C. *muris*[172]. Among these, *C. parvum* is mostly responsible for human infections. The life cycle of *C. parvum* (Figure 4.1) starts from the host's ingestion of oocysts, normally from water contaminated by faeces from the infected hosts (humans or livestock). Once ingested, *C. parvum* excysts in the small intestine and each oocyst releases four sporozoites which parasitise the epithelial cells of the small intestines to cause diseases[173] (Figure 4.1). Sporozoites multiply in the host's cells, and produce six to

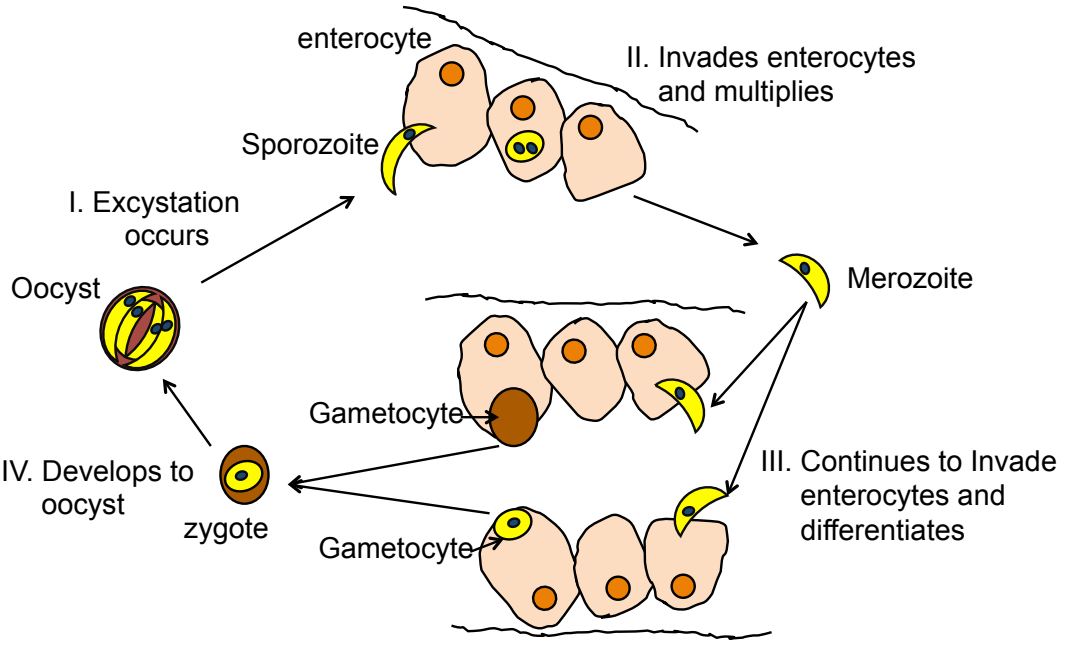

Figure 4.1 Generic life cycle of *C. parvum*.

eight merozoites. Merozoites continue to invade the epithelial cells of the host and asexually multiply. However, some merozoites develop differently and form either male or female gametocytes. Male and female gametocytes then join together to generate zygotes, which later undergo sporogony and finally develop into thin-wall and thick-wall oocysts. Thin-wall oocysts stay in the host and maintain infection by excysting and releasing sporozoites to invade enterocytes within intestines, while thick-wall oocysts pass through the digestive system into the environment, where they can survive and remain infective for over a year. If another host swallows them, a new cycle of *C. parvum* infection occurs.

Understanding the behaviour and fate of *C. parvum* in water treatment systems is essential to assess risk at existing plants and appropriately design future systems[174, 175]. Although it is known that the nature of the coagulation pre-treatment is very important for the efficiency of the subsequent water treatment processes, the exact adhesion and removal mechanisms have not been elucidated[174, 176]. Few field studies of *C. parvum* in water treatment systems have been undertaken, due to limitations in the assay techniques for determining a mass balance for oocysts and a lack of understanding of the mechanisms of interaction with chemicals or surfaces within the process[174]. Instead, laboratory studies have concentrated on the adhesion characteristics of *C. parvum* to a range of materials and measurement of interaction forces.

Numerous factors influence oocyst-surface interactions including oocyst treatment (*e.g.* formalin or heat treatment to inactivate oocysts or proteinase K to digest surface macromolecules), the nature of the surface (charge and hydrophobicity) and solution conditions (*e.g.* the presence of divalent metal ions or ionic strength)[174, 175, 177-180]. However these previous studies have demonstrated some deviation from the predicted theory developed by: Derjaguin and Landau; Verwey and Overbeek (DLVO). The attachment efficiency of *C. parvum* to surfaces (e.g. quartz or silane) has been observed to be generally low, even at high ionic strengths, where DLVO theory predicts no energy barrier to adhesion. These results have been explained by the presence of a fluffy glycoprotein layer[181] extending approximately

115 nm from the oocyst wall[182]. This brush-like arrangement of macromolecules contributes "electrosteric" repulsion preventing oocyst adhesion to surfaces.

While various studies of *C. parvum* adhesion have been undertaken, with materials ranging from metal oxides[180], quartz[177, 181], silanes[182], natural organic matter[178], biofilms[183] and clays to natural suspended sediments[179], little work, apart from a paper by Dai, have investigated polymeric materials[175]. In that paper, Dai and co-workers mixed *C. parvum* oocysts with glass beads and beads coated with aminosiloxane and fluorosiloxane, and recovered the oocysts using a flow cytometer to count the number of oocysts in suspension. They found oocysts preferred to bind on the positively charged, hydrophilic aminosiloxane beads (82% recovery relative to a control) and 100% of oocysts were recovered from both glass and fluorosiloxane beads. This indicated that surface charge was a more important factor than hydrophobic effects on oocyst adhesion.

Understanding the adhesion of *C. parvum* to polymers would be highly useful for numerous reasons: firstly, the membranes employed in filtration methods of water treatment and monitoring are made out of polymeric materials; secondly, polymers could easily be used as coatings in water treatment systems or sensing applications; thirdly, it is easy to systematically vary polymer properties to facilitate studies to elucidate structure-activity relationships.

Polymer microarrays have not previously been applied to investigate protozoa. In this chapter, 652 polymers were screened to determine which materials would enhance or limit *C. parvum* adhesion, investigating the role of *C. parvum* binding on surfaces as well as the influence of polymer hydrophobicity, surface roughness and composition to develop an understanding of how *C. parvum* interacts with surfaces.

4.2 Polymer Microarray Screening

4.2.1 Initial Polymer Microarray Screening

Polymer microarrays with 652 pre-synthesised and well characterised polymers were fabricated onto a glass slide, which was subsequently exposed to *C. parvum* oocysts for 3 hours at room temperature with agitation. Following staining of the slides, automated screening was performed to capture images for each polymer with automatic counting of the number of oocysts per polymer feature. The initial microarray of 652 polymers showed considerable differences in binding affinities between different polymers. From these initial experiments, 34 polymers were selected for further investigation (results shown in Figure 4.2), to increase our understanding of how polymer material properties influence oocyst adherence.

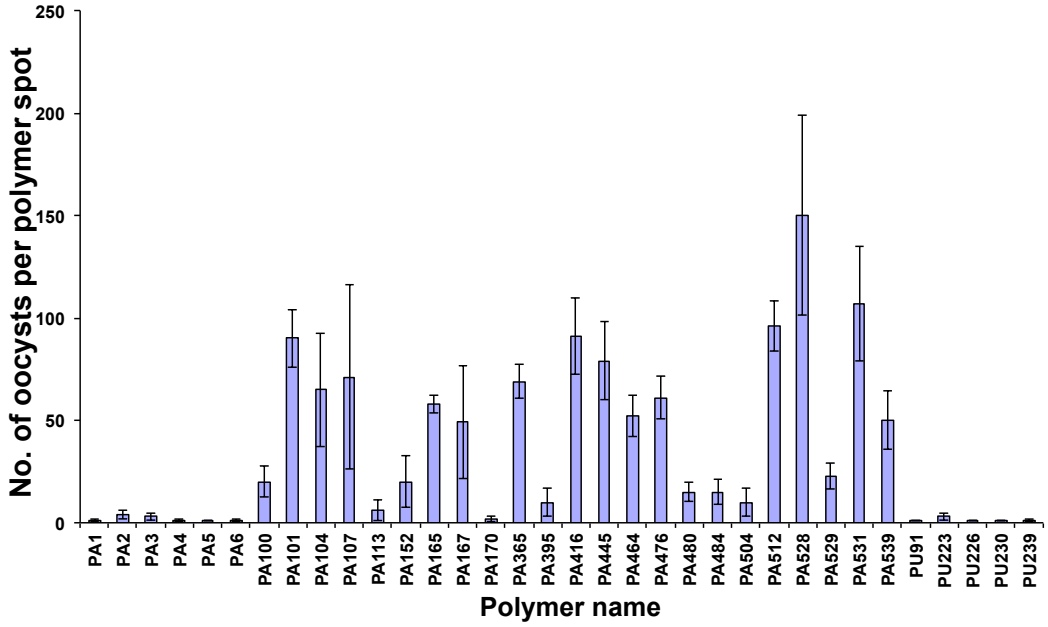

Figure 4.2 Results of the oocysts initial polymer microarray screening (n=3). Graph of oocyst binding on 34 hit polymers which promoted or limited *C. parvum* adherence.

4.2.2 Hit Polymer Microarray Screening

These selected polymers were re-printed in quintuplicate to give so-called "hit" arrays (results of hit arrays are shown in Figure 4.3). This included those polymers that promoted strong interaction (such as PA512, PA528 and PA531) and those which prevented adhesion (such as PAs, 1, 2, 3, 4, 5 and 6, and PUs, 91, 230, 239). The results of the hit arrays show that PA365, PA528 and PA531 most successfully bound *C. parvum* oocysts whereas PA 1-6 acted to prevent binding. PA6 and PA531 were selected for later investigation on larger surfaces in order to confirm suitability for practical applications (Figure 4.4a). The chemical structures of PA6 and PA531 are shown in Figure 4.4b; they were resynthesised and spin-coated onto glass surfaces and exposed to oocysts for large-scale binding experiments.

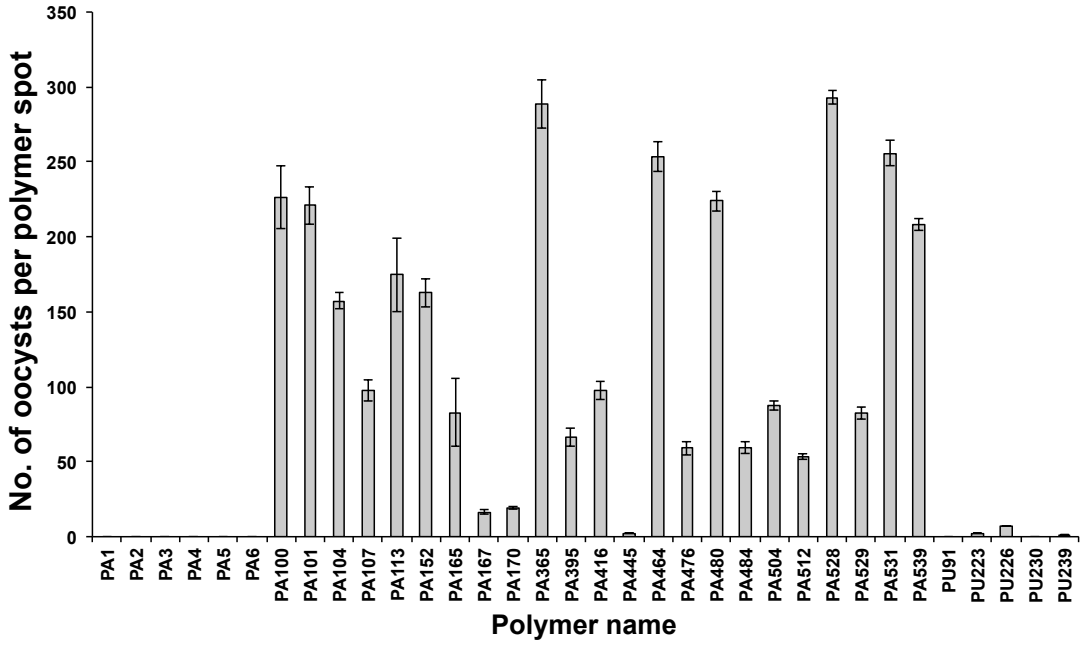

Figure 4.3 Results of the oocysts hit polymer microarray screening (n=5). Graph of oocyst binding on 34 hit polymers which promoted or limited *C. parvum* adherence.

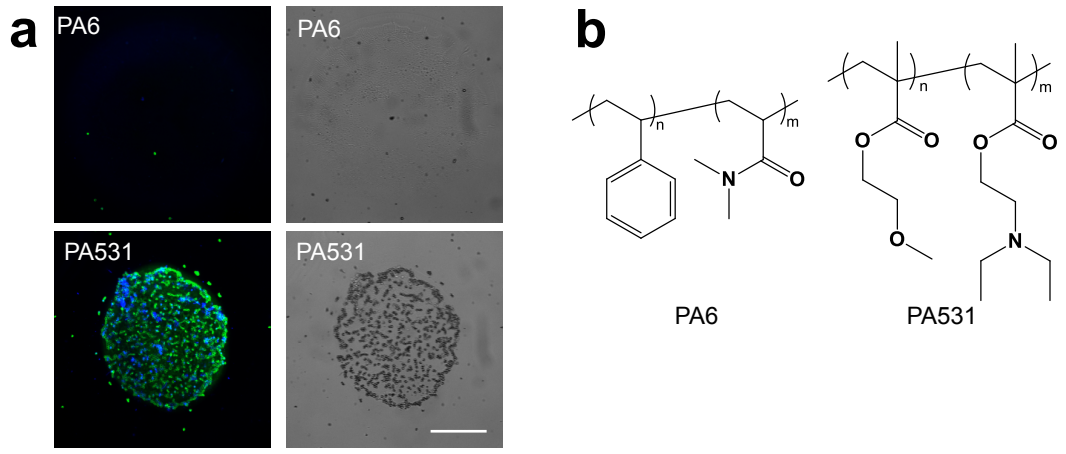

Figure 4.4 (a) Images of the polymer features on the hit arrays with *C. parvum* oocysts stained with Crypto-a-glo (green fluorescence), and DAPI (blue fluorescence). Fluorescent (left) and phase contrast (right) images of a polymer feature of a poor binding polymer (PA6) and a strong binding polymer (PA531). (b) Chemical structures for the two polymers. Scale bar = 100 μm.

4.3 Effects of Material Properties and Oocyst Viability on Adhesion of *C. parvum*

Analysis of the hit polymers was used to investigate the relationships between binding and material properties, including hydrophobicity, surface roughness and polymer composition, which influence cellular, bacterial and protozoan adhesion, as well as the influence of oocyst viability on *C. parvum* adherence[112, 175, 181, 184].

4.3.1 Wettability Analysis

Wettability is one of the most important properties utilised in the area of polymeric analysis, and is used as a measurement of the hydrophobicity/hydrophilicity of materials. The Bradley group developed the first high-throughput methods to evaluate wettability[91, 96]. Importantly, this measurement was dynamic as water contact angles (WCAs) vary with time (See Table 4.1 for the WCAs of the hit polymers in this study).

From the results, the eight best-binding polymers all had a WCA between 60° and 69° (Figure 4.3, 4.5 and Table 4.1), suggesting that this range of WCAs is optimal for oocyst binding. Furthermore, it appears (Figure 4.3, 4.5 and Table 4.1) that extremes of hydrophobicity or hydrophilicity have a negative influence on oocyst attachment. The identified poor binding polymers (PA1-6) all exhibited high WCAs as do the PUs 91, 223 and 226. Poor adhesion was also seen with the other polyurethanes, such as PU230 and PU239, which exhibited the lowest WCAs.

However, there was no direct correlation between oocyst adherence and WCA. This lack of correlation is supported by the observation that many poor-binding polymers had WCAs, in the so-called optimal binding range, between 60° and 72° (Figure 4.5 and Table 4.1). Additionally, PA104, noted for its strong interaction with *C. parvum* oocysts, had a high contact angle, comparable to PA1 and PA6 (Figure 4.5 and Table 4.1). Therefore, our results support the assertion by Dai[175] that hydrophobicity is not an important factor controlling the adhesion of *C. parvum*.

Table 4.1 Hit polymer wettability (water contact angle) and surface roughness (root mean square).

Polymer	Water contact angle (°)	Root mean square (nm)
PA1	74	32.4
PA2	72	23.6
PA3	71	36.7
PA4	85	19.0
PA5	83	16.7
PA6	79	1.7
PA100	67	0.79
PA101	66	3.8
PA104	86	5.0
PA107	40	2.1
PA113	74	0.96
PA152	68	1.1
PA165	59	12.2
PA167	64	1.1
PA170	69	1.5
PA365	64	1.4
PA395	61	8.3
PA416	62	1.8
PA445	66	2.4
PA464	69	6.7
PA476	74	7.2
PA480	64	1.7
PA484	54	2.1
PA504	67	1.6
PA512	64	3.1
PA528	61	3.5
PA529	61	0.91
PA531	61	2.0
PA539	60	5.6
PU91	82	17.0
PU223	83	6.4
PU226	83	0.73
PU230	32	59.0
PU239	28	8.8

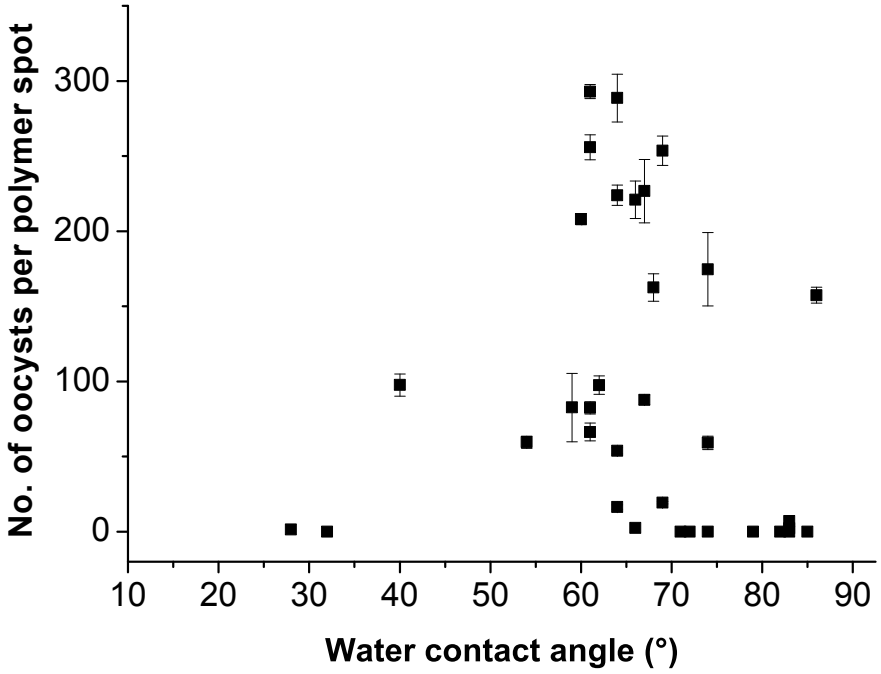

Figure 4.5 *C. parvum* oocyst adherence and polymer wettability (water contact angle) of hit polymers (n=5)

4.3.2 Surface Roughness

Atomic force microscopy (AFM) was employed to investigate the influence of the surface roughness on *C. parvum* adherence (Figure 4.6, 4.7). The root mean square surface (RMS) roughness value of strongly binding polymers such as PA531, PA528 and PA480 were 2.0 nm, 3.5 nm and 1.7 nm respectively, suggesting that low surface roughness may assist *C. parvum* oocyst attachment (Table 4.1). Accordingly, those polymers with the highest roughness value showed the lowest binding of *C. parvum* oocysts; for example, the inhibitory polyacrylates, PA1 (32.4 nm), PA2 (23.6 nm), PA3 (36.7 nm), PA4 (19.0 nm), and PA5 (16.7 nm) as well as PU230 (59.0 nm) and PU91 (17.0 nm). Fitting of linear, logarithmic and polynomial trend lines, to a plot of

oocyst adherence against RMS, all generated low R^2 values (0.17 or less) indicating a lack of correlation between the surface roughness and *C. parvum* adhesion.

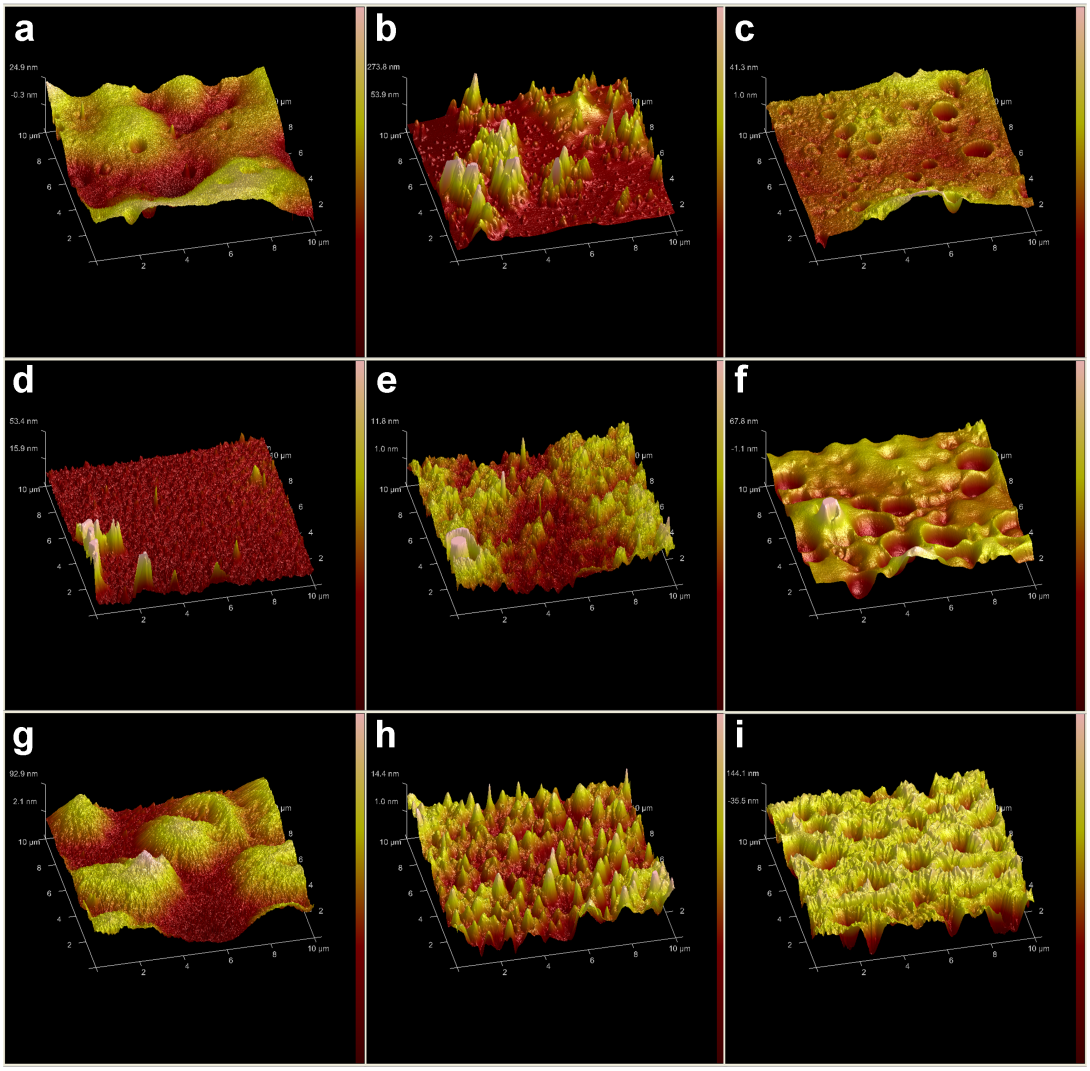

Figure 4.6 Surface roughness analysis of strong/poor oocyst binding polymers on hit arrays using atomic force microscopy (AFM, DimensionV Nanoscope, Veeco). The results were calculated using NanoScope analysis software (Veeco version 1.20). Polymer names listed at the top of each sub-image: (a) PA528, (b) PA4, (c) PA104, (d) PA101, (e) PA531, (f) PA464, (g) PU91, (h) PA512 and (i) PU230.

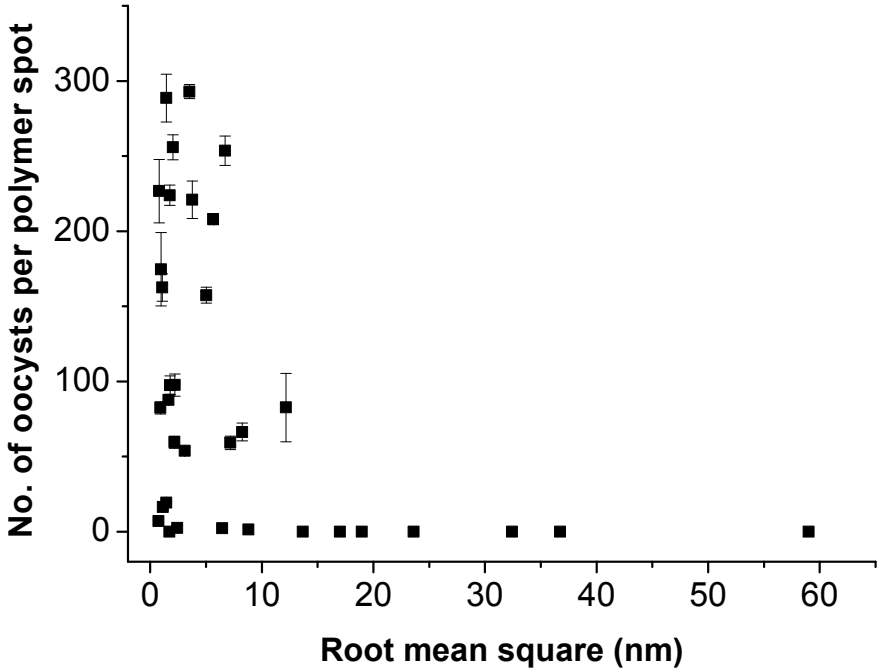

Figure 4.7 *C. parvum* oocyst adherence and polymer surface roughness (root mean square) of hit polymers (n=5)

The root mean square (RMS) surface roughness value ranged from 0.01 to 59.0 nm (Table 4.1 and Figure 4.7). However, Figure 4.7 shows that for polymers with RMS values of greater than 15 nm *C. parvum* interactions are inhibited. Interestingly, the surface roughness of oocysts was between 5-20 nm over micron-sized areas[174, 185] and for bacterial attachment it is known that irregularities that conform to the size of the bacteria increases the adhesion due to maximising bacteria-surface contact area[184, 186] perhaps for *C. parvum* a similar surface roughness for oocysts promotes attachment.

4.3.3 Polymer Composition

Figure 4.8 shows clearly that specific polymer compositions inhibit binding and includes polymers containing styrene and *N,N*-dimethyl acrylate (DMAA) or *N,N*-diethyl acrylate (DEAA), while three out of four of those polymers which had the highest adherence of oocysts contained methoxyethyl methacrylate (MEMA) with 2-(diethylamino)ethyl methacrylate (DEAEMA) or MEMA with 2-(dimethylamino) ethyl methacrylate (DMAEMA).

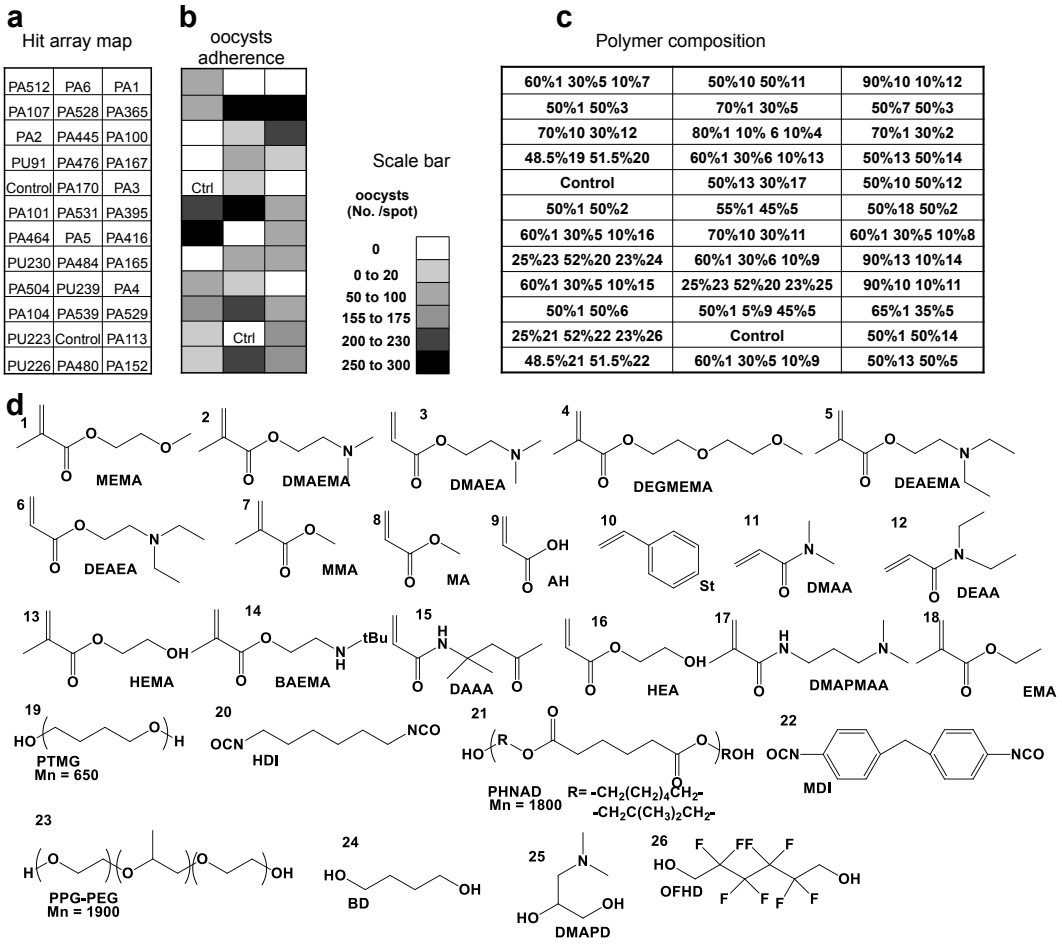

Figure 4.8 Mapping the binding behaviour of *C. parvum* oocysts. (a) Location map of the 34 selected polymers on the arrays; (b) oocyst adherence on the arrays; (c) composition of the polymers, with the monomers shown in (d).

Hydrogen bonding and acid-base interactions may play an important role in controlling surface adhesion of oocysts to polymers. Comparison of the structures of PA531 (strong interaction) and PA6 (inhibition of adhesion) supports this argument. PA531 contains MEMA and DEAEMA which possess several groups capable of participating in hydrogen bonding and ionic interactions, whereas PA6 is composed of styrene and DMAA and as such is less effective for these interactions (Figure 4.8). A key component of PA531 is DEAEMA, which has a reported pK_a of 8.4[187] which means that it will be protonated at all physiologically relevant pH's. This will thus ion-pair with the carboxylate/phosphate rich oocyst wall. The same argument holds for PA101 and PA480. The poor binding of PA1-6 can be rationalised by the non-charged nature of styrene and the acrylamides, DMAA and DEAA. Likewise, the PUs (PU91, PU223, and PU226) have no formal positive charge.

4.3.4 *C. parvum* Viability on Adhesion Characteristics

To investigate the influence of *C. parvum* viability for its adhesion onto polymer materials, non-viable oocysts obtained by heat treatment were exposed to the hit arrays. Some polymers, such as PA101, PA480 and PA531, showed high binding for both viable and non-viable oocysts (Figure 4.9). Additionally, polymers such as PA1, PA2, PA3, PA4, PA5 and PA6 completely prevented viable and non-viable oocyst adhesion (Figures 4.9). However, in general, notable differences in adhesion characteristics were obtained in the results for viable and non-viable oocysts. PA113 and PA531 were the top two polymers for adhesion of non-viable oocysts, while PA365 and PA528 demonstrated the highest affinity binding for viable oocysts, perhaps indicative of different mechanisms, and relative strengths, of interactions. Polymers PA104 and PA504 demonstrated the highest selectivity in favour of binding viable oocysts given that the ratio of viable to non-viable oocysts bound was greater than 20 as opposed to an average of 4.5 for all the polymers in the hit arrays (Figure 4.9b).

A lower number of oocysts per polymer spot for the non-viable oocysts were observed (Figure 4.9), contradicting previous work which suggested that heat treatment of oocysts enables better adhesion *via* alteration/removal of surface glycoproteins[176, 182]. However, the influence of viability on oocysts adhesion has not

been previously studied for polymer materials. Possibly, for polymer materials, the interaction is dominated by forces such as hydrogen bonding and Lewis acid base interactions[188], and non-viable oocysts, with a reduced proportion of surface glycoproteins, are less able to interact with polymer surfaces.

a

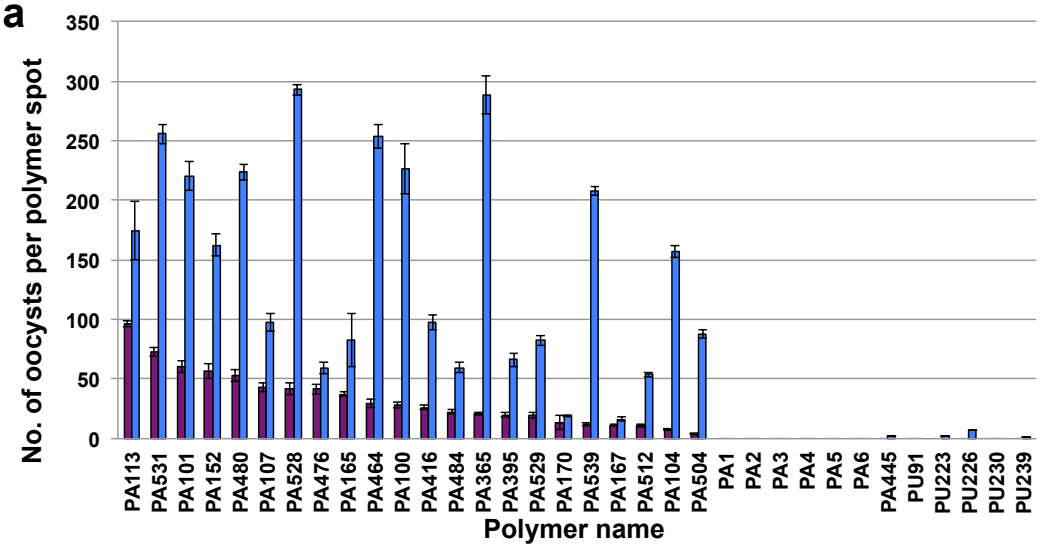

b

Polymer	Ratio viable/ non-viable	Polymer	Ratio viable/ non-viable	Polymer	Ratio viable/ non-viable	Polymer	Ratio viable/ non-viable)
PA113	1.8	PA464	8.5	PA167	1.4	PA5	no binding
PA531	3.5	PA100	8.0	PA512	4.9	PA4	no binding
PA101	3.7	PA416	3.7	PA104	20.7	PU230	no binding
PA152	2.9	PA484	2.6	PA504	22.5	PA3	no binding
PA480	4.2	PA365	13.7	PA2	no binding	PU91	no binding
PA107	2.3	PA395	3.3	PU226	no binding	PA1	no binding
PA528	6.9	PA529	4.3	PA445	no binding	PA6	no binding
PA476	1.4	PA170	1.4	PU223	no binding		
PA165	2.2	PA539	17.6	PU239	no binding		

Figure 4.9 (a) Bar graph indicating the average number of bound viable/non-viable oocysts for each polymer (averaged over the 5 spots). Purple: non-viable oocysts; Blue: viable oocysts. (b) Table compares the ratio of viable/non-viable oocysts on each polymer.

4.4 Large Scale Experiments

4.4.1 Fluorescence Microscopy Analysis

PA531 and PA6 were resynthesised and spin coated to 13 mm glass coverslips, followed by three hour exposure to oocysts and imaged by fluorescence microscopy. Figure 4.10 shows that polymer performance was maintained on the larger scale; with numerous oocysts observed to adhere to PA531 coated surface, in contrast to no oocysts on the surface of PA6.

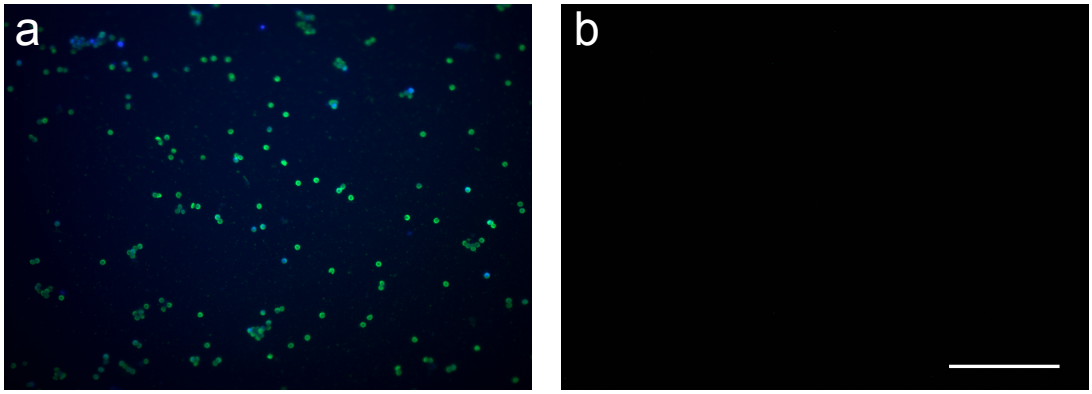

Figure 4.10 Viable oocysts stained with Crypto-a-glo (green fluorescence) and DAPI (blue fluorescence) on the polymer surface of (a) PA531 and (b) PA6 coated coverslips. Scale bar = 100 μm.

4.4.2 Scanning Electron Microscopy Analysis

Scanning electron microscopy (SEM) was utilised to study the binding of both viable and non-viable oocysts on these selected polymers. SEM images of the large scale substrates coated with PA531 and PA6 were consistent with the polymer microarray results and fluorescent images of the coated surfaces (Figure 4.11).

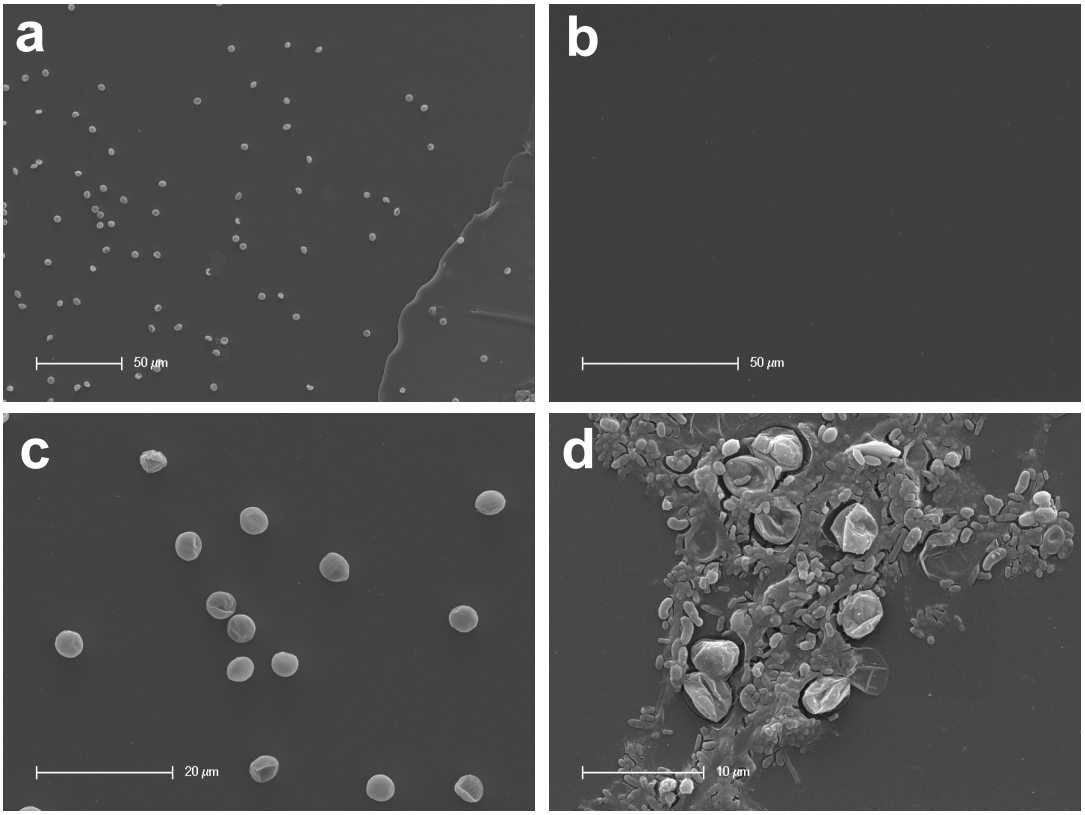

Figure 4.11 SEM images of viable/non-viable oocysts on coated substrates. (a) Viable oocyst attachment on the PA531; (b) viable oocysts did not attach on PA6; (c) morphology of viable oocyst attachment on a PA531; (d) non-viable oocysts adhering to PA531, showing excystation expelling their internal sporozoites. Scale bars are shown for (a) to (d).

The morphologies of viable oocysts on PA531 (Figure 4.11c) exhibited the expected oocyst features, with shape, size and presence of a central suture all in agreement with previous SEM studies of *C. parvum* oocysts[189]. Occasionally differences in morphology were observed, with a higher proportion of non-viable oocysts having undergone excystation and release of their sporozoites (Figure 4.11d).

4.5 Conclusion

From an analysis of over 652 polymers, materials were identified which enhance or prevent the binding of the waterborne, protozoan parasite *C. parvum*. Results from the initial array were confirmed on a hit array, containing the best and worst performing polymers, and on larger polymer coated surfaces. Differences were observed between the adhesion characteristics of viable and non-viable oocysts.

Comparison of the binding data with the physical properties of the polymers indicated that neither wettability nor surface roughness of the polymers were important factors in controlling the adhesion of *C. parvum* oocysts. However, the polymer composition was critical in determining oocyst-polymer interactions. The presence of certain monomers, e.g. DEAEMA or DMAEMA with MEMA, were associated with enhanced binding whereas other monomers, *e.g.* styrene with DEAA or DMAA, in the polymers appeared to prevent adhesion. This was explained by ion-pair interactions between the polymer surfaces and the oocyst wall.

Future work is necessary to investigate the kinetics of adhesion, and the influence of variation in pH and ionic strength of water samples on *C. parvum* oocyst binding. Additionally, further research is also desirable to look at the adhesion behaviour of different *Cryptosporidium* species and also explore potential applications, such as filters and sensor materials.

Chapter 5

Analysis of *Giardia lamblia* Interactions with Polymer Substrates

Published as: Harry Pickering, Mei Wu, Mark Bradley and Helen Bridle. Analysis of *Giardia lamblia* interactions with polymer surfaces using a microarray approach, *Environmental Science & Technology* **2012**, 46(4), 2179-86

Patent: Mei Wu, Helen Bridle and Mark Bradley. Water treatment and monitoring (GB 50893728.1).

5.1 Introduction

The protozoan parasite *Giardia lamblia* (*G. lamblia*), which has a low infectious dose (1-10 cysts), contaminates water supplies across the globe and causes giardiasis[190]. Treatment of giardiasis varies depending on the patient, as does the effectiveness of different drugs, which have common side effects[191]. This pathogen causes a major problem in the water industry as it is resistant to disinfection by chlorine treatment[192] and can also pass with up to 30% efficiency through advanced membrane filters[193]. Prevalence of *G. lamblia* is around 20-30% in the developing world[194], with up to 100% of children acquiring the infection before the age of three[191]. In the developed world, where water treatment is better and more widespread, prevalence is lower but outbreaks do occur. In 1985 there was a particularly serious outbreak in the UK[195] with 108 cases of giardiasis confirmed. In the US, *G. lamblia* is one of the most common intestinal protozoan infections, and in

New York State, the incidence of *G. lamblia* infectious diseases was 19 per 10,000 capita in 2001[196]. In 2004, over 1000 cases were reported in Norway, resulting from leaking sewage and ineffective water treatment[197].

The spread of *G. lamblia* infection is by the faecal-oral route with outbreaks commonly occurring *via* water contamination as cysts can survive in water for over 3 months. After ingestion, *G. lamblia* cysts pass through the stomach, excyst and release two trophozoites in the small intestine (Figure 5.1), which adhere to the epithelial surface and undergo asexual replication by binary fission[198]. Some of theses trophozoites and cysts pass through the digestive system into the faeces for transmission. However, trophozoites can not survive very long time outside the host, only cysts are able to survive and infect other hosts. There is a period of incubation after ingestion of *G. lamblia* ranging from 1 to 45 days[198], and symptoms of infected patients often include diarrhoea, abdominal pain, anaemia, anorexia and weight loss[199].

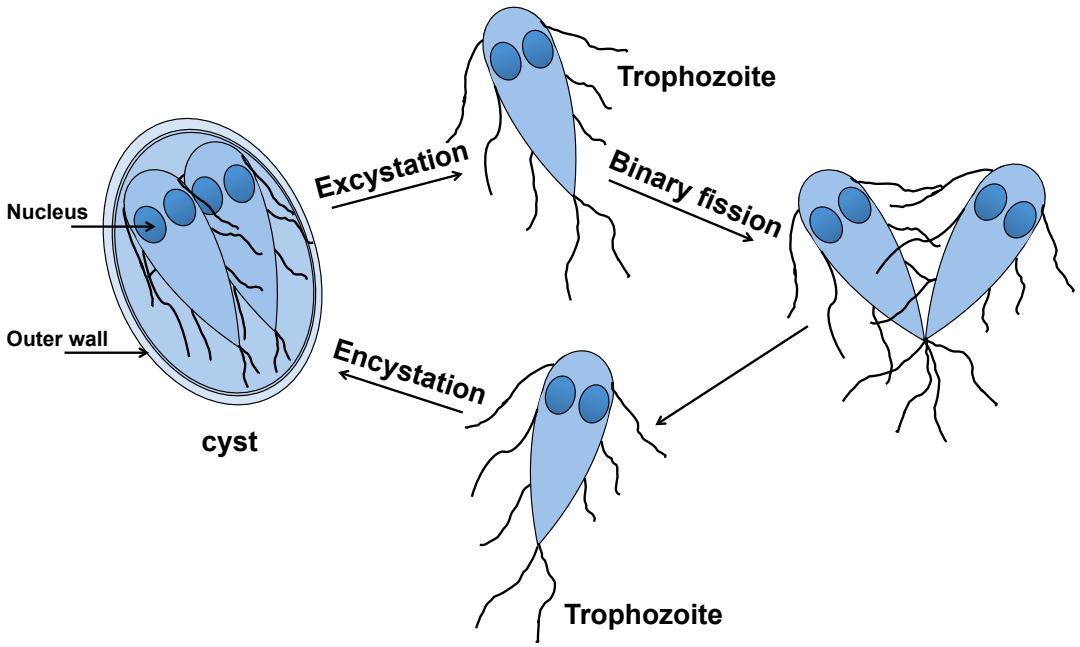

Figure 5.1 Genetic life cycle of *Giardia lamblia*.

The culmination of the lifecycle of *G. lamblia* in its host is the release of thick-walled cysts, which are resistant to a wide range of environmental stresses. The wall consists of a fibrillar extracellular matrix, lined by a double inner membrane and with an outer filamentous wall[200]. This outer wall is around 300 nm thick, and is the most important aspect when considering the adhesive abilities of the cysts. The outer wall is composed of around 43% carbohydrates[201], 86% of which comprises a homopolymer of *β*-(1-3)-*N*-acetyl-D-galactosamine[202]. The galactosamine forms curled fibrils, which bind to cyst wall proteins *via* internal lectin domains. Binding to these proteins compresses the homopolymers into a narrow, mesh-like structure in fully formed cyst walls[203].

Most previous studies of *G. lamblia* surface interactions have focused on the post-ingestion trophozoite stage with the aim of understanding host susceptibility and the process of infection (Figure 5.1). Relatively little work[204] has considered the cyst stage, which is more important in environmental analysis, for example: to understand the transport and fate of cysts in the environment; to predict and explain the performance of water treatment technologies; and to design novel materials for membranes and filters.

Cyst interaction with polymeric materials was investigated in a paper by Dai[175]. This work compared the adhesion of *G. lamblia* cysts on glass beads, fluoro- and amino-polymeric coated beads and polymer cationic resins. Results showed that both fluoro-coated beads (most hydrophobic) and polymer cationic resin (hydrophilic and with the strongest positive charge) bound *G. lamblia* cysts. However, after binding, cysts were recovered from the cationic resin (66% relative to a control), while no cysts were recovered from the fluoro-coated beads. This indicated that although both hydrophobicity and surface charge can influence the adhesion of *G. lamblia* cysts to solid surfaces, hydrophobicity appears to exert a greater influence than surface charge alone.

Since polymers are utilised in the production of membrane filters for water treatment and monitoring, pathogen-specific coatings could help to improve the performance of these methods[193]. Furthermore, the relative simplicity with which polymeric material properties can be modified readily provides a method to gain

insight into structure-activity relationships with respect to parasite/material interactions. Improved knowledge of *G. lamblia* interactions with polymers could thus assist in the design of improved water treatment processes.

In this chapter, the focus was on the identification of materials for *G. lamblia* adhesion and investigation of the mechanisms by which the protozoa attach to a specific polymer. 652 polymers were screened to determine which materials promoted or limited *G. lamblia* adhesion. The polymeric effect on surface interactions such as hydrophobicity, surface roughness and polymer structure/composition were investigated. In addition, *G. lamblia* viability and the influences of pH and proteinase K on *G. lamblia* interactions with surfaces were also studied.

5.2 Polymer Microarray Screening

Polymer microarray preparation and fluorescence microscopy analysis were carried out by Mei Wu in the School of Chemistry, University of Edinburgh. The incubation, fixing and staining of the polymer microarrays with cysts were undertaken by Harry Pickering in the School of Engineering, University of Edinburgh.

5.2.1 Initial Polymer Microarray Screening

652 polymers were examined in initial microarray studies and showed significant variation in parasite binding ability. Viable *G. lamblia* cysts (1 million cysts per experiment) were exposed to the initial microarrays for 3 hours. From these results, 34 polymers were selected to undergo a more detailed investigation to understand how their properties influence cyst adherence. Polymers showing either very strong cyst binding or the prevention of cyst adherence in initial polymer microarrays are shown in Figure 5.2.

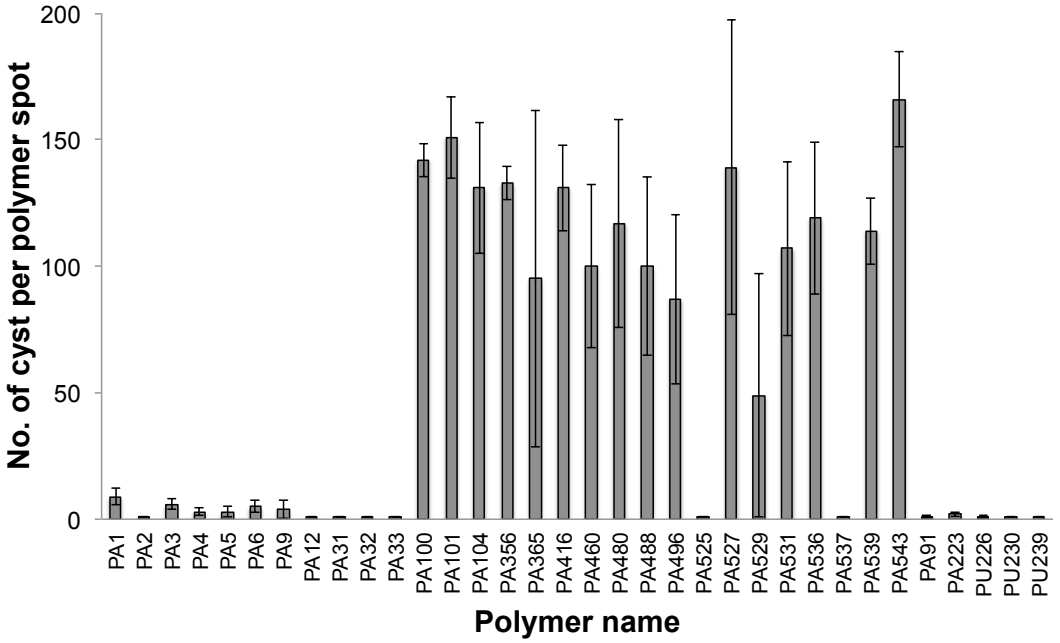

Figure 5.2 Screening of *G. lamblia* cysts on polymer microarrays. Graph of cyst binding on 34 hit polymers which promoted or inhibited *G. lamblia* adhesion (n=3).

5.2.2 Hit Polymer Microarray Screening

Six copies of each selected polymer (34 members) were printed onto a microscope slide to form a so-called "hit-array". The polymers chosen were a mix of those which promoted strong adhesion (PA101 (Figure 5.3), PA104, PA531 and PA480), and those which prevented binding (PAs 1 to 6, PA31 to 33 and some polyurethanes, PU91, PU223 and PU226). These results confirmed PA104, PA531 and PA480 as the best binding polymers, while highlighting PA6 and PA32 as polymers which prevented binding (Figure 5.4). These polymers were selected for a detailed investigation of their physical/chemical/biological properties which influence cyst binding, such as wettability, surface roughness, polymer composition, cyst viability, the presence of enzyme and variance in pH, as well as on larger surfaces to demonstrate their utility for practical applications.

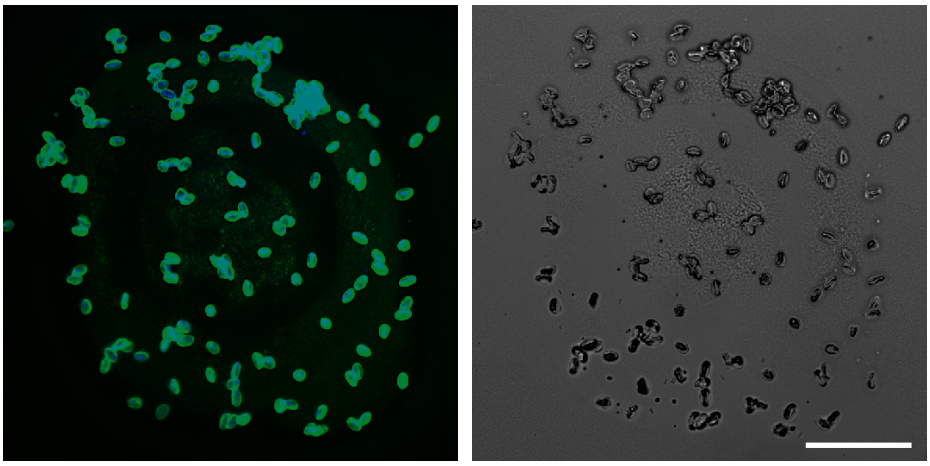

Figure 5.3 Image of the cysts stained with Giardia-a-glo (green), and DAPI (blue) bound to polymer spot (PA101). Fluorescent (left) and phase contrast (right) images of selected polymers are shown. Scale bar = 100 μm.

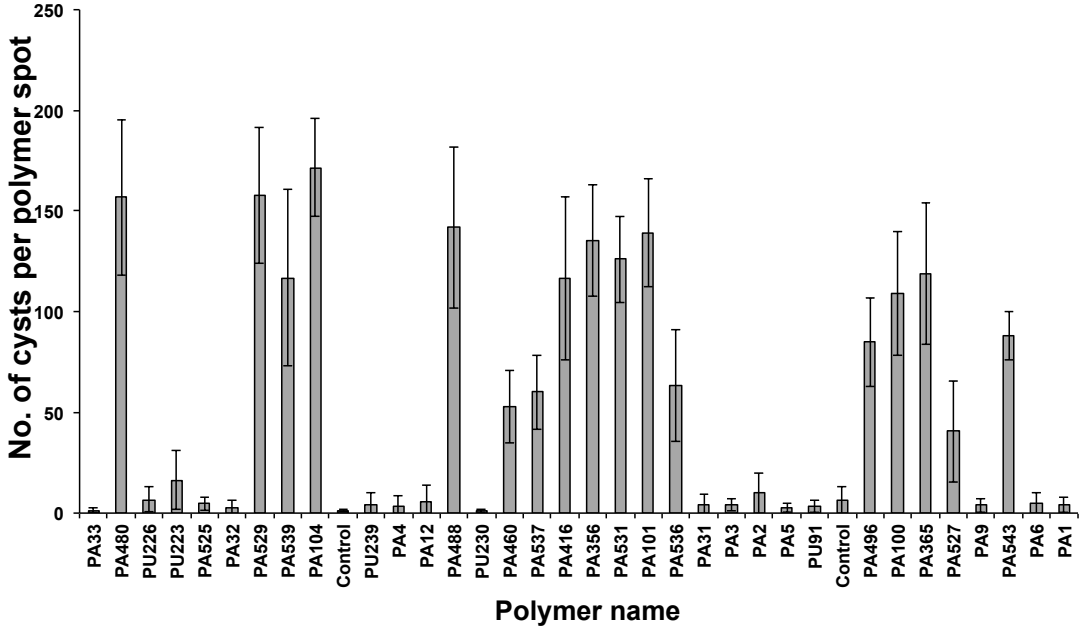

Figure 5.4 Screening of *G. lamblia* cysts on hit polymer microarrays. Graph of cyst binding on 34 hit polymers that promoted or limited *G. lamblia* adhesion (n=6).

5.3 Effects of Polymer Properties on Adhesion of *G. lamblia*

5.3.1 Effect of Polymer Hydrophobicity/Wettability

Wettability is a crucial property for polymers, with dynamic water contact angles (WCA) being the most common values used to quantify wettability or hydrophobicity. One previous work by Dai demonstrated that hydrophobic forces dominate surface charges when considering surface/*G. lamblia* interactions[175]. However, in this work, the binding of the polymers to cysts demonstrated no correlation between wettability and cyst adhesion (Table 5.1 and Figure 5.5).

Table 5.1 Hit polymer wettability (water contact angle).

Polymer	Water contact angle (^{o})	Polymer	Water contact angle (^{o})
PA1	74	PA460	70
PA2	72	PA480	64
PA3	71	PA488	64
PA4	85	PA496	47
PA5	83	PA525	83
PA6	79	PA527	61
PA9	80	PA529	61
PA12	75	PA531	61
PA31	40	PA536	60
PA32	17	PA537	61
PA33	18	PA539	60
PA100	67	PA543	64
PA101	66	PU91	82
PA104	86	PU223	83
PA356	60	PU226	83
PA365	64	PU230	32
PA416	62	PU239	28

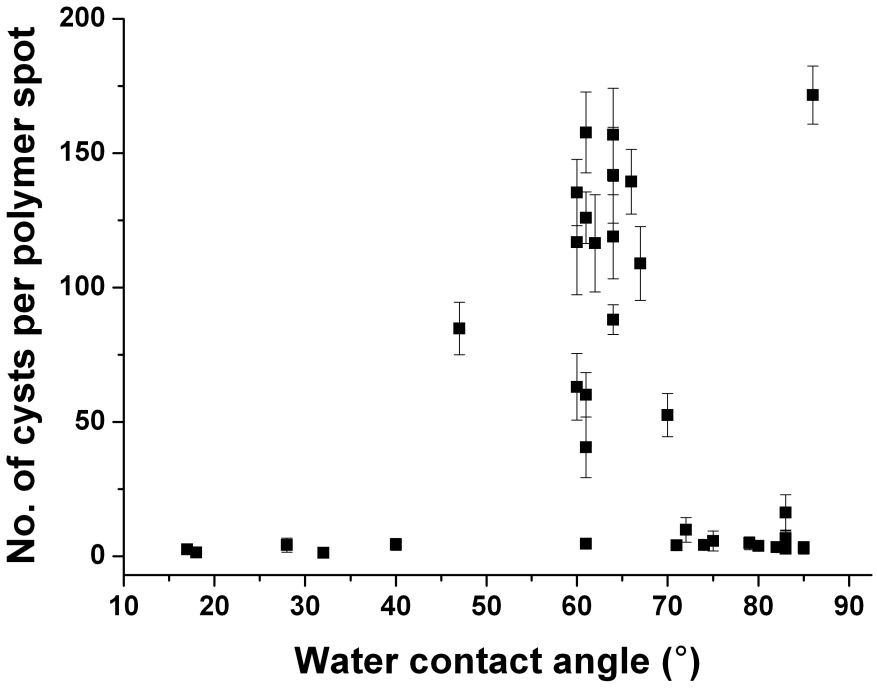

Figure 5.5 *G. lamblia* cyst binding per polymer spot (n=6) in relation to polymer wettability (water contact angle).

Figure 5.5 shows that the majority of the polymers with significant binding had a WCA between 60º and 65º. The WCAs of two of the best binding polymers, PA531 and PA480, were of 61º and 64º respectively. Values of wettability outside this range generally indicated poor adhesion; for example PA32, PA33 and PU230 all prevented cyst adhesion and had low WCAs of 17º, 18º and 32º respectively, while PA6, PA4 and PU91, which also prevented adhesion, had high WCAs of 79º, 85º, and 82º respectively (Table 5.1). This is in direct contrast with the previous work by Dai[175], who observed that *G. lamblia* cysts demonstrated the strongest adhesion to hydrophobic (WCA 95º) fluorosiloxane-coated glass beads and considerable interactions with cationic polymer (commercial polyquaternary ammonium resin) beads (WCA 45º), whereas aminosiloxane coated beads (WCA 70º) prevented adhesion[175]. From these results, it can be concluded that the

wettability/hydrophobicity of a polymeric material is not a property which could be employed to predict the degree of *G. lamblia* cyst interaction. Other factors must play an important role, and it highlights the advantages of microarray approaches in which multiple polymer properties can be screened to allow the optimal properties to be rapidly selected.

5.3.2 Effect of Polymer Surface Roughness

Atomic force microscopy (AFM) was employed to investigate the influence of surface roughness on *G. lamblia* adherence. For each polymer surface, analysis was taken over a 100 μm^2 area and the root mean square (RMS) surface roughness was determined from an average of three random positions. The RMS ranged from 0.01 to 59.0 nm, and did not show any correlation with WCA (Table 5.1, 5.2 and Figure 5.6).

Table 5.2 Hit polymer surface roughness (root mean square).

Polymer	Root mean square (nm)	Polymer	Root mean square (nm)
PA1	32.4	PA460	7.4
PA2	23.6	PA480	1.7
PA3	36.7	PA488	3.9
PA4	19.0	PA496	1.6
PA5	13.6	PA525	0.6
PA6	1.7	PA527	4.2
PA9	3.8	PA529	0.9
PA12	12.9	PA531	2.0
PA31	4.8	PA536	9.1
PA32	1.0	PA537	2.3
PA33	0.2	PA539	5.6
PA100	0.8	PA543	7.3
PA101	3.8	PU91	17.0
PA104	5.0	PU223	6.4
PA356	5.6	PU226	0.7
PA365	1.4	PU230	59.0
PA416	1.8	PU239	8.8

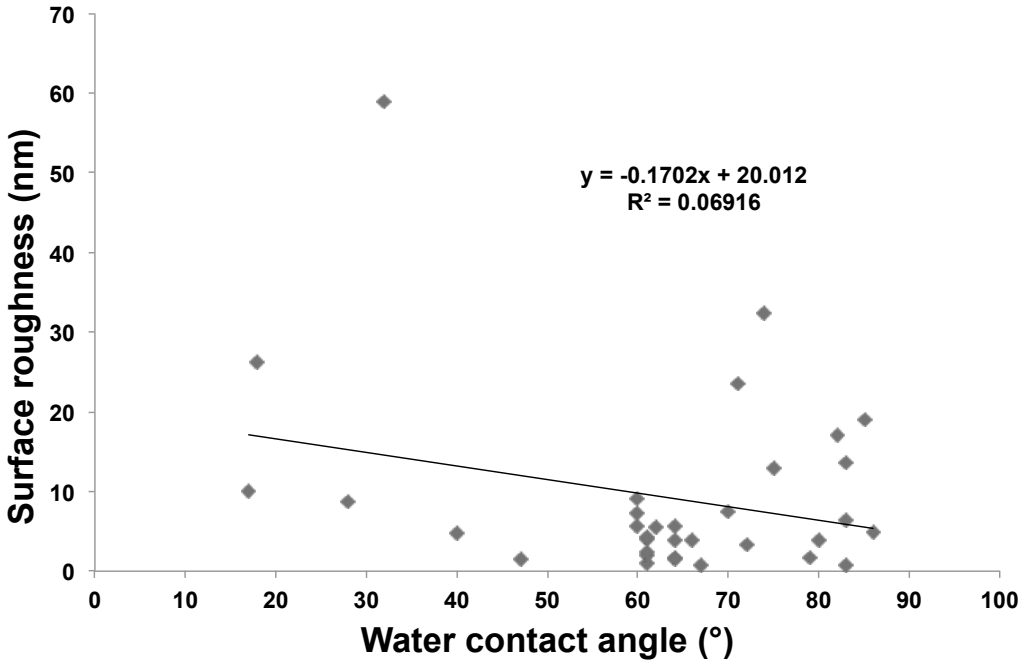

Figure 5.6 Water contact angle against surface roughness, showing minimal correlation.

Similar to the wettability analysis, surface roughness demonstrated no correlation with cyst adhesion (Figure 5.7). PA6, PA32 and PU230 which prevented adhesion, had RMS values of 1.7 nm, 1.0 nm and 59.0 nm, respectively, while PA104, PA480 and PA531, the strongest binding polymers, had RMS values of 5.0 nm, 1.7 nm and 2.0 nm, respectively (Table 5.2). It is clear from Figure 5.7 that high values of RMS, specifically those greater than 10 nm, appear to prevent adhesion, including polymers such as PA1, PA3-5 and polyurethanes, PU91 and PU230. This suggests that while surface roughness is not well correlated with cyst adhesion, high RMS values are likely to limit binding ability.

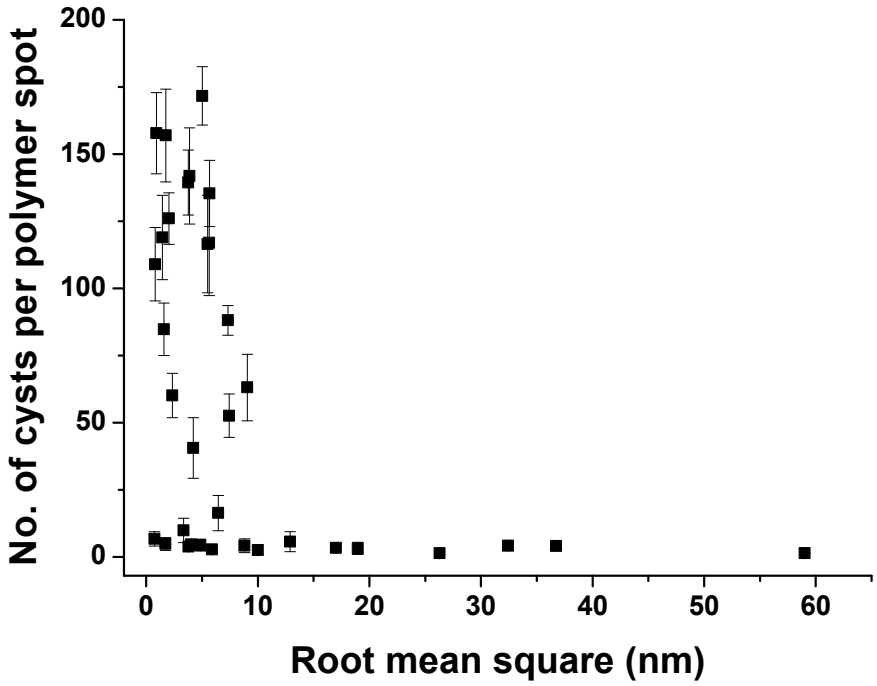

Figure 5.7 *G. lamblia* cyst binding per polymer spot (n=6) and polymer surface roughness (root mean square).

For bacterial attachment it is known that the presence of irregularities that conform to the size of the bacteria increases adhesion due to maximising bacteria-surface contact area[184, 186]. If this hypothesis were correct for *G. lamblia*, it would imply that the surface roughness of cysts is likely to be on the order of 1-10 nm (the RMS value above which no adhesion was observed for *G. lamblia*). AFM measurement of *G. lamblia* cysts was carried out by binding *G. lamblia* cysts on a PA104 coated surface, and gave a surface roughness of 53.0 nm (Figure 5.8), higher than all of the hit polymers except PU230 (Table 5.2).

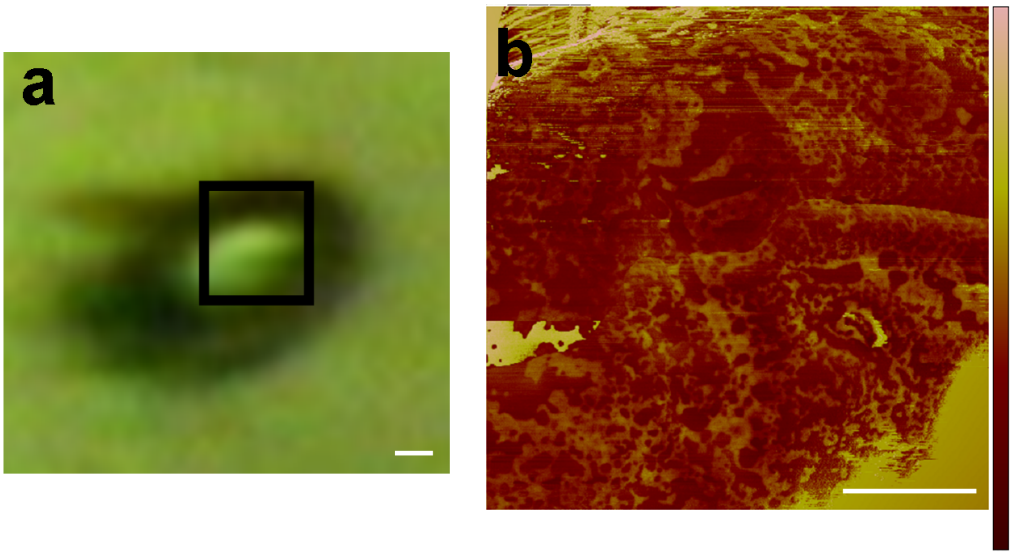

Figure 5.8 AFM analysis of the surface roughness of *G. lamblia*. (a) Image of the measured *G. lamblia* cyst. (b) Associated phase image for surface roughness determination. Scale bar = 2 μm.

5.3.3 Effect of Polymer Composition

To investigate the relationship between chemical composition of the polymers and cyst adhesion, the monomeric composition was mapped against binding (Figure 5.9).

Figure 5.9 indicates that inhibition of cyst binding was greatest in polyacrylates containing *N,N*-dimethyl acrylamide (DMAA), *N,N*-diethyl acrylate (DEAA) or styrene, as well as polyurethanes containing Poly(1,6-hexanediol/neopentyl glycol-*alt*-adipic acid)diol (PHNAD), such as PU223 and PU226. Monomers promoting strong binding included 2-(dimethylamino)ethyl methacrylate (DMAEMA), 2-(diethylamino)ethyl methacrylate (DEAEMA), 2-(dimethylamino)ethyl acrylate (DMAEA), or 2-(diethylamino)ethyl acrylate (DEAEA); these were found in the best performing polymers, PA104, PA480 and PA531.

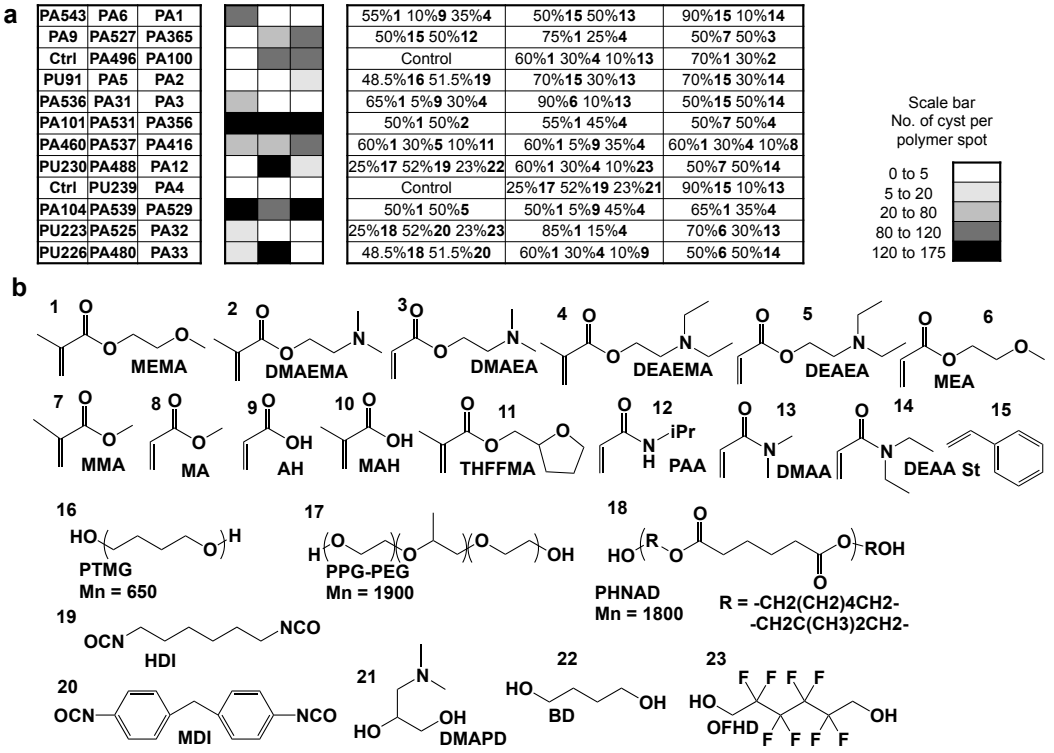

Figure 5.9 Analysis of hit array results and polymer structures. (a) Left to right: polymer identity; the binding of cysts; and the polymer composition. Bars relating colour intensity to cyst binding. (b) Structures of the monomers.

For cellular adhesion it has been reported that glycol functionalities act in a preventative manner[112]. Binding to surfaces is often attributed to the protein-repellent nature of functional group moieties. For the majority of cell types adhesion is considered to occur *via* initial protein adsorption, which subsequently mediates cellular adhesion. Accordingly, the repellent nature of glycol functionalities is consistent with the results in this chapter, since none of the polyurethanes containing monomers with glycols, such as PU230 and PU239, showed strong interactions with the cysts. In this case, poor interactions between the proteins and the glycol moieties could inhibit binding of the cyst surface proteins, thus limiting interactions between these polymers and the cyst outer wall.

In terms of amine functionalities, on the hit arrays, the monomers DMAEA, DEAEA, DMAEMA and DEAEMA, present in polymers also containing MEMA and MMA, all contain secondary amine groups and were associated with high levels of cyst adhesion. For cyst adhesion, the hypothesis is that at physiological pH values, the amines will be protonated and thus can ion-pair with the cyst wall. DMAA and DEAA contain amide groups and are present in polymers which prevent adhesion. Since amide groups will not be protonated at physiologically relevant pH values; this explains the lack of interaction with *G. lamblia*.

Thus, it could be hypothesised that glycol, aromatic and amide functional groups act to prevent adhesion whereas amine groups promote adhesion.

5.4 Non-polymeric Effects on Adhesion of *G. lamblia*

5.4.1 Effect of *G. lamblia* Viability

Non-viable cysts were also investigated for their ability to bind to the polymers. Non-viable *G. lamblia* cysts were obtained *via* heat treatment[205] and confirmed by staining with a membrane impermeable dye, propidium iodide (Figure 5.10).

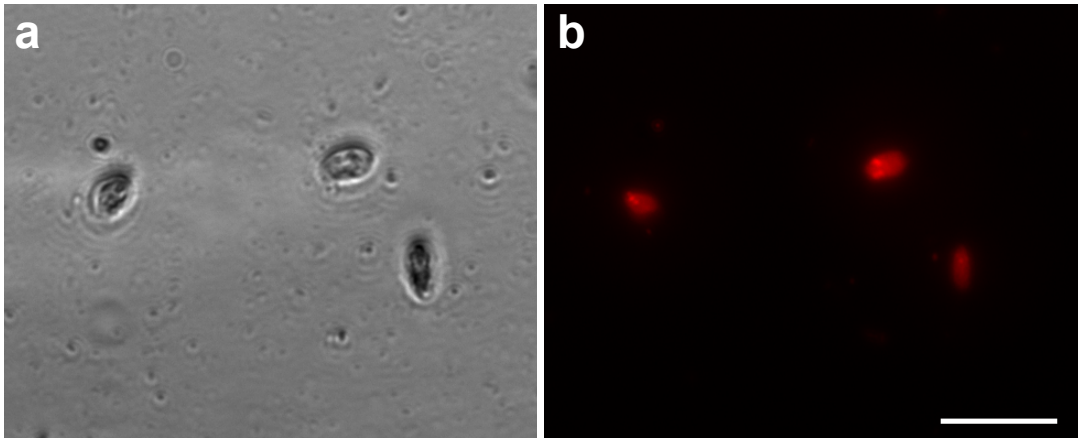

Figure 5.10 Propidium iodide staining to confirm that heat treatment resulted in non-viable cysts. (a) Phase contrast image of three cysts after 5 minutes of heat treatment at 70˚C. (b) Fluorescent image of the same three cysts after treatment with propidium iodide. Scale bar = 20 μm.

The viability of the cysts had a low impact upon whether binding to the polymer surfaces was observed, as supported by an R^2 value of 0.857 (Figure 5.11) between viable and non-viable cyst adhesion, suggesting that viability does not have a significant effect on adhesion characteristics of *G. lamblia* cysts. Specific polymers, such as PA531 and PA104, showed high binding regardless of the viability of the cysts (Figure 5.12b). There was also a considerable number of polymers, such as PA1-6, which effectively prevented binding of both viable and non-viable cysts (Figure 5.12b).

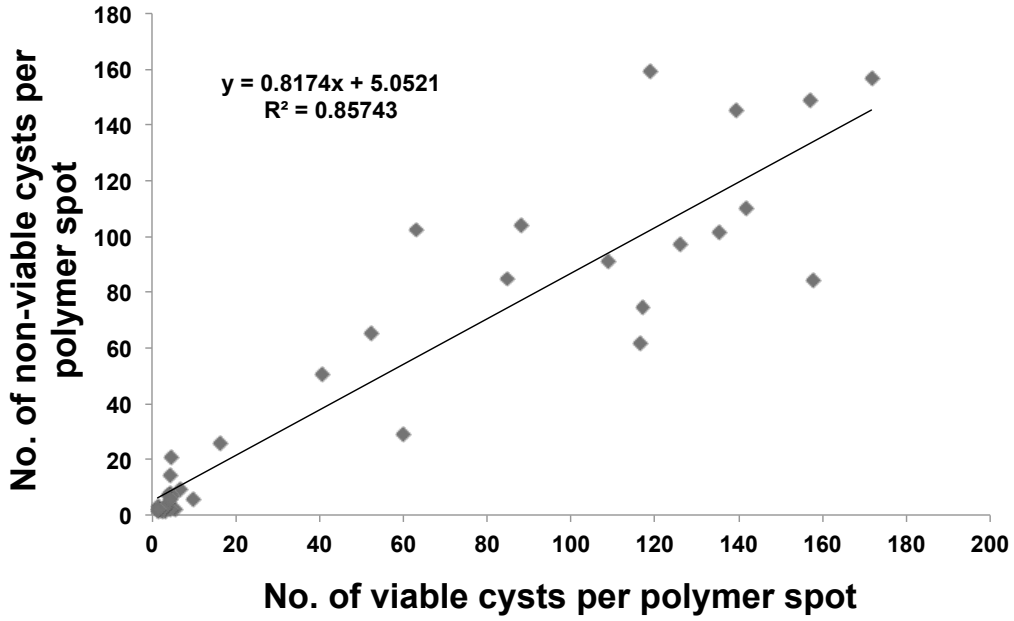

Figure 5.11 Graphs comparing viable and non-viable cyst binding in hit arrays, showing good correlation.

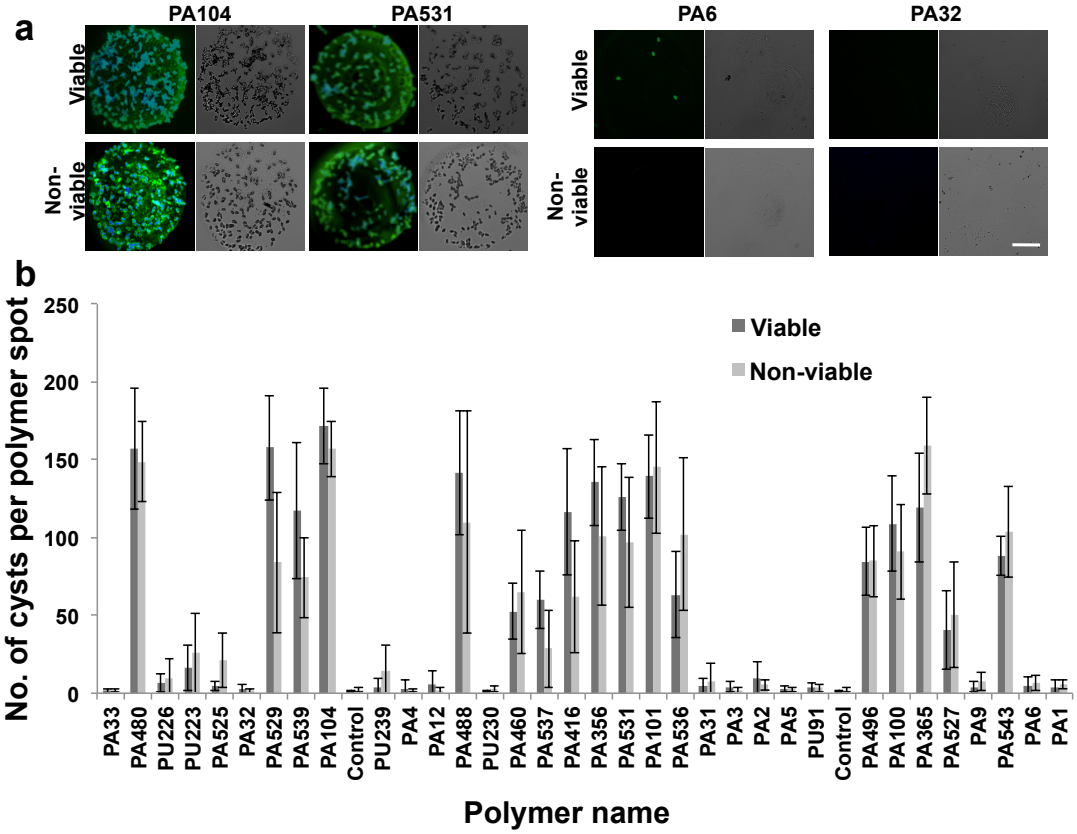

Figure 5.12 Hit array screening for viable/non-viable *G. lamblia* cyst binding. (a) Images of the cysts stained with Giardia-a-glo (green), and DAPI (blue) bound to polymer spots. Fluorescent (left) and phase contrast (right) images of selected polymers are shown. Left: two strong binding polymers (PA104 and PA531). Right: two poor binding polymers (PA6 and PA32). Scale bar = 100 μm. (b) Graph comparing the results of 34 polymers on hit arrays with viable (dark grey) and non-viable cysts (light grey), showing the strong correlation between them.

5.4.2 Effect of Proteinase K Treatment

Proteinase K has previously been employed to study the nature of surface macromolecules of *Giardia*[202]. To further understand the cysts' surface interactions, viable cysts were treated with proteinase K, to remove proteins from the outer layers of the cyst wall, before analysis on a hit array. Proteinase K removes any proteins stretching out from the cyst and also contributes to degradation of those involved in the mesh-like outer wall. SEM images (Figure 5.13) illustrate changes in cyst morphology, *e.g.* cysts either revealing a clearly delineated cyst wall (Figure 5.13a) or appearing rounded with slightly thicker outer walls (Figure 5.13b), as expected. Chatterjee previously reported that removal of the cyst wall proteins decompresses the galactosamine fibrils, thus thickening the cyst wall[203]. The results showed that binding to the polymers was severely limited for all polymers on the hit arrays, with the number of cysts bound reduced by 70% (Figure 5.14), although polymers which normally promoted strong adhesion, such as PA104 and PA480, still bound the highest number of cysts. The reduction in adhesive ability suggests that the cyst wall proteins that bind the galactosamine fibrils play a crucial role in surface interactions. This supports the theory that protein-specific interactions with the polymers control the adhesion of the cysts to the surfaces.

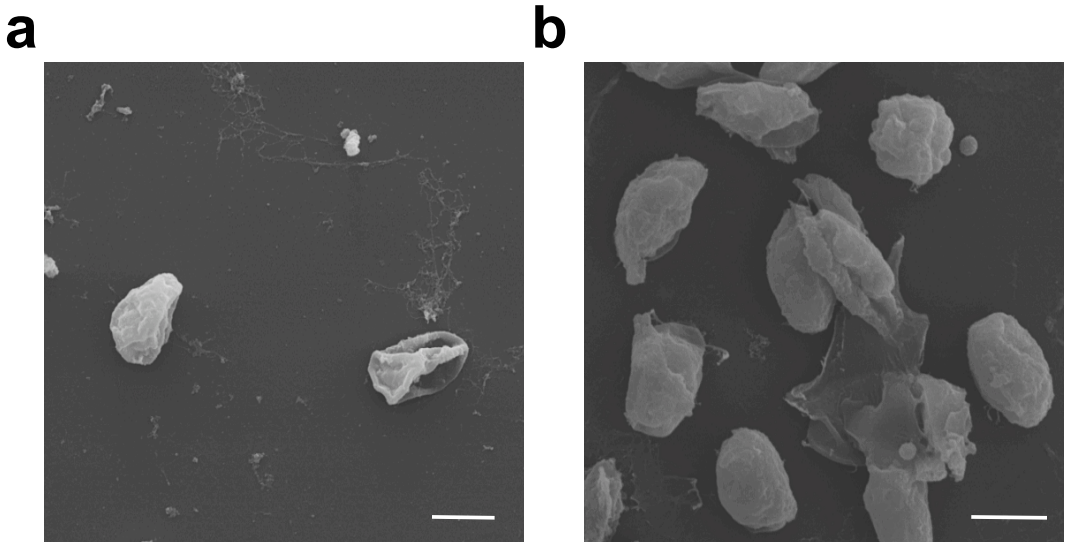

Figure 5.13 SEM images of the proteinase K treated cysts on a polymer spots of the hit arrays. (a) PA104 and (b) PA531. Scale bar = 10 μm.

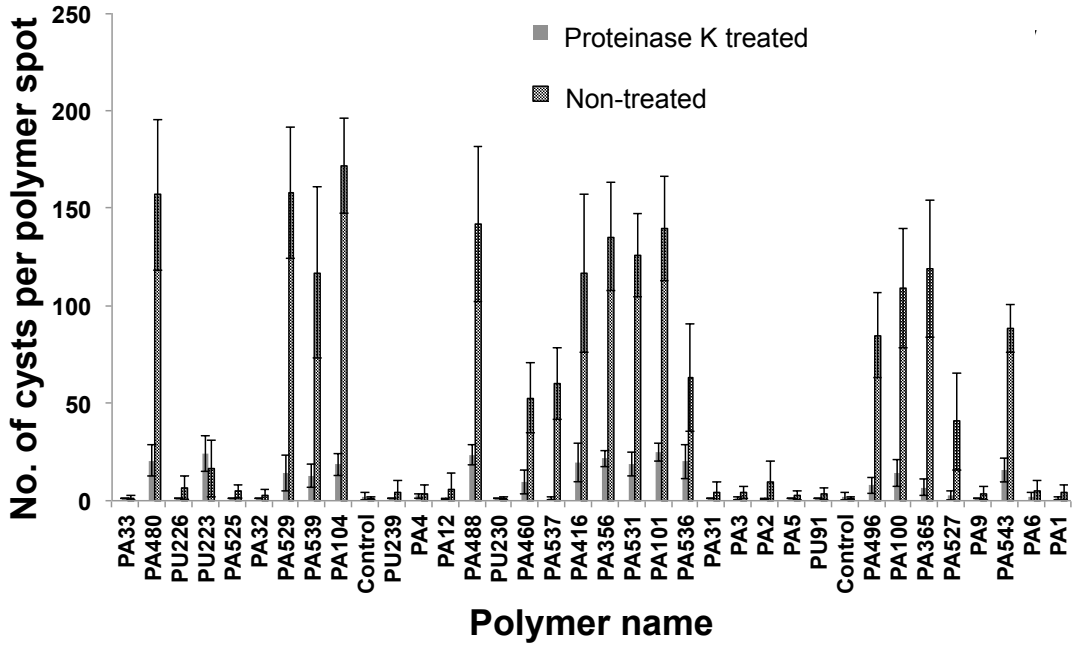

Figure 5.14 Graph comparing binding of viable cysts on the hit arrays before (dark grey) and after (light grey) proteinase K treatment.

5.4.3 Influence of pH

Analysis of cyst adhesion at different pH values (pH 2 and 12) showed an overall reduction in binding (Figures 5.15 and 5.16). Those polymers (PA12, PA33 and PU91) with weak adhesion at pH 7 did not exhibit significantly different results at extremes of pH, whereas those which demonstrated strong adhesion at pH 7 showed severe reductions in binding at both pH 2 and 12. In previous discussions, analysis of the effects of polymer composition and proteinase K treatment on cyst adhesion suggested that ion-pair interactions play a key role in controlling the binding of *G. lamblia* to a polymer surface. At pH 2, the cyst wall will have high net positive charges and therefore will not be attracted to protonated amines. At pH 12, whilst the cyst wall will be negatively charged, amines on the surface will not be protonated and again no interactions will occur. Thus, performing experiments at different pH values significantly worsened the adhesive capacity of *G. lamblia* cysts to the polymers.

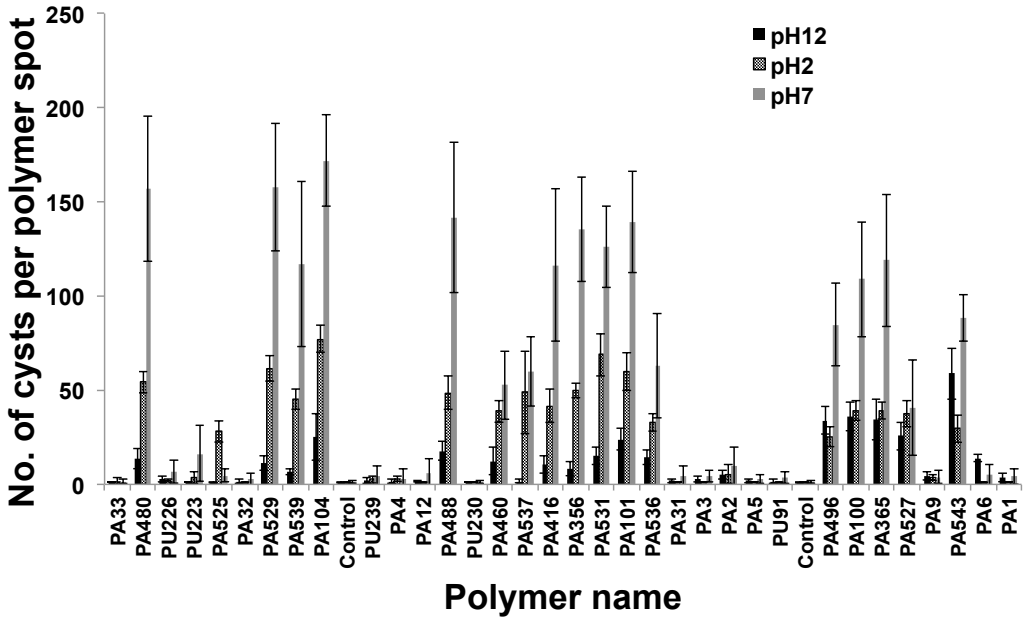

Figure 5.15 Effects of pH on *G. lamblia* cyst binding at pH 2 (patterned grey), pH 7 (medium grey) and pH 12 (dark grey).

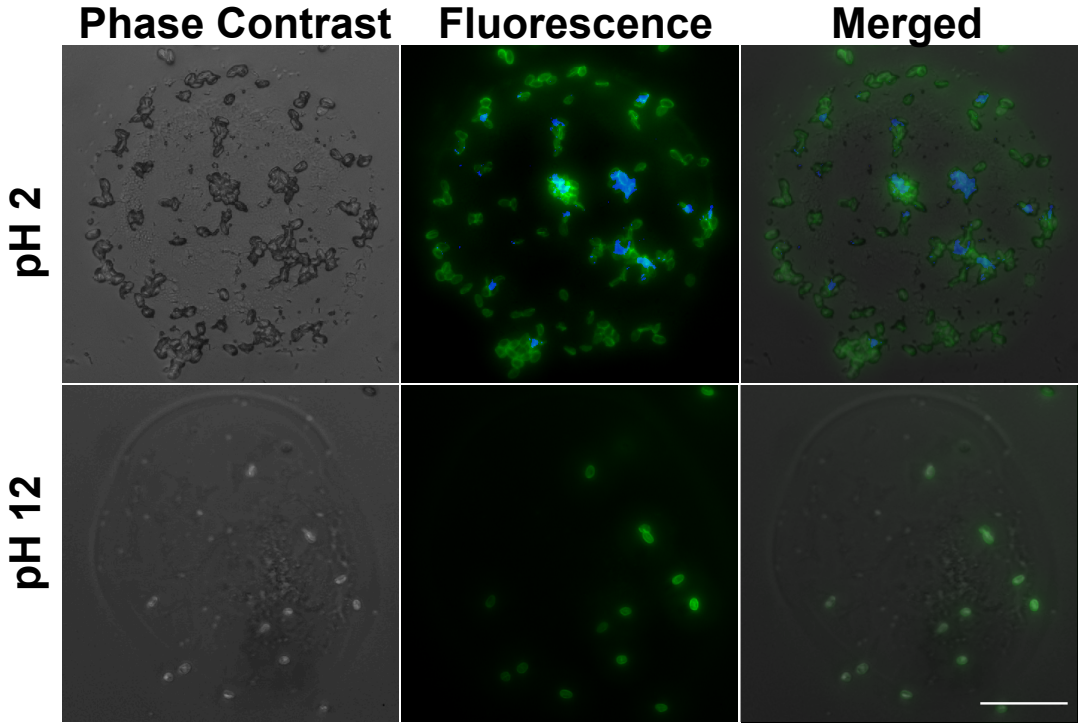

Figure 5.16 Fluorescence and phase contrast images showing cysts bound on polymer spots stained with Giardia-a-glo (green), and DAPI (blue). Scale bar =100 μm.

5.5 Large-scale Polymer Experiments

5.5.1 Fluorescence Microscopy Analysis

Polymers (PA6, PA32, PA104, PA480, and PA531) that showed strong affinity/repulsion to both viable and non-viable cysts were resynthesised and spin-coated onto glass surfaces (coverslips, 13 mm in diameter), followed by exposure to cysts and imaging by fluorescence microscopy. The performances of large-scale polymer coated surfaces were as expected (Figure 5.17), with PA531, PA104 and PA480 significantly promoting strong binding, and PA6 and PA32 considerably preventing cyst adhesion.

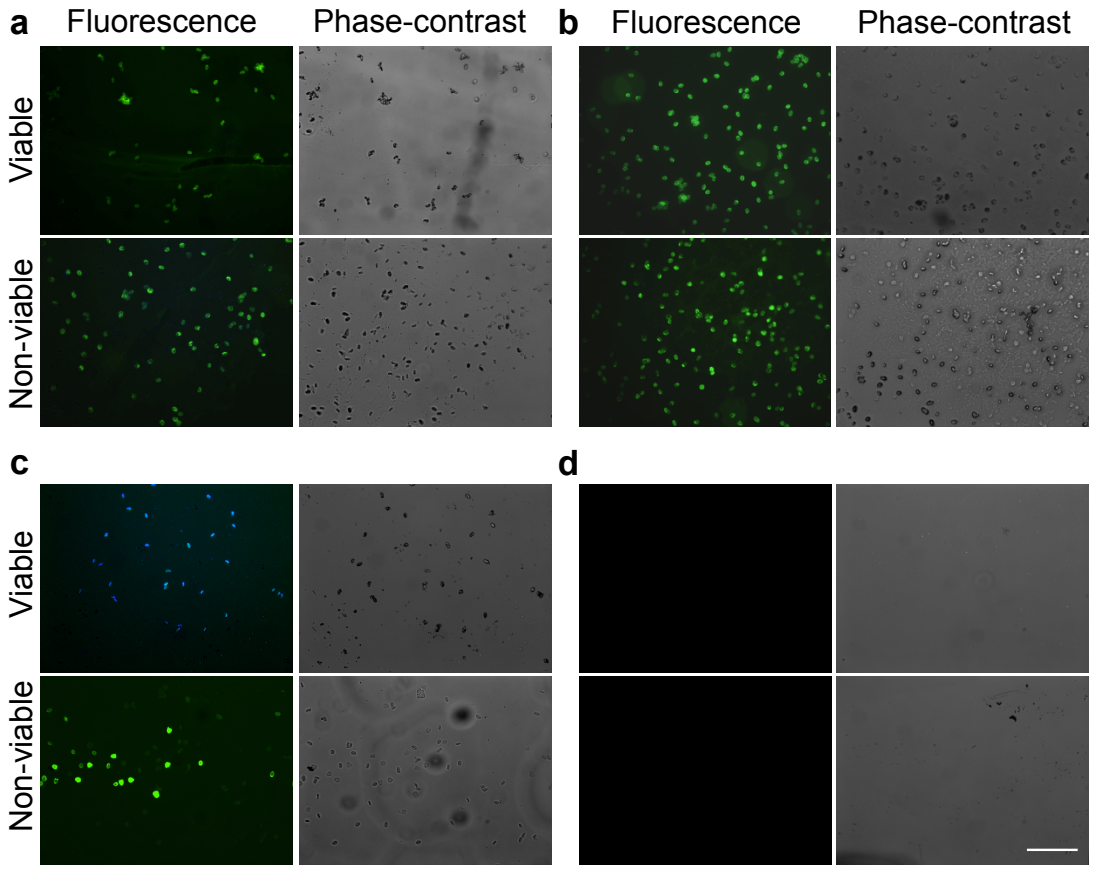

Figure 5.17 Polymer scale-up experiments for *G. lamblia* cyst binding. Fluorescence (left) and phase contrast (right) images of viable/non-viable cysts were shown on polymer coated surfaces (a-d). (a-c) Selected polymers for strong cyst binding: (a) PA531; (b) PA104; (c) PA480. (d) No cyst binding on PA32. For the fluorescence images cysts were stained with Giardia-a-glo (green), and DAPI (blue). Scale bar = 100 μm.

5.5.2 Scanning Electron Microscopy (SEM) Analysis

SEM imaging of *G. lamblia* cysts on polymer coated surfaces (Figure 5.18) demonstrated the features expected of *G. lamblia* cysts, with their shapes and sizes consistent with previous studies[206]. All *G. lamblia* viable cysts showed a similar appearance (Figure 5.18c), while non-viable cysts displayed more intercellular details and a granular texture (Figure 5.18d). These images also highlight the differences between viable and non-viable cysts, with the walls being generally rougher and thicker in the latter[207].

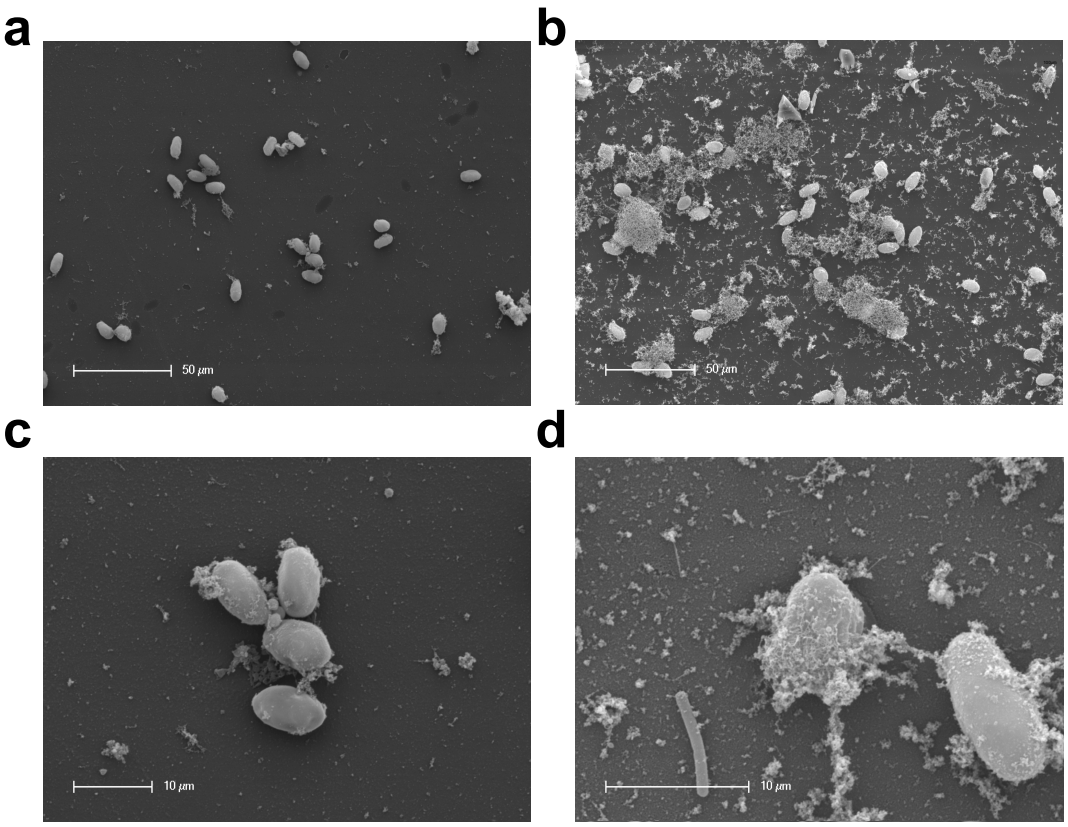

Figure 5.18 SEM images of polymer scale-up experiments for *G. lamblia* cyst binding. Strong binding PA531 coated surfaces with (a) viable and (b) non-viable cysts. High magnification images of (c) viable and (d) non-viable cysts on a PA531 coated surface. Scale bar is shown.

5.6 Conclusions

In summary, this work shows the results of a polymer microarray investigation into the adhesion characteristics of the water-borne protozoan parasite *G. lamblia*. From 652 screened polymers, several materials were identified which either promoted or prevented the binding of *G. lamblia* cysts. The performance of these polymers was confirmed by scale-up.

Comparison of the adhesion results with polymer properties, such as wettability, surface roughness and polymer composition, was undertaken to elucidate which factors control cyst-polymer surface interactions. Firstly, it appeared as though overall high hydrophobicity or hydrophilicity (outside 50º-70º) seemed to prevent cyst adhesion, as did high RMS values (greater than 10 nm). This is illustrated by polymers, such as PA5 (83º; 13.6 nm) and PU230 (32º; 59.0 nm). Additionally, the strong binding polymers, PA480 and PA531, had wettability values within the range 60º-65º and RMS values of 2 nm or below. However, no correlation of adhesion was observed with wettability or surface roughness, though extremes of hydrophobicity/ hydrophilicity and surface roughness were generally associated with poor adhesion.

In terms of polymer composition, the presence of aromatic monomers, such as styrene, amide groups (*e.g.* DEAA and DMAA) and glycol moieties appeared to prevent adhesion. In contrast, secondary amine functionalities were linked with good adhesion. MEMA and MMA, copolymerised with amine monomers, such as DEAEMA and DEAEA, were also identified as monomers which enhanced adhesion. Certain monomers appear to be capable of participating in specific chemical associations with the outer wall of the cysts, suggested to be ion-pair interactions between protonated amines and negatively charged groups on the cyst wall. These interactions do not occur following particular cyst treatments. Specifically, removal of surface proteins *via* proteinase K treatment, or performing experiments at different pH values, significantly reduced the adhesive capacity of *G. lamblia* cysts to the polymers.

The work reported here is the first polymer microarray study of *G. lamblia* cyst adhesion, allowing for interactions with a wide range of polymers to be probed and a deeper understanding to be gained of the mechanisms by which parasites attach to polymer surfaces. Such improved understanding is likely to contribute to better design of water treatment processes for this pathogen, and the polymers identified in this chapter may find applications in coatings for membrane filters or even in the development of sensing technology.

Chapter 6

Experimental

6.1 General Information

6.1.1 Equipment

QArray^{mini} microarrayer (**Genetix**)

BioAnalyzer 4F/4S white light scanner and FIPS software (**LaVision BioTech**)

HCS platform and Pathfinder™ software (**IMSTAR**)

Biosafety cabinet: HERAsafe KS 18 class II (**Heraeus**)

Incubator: HERAcell 150 (**Heraeus**)

Vacuum oven: Vacutherm VT6025 (**Heraeus**)

Freeze dryer Micro Modulyo (**Edwards**)

Plasma machine (**Europlasma**)

P6708 Spin-coater (**Speedlines Technologies**)

Critical point drier (**Polaron**)

Sputter coater (**Edwards**)

XL30CP Scanning electron microscope (**Philips**)

Dimension NanoScope V Atomic force microscope (**Veeco**)

6.1.2 Polymers

The polymer libraries, including 475 members of polyacrylate (Appendix I) and 219 members of polyurethane (Appendix II), were synthesised by Jean-Francois Thaburet, Hitoshi Mizomoto and Ann Jasmine Jose as part of a previous project[91, 95, 96], and were previously characterised in terms of molecular weight (by gel

permeation chromatography (GPC)), wettability and glass transition temperature (by differential scanning calorimetry (DSC))[91, 96].

6.1.3 Chemicals and Materials

All chemicals were of analytical grade and used as received without further purification. Phosphate buffered saline (PBS) tablets were form Oxoid. Tetracycline, sodium cacodylate trihydrate, amino-alkylsilane microscope slides and all the monomers used were obtained from Sigma-Aldrich, and the coverslips were from VWR. GeneFrames (AB-0630) were purchased from Thermo Scientific, and 2.5% (w/v) glutaraldehyde and 1% (w/v) osmium tetroxide were purchased from Electron Microscopy Sciences. The rectangular four-well plates were purchased from Nunc. Gridded glass coverslips were purchased from CELL-VU.

6.1.4 Polymer Microarray Fabrication

Polymer microarrays were fabricated by contact printing (QArray^{mini}, Genetix, UK) with 32 aQu solid pins (K2785, Genetix) using 1% (w/v) polymer solutions in 1-methyl-2-pyrrolidinone (NMP) placed in polypropylene 384-well microplates (X7020, Genetix, Figure 6.1). The printing conditions used were 5 stamps per spot, with a 200 ms inking time and a 100 ms stamping time on amino-alkylsilane treated microscope slides (25 × 75 mm), previously dip-coated with agarose Type I-B[94] (1% w/v in deionised water) at 65˚C. The typical spot size was 300-320 µm in diameter. After printing, the polymer microarrays were dried under vacuum at 45˚C overnight.

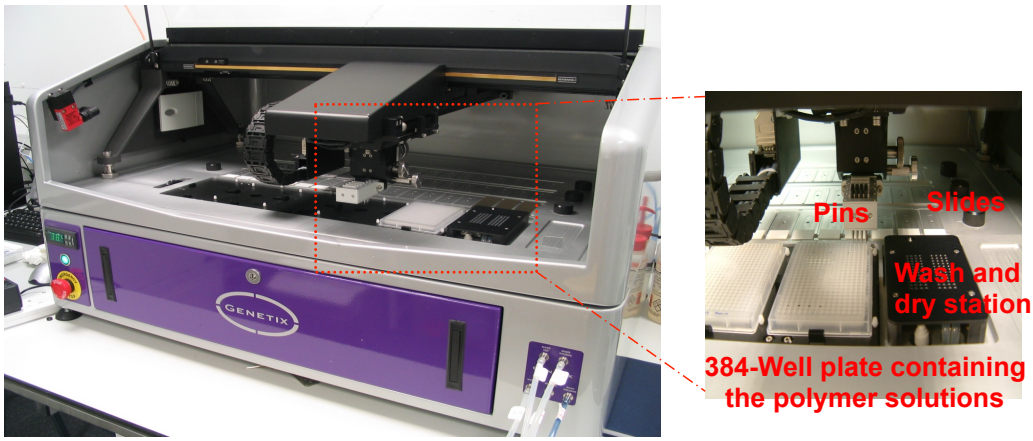

Figure 6.1 QArray^{mini} (Genetix) contact microarrayer

6.1.5 Scale-up

Glass coverslips (13 mm in diameter) were cleaned with tetrahydrofuran (THF). Selected polymers were prepared in THF solutions (2% w/v), and filtered before use. 100 µl of each polymer solution was placed onto the glass coverslips and spin-coated *via* a spin-coater (P6708, Speedlines Technologies) at 2000 revolutions per minute (rpm) for 20 seconds. Coated coverslips were dried in a vacuum oven at 45˚C and 200 mbar overnight (Figure 6.2).

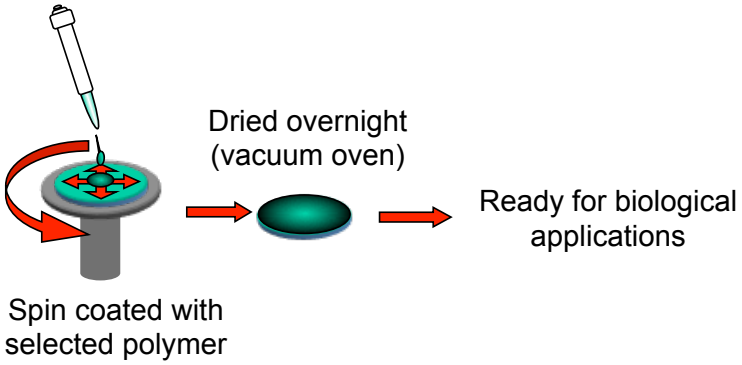

Figure 6.2 Spin coating.

6.2 Experimental for Chapter 2

6.2.1 Polymer Microarray Fabrication

Polymer microarrays were prepared as described in section 6.1.4. The initial polymer microarrays including 1480 polymer spots (quadruplicates of 370 polymers including 195 polyacrylates and 175 polyurethanes), were fabricated using 32 aQu solid pins (k2785, Genetix) in a 32 × 48 pattern with a pitch distance of 560 μm (x-axis) and 750 μm (y-axis).

6.2.2 Culture of Bacteria

S. Typhimurium and *E. coli* were transformed with pHC60 (expressing GFP)[124, 208]. *S.* Typhimurium and *E. coli* were grown with aeration at 37˚C and 30˚C respectively on Luria-Bertani (LB) agar plates containing tetracycline (10 μg ml^{-1}). Bacterial cultures were then grown in 5 ml of LB broth with continual shaking overnight under the same conditions used for culturing on agar. Cultures were collected by centrifugation at 6000 rpm for 3 minutes, washed and resuspended with fresh LB broth and diluted tenfold to a final concentration of approximately 2×10^8 CFU ml^{-1}.

6.2.3 Bacterial Binding

6 ml of *S.* Typhimurium or *E. coli* culture (2×10^8 CFU ml^{-1}) were added to polymer microarrays (in duplicate) in a four-well plate (Nunc) and incubated overnight (except where stated) at room temperature. Subsequently, the polymer microarray slides were gently washed three times with 6 ml of PBS, rinsed in 6 ml of deionised water, and dried with a stream of air. A GeneFrame and coverslip (1.9 × 6.0 cm, AB-0630, Thermo Scientific) was then applied to each slide, and the outside was washed with 70% ethanol. Polymer microarrays were analysed with a LaVision BioAnalyzer 4F/4S scanner with a FITC filter. Bacterial adhesion was evaluated *via* integration of the fluorescence intensity after background correction. The mean and standard deviation for sets of four identical polymer features were determined, with the reproducibility between two identical microarrays evaluated by a student t-test. Polymers with p-values < 0.001 and 6 degrees of freedom were considered

statistically significant. Raw data of *S.* Typhimurium and *E. coli*-polymer binding analysis are presented in appendix III.

6.2.4 Fluorescence-based High-Content Imaging

High-content imaging was carried out using an automated high-content screening (HCS) fluorescent microscope platform (Nikon 50i) with an X-Y-Z stage running Pathfinder^{TM} (IMSTAR) that allowed the capture of single images for each polymer spot. Bacteria were imaged with both brightfield and fluorescein channels with a 20× objective.

6.2.5 Polymer Microarray Reproducibility

Polymer microarrays were prepared as described in section 6.1.4. Eight members of the hit polyurethanes (PU104, PU120 and PU126) and polyacrylates (PA155, PA235, PA325, PA422 and PA426) were printed using 8 aQu solid pins (k2785, Genetix), following a four-replicate pattern with 8 single fields of 5 × 5 spots in a pitch distance of 900 μm (y-axis) and 900 μm (x-axis). *S.* Typhimurium binding on hit polymers was imaged *via* a HCS platform with the Pathfinder^{TM} software package as described in section 6.2.4.

6.2.6 Polymer Microarrays for Time-Dependent Binding

Polymer microarrays with letters U and K were fabricated with polymers PU104 and PA325 using 1 aQu solid pin (k2785, Genetix) under the same conditions as in section 6.1.2. Microarrays were incubated with 6 ml of *S.* Typhimurium (2×10^8 CFU ml^{-1}) for four hours at room temperature, scanned *via* a LaVision BioAnalyzer 4F/4S scanner and imaged *via* a HCS platform with the Pathfinder^{TM} software package as described in sections 6.2.3 and 6.2.4, respectively.

6.2.7 Scanning Electron Microscopy (SEM) Analysis

After incubation with *S.* Typhimurium (2×10^8 CFU ml^{-1}) overnight, the hit polymer microarrays with eight hit polymer members (PU104, PU120, PU126 PA155, PA235, PA325, PA422 and PA426) was washed twice with 6 ml of 0.1 M cacodylate buffer (pH 7.4) and then fixed with 5 ml of glutaraldehyde solution (2.5% w/v in 0.1

M cacodylate buffer, pH 7.4) at room temperature for 2 hours. Polymer microarrays were post fixed with 2 ml of an aqueous solution of osmium tetroxide (1% w/v) for 1 hour at room temperature. Microarrays were dehydrated stepwise with ethanol (50, 70, 90 and 100% v/v), critical point dried in CO_2 (Critical Point Drier, Polaron) and gold coated by sputtering (Edwards S150B Sputter coater). The samples were examined with a Philips XL30CP Scanning Electron Microscope.

6.2.8 Scale-up

Polymers (PA155 and PA325) were spin-coated onto grided glass coverslips (CELL-VU DRM 800) as described in section 6.1.5. Each coated (PA155 and PA325) or uncoated (glass as control) coverslip was incubated with 1 ml of *S.* Typhimurium (2×10^8 CFU ml^{-1}) overnight. Uncoated and coated coverslips were washed twice with 1ml of 0.1 M cacodylate buffer (pH 7.4) and fixed with 1 ml of glutaraldehyde solution (2.5% w/v in 0.1 M cacodylate buffer, pH 7.4) for 2 hours and then post fixed with 800 µl of an aqueous solution of osmium tetroxide (1% w/v) for 1 hour. Coverslips were dehydrated, dried, gold coated as described in section 6.2.7, and imaged by SEM. SEM images were transferred into Image-Pro Plus 4.5 software (©2001 Media Cybernetics) for processing. The numbers of bacteria in randomly selected sub-squares (four identical areas with 10 µm sides for each coverslip) were counted automatically[125] (Figure 6.3). Reproducibility was determined by calculating the mean and the standard deviation for the four identical sub-squares.

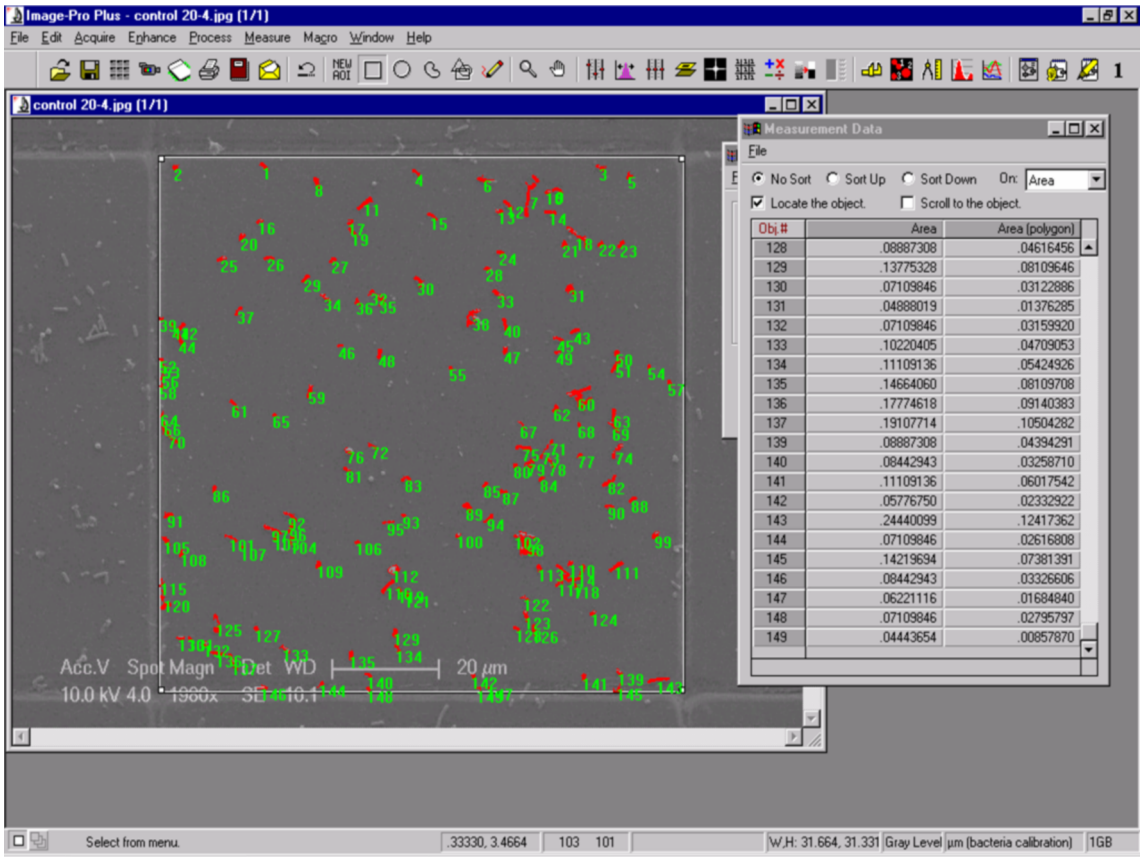

Figure 6.3 Automated counting of *S.* Typhimurium binding. In this example, the number of *S.* Typhimurium on one single square of the uncoated coverslip (control) was counted. *S.* Typhimurium identified by Image-Pro Plus 4.5 are in red with an associated number in green.

6.3 Experimental for Chapter 3

6.3.1 Polymer Microarray Preparation

Polymer microarrays were prepared as described in section 6.1.4. The initial microarrays contained 1524 polymer spots (quadruplicates of 381 polymers, including 207 polyacrylates and 174 polyurethanes), and were fabricated in a 32 × 48 pattern with a pitch distance of 560 μm (x-axis) and 750 μm (y-axis).

6.3.2 Culture of Bacteria

6.3.2.1 Culture of *Campylobacter jejuni*

C. jejuni strains (CH4 and NCTC 11168) were kindly provided by Dr. Bruce Ward in the School of Biological Sciences, University of Edinburgh. *C. jejuni* strains were grown in Brucella broth, supplemented with *Campylobacter* growth supplement (FBP) consisting of iron (II) sulphate (0.15 mg ml^{-1}), sodium pyruvate (0.15 mg ml^{-1}) and sodium metabisulphite (0.15 mg ml^{-1}), vancomycin (2500 units L^{-1}) and trimethoprim (5 mg L^{-1}). *C. jejuni* were grown in a micro-aerophilic atmosphere of 85% Nitrogen, 10% CO_2 and 5% O_2.

6.3.2.2 Culture of *Clostridium perfringens* and *Clostridium difficile*

C. perfringens (strain NCTC 8257) and *C. difficile* (strain NCTC 630) were kindly provided by Elena S. Theophilou and Dr. Garry Blakely in the School of Biological Sciences, University of Edinburgh, and were grown in brain-heart infusion (BHI) with supplements of L-cysteine (0.5 mg L^{-1}), sodium bicarbonate (1 mg L^{-1}) and hemin (5 mg L^{-1}) /menadione (0.5 mg L^{-1}) in an anaerobic environment.

6.3.2.3 Culture of *Streptococcus mutans*

S. mutans (strain NCTC 10923) was grown in Luria-Bertani (LB) broth.

6.3.2.4 Culture of Clinical Cocktail 1

This consists of *Klebsiella pneumoniae* (*K. pneumoniae*), *Staphylococcus saprophyticus* (*S. saprophyticus*), and *Staphylococcus aureus* (*S. aureus*). These strains of bacteria had been previously isolated from endotracheal tubes from ICU patients, and then genotyped by PCR analysis so that the specific species could be identified. The strains were grown in LB broth.

6.3.2.5 Culture of Clinical Cocktail 2

This consists of *S. mutans*, *S. aureus*, *K. pneumonia* and *Enterococcus faecalis* (*E. faecalis*). All strains were grown in brain-heart infusion (BHI) broth in a micro-aerophilic environment (85% N_2, 10% CO_2, 5% O_2) at 37˚C.

6.3.3 Bacterial Attachment to the Microarrays

Each bacterial strain was grown in 5 ml of the appropriate medium (e.g. *C. jejuni* in brucella broth described in section 6.3.2.1), and incubated at 37˚C overnight with shaking to a constant density.

For experiments with a single bacterial strain, 2 ml of each culture was collected by centrifugation (6000 rpm for 3 minutes), washed, resuspended in 2 ml of fresh medium and diluted with a further 18 ml of fresh medium. 6 ml of this diluted bacteria culture was added to each of two polymer microarrays. These were placed in a four-well plate (Nunc), so that the microarrays were completely submerged with medium. Microarrays were incubated overnight at room temperature. For the anaerobic and micro-aerophilic bacterial strains, the four-well plate was placed in a gas jar. Overnight cultures of bacteria in clinical cocktail 1 were combined in equal amounts and then diluted fourfold with fresh media prior to incubation with the polymer microarrays. Bacteria in clinical cocktail 2 were prepared similarly but were incubated with microarrays at 37˚C over 5 days, under micro-aerophilic conditions with agitation (30 rpm).

After incubation, polymer microarrays were washed gently with 6 ml of PBS and stained with 4',6-diamidino-2-phenylindole (DAPI) (1 μg ml^{-1} in PBS, 6 ml) for 20 minutes. Subsequently, the polymer microarray slides were washed three times with 6 ml of PBS, rinsed in 6 ml of deionised water, and then dried with a stream of air. A GeneFrame and coverslip (1.9 × 6.0 cm, AB-0630) were applied to each slide and were sprayed with 1% Virkon disinfectant (w/v, aq).

6.3.4 Analysis of Bacterial Attachment

The polymer microarrays were analysed using a LaVision Bioanalyzer 4F/4S scanner with a DAPI filter using an exposure time of 30 ms. An automated fluorescent microscope (with an X-Y-Z stage running Pathfinder™, IMSTAR) allowed the capture of single images for each polymer spot. Brightfield and DAPI-like band channels were used for imaging under a 20× objective.

Bacterial adhesion was evaluated by calculating the average fluorescence intensity of the quadruplicate polymer spots after background correction. The population standard deviation of the eight spots was also measured (four spots for each polymer on the microarray, with two microarrays used for each bacterial strain). The mean and standard deviation for sets of four identical polymer features were determined, with the reproducibility between two identical microarrays evaluated by a student t-test. Polymers with p-values < 0.001 and 6 degrees of freedom were considered statistically significant. Raw data of bacteria-polymer binding analysis are presented in appendix III.

6.3.5 Scale-up

Glass coverslips coated three polyacrylates (PA13, PA338, PA515) and four polyurethanes (PU5, PU20, PU83, PU179) were prepared as described in section 6.1.5.

Glass coverslips used as negative controls were coated agarose to inhibit unspecific cellular adhesion; these were pre-treated with aminosilane to improve agarose coating. For aminosilane treatment, clean, dry glass coverslips (13 mm in diameter, VWR) were treated with 3-aminopropyltriethoxysilane (APTES) solution

(1.5% w/v in acetonitrile) for one hour at room temperature, rinsed in dry acetonitrile and acetone, and treated in an oven at 100˚C for 3 hours. Coating with agarose was performed by dip-coating these aminosilane-treated coverslips into agarose Type-B aqueous solution (1% w/v) at 65˚C, followed by wiping off the coating on the bottom side with a clean piece of tissue. The coverslips were dried overnight at room temperature in a dust free environment.

Two mixed bacterial cultures, clinical cocktails 1 and 2, were prepared as described in section 6.3.2 and 6.3.3, and applied to the polymer coated, agarose-coated and uncoated glass coverslip samples. Each coverslip was incubated with 600 µl of mixed culture in a 24 well plate overnight under micro-aerophilic conditions with agitation (30 rpm). Samples were washed twice with 6 ml of 0.1 M cacodylate buffer (pH 7.4) and then fixed and visualised as described in section 6.2.8. Starting cell numbers were determined by serial dilution for each of the constituent parts of the clinical cocktails. Bacterial concentration ranged from 1.4×10^6 to 3×10^8 CFU ml^{-1}, depending on the organism.

Coverslips were analysed using a scanning electron microscopy (Philips XL30CP). The average numbers of bacteria attached on the coated/uncoated coverslips (randomly selected areas for each coverslip) were counted.

6.4 Experimental for Chapter 4

6.4.1 Polymer Microarray Printing

Polymer microarrays were prepared as described in section 6.1.4. The initial polymer microarrays contained 1956 polymer spots (triplicate of 652 polymers, including 468 polyacrylates and 164 polyurethanes) and were fabricated using 32 aQu solid pins (k2785, Genetix) in a 36 × 56 pattern with a pitch distance of 500 μm (x-axis) and 640 μm (y-axis).

6.4.2 Scanning for Oocyst Interactions

Cryptosporidium parvum (*C. parvum*) oocysts (Creative Science, Moredun, UK) were diluted in sterilised water to a count of 1.66×10^5 oocysts per ml. When required, heat treatment of the samples for 5 minutes at 70˚C was performed, using a Trechne Dri-Heat heating block, to obtain non-viable oocysts. Polymer microarrays were sterilised by exposure under UV irradiation for 15 minutes and freshly prepared 6 ml aliquots (1 million oocysts per experiment) were added to a polymer microarray in a four-well plate (Nunc). The slides were incubated with oocysts on a plate shaker at 20-50 rpm for 3 hours at room temperature. Subsequently, the slides were rinsed with sterilised water and then fluorescently stained.

6.4.3 Fluorescent Staining of *C. parvum* Oocysts

The standard *C. parvum* staining protocol (EPA1623) was adapted for the larger array area. After the slide was rinsed and air dried, 1 ml of MeOH was added to the slide and allowed to air dry; 2 ml of DAPI (1 μg ml^{-1} in PBS) was applied to the slide for 1 minute followed by a sterilised water rinse; finally, 2 ml of Crypto-a-glo (Waterborne Inc, USA) was added to the slide for 2 hours at 37˚C before rinsing in sterilised water and being left to air dry. A GeneFrame and coverslip (1.9 × 6.0 cm, AB-0630) were then applied to each slide and cleaned with 70% ethanol. Image capture of the polymer microarray was performed *via* a Nikon 50i fluorescence microscope (20× objective) with an automated X-Y-Z stage, using the IMSTAR Pathfinder™ software package (IMSTAR S.A., Paris, France). Oocyst number and morphology of each polymer was determined using the automated scanning

IMSTAR software. Raw data of oocyst-polymer binding analysis are presented in appendix III.

6.4.4 Polymer Microarray Reproducibility

Hit polymer microarrays contained a selection of 34 members of the best and worst polymers (listed in Table 6.1) and were prepared as described in section 6.1.4. Polyurethanes and polyacrylates were printed using 9 aQu solid pins (k2785, Genetix), in a 15 × 12 pattern with a pitch distance of 900 μm (x-axis) and 1120 μm (y-axis). 6 ml (1.66×10^5 oocysts per ml in sterilised water) viable oocysts or non-viable oocysts were applied to hit arrays as described in section 6.4.2. The hit array slides were fixed and either analysed by fluorescence microscopy using a HCS platform with the Pathfinder™ software package as described in section 6.4.3 or analysed by SEM as described in section 6.2.7.

Table 6.1 Map of hit polymer microarrays. 5 spots of each polymer were fabricated, allowing 2 empty areas for controls.

PA512	PA6	PA1
PA107	PA528	PA365
PA2	PA445	PA100
PU91	PA476	PA167
Control	PA170	PA3
PA101	PA531	PA395
PA464	PA5	PA416
PU230	PA484	PA165
PA504	PU239	PA4
PA104	PA539	PA529
PU223	Control	PA113
PU226	PA480	PA152

6.4.5 Scale-up Experiment

Polymers (PA531, PA480, PA6, and PA104, PA504) were spin-coated on glass coverslips as described in section 6.1.5. One of each coverslip was incubated with 600 µl of viable oocysts or non-viable oocysts (1.66×10^5 oocysts per ml in sterilised water) in a 24 well plate as described in 6.4.2. The coverslips were then fixed and imaged by fluorescence microscopy as described in section 6.4.3 and SEM as described in section 6.2.7.

6.4.6 Atomic Force Microscopy

Surface roughness of all the 34 hit polymers (listed in Table 6.1) was measured. An atomic force microscope (AFM, DimensionV Nanoscope, Veeco) was used to scan the polymer surface within a square area with 10 µm sides (Figure 6.4). The scan rate ranged from 1.32 Hz to 1.60 Hz, and the height values (Z values) of the surface were obtained with a resolution of 512 × 512 in the scanned region. The root mean squares (RMS) of all the spots in the hit array were calculated (by averaging over three 9 μm^2 areas) using the NanoScope analysis software (Veeco version 1.20). Root mean square averages of height deviations taken from the mean image data plane are expressed as:

$$R_q = \sqrt{\frac{\sum (Z_i)^2}{N}}$$

where Z_i is the current Z value, and N is the number of points within the box cursor.

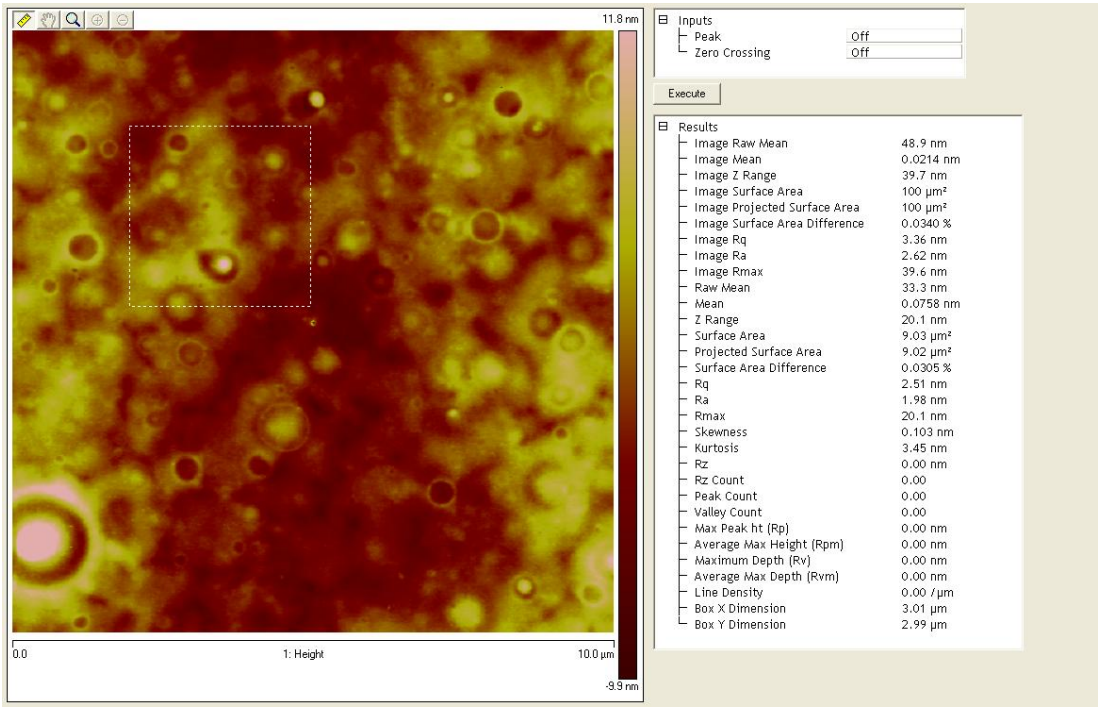

Figure 6.4 Surface roughness analysis of PA531 using atomic force microscopy (AFM, DimensionV Nanoscope, Veeco). The dotted area (3 × 3 µm by side) was randomly selected for calculating the root mean square result using the NanoScope analysis software (Veeco version 1.20).

6.5 Experimental for Chapter 5

6.5.1 Polymer Microarray Manufacture

Polymer microarrays were prepared as described in sections 6.1.4 and 6.4.2. The initial array contained 1956 polymer spots (triplicates of 652 polymers, including 468 polyacrylates and 164 polyurethanes) in a 36 × 56 pattern with a pitch distance of 500 μm (x-axis) and 640 μm (y-axis).

6.5.2 Scanning for Cyst Interactions

Giardia lamblia (*G. lamblia*) cysts (Waterborne Inc, USA, Catalog number: P101) were diluted in sterilised water to 1.66×10^5 cysts per ml. When required, heat treatment of the samples for 5 minutes at 70˚C was performed[205], using a Trechne Dri-Heat heating block, to obtain non-viable cysts, confirmed by staining with propidium iodide (PI, 1 μg ml^{-1} in sterilised water). Cyst exposure to polymer microarrays was as described in section 6.4.2. Subsequently, the slides were rinsed with sterilised water and the cysts were fluorescently stained, using an adapted version of the standard EPA1623 protocol.

6.5.3 Fluorescent Staining of Cysts

The standard *G. lamblia* staining protocol (EPA1623) was adapted for the larger array area. Slides were rinsed with sterilised water, fixed with MeOH and stained with DAPI (1 μg ml^{-1} in PBS) as described in section 6.4.3. Finally, 2 ml of Giardia-a-glo (Waterborne Inc, USA) was added to slides (25 minutes) before rinsing in sterilised water and being left to air dry. Slides were imaged with a Nikon 50i fluorescence microscope (20× objective) with an automated X-Y-Z stage, using the Pathfinder™ software package (IMSTAR S.A., Paris, France) as described in section 6.4.3. Cyst number and morphology of each polymer was determined using the automated scanning IMSTAR software. Raw data of cyst-polymer binding analysis are presented in appendix III.

6.5.4 Polymer Microarray Reproducibility

Hit polymer microarrays containing a selection of 34 members of the best and worst polymers (listed in Table 6.2) were prepared with the same conditions as described in section 6.1.4. Polyurethanes and polyacrylates were printed using 9 aQu solid pins (k2785, Genetix), in an 18 × 12 pattern with a pitch distance of 750 μm (x-axis) and 1120 μm (y-axis). 6 ml of viable or non-viable cysts (1.66×10^5 cysts per ml in sterilised water) were applied to hit arrays as described in section 6.5.2. The hit array slides were fixed and analysed by fluorescence microscopy *via* a HCS platform with the Pathfinder™ software package as described in section 6.5.3.

Table 6.2 Map of hit polymer microarrays. 6 spots of each polymer were fabricated, allowing 2 empty areas for controls.

PA543	PA6	PA1
PA9	PA527	PA365
Control	PA496	PA100
PU91	PA5	PA2
PA536	PA31	PA3
PA101	PA531	PA356
PA460	PA537	PA416
PU230	PA488	PA12
Control	PU239	PA4
PA104	PA539	PA529
PU223	PA525	PA32
PU226	PA480	PA33

6.5.5 Surface Roughness

Surface roughness of all the 34 hit polymers (listed in Table 6.2) was quantified using Atomic Force Microscopy (AFM) as described in section 6.4.6. For the *Giardia lamblia* surface roughness measurement, the sample was prepared by overnight incubation of *G. lamblia* cysts on a PA104 coated coverslip (13 mm in diameter), followed by fixing in glutaraldehyde solution (2.5% w/v in 0.1 M cacodylate buffer, pH 7.4) for 2 hours, rinsing with sterilised water and air drying.

The AFM was performed with a contact cantilever in air at a scan rate of 0.788 Hz and the roughness was determined over a scanned square area with 6 µm sides (Figure 6.5).

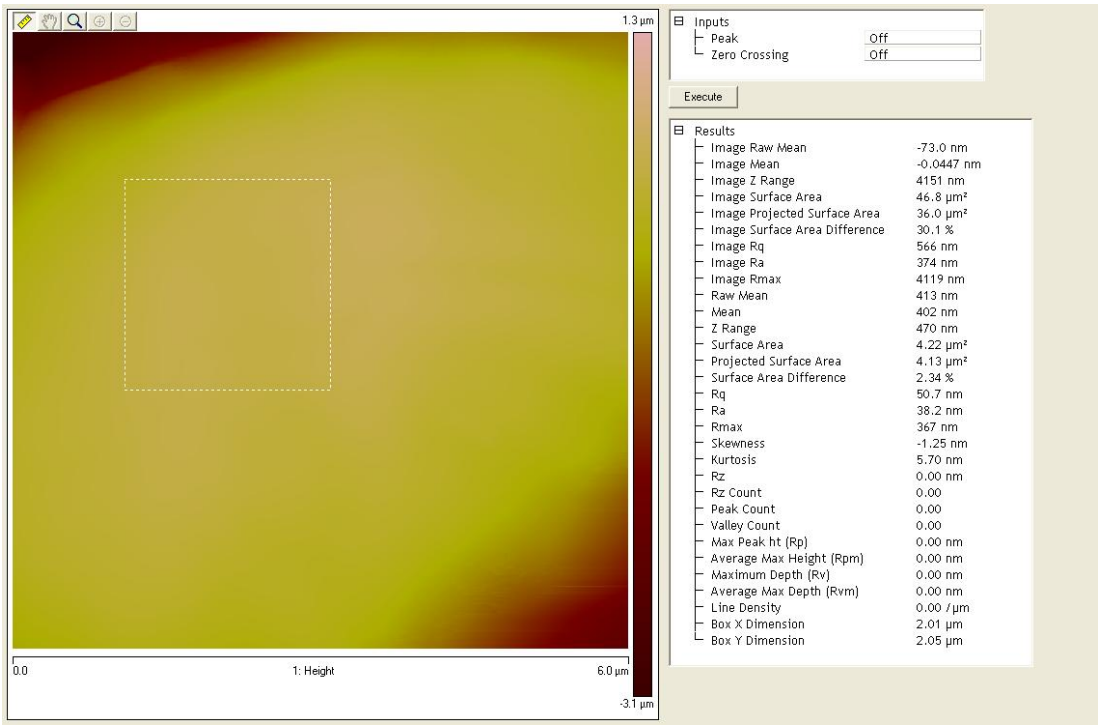

Figure 6.5 Surface roughness analysis of *Giardia lamblia* using atomic force microscopy (AFM, DimensionV Nanoscope, Veeco). The dotted area (2 × 2 µm by side) was randomly selected for calculating the root mean square result using the NanoScope analysis software (Veeco version 1.20).

6.5.6 Proteinase K Treatment

G. lamblia (1 million cysts) were incubated at 37˚C on a plate shaker for 3 hours with 1 ml of an aqueous solution containing 9 mg ml^{-1} proteinase K, 1 M Tris and 10 mM $CaCl_2$. Subsequently, the solution was centrifuged for 5 minutes at 12000 rpm. The supernatant was removed, the pellet was washed and resuspended in 1 ml of sterilised water and this solution was centrifuged for a further 5 minutes. The supernatant was again removed, the pellet was resuspended in 5 ml of sterilised

water and the solution was applied to the hit arrays (polymers listed in Table 6.2) using the protocol described in section 6.5.2. The proteinase K treated cysts on hit arrays were examined, fixed and imaged by fluorescence microscopy as described in 6.5.3 and analysed by SEM as described in section 6.2.7.

6.5.7 Influence of pH

1 M hydrochloric acid and 1 M sodium hydroxide were used to prepare pH 2 and pH 12 aqueous solutions respectively, and 5.2 ml of the acidified/basified solution was added to 800 µl of *G. lamblia* (1 million cysts in sterilised water) to give a cyst concentration of 1.66×10^5 cysts per ml. The pH-influenced cysts were applied to the hit arrays (polymers listed in Table 6.2) using the protocol described in section 6.5.2, and the hit arrays were washed, fixed and imaged by fluorescence microscopy as described in section 6.5.3.

6.5.8 Scale-up Experiments on Viable/non-viable cysts

Polymers (PA6, PA32, PA104, PA480 and PA531) were spin-coated on glass coverslips as described in section 6.1.5. Each of the coverslips was incubated with 600 µl of either viable or non-viable *G. lamblia* (0.833×10^5 cysts per ml in sterilised water) in 24 well plates as described in section 6.5.2. The coverslips were washed, fixed and imaged by fluorescence microscopy as described in section 6.5.3 and SEM as described in section 6.2.8.

References

1. Moyer, C.A., Brentano, L., Gravens, D.L., Margraf, H.W. & Monafo, W.W., Jr. Treatment of large human burns with 0.5 percent silver nitrate solution. *Arch. Surg. Chigago (Chicago, Ill.: 1960)* **90**, 812-867 (1965).
2. Chopra, I. The increasing use of silver-based products as antimicrobial agents: A useful development or a cause for concern? *J. Antimicrob. Chemother.* **59**, 587-590 (2007).
3. Klasen, H.J. A historical review of the use of silver in the treatment of burns. II. Renewed interest for silver. *Burns* **26**, 131-138 (2000).
4. Asimov, I. Asimov's biographical encyclopedia of science and technology: the living stories of more than 1000 great scientists from the age of Greece to the space age, chronologically arranged. (Garden City, N.Y. : Doubleday, 1964).
5. Toledo-Pereyra, L.H. Joseph Lister's surgical revolution. *J. Invest. Surg.* **23**, 241-243 (2010).
6. Florey, H.W. in Nobel lectures (the Nobel Foundation, Stockholm; 1945).
7. Fleming, A. in Nobel lectures (the Nobel Foundation, Stockholm; 1945).
8. Chain, E.B. in Nobel lectures (the Nobel Foundation, Stockholm; 1946).
9. Mann, J.M. & Tarantola, D.J.M. AIDS in the world. (Cambridge, Mass.; London: Harvard University Press, 1992).
10. Culotta, E. Funding crunch hobbles antibiotic-resistance research. *Science* **264**, 362-363 (1994).
11. Cohen, M.L. Changing patterns of infectious disease. *Nature* **406**, 762-767 (2000).
12. Moran, G.J. et al. Methicillin-resistant S. aureus infections among patients in the emergency department. *N. Engl. J. Med.* **355**, 666-674 (2006).
13. Jean, S.S. & Hsueh, P.R. High burden of antimicrobial resistance in Asia. *Int. J. Antimicrob. Ag.* **37**, 291-295 (2011).
14. World health statistics 2010 (World Health Organisation, Geneva; 2010).
15. Frank C.F.M., Askar M., Bernard H., Fruth A., Gilsdorf A., Höhle M., Karch H., Krause G., Prager R., Spode A., Stark K., Werber D., on behalf of the HUS investigation & team. Large and ongoing outbreak of haemolytic uraemic syndrome, Germany, May 201. *Eurosurveillance* **16**, 19878 (2011).
16. No, H.K., Park, N.Y., Lee, S.H., Hwang, H.J. & Meyers, S.P. Antibacterial activities of chitosans and chitosan oligomers with different molecular weights on spoilage bacteria isolated from tofu. *J. Food Sci.* **67**, 1511-1514 (2002).
17. Senel, S. & McClure, S.J. Potential applications of chitosan in veterinary medicine. *Adv. Drug Deliv. Rev.* **56**, 1467-1480 (2004).
18. Kenawy, E.R., Worley, S.D. & Broughton, R. The chemistry and applications of antimicrobial polymers: A state-of-the-art review. *Biomacromolecules* **8**, 1359-1384 (2007).
19. Timofeeva, L. & Kleshcheva, N. Antimicrobial polymers: Mechanism of action, factors of activity, and applications. *Appl. Microbiol. Biotechnol.* **89**, 475-492 (2011).

20. Lienkamp, K. et al. Antimicrobial polymers prepared by ROMP with unprecedented selectivity: A molecular construction kit approach. *J. Am. Chem. Soc.* **130**, 9836-9843 (2008).
21. Palermo, E.F. & Kuroda, K. Chemical structure of cationic groups in amphiphilic polymethacrylates modulates the antimicrobial and hemolytic activities. *Biomacromolecules* **10**, 1416-1428 (2009).
22. Kuroda, K. & DeGrado, W.F. Amphiphilic polymethacrylate derivatives as antimicrobial agents. *J. Am. Chem. Soc.* **127**, 4128-4129 (2005).
23. Palermo, E.F., Sovadinova, I. & Kuroda, K. Structural determinants of antimicrobial activity and biocompatibility in membrane-disrupting methacrylamide random copolymers. *Biomacromolecules* **10**, 3098-3107 (2009).
24. Munoz-Bonilla, A. & Fernandez-Garcia, M. Polymeric materials with antimicrobial activity. *Prog. Polym. Sci.* **37**, 281-339 (2012).
25. Al-Muaikel, N.S., Al-Diab, S.S., Al-Salamah, A.A. & Zaid, A.M.A. Synthesis and characterization of novel organotin monomers and copolymers and their antibacterial activity. *J. Appl. Polym. Sci.* **77**, 740-745 (2000).
26. Kanazawa, A., Ikeda, T. & Endo, T. Antibacterial activity of polymeric sulfonium salts. *J. Polym. Sci. Pol. Chem.* **31**, 2873-2876 (1993).
27. Kanazawa, A., Ikeda, T. & Endo, T. Synthesis and antimicrobial activity of dimethyl-substituted and trimethyl-substituted phosphonium salts with alkyl chains of various lengths. *Antimicrob. Agents Chemother.* **38**, 945-952 (1994).
28. Tashiro, T. Antibacterial and bacterium adsorbing macromolecules. *Macromol. Mater. Eng.* **286**, 63-87 (2001).
29. Woo, G.L.Y., Mittelman, M.W. & Santerre, J.P. Synthesis and characterization of a novel biodegradable antimicrobial polymer. *Biomaterials* **21**, 1235-1246 (2000).
30. Woo, G.L.Y. et al. Biological characterization of a novel biodegradable antimicrobial polymer synthesized with fluoroquinolones. *J. Biomed. Mater. Res.* **59**, 35-45 (2002).
31. Yang, M.L. & Santerre, J.P. Utilization of quinolone drugs as monomers: Characterization of the synthesis reaction products for poly(norfloxacin diisocyanatododecane polycaprolactone). *Biomacromolecules* **2**, 134-141 (2001).
32. Patel, S.A., Patel, M.V., Ray, A. & Patel, R.M. Synthesis, characterization, and antimicrobial activity of some novel poly(ether ketone)s. *J. Polym. Sci. Pol. Chem.* **41**, 2335-2344 (2003).
33. Monteiro, D.R. et al. The growing importance of materials that prevent microbial adhesion: antimicrobial effect of medical devices containing silver. *Int. J. Antimicrob. Ag.* **34**, 103-110 (2009).
34. Kong, H. & Jang, J. Antibacterial properties of novel poly(methyl methacrylate) nanofiber containing silver nanoparticles. *Langmuir* **24**, 2051-2056 (2008).
35. Tarnavchyk, I. et al. Reactive hydrogel networks for the fabrication of metal–polymer nanocomposites. *Macromol. Rapid Commun.* **30**, 1564-1569 (2009).
36. Kamrupi, I.R. & Dolui, S.K. Synthesis of copper-polystyrene nanocomposite particles using water in supercritical carbon dioxide medium and its antimicrobial activity. *J. Appl. Polym. Sci.* **120**, 1027-1033 (2011).

37. Kong, H., Song, J. & Jang, J. Photocatalytic antibacterial capabilities of TiO2, biocidal polymer nanocomposites synthesized by a surface-initiated photopolymerization. *Environ. Sci. Technol.* **44**, 5672-5676 (2010).
38. biolfilms, R.o.m. (NIH, National Heart, Lung, and Blood Institute, 2002).
39. Henrici, A.T. Studies of freshwater bacteria I. A direct microscopic technique. *J. Bacteriol.* **25**, 277-287 (1933).
40. Heilmann, C. et al. Molecular basis of intercellular adhesion in the biofilm-forming Staphylococcus epidermidis. *Mol. Microbiol.* **20**, 1083-1091 (1996).
41. Heilmann, C., Gerke, C., PerdreauRemington, F. & Gotz, F. Characterization of Tn917 insertion mutants of Staphylococcus epidermidis affected in biofilm formation. *Infect. Immun.* **64**, 277-282 (1996).
42. Cunliffe, D., Smart, C.A., Alexander, C. & Vulfson, E.N. Bacterial adhesion at synthetic surfaces. *Appl. Environ. Microb.* **65**, 4995-5002 (1999).
43. O'Toole, G. & Kaplan, H.B. Biofilm formation as microbial development. *Annu. Rev. Microbiol.* **54**, 49 (2000).
44. Davey, M.E. & O'Toole, G.A. Microbial biofilms: From ecology to molecular genetics. *Microbiol. Mol. Biol. Rev.* **64** (2000).
45. An, Y.H. & Friedman, R.J. Handbook of bacterial adhesion: Principles, methods, and applications. (Humana Pr Inc, 2000).
46. Bos, R., van der Mei, H.C. & Busscher, H.J. Physico-chemistry of initial microbial adhesive interactions-its mechanisms and methods for study. *Fems Microbiol. Rev.* **23**, 179-230 (1999).
47. Lichter, J.A., Van Vliet, K.J. & Rubner, M.F. Design of antibacterial surfaces and interfaces: Polyelectrolyte multilayers as a multifunctional platform. *Macromolecules* **42**, 8573-8586 (2009).
48. Ferreira, L. & Zumbuehl, A. Non-leaching surfaces capable of killing microorganisms on contact. *J. Mater. Chem.* **19**, 7796 (2009).
49. Callow, M.E. & Fletcher, R.L. The influence of low surface energy materials on bioadhesion - A review. *Int. Biodeterior. Biodegrad.* **34**, 333-348 (1994).
50. Donlan, R.M. Biofilms: Microbial life on surfaces. *Emerg. Infecti. Dis.* **8**, 881-890 (2002).
51. Characklis, W.G. & Marshall, K.C. Biofilms. (New York; Chichester: Wiley, 1990).
52. Fletcher, M. & Loeb, G.I. Influence of substratum characteristics on the attachment of a marine pseudomonad to solid surfaces. *Appl. Environ. Microb.* **37**, 67-72 (1979).
53. Pringle, J.H. & Fletcher, M. Influence of substratum wettability on attachment of freshwater bacteria to solid surfaces. *Appl. Environ. Microb.* **45**, 811-817 (1983).
54. Bendinger, B., Rijnaarts, H.H.M., Altendorf, K. & Zehnder, A.J.B. Physicochemical cell surface and adhesive properties of 'coryneform bacteria related to the presence and chain length of mycolic acids. *Appl. Environ. Microb.* **59**, 3973-3977 (1993).
55. Park, K.D. et al. Bacterial adhesion on PEG modified polyurethane surfaces. *Biomaterials* **19**, 851-859 (1998).
56. Boulmedais, F. et al. Polyelectrolyte multilayer films with pegylated polypeptides as a new type of anti-microbial protection for biomaterials. *Biomaterials* **25**, 2003-2011 (2004).

57. Tiller, J.C., Lee, S.B., Lewis, K. & Klibanov, A.M. Polymer surfaces derivatized with poly(vinyl-N-hexylpyridinium) kill airborne and waterborne bacteria. *Biotechnol. Bioeng.* **79**, 465-471 (2002).
58. Palermo, E.F. & Kuroda, K. Structural determinants of antimicrobial activity in polymers which mimic host defense peptides. *Appl. Microbiol. Biotechnol.* **87**, 1605-1615 (2010).
59. Nederberg, F. et al. Biodegradable nanostructures with selective lysis of microbial membranes. *Nat. Chem.* **3**, 409-414 (2011).
60. Kanazawa, A., Ikeda, T. & Endo, T. Polymeric phosphonium salts as as novel class of cationic biocides .5. Sthnthesis and antibacterial activity of polyesters releasing phosphonium biocides *J. Polym. Sci. Pol. Chem.* **31**, 3003-3011 (1993).
61. Nonaka, T., Li, H., Makinose, K., Ogata, T. & Kurihara, S. Synthesis and functions of water-soluble and thermosensitive copolymers having phosphonium groups from acryloyloxyethyl trialkyl phosphonium chloride, N-isopropylacrylamide, and without/with butylmethacrylate. *J. Appl. Polym. Sci.* **90**, 1139-1147 (2003).
62. Lee, S.B. et al. Permanent, nonleaching antibacterial surfaces. 1. Synthesis by atom transfer radical polymerization. *Biomacromolecules* **5**, 877-882 (2004).
63. Hetrick, E.M. & Schoenfisch, M.H. Reducing implant-related infections: Active release strategies. *Chem. Soc. Rev.* **35**, 780-789 (2006).
64. Schierholz, J.M., Steinhauser, H., Rump, A.F.E., Berkels, R. & Pulverer, G. Controlled release of antibiotics from biomedical polyurethanes: Morphological and structural features. *Biomaterials* **18**, 839-844 (1997).
65. Schierholz, J.M. Physico-chemical properties of a rifampicin-releasing polydimethylsiloxane shunt. *Biomaterials* **18**, 635-641 (1997).
66. Southern, E.M. DNA microarrays. History and overview. *Methods Mol. Biol.* **170**, 1-15 (2001).
67. Frank, R. The SPOT synthesis technique. Synthetic peptide arrays on membrane supports-principles and applications. *J. Immunol. Methods* **267**, 13-26 (2002).
68. Hoheisel, J.D., Lennon, G.G., Zehetner, G. & Lehrach, H. Use of high coverage reference libraries of drosophila-melanogaster for relational data-analysis - a step towaords mapping and sequencing of genome. *J. Mol. Biol.* **220**, 903-914 (1991).
69. Erlich, H. et al. HLA-DR, DQ and DP typing using PCR amplification and immobilized probes. *Eur. J. Immunogenet.* **18**, 33-55 (1991).
70. Southern, E.M., Maskos, U. & Elder, J.K. Analyzing and comparing nucleic-acid sequences by hybridazation to arrays of oligonucleotides: Evalution using experimental models *Genomics* **13**, 1008-1017 (1992).
71. Maskos, U. & Southern, E.M. Oligonucleotide hybridizations on glass supports: A novel linker oligobucleotide synthesis and hybridization properties of oligonucleotides synthesized in situ. *Nucleic Acids Res.* **20**, 1679-1684 (1992).
72. Maskos, U. & Southern, E.M. A study of oligonucleotide reasssociation using large arrays of oligonucleotedes synthesized on a glass support *Nucleic Acids Res.* **21**, 4663-4669 (1993).

73. Fodor, S.P.A. et al. Light-directed, spatially addressable parallel chemical synthesis. *Science* **251**, 767-773 (1991).
74. Pease, A.C. et al. Light-generated oligonucleotide arrays for rapid DNA sequence analysis. *Proc. Natl. Acad. Sci. U. S. A.* **91**, 5022-5026 (1994).
75. Frank, R., Guler, S., Krause, S. & Lindenmaier, W. Facile and rapid spot-synthesis of large number of peptides on membrane sheets (Escom Science Publ Bv, Ae Leiden; 1991).
76. Frank, R. Spot-synthesis: an easy technique for the positionally addressable, parallel chemical synthesis on a membrane support. *Tetrahedron* **48**, 9217-9232 (1992).
77. Adames, N., Blundell, K., Ashby, M.N. & Boone, C. Role of Yeast Insulin-Degrading Enzyme Homologs in Propheromone Processing and Bud Site Selection. *Science* **270**, 464-467 (1995).
78. Lashkari, D.A. et al. Yeast microarrays for genome wide parallel genetic and gene expression analysis. *Proc. Natl. Acad. Sci. U. S. A.* **94**, 13057-13062 (1997).
79. Wang, D.N., Liu, S.Y., Trummer, B.J., Deng, C. & Wang, A.L. Carbohydrate microarrays for the recognition of cross-reactive molecular markers of microbes and host cells. *Nat. Biotechnol.* **20**, 275-281 (2002).
80. Feizi, T., Fazio, F., Chai, W. & Wong, C.-H. Carbohydrate microarrays - a new set of technologies at the frontiers of glycomics. *Curr. Opin. Struc. Biol.* **13**, 637-645 (2003).
81. Huang, C.Y. et al. Carbohydrate microarray for profiling the antibodies interacting with Globo H tumor antigen. *Proc. Natl. Acad. Sci. U. S. A.* **103**, 15-20 (2006).
82. MacBeath, G., Koehler, A.N. & Schreiber, S.L. Printing small molecules as microarrays and detecting protein-ligand interactions en masse. *J. Am. Chem. Soc.* **121**, 7967-7968 (1999).
83. Diaz-Mochon, J.J., Tourniaire, G. & Bradley, M. Microarray platforms for enzymatic and cell-based assays. *Chem. Soc. Rev.* **36**, 449-457 (2007).
84. Pernagallo, S., Unciti-Broceta, A., Diaz-Mochon, J.J. & Bradley, M. Deciphering cellular morphology and biocompatibility using polymer microarrays. *Biomed. Mater.* **3**, 034112 (2008).
85. Pernagallo, S., Diaz-Mochon, J.J. & Bradley, M. A cooperative polymer-DNA microarray approach to biomaterial investigation. *Lab Chip* **9**, 397-403 (2009).
86. Svensen, N. et al. Screening of a combinatorial homing peptide library for selective cellular delivery. *Angew. Chem. Int. Ed.* **50**, 6133-6136 (2011).
87. Svensen, N., Diaz-Mochon, J.J. & Bradley, M. Encoded peptide libraries and the discovery of new cell binding ligands. *Chem. Commun.* **47**, 7638-7640 (2011).
88. David, C., Amandine, P., Marie-Anne, D. & Xavier, G. ReviewGene to screen: Cell microarrays in drug discovery. *Drug Discov. Today* **11**, 616-622 (2006).
89. Castel, D., Pitaval, A., Debily, M.-A. & Gidrol, X. Cell microarrays in drug discovery. *Drug Discov. Today* **11**, 616-622 (2006).
90. Tourniaire, G. PhD thesis in School of Chemistry (Univeristy of Edinburgh, Edinburgh; 2006).

91. Mizomoto, H. PhD thesis in School of Chemistry (University of Southampton, Southampton; 2004).
92. How, S.E. et al. Polyplexes and lipoplexes for mammalian gene delivery: From traditional to microarray screening. *Comb. Chem. High Throughput Screen* **7**, 423-430 (2004).
93. Anderson, D.G., Levenberg, S. & Langer, R. Nanoliter-scale synthesis of arrayed biomaterials and application to human embryonic stem cells. *Nat. Biotechnol.* **22**, 863-866 (2004).
94. Tourniaire, G. et al. Polymer microarrays for cellular adhesion. *Chem. Commun.*, 2118-2120 (2006).
95. Jose, A.J. PhD thesis in School of Chemistry (University of Southampton, Southampton; 2005).
96. Thaburet, J.F.O., Mizomoto, H. & Bradley, M. High-throughput evaluation of the wettability of polymer libraries. *Macromol. Rapid Commun.* **25**, 366-370 (2004).
97. Urquhart, A.J. et al. TOF-SIMS analysis of a 576 micropatterned copolymer array to reveal surface moieties that control wettability. *Anal. Chem.* **80**, 135-142 (2008).
98. Anderson, D.G., Putnam, D., Lavik, E.B., Mahmood, T.A. & Langer, R. Biomaterial microarrays: rapid, microscale screening of polymer-cell interaction. *Biomaterials* **26**, 4892-4897 (2005).
99. Mant, A. et al. Polymer microarrays: Identification of substrates for phagocytosis assays. *Biomaterials* **27**, 5299-5306 (2006).
100. Urquhart, A.J. et al. High throughput surface characterisation of a combinatorial material library. *Adv. Mater.* **19**, 2486-2491 (2007).
101. Unciti-Broceta, A., Diaz-Mochon, J.J., Mizomoto, H. & Bradley, M. Combining nebulization-mediated transfection and polymer microarrays for the rapid determination of optimal transfection substrates. *J. Comb. Chem.* **10**, 179-184 (2008).
102. Tare, R.S. et al. A microarray approach to the identification of polyurethanes for the isolation of human skeletal progenitor cells and augmentation of skeletal cell growth. *Biomaterials* **30**, 1045-1055 (2009).
103. Zhang, R., Liberski, A., Khan, F., Diaz-Mochon, J.J. & Bradley, M. Inkjet fabrication of hydrogel microarrays using in situ nanolitre-scale polymerisation. *Chem. Commun.* 1317-1319 (2008).
104. Zhang, R., Liberski, A., Sanchez-Martin, R. & Bradley, M. Microarrays of over 2000 hydrogels - Identification of substrates for cellular trapping and thermally triggered release. *Biomaterials* **30**, 6193-6201 (2009).
105. Liberski, A., Zhang, R. & Bradley, M. Inkjet fabrication of polymer microarrays and grids-solving the evaporation problem. *Chem. Commun.* 334-336 (2009).
106. Mei, Y. et al. Mapping the Interactions among Biomaterials, Adsorbed Proteins, and Human Embryonic Stem Cells. *Adv. Mater.* **21**, 2781-2786 (2009).
107. Khan, F., Tare, R.S., Kanczler, J.M., Oreffo, R.O.C. & Bradley, M. Strategies for cell manipulation and skeletal tissue engineering using high-throughput polymer blend formulation and microarray techniques. *Biomaterials* **31**, 2216-2228 (2010).

108. Mei, Y. et al. Combinatorial development of biomaterials for clonal growth of human pluripotent stem cells. *Nat. Mater.* **9**, 768-778 (2010).
109. Hay, D.C. et al. Unbiased screening of polymer libraries to define novel substrates for functional hepatocytes with inducible drug metabolism. *Stem Cell Res.* **6**, 92-102 (2011).
110. Hansen, A., McMillan, L., Morrison, A., Petrik, J. & Bradley, M. Polymers for the rapid and effective activation and aggregation of platelets. *Biomaterials* **32**, 7034-7041 (2011).
111. Pernagallo, S. et al. The discovery of a novel biopolymers to enhance endothelialisation of intra-vascular devices. *Adv. Health. Mater., accepted* (2012).
112. Yang, J. et al. Polymer surface functionalities that control human embryoid body cell adhesion revealed by high throughput surface characterization of combinatorial material microarrays. *Biomaterials* **31**, 8827-8838 (2010).
113. Tourniaire, G., Diaz-Mochon, J.J. & Bradley, M. Fingerprinting Polymer Microarrays. *Comb. Chem. High Throughput Screen* **12**, 690-696 (2009).
114. Wu, M., Bridle, H. & Bradley, M. Targeting Cryptosporidium parvum capture. *Water Res.* **46**, 1715-1722 (2012).
115. Rieger, B., van den Doel, L.R. & van Vliet, L.J. Ring formation in nanoliter cups: Quantitative measurements of flow in micromachined wells. *Phys. Rev. E. Stat. Nonlin. Soft Matter. Phys.* **68**, 036312 (2003).
116. Morisaki, H. & Tabuchi, H. Bacterial attachment over a wide range of ionic strengths. *Colloid Surf. B-Biointerfaces* **74**, 51-55 (2009).
117. Hoiseth, S.K. & Stocker, B.A.D. Aromatic-dependent *Salmonella typhimurium* are non-virulent and effective as live vaccines. *Nature* **291**, 238-239 (1981).
118. Coburn, B., Grassl, G.A. & Finlay, B.B. *Salmonella*, the host and disease: a brief review. *Immunol. Cell Biol.* **85**, 112-118 (2007).
119. Riley, M. et al. *Escherichia coli* K-12: A cooperatively developed annotation snapshot-2005. *Nucleic Acids Res.* **34**, 1-9 (2006).
120. Kwon, Y.M. & Ricke, S.C. Induction of acid resistance of Salmonella typhimurium by exposure to short-chain fatty acids. *Appl. Environ. Microb.* **64**, 3458-3463 (1998).
121. Examination of federal food safety oversight in the wake of peanut products recall: Hearing before the Committee on Agriculture, Nutrition, and Forestry, United States Senate, One Hundred Eleventh Congress, first session, February 5, 2009. (Washington : U.S. G.P.O., 2010).
122. Trombert, A.N., Berrocal, L., Fuentes, J. & Mora, G. S. Typhimurium sseJ gene decreases the S. Typhi cytotoxicity toward cultured epithelial cells. *BMC Microbiol.* **10**, 312 (2010).
123. D'Haeze, W., Gao, M. & Holsters, M. A gfp reporter plasmid to visualize Azorhizobium caulinodans during nodulation of Sesbania rostrata. *Plasmid* **51**, 185-191 (2004).
124. Heim, R., Cubitt, A.B. & Tsien, R.Y. Improved green fluorescence. *Nature* **373**, 663-664 (1995).
125. Jose, A.J., Wong, L.S., Merrington, J. & Bradley, M. Automated image analysis of polymer beads and size distribution. *Ind. Eng. Chem. Res.* **44**, 8659-8662 (2005).

126. Falguera, V., Quintero, J.P., Jimenez, A., Munoz, J.A. & Ibarz, A. Edible films and coatings: Structures, active functions and trends in their use. *Trends Food Sci. Technol.* **22**, 292-303 (2011).
127. Costerton, J.W., Stewart, P.S. & Greenberg, E.P. Bacterial biofilms: A common cause of persistent infections. *Science* **284**, 1318-1322 (1999).
128. Benvenis, R. & Davies, J. Mechanisms of antibiotic-resistance in bacteria. *Annu. Rev. Biochem.* **42**, 471-506 (1973).
129. Giaouris, E., Chorianopoulos, N. & Nychas, G.J.E. Effect of temperature, pH, and water activity on biofilm formation by Salmonella enterica Enteritidis PT4 on stainless steel surfaces as indicated by the bead vortexing method and conductance measurements. *J. Food Prot.* **68**, 2149-2154 (2005).
130. Thomas, R.J. PhD thesis in School of Biological Science (University of Edinburgh, Edinburgh; 2001).
131. Parkhill, J. et al. The genome sequence of the food-borne pathogen Campylobacter jejuni reveals hypervariable sequences. *Nature* **403**, 665-668 (2000).
132. Sebaihia, M. et al. The multidrug-resistant human pathogen Clostridium difficile has a highly mobile, mosaic genome. *Nat. Genet.* **38**, 779-786 (2006).
133. Gibbons, R.J., Berman, K.S., Knoettner, P. & Kapsimalis, B. Dental caries and alveolar bone loss in gnotobiotic rats infected with capsule forming streptococci of human origin. *Arch. Oral Biol.* **11**, 549-IN544 (1966).
134. Feldman, C. et al. The presence and sequence of endotracheal tube colonization in patients undergoing mechanical ventilation. *Eur. Resp. J.* **13**, 546-551 (1999).
135. Tleyjeh, I.M. et al. Temporal trends in infective endocarditis - A population-based study in Olmsted County, Minnesota. *JAMA-J. Am. Med. Assoc.* **293**, 3022-3028 (2005).
136. Lacassin, F. et al. Procedures associated with infective endocarditis in adults - A case control study. *Eur. Heart J.* **16**, 1968-1974 (1995).
137. Young, K.T., Davis, L.M. & DiRita, V.J. Campylobacter jejuni: molecular biology and pathogenesis. *Nat. Rev. Microb.* **5**, 665-679 (2007).
138. Wilson, D.J. et al. Tracing the source of Campylobacteriosis. *PLoS Genet.* **4**, e1000203 (2008).
139. Musgrave, C.R., Bookstaver, P.B., Sutton, S.S. & Miller, A.D. Use of alternative or adjuvant pharmacologic treatment strategies in the prevention and treatment of Clostridium difficile infection. *Int. J. Infect. Dis.* **15**, 438-448 (2011).
140. Wroe, A.J. Immune response to Clostridium difficile infection and an investigation of the mechanisms of moxifloxacin resistance in clinical C. difficile isolates (2009).
141. Uzal, F.A. et al. Clostridium perfringens type C and Clostridium difficile co-infection in foals. *Vet. Microbiol.* **156**, 395-402 (2012).
142. Johnson, S. et al. Fatal Pseudomembranous Colitis associated with a variant Clostridium difficile strain not detected by toxin A immunoassay. *Ann. Intern. Med.* **135**, 434-438 (2001).
143. Paredes-Sabja, D. & Sarker, M.R. Germination response of spores of the pathogenic bacterium Clostridium perfringens and Clostridium difficile to cultured human epithelial cells. *Anaerobe* **17**, 78-84 (2011).

144. Canard, B. & Cole, S.T. Genome organization of the anaerobic pathogen Clostridium perfringens. *Proc. Natl. Acad. Sci. U. S. A.* **86**, 6676-6680 (1989).
145. Kennedy, C.L. et al. Cross-complementation of Clostridium perfringens PLC and Clostridium septicum alpha-toxin mutants reveals PLC is sufficient to mediate gas gangrene. *Microbes Infect.* **11**, 413-418 (2009).
146. Bryant, A.E. et al. Clostridial gas gangrene. II. Phospholipase C-induced activation of platelet gpIIbIIIa mediates vascular occlusion and myonecrosis in Clostridium perfringens gas gangrene. *J. Infecti. Dis.* **182**, 808-815 (2000).
147. Merritt, J. & Qi, F. The mutacins of Streptococcus mutans: regulation and ecology. *Mol. Oral Microbiol.* **27**, 57-69 (2012).
148. Younson, J. & Kelly, C. The rational design of an anti-caries peptide against Streptococcus mutans. *Mol. Divers.* **8**, 121-126 (2004).
149. Gussy, M.G., Waters, E.G., Walsh, O. & Kilpatrick, N.M. Early childhood caries: Current evidence for aetiology and prevention. *J. Paediatr. Child Health* **42**, 37-43 (2006).
150. Jukka, H.M. & Lisa, G.n. Review: Oral and dental health care of oral cancer patients: hyposalivation, caries and infections. *Oral Oncol.* **46**, 464-467 (2010).
151. Podschun, R. & Ullmann, U. Klebsiella spp. as nosocomial pathogens: Epidemiology, taxonomy, typing methods, and pathogenicity factors. *Clin. Microbiol. Rev.* **11**, 589-603 (1998).
152. Brisse, S. & Verhoef, J. Phylogenetic diversity of Klebsiella pneumoniae and Klebsiella oxytoca clinical isolates revealed by randomly amplified polymorphic DNA, gyrA and parC genes sequencing and automated ribotyping. *Int. J. Syst. Evol. Microb.* **51**, 915-924 (2001).
153. Wang, J.-H. et al. Primary liver abscess due to Klebsiella pneumoniae in Taiwan. *Clin. Infect. Dis.* **26**, 1434-1438 (1998).
154. Raz, R., Colodner, R. & Kunin, C.M. Who are you - Staphylococcus saprophyticus? *Clin. Infect. Dis.* **40**, 896-898 (2005).
155. Gupta, K., Hooton, T.M., Wobbe, C.L. & Stamm, W.E. The prevalence of antimicrobial resistance among uropathogens causing acute uncomplicated cystitis in young women. *Int. J. Antimicrob. Ag.* **11**, 305-308 (1999).
156. Nickerson, E.K., West, T.E., Day, N.P. & Peacock, S.J. Staphylococcus aureus disease and drug resistance in resource-limited countries in south and east Asia. *Lancet Infect. Dis.* **9**, 130-135 (2009).
157. Schwartz, K. & Nourse, C. Panton-Valentine leukocidin-associated Staphylococcus aureus necrotizing pneumonia in infants: a report of four cases and review of the literature. *Eur. J. Pediatr.* **171**, 711-717 (2012).
158. Kahl, B.C. Impact of Staphylococcus aureus on the pathogenesis of chronic cystic fibrosis lung disease. *Int. J. Med. Microb.* **300**, 514-519 (2010).
159. Murray, B.E. Diversity among multidrug-resistant Enterococci. *Emerg. Infect. Dis.* **4**, 37 (1998).
160. Lahiri, S.D., Zhang, G., Dunaway-Mariano, D. & Allen, K.N. The pentacovalent phosphorus intermediate of a phosphoryl transfer reaction. *Science* **299**, 2067-2071 (2003).
161. Macovei, L. & Zurek, L. Ecology of antibiotic resistance genes: Characterization of Enterococci from houseflies collected in food settings. *Appl. Environ. Microb.* **72**, 4028-4035 (2006).

162. Murray, B.E. The life and times of the Enterococcus. *Clin. Microbiol. Rev.* **3**, 46-65 (1990).
163. Tsigrelis, C., Singh, K.V., Coutinho, T.D., Murray, B.E. & Baddour, L.M. Vancomycin-resistant Enterococcus faecalis Endocarditis: Linezolid failure and strain characterization of virulence factors. *J. Clin. Microb.* **45**, 631-635 (2007).
164. Pernagallo, S., Wu, M., Gallagher, M.P. & Bradley, M. Colonising new frontiers-microarrays reveal biofilm modulating polymers. *J. Mater. Chem.* **21**, 96-101 (2011).
165. Snelling, W.J. et al. Cryptosporidiosis in developing countries. *J. Infect. Dev. Ctries.* **1**, 242-256 (2007).
166. Casemore, D.P., Hoyle, B., Tynan, P. & Smith, M.S. in Cryptosporidium: the Analytical Challenge. (eds. M. Smith & K.C. Thompson) 73-83 (Royal Soc Chemistry, Cambridge; 2001).
167. Smith, H.V. & Nichols, R.A.B. Cryptosporidium: Detection in water and food. *Exp. Parasitol.*, 61-79 (2010).
168. Davies, A.P. & Chalmers, R.M. Cryptosporidiosis. *Br. Med. J.* **339**, b4168 (2009).
169. Mackenzie, W.R. et al. A massive outbreak in milwaukee of Cryptosporidium infection transmitted through the public water-supply. *N. Engl. J. Med.* **331**, 161-167 (1994).
170. Ng, J.S.Y., Pingault, N., Gibbs, R., Koehler, A. & Ryan, U. Molecular characterisation of Cryptosporidium outbreaks in Western and South Australia. *Exp. Parasitol.* **125**, 325-328 (2010).
171. Smittskyddsinstitutet (news archive SMI, 2011).
172. Santin, M. & Fayer, R. Intragenotypic variations in the Cryptosporidium sp cervine genotype from sheep with implications for public health. *J. Parasitol.* **93**, 668-672 (2007).
173. Abrahamsen, M.S. et al. Complete genome sequence of the apicomplexan, Cryptosporidium parvum. *Science* **304**, 441-445 (2004).
174. Tufenkji, N., Dixon, D.R., Considine, R. & Drummond, C.J. Multi-scale Cryptosporidium/sand interactions in water treatment. *Water Res.* **40**, 3315-3331 (2006).
175. Dai, X., Boll, J., Hayes, M.E. & Aston, D.E. Adhesion of Cryptosporidium parvum and Giardia lamblia to solid surfaces: the role of surface charge and hydrophobicity. *Colloid Surf. B-Biointerfaces* **34**, 259-263 (2004).
176. Gao, X. & Chorover, J. In-situ monitoring of Cryptosporidium parvum oocyst surface adhesion using ATR-FTIR spectroscopy. *Colloid Surf. B-Biointerfaces* **71**, 169-176 (2009).
177. Kuznar, Z.A. & Elimelech, M. Adhesion kinetics of viable Cryptosporidium parvum oocysts to quartz surfaces. *Environ. Sci. Technol.* **38**, 6839-6845 (2004).
178. Janjaroen, D., Liu, Y., Kuhlenschmidt, M.S., Kuhlenschmidt, T.B. & Nguyen, T.H. Role of divalent cations on deposition of Cryptosporidium parvum oocysts on natural organic matter surfaces. *Environ. Sci. Technol.* **44**, 4519-4524 (2010).

179. Searcy, K.E., Packman, A.I., Atwill, E.R. & Harter, T. Association of Cryptosporidium parvum with suspended particles: Impact on oocyst sedimentation. *Appl. Environ. Microb.* **71**, 1072-1078 (2005).
180. Walker, M.J. Sorption of Cryptosporidium parvum Oocysts in Aqueous Solution to Metal Oxide and Hydrophobic Substrates. *Environ. Sci. Technol.* **33**, 3134-3139 (1999).
181. Liu, Y., Kuhlenschmidt, M.S., Kuhlenschmidt, T.B. & Nguyen, T.H. Composition and conformation of Cryptosporidium parvum oocyst wallsurface macromolecules and their effect on adhesion kinetics of oocysts on quartz surface. *Biomacromolecules* **11**, 2109-2115 (2010).
182. Byrd, T.L. & Walz, J.Y. Investigation of the interaction force between Cryptosporidium parvum oocysts and solid surfaces. *Langmuir* **23**, 7475-7483 (2007).
183. Searcy, K.E., Packman, A.I., Atwill, E.R. & Harter, T. Capture and retention of Cryptosporidium parvum oocysts by Pseudomonas aeruginosa biofilms. *Appl. Environ. Microb.* **72**, 6242-6247 (2006).
184. Bazaka, K., Jacob, M.V., Crawford, R.J. & Ivanova, E.P. Plasma-assisted surface modification of organic biopolymers to prevent bacterial attachment. *Acta Biomater.* **7**, 2015-2028 (2011).
185. Considine, R.F., Dixon, D.R. & Drummond, C.J. Laterally-resolved force microscopy of biological microspheres-oocysts of Cryptosporidium parvum. *Langmuir* **16**, 1323-1330 (2000).
186. Whitehead, K.A., Colligon, J. & Verran, J. Retention of microbial cells in substratum surface features of micrometer and sub-micrometer dimensions. *Colloid Surf. B-Biointerfaces* **41**, 129-138 (2005).
187. van de Wetering, P. et al. A mechanistic study of the hydrolytic stability of poly(2-(dimethylamino)ethyl methacrylate). *Macromolecules* **31**, 8063-8068 (1998).
188. Grasso, D., Subramaniam, K., Butkus, M., Strevett, K. & Bergendahl, J. A review of non-DLVO interactions in environmental colloidal systems. *Rev. Environ. Sci. Biotechnol.* **1**, 17-38 (2002).
189. Poitras, C., Fatisson, J. & Tufenkji, N. Real-time microgravimetric quantification of Cryptosporidium parvum in the presence of potential interferents. *Water Res.* **43**, 2631-2638 (2009).
190. Caccio, S.M., Thompson, R.C., McLauchlin, J. & Smith, H.V. Unravelling Cryptosporidium and Giardia epidemiology. *Trends Parasitol.* **21**, 430-437 (2005).
191. Heresi, G.P., Murphy, J.R. & Cleary, T.G. Giardiasis. *Semin. Pediatr. Infect. Dis.* **11**, 189-195 (2000).
192. Owen, R.L. The ultrastructural basis of Giardia function. *Trans. Roy. Soc. Trop. Med. Hyg.* **74**, 429-433 (1980).
193. Falk, C.C., Karanis, P., Schoenen, D. & Seitz, H.M. Bench scale experiments for the evaluation of a membrane filtration method for the recovery efficiency of Giardia and Cryptosporidium from water. *Water Res.* **32**, 565-568 (1998).
194. Farthing, M.J.G. in Giardia: From molecules to disease. (eds. R.C.A. Thompson, J.A. Reynoldson & A.J. Lymbery) 15-37 (CABI Publishing, Wallingford, UK; 1994).

195. Jephcott, A.E., Begg, N.T. & Baker, I.A. Outbreak of giardiasis associated with mains water in the United Kingdom. *Lancet* **1**, 730-732 (1986).
196. Lebwohl, B., Deckelbaum, R.J. & Green, P.H.R. Giardiasis. *Gastrointest. Endosc.* **57**, 906-913 (2003).
197. Nygard, K. et al. A large community outbreak of waterborne giardiasis-delayed detection in a non-endemic urban area. *BMC Public Health* **6**, 141 (2006).
198. Ortega, Y.R. & Adam, R.D. Giardia: overview and update. *Clin. Infect. Dis.* **25**, 545-549 (1997).
199. Thompson, R.C.A. Giardiasis as a re-emerging infectious disease and its zoonotic potential. *Int. J. Parasitol.* **30**, 1259-1267 (2000).
200. Reiner, D.S. PhD thesis in Department of Microbiology, Tumour and cell biology (Karolinska Institutet, Stockholm; 2008).
201. Manning, P., Erlandsen, S.L. & Jarroll, E.L. Carbohydrate and amino acid analyses of Giardia muris cysts. *J. Protozool.* **39**, 290-296 (1992).
202. Gerwig, G.J. et al. The Giardia intestinalis filamentous cyst wall contains a novel beta(1-3)-N-acetyl-D-galactosamine polymer: a structural and conformational study. *Glycobiology* **12**, 499-505 (2002).
203. Chatterjee, A. et al. Giardia cyst wall protein 1 is a lectin that binds to curled fibrils of the GalNAc homopolymer. *PLoS Pathog* **6** (2010).
204. Dai, X. & Boll, J. Evaluation of attachment of Cryptosporidium parvum and Giardia lamblia to soil particles. *J. Environ. Qual.* **32**, 296-304 (2003).
205. Ongerth, J.E., Johnson, R.L., Macdonald, S.C., Frost, F. & Stibbs, H.H. Backcountry Water Treatment to Prevent Giardiasis. *Am. J. Public Health* **79**, 1633-1637 (1989).
206. Deng, M.Y. & Cliver, D.O. Degradation of Giardia lambia cysts in mixed human and swine wates. *Appl. Environ. Microb.* **58**, 2368-2374 (1992).
207. Schupp, D.G. & Erlandsen, S.L. Determination of Giardia muris cyst viability by differential interference contrast, phase, or brightfield microscopy *J. Parasitol.* **73**, 723-729 (1987).
208. Cheng, H.P. & Walker, G.C. Succinoglycan is required for initiation and elongation of infection threads during nodulation of alfalfa by Rhizobium meliloti. *J. Bacteriol.* **180**, 5183-5191 (1998).

Appendix I: Polyacrylate library

List of polyacrylates used in this thesis with their corresponding monomers and monomer ratio in the synthesis.

PA	Monomer (1)	Monomer (2)	Monomer (3) or functional amine	Monomer ratio (%)		
				Monomer (1)	Monomer (2)	Monomer (3)
1	St	DEAA	-	90	10	-
2	St	DEAA	-	70	30	-
3	St	DEAA	-	50	50	-
4	St	DMAA	-	90	10	-
5	St	DMAA	-	70	30	-
6	St	DMAA	-	50	50	-
7	St	NiPAA	-	90	10	-
8	St	NiPAA	-	70	30	-
9	St	NiPAA	-	50	50	-
10	MMA	DEAA	-	90	10	-
11	MMA	DEAA	-	70	30	-
12	MMA	DEAA	-	50	50	-
13	MMA	DMAA	-	90	10	-
14	MMA	DMAA	-	70	30	-
15	MMA	DMAA	-	50	50	-
16	MMA	NiPAA	-	90	10	-
17	MMA	NiPAA	-	70	30	-
18	MMA	NiPAA	-	50	50	-
19	MEMA	DEAA	-	90	10	-
20	MEMA	DEAA	-	70	30	-
21	MEMA	DEAA	-	50	50	-
22	MEMA	DMAA	-	90	10	-
23	MEMA	DMAA	-	70	30	-
24	MEMA	DMAA	-	50	50	-
25	MEMA	NiPAA	-	90	10	-
26	MEMA	NiPAA	-	70	30	-
27	MEMA	NiPAA	-	50	50	-
28	MEA	DEAA	-	90	10	-
29	MEA	DEAA	-	70	30	-
30	MEA	DEAA	-	50	50	-
31	MEA	DMAA	-	90	10	-
32	MEA	DMAA	-	70	30	-
33	MEA	DMAA	-	50	50	-
34	MEA	NiPAA	-	90	10	-
35	MEA	NiPAA	-	70	30	-
36	MEA	NiPAA	-	50	50	-
37	HEMA	DEAA	-	90	10	-
38	HEMA	DEAA	-	70	30	-
39	HEMA	DEAA	-	50	50	-
40	HEMA	DMAA	-	90	10	-
41	HEMA	DMAA	-	70	30	-
42	HEMA	DMAA	-	50	50	-
43	HEMA	NiPAA	-	90	10	-
44	HEMA	NiPAA	-	70	30	-
45	HEMA	NiPAA	-	50	50	-
46	HPMA	DEAA	-	90	10	-
47	HPMA	DEAA	-	70	30	-
48	HPMA	DEAA	-	50	50	-
49	HPMA	DMAA	-	90	10	-
50	HPMA	DMAA	-	70	30	-
51	HPMA	DMAA	-	50	50	-
52	HPMA	NiPAA	-	90	10	-
53	HPMA	NiPAA	-	70	30	-
54	HPMA	NiPAA	-	50	50	-
55	HBMA	DEAA	-	90	10	-
56	HBMA	DEAA	-	70	30	-
57	HBMA	DEAA	-	50	50	-
58	HBMA	DMAA	-	90	10	-

PA	Monomer (1)	Monomer (2)	Monomer (3) or functional amine	Monomer ratio (%)		
				Monomer (1)	Monomer (2)	Monomer (3)
59	HBMA	DMAA	-	70	30	-
60	HBMA	DMAA	-	50	50	-
61	HBMA	NiPAA	-	90	10	-
62	HBMA	NiPAA	-	70	30	-
63	HBMA	NiPAA	-	50	50	-
96	MEMA	DEAEMA	-	90	10	-
97	MEMA	DEAEMA	-	70	30	-
98	MEMA	DEAEMA	-	50	50	-
99	MEMA	DMAEMA	-	90	10	-
100	MEMA	DMAEMA	-	70	30	-
101	MEMA	DMAEMA	-	50	50	-
102	MEMA	DEAEA	-	90	10	-
103	MEMA	DEAEA	-	70	30	-
104	MEMA	DEAEA	-	50	50	-
105	MEMA	DMAEA	-	90	10	-
106	MEMA	DMAEA	-	70	30	-
107	MEMA	DMAEA	-	50	50	-
108	MEMA	MTEMA	-	90	10	-
109	MEMA	MTEMA	-	70	30	-
110	MEMA	MTEMA	-	50	50	-
111	MEMA	BAEMA	-	90	10	-
112	MEMA	BAEMA	-	70	30	-
113	MEMA	BAEMA	-	50	50	-
114	MEMA	DMAPMAA	-	90	10	-
115	MEMA	DMAPMAA	-	70	30	-
116	MEMA	DMAPMAA	-	50	50	-
117	MEMA	BACOEA	-	90	10	-
118	MEMA	BACOEA	-	70	30	-
119	MEMA	BACOEA	-	50	50	-
120	MEMA	DMVBA	-	90	10	-
121	MEMA	DMVBA	-	70	30	-
122	MEMA	DMVBA	-	50	50	-
123	MEMA	VAA	-	90	10	-
124	MEMA	VAA	-	70	30	-
125	MEMA	VAA	-	50	50	-
126	MEMA	VI	-	90	10	-
127	MEMA	VI	-	70	30	-
128	MEMA	VI	-	50	50	-
129	MEMA	VPNO	-	90	10	-
130	MEMA	VPNO	-	70	30	-
131	MEMA	VPNO	-	50	50	-
132	MEMA	VP-4	-	90	10	-
133	MEMA	VP-4	-	70	30	-
134	MEMA	VP-4	-	50	50	-
135	MEMA	VP-2	-	90	10	-
136	MEMA	VP-2	-	70	30	-
137	MEMA	VP-2	-	50	50	-
138	MEMA	DAAA	-	90	10	-
139	MEMA	DAAA	-	70	30	-
140	MEMA	DAAA	-	50	50	-
141	MEMA	MNPMA	-	90	10	-
142	MEMA	MNPMA	-	70	30	-
143	MEMA	MNPMA	-	50	50	-
150	HEMA	DEAEMA	-	90	10	-
152	HEMA	DEAEMA	-	50	50	-
153	HEMA	DMAEMA	-	90	10	-
154	HEMA	DMAEMA	-	70	30	-
155	HEMA	DMAEMA	-	50	50	-
156	HEMA	DEAEA	-	90	10	-
157	HEMA	DEAEA	-	70	30	-
158	HEMA	DEAEA	-	50	50	-
159	HEMA	DMAEA	-	90	10	-
160	HEMA	DMAEA	-	70	30	-
161	HEMA	DMAEA	-	50	50	-
162	HEMA	MTEMA	-	90	10	-
163	HEMA	MTEMA	-	70	30	-
164	HEMA	MTEMA	-	50	50	-

PA	Monomer (1)	Monomer (2)	Monomer (3) or functional amine	Monomer ratio (%)		
				Monomer (1)	Monomer (2)	Monomer (3)
165	HEMA	BAEMA	-	90	10	-
167	HEMA	BAEMA	-	50	50	-
168	HEMA	DMAPMAA	-	90	10	-
169	HEMA	DMAPMAA	-	70	30	-
170	HEMA	DMAPMAA	-	50	50	-
171	HEMA	BACOEA	-	90	10	-
172	HEMA	BACOEA	-	70	30	-
173	HEMA	BACOEA	-	50	50	-
174	HEMA	DMVBA	-	90	10	-
175	HEMA	DMVBA	-	70	30	-
176	HEMA	DMVBA	-	50	50	-
177	HEMA	VAA	-	90	10	-
178	HEMA	VAA	-	70	30	-
179	HEMA	VAA	-	50	50	-
180	HEMA	VI	-	90	10	-
181	HEMA	VI	-	70	30	-
182	HEMA	VI	-	50	50	-
183	HEMA	VPNO	-	90	10	-
184	HEMA	VPNO	-	70	30	-
185	HEMA	VPNO	-	50	50	-
186	HEMA	VP-4	-	90	10	-
187	HEMA	VP-4	-	70	30	-
188	HEMA	VP-4	-	50	50	-
189	HEMA	VP-2	-	90	10	-
190	HEMA	VP-2	-	70	30	-
191	HEMA	VP-2	-	50	50	-
192	HEMA	DAAA	-	90	10	-
193	HEMA	DAAA	-	70	30	-
194	HEMA	DAAA	-	50	50	-
195	HEMA	MNPMA	-	90	10	-
196	HEMA	MNPMA	-	70	30	-
197	HEMA	MNPMA	-	50	50	-
198	MMA	A-H	-	90	10	-
199	MMA	A-H	-	70	30	-
200	MMA	A-H	-	50	50	-
201	MMA	AES-H	-	90	10	-
202	MMA	AES-H	-	70	30	-
203	MMA	AES-H	-	50	50	-
204	MMA	MA-H	-	90	10	-
205	MMA	MA-H	-	70	30	-
206	MMA	MA-H	-	50	50	-
207	MMA	AAG-H	-	90	10	-
208	MMA	AAG-H	-	70	30	-
209	MMA	AAG-H	-	50	50	-
210	MMA	EGMP-H	-	90	10	-
213	MEMA	A-H	-	90	10	-
214	MEMA	A-H	-	70	30	-
215	MEMA	A-H	-	50	50	-
216	MEMA	AES-H	-	90	10	-
218	MEMA	AES-H	-	50	50	-
219	MEMA	MA-H	-	90	10	-
220	MEMA	MA-H	-	70	30	-
221	MEMA	MA-H	-	50	50	-
222	MEMA	AAG-H	-	90	10	-
223	MEMA	AAG-H	-	70	30	-
224	MEMA	AAG-H	-	50	50	-
225	MEMA	EGMP-H	-	90	10	-
226	MEMA	EGMP-H	-	70	30	-
227	MEMA	EGMP-H	-	50	50	-
228	MMA	A-H	DEAEMA	70	20	10
229	MMA	A-H	DEAEMA	70	15	15
230	MMA	A-H	DEAEMA	70	10	20
231	MMA	A-H	DEAEA	70	20	10
232	MMA	A-H	DEAEA	70	15	15
233	MMA	A-H	DEAEA	70	10	20
234	MMA	MA-H	DEAEMA	70	20	10
235	MMA	MA-H	DEAEMA	70	15	15

PA	Monomer (1)	Monomer (2)	Monomer (3) or functional amine	Monomer ratio (%)		
				Monomer (1)	Monomer (2)	Monomer (3)
236	MMA	MA-H	DEAEMA	70	10	20
237	MMA	MA-H	DEAEA	70	20	10
238	MMA	MA-H	DEAEA	70	15	15
240	MEMA	A-H	DEAEMA	70	20	10
241	MEMA	A-H	DEAEMA	70	15	15
242	MEMA	A-H	DEAEMA	70	10	20
243	MEMA	A-H	DEAEA	70	20	10
244	MEMA	A-H	DEAEA	70	15	15
245	MEMA	A-H	DEAEA	70	10	20
246	MEMA	MA-H	DEAEMA	70	20	10
247	MEMA	MA-H	DEAEMA	70	15	15
248	MEMA	MA-H	DEAEMA	70	10	20
249	MEMA	MA-H	DEAEA	70	20	10
250	MEMA	MA-H	DEAEA	70	15	15
251	MEMA	MA-H	DEAEA	70	10	20
252	MEMA	GMA	-	90	10	-
253	MEMA	GMA	-	70	30	-
254	MEMA	GMA	-	50	50	-
255	MEMA	GMA	DnBA	90	10	-
256	MEMA	GMA	DnBA	70	30	-
257	MEMA	GMA	DnBA	50	50	-
258	MEMA	GMA	DnHA	90	10	-
259	MEMA	GMA	DnHA	70	30	-
260	MEMA	GMA	DnHA	50	50	-
261	MEMA	GMA	DcHA	90	10	-
262	MEMA	GMA	DcHA	70	30	-
264	MEMA	GMA	DBnA	90	10	-
265	MEMA	GMA	DBnA	70	30	-
266	MEMA	GMA	DBnA	50	50	-
267	MEMA	GMA	MnHA	90	10	-
268	MEMA	GMA	MnHA	70	30	-
270	MEMA	GMA	cHMA	90	10	-
271	MEMA	GMA	cHMA	70	30	-
273	MEMA	GMA	BnMA	90	10	-
274	MEMA	GMA	BnMA	70	30	-
276	MEMA	GMA	MAEPy	90	10	-
277	MEMA	GMA	MAEPy	70	30	-
279	MEMA	GMA	Pyrle	90	10	-
280	MEMA	GMA	Pyrle	70	30	-
281	MEMA	GMA	Pyrle	50	50	-
285	MEMA	GMA	MAn	90	10	-
291	MEMA	GMA	DEMEDA	90	10	-
296	MEMA	GMA	TMPDA	50	50	-
303	MMA	GMA	-	90	10	-
304	MMA	GMA	-	70	30	-
305	MMA	GMA	-	50	50	-
306	MMA	GMA	DnBA	90	10	-
307	MMA	GMA	DnBA	70	30	-
309	MMA	GMA	DnHA	90	10	-
313	MMA	GMA	DcHA	70	30	-
315	MMA	GMA	DBnA	90	10	-
316	MMA	GMA	DBnA	70	30	-
317	MMA	GMA	DBnA	50	50	-
318	MMA	GMA	MnHA	90	10	-
319	MMA	GMA	MnHA	70	30	-
320	MMA	GMA	MnHA	50	50	-
321	MMA	GMA	cHMA	90	10	-
322	MMA	GMA	cHMA	70	30	-
323	MMA	GMA	cHMA	50	50	-
324	MMA	GMA	BnMA	90	10	-
325	MMA	GMA	BnMA	70	30	-
326	MMA	GMA	BnMA	50	50	-
327	MMA	GMA	MAEPy	90	10	-
329	MMA	GMA	MAEPy	50	50	-
330	MMA	GMA	Pyrle	90	10	-
331	MMA	GMA	Pyrle	70	30	-
332	MMA	GMA	Pyrle	50	50	-

PA	Monomer (1)	Monomer (2)	Monomer (3) or functional amine	Monomer ratio (%)		
				Monomer (1)	Monomer (2)	Monomer (3)
335	MMA	GMA	2-MAPy	50	50	-
336	MMA	GMA	MAn	90	10	-
337	MMA	GMA	MAn	70	30	-
338	MMA	GMA	MAn	50	50	-
339	MMA	GMA	TMEDA	90	10	-
340	MMA	GMA	TMEDA	70	30	-
341	MMA	GMA	TMEDA	50	50	-
342	MMA	GMA	DEMEDA	90	10	-
345	MMA	GMA	TMPDA	90	10	-
346	MMA	GMA	TMPDA	70	30	-
348	MMA	GMA	Mpi	90	10	-
349	MMA	GMA	Mpi	70	30	-
354	MMA	DEAEMA	-	90	10	-
355	MMA	DEAEMA	-	70	30	-
356	MMA	DEAEMA	-	50	50	-
357	MMA	DMAEMA	-	90	10	-
358	MMA	DMAEMA	-	70	30	-
359	MMA	DMAEMA	-	50	50	-
360	MMA	DEAEA	-	90	10	-
361	MMA	DEAEA	-	70	30	-
363	MMA	DMAEA	-	90	10	-
364	MMA	DMAEA	-	70	30	-
365	MMA	DMAEA	-	50	50	-
366	HPMA	DEAEMA	-	90	10	-
367	HPMA	DEAEMA	-	70	30	-
368	HPMA	DEAEMA	-	50	50	-
369	HPMA	DMAEMA	-	90	10	-
370	HPMA	DMAEMA	-	70	30	-
371	HPMA	DMAEMA	-	50	50	-
372	HPMA	DEAEA	-	90	10	-
373	HPMA	DEAEA	-	70	30	-
374	HPMA	DEAEA	-	50	50	-
375	HPMA	DMAEA	-	90	10	-
376	HPMA	DMAEA	-	70	30	-
377	HPMA	DMAEA	-	50	50	-
378	HBMA	DEAEMA	-	90	10	-
381	HBMA	DMAEMA	-	90	10	-
384	HBMA	DEAEA	-	90	10	-
385	HBMA	DEAEA	-	70	30	-
386	HBMA	DEAEA	-	50	50	-
387	HBMA	DMAEA	-	90	10	-
388	HBMA	DMAEA	-	70	30	-
389	HBMA	DMAEA	-	50	50	-
390	EMA	DEAEMA	-	90	10	-
391	EMA	DEAEMA	-	70	30	-
392	EMA	DEAEMA	-	50	50	-
393	EMA	DMAEMA	-	90	10	-
394	EMA	DMAEMA	-	70	30	-
395	EMA	DMAEMA	-	50	50	-
396	EMA	DEAEA	-	90	10	-
397	EMA	DEAEA	-	70	30	-
398	EMA	DEAEA	-	50	50	-
399	EMA	DMAEA	-	90	10	-
400	EMA	DMAEA	-	70	30	-
401	EMA	DMAEA	-	50	50	-
402	BMA	DEAEMA	-	90	10	-
403	BMA	DEAEMA	-	70	30	-
404	BMA	DEAEMA	-	50	50	-
405	BMA	DMAEMA	-	90	10	-
406	BMA	DMAEMA	-	70	30	-
407	BMA	DMAEMA	-	50	50	-
408	BMA	DEAEA	-	90	10	-
410	BMA	DEAEA	-	50	50	-
411	BMA	DMAEA	-	90	10	-
412	BMA	DMAEA	-	70	30	-
413	BMA	DMAEA	-	50	50	-
414	MEMA	DEAEMA	MA	40	30	30

PA	Monomer (1)	Monomer (2)	Monomer (3) or functional amine	Monomer ratio (%)		
				Monomer (1)	Monomer (2)	Monomer (3)
415	MEMA	DEAEMA	MA	60	10	30
416	MEMA	DEAEMA	MA	60	30	10
417	MEMA	DEAEMA	MA	80	10	10
418	MEMA	DEAEA	MA	40	30	30
419	MEMA	DEAEA	MA	60	10	30
420	MEMA	DEAEA	MA	60	30	10
421	MEMA	DEAEA	MA	80	10	10
422	MEMA	DEAEMA	BMA	40	30	30
423	MEMA	DEAEMA	BMA	60	10	30
424	MEMA	DEAEMA	BMA	60	30	10
425	MEMA	DEAEMA	BMA	80	10	10
426	MEMA	DEAEA	BMA	40	30	30
427	MEMA	DEAEA	BMA	60	10	30
428	MEMA	DEAEA	BMA	60	30	10
429	MEMA	DEAEA	BMA	80	10	10
430	MEMA	DEAEMA	MEA	40	30	30
431	MEMA	DEAEMA	MEA	60	10	30
432	MEMA	DEAEMA	MEA	60	30	10
433	MEMA	DEAEMA	MEA	80	10	10
434	MEMA	DEAEA	MEA	40	30	30
435	MEMA	DEAEA	MEA	60	10	30
436	MEMA	DEAEA	MEA	60	30	10
437	MEMA	DEAEA	MEA	80	10	10
442	MEMA	DEAEA	DEGMEMA	40	30	30
443	MEMA	DEAEA	DEGMEMA	60	10	30
444	MEMA	DEAEA	DEGMEMA	60	30	10
445	MEMA	DEAEA	DEGMEMA	80	10	10
446	MEMA	DEAEMA	THFFA	40	30	30
447	MEMA	DEAEMA	THFFA	60	10	30
448	MEMA	DEAEMA	THFFA	60	30	10
449	MEMA	DEAEMA	THFFA	80	10	10
450	MEMA	DEAEA	THFFA	40	30	30
451	MEMA	DEAEA	THFFA	60	10	30
452	MEMA	DEAEA	THFFA	60	30	10
453	MEMA	DEAEA	THFFA	80	10	10
454	MEMA	DEAEMA	THFFMA	40	30	30
455	MEMA	DEAEMA	THFFMA	60	10	30
457	MEMA	DEAEMA	THFFMA	80	10	10
458	MEMA	DEAEA	THFFMA	40	30	30
459	MEMA	DEAEA	THFFMA	60	10	30
460	MEMA	DEAEA	THFFMA	60	30	10
461	MEMA	DEAEA	THFFMA	80	10	10
462	MEMA	DEAEMA	HEA	40	30	30
463	MEMA	DEAEMA	HEA	60	10	30
464	MEMA	DEAEMA	HEA	60	30	10
465	MEMA	DEAEMA	HEA	80	10	10
467	MEMA	DEAEA	HEA	60	10	30
468	MEMA	DEAEA	HEA	60	30	10
469	MEMA	DEAEA	HEA	80	10	10
470	MEMA	DEAEMA	HEMA	40	30	30
474	MEMA	DEAEA	HEMA	40	30	30
475	MEMA	DEAEA	HEMA	60	10	30
476	MEMA	DEAEA	HEMA	60	30	10
477	MEMA	DEAEA	HEMA	80	10	10
478	MEMA	DEAEMA	A-H	40	30	30
480	MEMA	DEAEMA	A-H	60	30	10
481	MEMA	DEAEMA	A-H	80	10	10
482	MEMA	DEAEA	A-H	40	30	30
483	MEMA	DEAEA	A-H	60	10	30
484	MEMA	DEAEA	A-H	60	30	10
485	MEMA	DEAEA	A-H	80	10	10
486	MEMA	DEAEMA	MA-H	40	30	30
488	MEMA	DEAEMA	MA-H	60	30	10
489	MEMA	DEAEMA	MA-H	80	10	10
490	MEMA	DEAEA	MA-H	40	30	30
491	MEMA	DEAEA	MA-H	60	10	30
492	MEMA	DEAEA	MA-H	60	30	10

PA	Monomer (1)	Monomer (2)	Monomer (3) or functional amine	Monomer ratio (%)		
				Monomer (1)	Monomer (2)	Monomer (3)
493	MEMA	DEAEA	MA-H	80	10	10
494	MEMA	DEAEMA	DMAA	40	30	30
495	MEMA	DEAEMA	DMAA	60	10	30
496	MEMA	DEAEMA	DMAA	60	30	10
497	MEMA	DEAEMA	DMAA	80	10	10
498	MEMA	DEAEA	DMAA	40	30	30
499	MEMA	DEAEA	DMAA	60	10	30
500	MEMA	DEAEA	DMAA	60	30	10
501	MEMA	DEAEA	DMAA	80	10	10
502	MEMA	DEAEMA	DAAA	40	30	30
504	MEMA	DEAEMA	DAAA	60	30	10
507	MEMA	DEAEA	DAAA	60	10	30
508	MEMA	DEAEA	DAAA	60	30	10
509	MEMA	DEAEA	DAAA	80	10	10
510	MEMA	DEAEMA	MMA	40	30	30
511	MEMA	DEAEMA	MMA	60	10	30
512	MEMA	DEAEMA	MMA	60	30	10
513	MEMA	DEAEMA	MMA	80	10	10
514	MEMA	DEAEA	MMA	40	30	30
515	MEMA	DEAEA	MMA	60	10	30
517	MEMA	DEAEA	MMA	80	10	10
518	MEMA	DEAEMA	St	40	30	30
519	MEMA	DEAEMA	St	60	10	30
520	MEMA	DEAEMA	St	60	30	10
522	MEMA	DEAEA	St	40	30	30
523	MEMA	DEAEA	St	60	10	30
524	MEMA	DEAEA	St	60	30	10
525	MEMA	DEAEMA	-	85	15	-
526	MEMA	DEAEMA	-	80	20	-
527	MEMA	DEAEMA	-	75	25	-
528	MEMA	DEAEMA	-	70	30	-
529	MEMA	DEAEMA	-	65	35	-
530	MEMA	DEAEMA	-	60	40	-
531	MEMA	DEAEMA	-	55	45	-
532	MEMA	A-H	DEAEMA	85	5	10
533	MEMA	A-H	DEAEMA	80	5	15
534	MEMA	A-H	DEAEMA	75	5	20
535	MEMA	A-H	DEAEMA	70	5	25
536	MEMA	A-H	DEAEMA	65	5	30
537	MEMA	A-H	DEAEMA	60	5	35
538	MEMA	A-H	DEAEMA	55	5	40
539	MEMA	A-H	DEAEMA	50	5	45
540	MEMA	A-H	DEAEMA	75	10	15
541	MEMA	A-H	DEAEMA	70	10	20
542	MEMA	A-H	DEAEMA	65	10	25
543	MEMA	A-H	DEAEMA	55	10	35
544	MEMA	A-H	DEAEMA	50	10	40
545	MEMA	A-H	DEAEMA	65	15	20
546	MEMA	A-H	DEAEMA	60	15	25
547	MEMA	A-H	DEAEMA	55	15	30
548	MEMA	A-H	DEAEMA	50	15	35
549	MEMA	A-H	DEAEMA	55	20	25
550	MEMA	A-H	DEAEMA	50	20	30
551	MEMA	A-H	DEAEMA	90	5	5
552	MEMA	A-H	DEAEMA	80	15	5
553	MEMA	A-H	DEAEMA	70	25	5
554	MEMA	A-H	DEAEMA	60	35	5
555	MEMA	A-H	DEAEMA	50	45	5
556	MEMA	A-H	DEAEMA	50	40	10
557	MEMA	A-H	DEAEMA	60	25	15
558	MEMA	A-H	DEAEMA	50	35	15
559	MEMA	A-H	DEAEMA	60	20	20
560	MEMA	A-H	DEAEMA	50	30	20
561	MEMA	A-H	DEAEMA	50	25	25
563/pg1	MEMA	A-H	DEAEA	85	5	10
564/pg2	MEMA	A-H	DEAEA	80	5	15
565/pg3	MEMA	A-H	DEAEA	75	5	20

PA	Monomer (1)	Monomer (2)	Monomer (3) or functional amine	Monomer ratio (%)		
				Monomer (1)	Monomer (2)	Monomer (3)
pg4	MEMA	A-H	DEAEA	70	5	25
pg5	MEMA	A-H	DEAEA	65	5	30
pg6	MEMA	A-H	DEAEA	60	5	35
pg7	MEMA	A-H	DEAEA	55	5	40
pg8	MEMA	A-H	DEAEA	50	5	45
pg9	MEMA	A-H	DEAEA	75	10	15
pg10	MEMA	A-H	DEAEA	70	10	20
pg11	MEMA	A-H	DEAEA	65	10	25
pg12	MEMA	A-H	DEAEA	55	10	35
pg13	MEMA	A-H	DEAEA	50	10	40
pg14	MEMA	A-H	DEAEA	65	15	20
pg15	MEMA	A-H	DEAEA	60	15	25
pg16	MEMA	A-H	DEAEA	55	15	30
pg17	MEMA	A-H	DEAEA	50	15	35
pg19	MEMA	A-H	DEAEA	50	20	30

Appendix II: Polyurethane library

List of polyurethanes used in this thesis with their corresponding monomers and monomer ratio in the synthesis.

PU	Diol	Mn (Da)	Disocyanate	Chain extender	Monomer ratio (%)		
					Diol	Diisocyanate	Extender
1	PEG	2000	HDI	-	48.5	51.5	0
2	PEG	900	HDI	-	48.5	51.5	0
3	PEG	400	HDI	-	48.5	51.5	0
4	PPG	2000	HDI	-	48.5	51.5	0
5	PTMG	2000	HDI	-	48.5	51.5	0
6	PEG	2000	BICH	-	48.5	51.5	0
7	PEG	900	BICH	-	48.5	51.5	0
8	PEG	400	BICH	-	48.5	51.5	0
10	PTMG	2000	BICH	-	48.5	51.5	0
11	PEG	2000	TDI	-	48.5	51.5	0
12	PEG	900	TDI	-	48.5	51.5	0
13	PEG	400	TDI	-	48.5	51.5	0
14	PPG	2000	TDI	-	48.5	51.5	0
15	PTMG	2000	TDI	-	48.5	51.5	0
16	PEG	2000	MDI	-	48.5	51.5	0
17	PEG	900	MDI	-	48.5	51.5	0
18	PEG	400	MDI	-	48.5	51.5	0
19	PPG	2000	MDI	-	48.5	51.5	0
20	PTMG	2000	MDI	-	48.5	51.5	0
21	PEG	2000	PDI	-	48.5	51.5	0
22	PEG	900	PDI	-	48.5	51.5	0
23	PEG	400	PDI	-	48.5	51.5	0
24	PPG	2000	PDI	-	48.5	51.5	0
25	PTMG	2000	PDI	-	48.5	51.5	0
26	PEG	2000	HMDI	-	48.5	51.5	0
27	PEG	900	HMDI	-	48.5	51.5	0
28	PEG	400	HMDI	-	48.5	51.5	0
29	PPG	2000	HMDI	-	48.5	51.5	0
33	PEG	900	HDI	BD	0.25	0.52	0.23
35	PEG	400	HDI	BD	0.25	0.52	0.23
37	PPG	2000	HDI	BD	0.25	0.52	0.23
39	PTMG	2000	HDI	BD	0.25	0.52	0.23
41	PEG	2000	BICH	BD	0.25	0.52	0.23
46	PEG	400	BICH	ED	0.25	0.52	0.23
48	PPG	2000	BICH	ED	0.25	0.52	0.23
49	PTMG	2000	BICH	BD	0.25	0.52	0.23
53	PEG	900	TDI	BD	0.25	0.52	0.23
61	PEG	2000	MDI	BD	0.25	0.52	0.23
63	PEG	900	MDI	BD	0.25	0.52	0.23
65	PEG	400	MDI	BD	0.25	0.52	0.23
67	PPG	2000	MDI	BD	0.25	0.52	0.23
69	PTMG	2000	MDI	BD	0.25	0.52	0.23
71	PEG	2000	PDI	BD	0.25	0.52	0.23
73	PEG	900	PDI	BD	0.25	0.52	0.23
77	PPG	2000	PDI	BD	0.25	0.52	0.23
79	PTMG	2000	PDI	BD	0.25	0.52	0.23
81	PEG	2000	HMDI	BD	0.25	0.52	0.23
83	PEG	900	HMDI	BD	0.25	0.52	0.23
85	PEG	400	HMDI	BD	0.25	0.52	0.23
87	PPG	2000	HMDI	BD	0.25	0.52	0.23
89	PTMG	2000	HMDI	BD	0.25	0.52	0.23
39DE	PTMG	2000	HDI	DEAPD	0.25	0.52	0.23
49DE	PTMG	2000	BICH	DEAPD	0.25	0.52	0.23
91	PTMG	650	HDI	BD	0.485	0.515	0
92	PTMG	1000	HDI	BD	0.485	0.515	0
93	PTMG	650	BICH	BD	0.485	0.515	0
94	PTMG	1000	BICH	BD	0.485	0.515	0
95	PTMG	650	MDI	BD	0.485	0.515	0
96	PTMG	1000	MDI	BD	0.485	0.515	0

PU	Diol	Mn (Da)	Disocyanate	Chain extender	Monomer ratio (%)		
					Diol	Diisocyanate	Extender
97	PHNGAD	1800	BICH	DMAPD	0.25	0.52	0.23
98	PHNGAD	1800	BICH	DEAPD	0.25	0.52	0.23
99	PTMG	650	HDI	DMAPD	0.25	0.52	0.23
100	PTMG	1000	HDI	DMAPD	0.25	0.52	0.23
101	PTMG	650	BICH	DMAPD	0.25	0.52	0.23
102	PTMG	1000	BICH	DMAPD	0.25	0.52	0.23
103	PHNGAD	1800	MDI	DMAPD	0.25	0.52	0.23
104	PHNGAD	1800	MDI	DEAPD	0.25	0.52	0.23
105	PHNGAD	1800	HDI	DMAPD	0.25	0.52	0.23
106	PHNGAD	1800	HDI	DEAPD	0.25	0.52	0.23
107	PTMG	650	HDI	DEAPD	0.25	0.52	0.23
108	PTMG	1000	HDI	DEAPD	0.25	0.52	0.23
110	PTMG	1000	BICH	DEAPD	0.25	0.52	0.23
111	PTMG	650	MDI	DEAPD	0.25	0.52	0.23
112	PTMG	1000	MDI	DEAPD	0.25	0.52	0.23
114	PPG	425	HDI	BD	0.485	0.515	0
115	PPG	1000	HDI	BD	0.485	0.515	0
116	PPG	425	BICH	BD	0.485	0.515	0
117	PPG	1000	BICH	BD	0.485	0.515	0
118	PPG	425	MDI	DMAPD	0.25	0.52	0.23
119	PPG	1000	MDI	DMAPD	0.25	0.52	0.23
120	PPG	425	BICH	DEAPD	0.25	0.52	0.23
121	PPG	1000	BICH	DEAPD	0.25	0.52	0.23
122	PPG	2000	BICH	DEAPD	0.25	0.52	0.23
123	PPG	2000	MDI	DMAPD	0.25	0.52	0.23
124	PPG	2000	TDI	DMAPD	0.25	0.52	0.23
125	PPG	1000	TDI	DMAPD	0.25	0.52	0.23
126	PPG	425	TDI	DMAPD	0.25	0.52	0.23
127	PPG	1000	BICH	DMAPD	0.25	0.52	0.23
128	PPG	2000	BICH	DMAPD	0.25	0.52	0.23
129	PPG	425	BICH	DMAPD	0.25	0.52	0.23
130	PTMG	650	TDI	DMAPD	0.25	0.52	0.23
131	PTMG	1000	TDI	DMAPD	0.25	0.52	0.23
132	PHNGAD	1800	BICH	BD	0.25	0.52	0.23
133	PHNGAD	1800	HDI	BD	0.25	0.52	0.23
134	PHNGAD	1800	MDI	BD	0.25	0.52	0.23
135	PTMG	250	BICH	DMAPD	0.25	0.52	0.23
136	PTMG	250	BICH	DEAPD	0.25	0.52	0.23
137	PTMG	250	BICH	BD	0.25	0.52	0.23
138	PTMG	250	BICH	EG	0.25	0.52	0.23
139	PTMG	650	BICH	EG	0.25	0.52	0.23
140	PTMG	1000	BICH	EG	0.25	0.52	0.23
141	PTMG	2000	BICH	EG	0.25	0.52	0.23
142	PTMG	250	BICH	PG	0.25	0.52	0.23
143	PTMG	650	BICH	PG	0.25	0.52	0.23
144	PTMG	1000	BICH	PG	0.25	0.52	0.23
145	PTMG	2000	BICH	PG	0.25	0.52	0.23
146	PTMG	250	HDI	DMAPD	0.25	0.52	0.23
147	PTMG	250	HDI	DEAPD	0.25	0.52	0.23
148	PTMG	250	HDI	BD	0.25	0.52	0.23
149	PTMG	250	HDI	EG	0.25	0.52	0.23
150	PTMG	650	HDI	EG	0.25	0.52	0.23
151	PTMG	1000	HDI	EG	0.25	0.52	0.23
152	PTMG	2000	HDI	EG	0.25	0.52	0.23
153	PTMG	250	HDI	PG	0.25	0.52	0.23
154	PTMG	650	HDI	PG	0.25	0.52	0.23
156	PTMG	2000	HDI	PG	0.25	0.52	0.23
157	PTMG	250	MDI	DMAPD	0.25	0.52	0.23
158	PTMG	250	MDI	OFHD	0.25	0.52	0.23
159	PTMG	250	MDI	BD	0.25	0.52	0.23
161	PTMG	650	MDI	EG	0.25	0.52	0.23
162	PTMG	1000	MDI	EG	0.25	0.52	0.23
163	PTMG	2000	MDI	EG	0.25	0.52	0.23
164	PTMG	250	MDI	PG	0.25	0.52	0.23
165	PTMG	650	MDI	PG	0.25	0.52	0.23
166	PTMG	1000	MDI	PG	0.25	0.52	0.23
167	PTMG	2000	MDI	PG	0.25	0.52	0.23

PU	Diol	Mn (Da)	Disocyanate	Chain extender	Monomer ratio (%)		
					Diol	Diisocyanate	Extender
168	PTMG	250	BICH	-	48.5	51.5	0
169	PTMG	650	BICH	-	48.5	51.5	0
170	PTMG	1000	BICH	-	48.5	51.5	0
171	PTMG	250	HDI	-	48.5	51.5	0
172	PTMG	650	HDI	-	48.5	51.5	0
173	PTMG	1000	HDI	-	48.5	51.5	0
174	PTMG	250	MDI	-	48.5	51.5	0
175	PTMG	650	MDI	-	48.5	51.5	0
176	PTMG	1000	MDI	-	48.5	51.5	0
178	PTMG	1000	HDI	NMPD	0.25	0.52	0.23
179	PTMG	2000	HDI	NMPD	0.25	0.52	0.23
180	PTMG	1000	BICH	NMPD	0.25	0.52	0.23
181	PTMG	2000	BICH	NMPD	0.25	0.52	0.23
182	PTMG	650	MDI	NMPD	0.25	0.52	0.23
183	PTMG	1000	MDI	NMPD	0.25	0.52	0.23
184	PTMG	2000	MDI	NMPD	0.25	0.52	0.23
185	PHNAD	900	MDI	OFHD	0.17	0.52	0.33
186	PTMG	650	BICH	OFHD	0.25	0.52	0.23
187	PTMG	1000	BICH	OFHD	0.25	0.52	0.23
188	PTMG	2000	BICH	OFHD	0.25	0.52	0.23
189	PPG	1000	BICH	OFHD	0.17	0.52	0.33
190	PTMG	650	HDI	OFHD	0.25	0.52	0.23
191	PTMG	1000	HDI	OFHD	0.25	0.52	0.23
192	PTMG	2000	HDI	OFHD	0.25	0.52	0.23
194	PTMG	650	MDI	OFHD	0.25	0.52	0.23
195	PTMG	1000	MDI	OFHD	0.25	0.52	0.23
196	PTMG	2000	MDI	OFHD	0.25	0.52	0.23
197	PTMG	650	BICH	DHM	0.25	0.52	0.23
199	PTMG	2000	BICH	DHM	0.25	0.52	0.23
200	PTMG	650	HDI	DHM	0.25	0.52	0.23
201	PTMG	1000	HDI	DHM	0.25	0.52	0.23
202	PTMG	2000	HDI	DHM	0.25	0.52	0.23
203	PTMG	650	MDI	DHM	0.25	0.52	0.23
204	PTMG	1000	MDI	DHM	0.25	0.52	0.23
205	PTMG	2000	MDI	DHM	0.25	0.52	0.23
206	PPG	1000	HDI	OFHD	0.25	0.52	0.23
207	PPG	1000	BICH	OFHD	0.25	0.52	0.23
208	PPG	1000	MDI	OFHD	0.25	0.52	0.23
210	PPG	1000	BICH	PG	0.25	0.52	0.23
212	PHNAD	900	HDI	PG	0.25	0.52	0.23
213	PHNAD	900	BICH	PG	0.25	0.52	0.23
214	PHNAD	900	MDI	PG	0.25	0.52	0.23
215	PHNAD	900	HDI	BD	0.25	0.52	0.23
216	PHNAD	900	BICH	BD	0.25	0.52	0.23
217	PHNAD	900	MDI	BD	0.25	0.52	0.23
218	PHNAD	900	HDI	DMAPD	0.25	0.52	0.23
219	PHNAD	900	BICH	DMAPD	0.25	0.52	0.23
220	PHNAD	900	MDI	DMAPD	0.25	0.52	0.23
221	PHNAD	900	HDI	OFHD	0.25	0.52	0.23
222	PHNAD	900	BICH	OFHD	0.25	0.52	0.23
223	PHNAD	900	MDI	OFHD	0.25	0.52	0.23
224	PHNAD	900	HDI	-	48.5	51.5	0
225	PHNAD	900	BICH	-	48.5	51.5	0
226	PHNAD	900	MDI	-	48.5	51.5	0
227	PPG-PEG	1900	HDI	-	48.5	51.5	0
228	PPG-PEG	1900	BICH	-	48.5	51.5	0
229	PPG-PEG	1900	MDI	-	48.5	51.5	0
230	PPG-PEG	1900	HDI	BD	0.25	0.52	0.23
233	PPG-PEG	1900	HDI	OFHD	0.25	0.52	0.23
234	PPG-PEG	1900	BICH	OFHD	0.25	0.52	0.23
235	PPG-PEG	1900	MDI	OFHD	0.25	0.52	0.23
236	PPG-PEG	1900	HDI	PG	0.25	0.52	0.23
238	PPG-PEG	1900	MDI	PG	0.25	0.52	0.23
239	PPG-PEG	1900	HDI	DMAPD	0.25	0.52	0.23
241	PPG-PEG	1900	MDI	DMAPD	0.25	0.52	0.23
242	PPG-PEG	1900	HDI	EG	0.25	0.52	0.23
244	PPG-PEG	1900	MDI	EG	0.25	0.52	0.23

PU	Diol	Mn (Da)	Disocyanate	Chain extender	Monomer ratio (%)		
					Diol	Diisocyanate	Extender
245	PHNGAD	1800	HDI	OFHD	0.25	0.52	0.23
246	PHNGAD	1800	BICH	OFHD	0.25	0.52	0.23
247	PHNGAD	1800	MDI	OFHD	0.25	0.52	0.23
249	PHNGAD	1800	HDI	-	48.5	51.5	0
250	PHNGAD	1800	BICH	-	48.5	51.5	0
252	PHNGAD	1800	HDI	DHM	0.25	0.52	0.33
253	PPG-PEG	1900	MDI	DMAPD	0.17	0.52	0.33
254	PHNGAD	1800	BICH	BD	0.17	0.52	0.33
255	PPG-PEG	1900	MDI	BD	0.17	0.52	0.33
256	PPG	425	MDI	-	48.5	51.5	0
257	PTMG	1000	BICH	DMAPD	0.17	0.52	0.33
259	PTMG	2000	BICH	DMAPD	0.17	0.52	0.33
260	PTMG	2000	BICH	OFHD	0.17	0.52	0.33
263	PTMG	1000	HDI	OFHD	0.17	0.52	0.33
264	PTMG	1000	HDI	DMAPD	0.17	0.52	0.33
269	PPG	2000	MDI	DEAPD	0.25	0.52	0.23
271	PEG	400	MDI	DMAPD	0.25	0.52	0.23
273	PPG	425	MDI	DMAPD	0.25	0.52	0.23
275	PEG	400	MDI	-	48.5	51.5	0
276	PTMG	1000	MDI	OFHD	0.17	0.52	0.33
277	PTMG	2000	MDI	OFHD	0.17	0.52	0.33
278	PPG-PEG	1900	MDI	OFHD	0.17	0.52	0.33

Appendix III: Raw Data of Microbe-polymer Binding

Results for *E. coli* and *S.* Typhimurium-polyacrylate binding analysis. The fluorescence intensities were normalised by dividing the whole set of the highest fluorescence value examined per polymer microarray. Mean: Mean normalised fluorescence intensity; SD: Standard deviation.

PA	*E. col* binding						*S.* Typhimurium binding					
	Array 1		Array 2		Array 1 vs Array 2		Array 3		Array 4		Array 3 vs Array 4	
	Mean	SD	Mean	SD	t-Student	AVG	Mean	SD	Mean	SD	t-Student	AVG
1	0.1	0.0	0.0	0.0	9.8	0.1	0.6	0.0	0.2	0.0	3.5	0.4
2	0.1	0.0	0.1	0.0	1.3	0.1	0.3	0.1	0.1	0.0	0.1	0.2
14	0.1	0.0	0.0	0.0	8.8	0.1	0.2	0.1	0.1	0.0	0.6	0.1
18	0.2	0.0	0.3	0.2	1.6	0.2	0.1	0.0	0.1	0.0	0.8	0.1
21	0.1	0.0	0.0	0.0	5.2	0.1	0.4	0.1	0.1	0.0	0.7	0.2
26	0.2	0.0	0.0	0.0	12.8	0.1	0.3	0.1	0.2	0.1	0.6	0.3
46	0.2	0.0	0.1	0.0	8.7	0.2	0.4	0.0	0.3	0.0	3.5	0.3
49	0.2	0.0	0.1	0.0	5.4	0.2	0.3	0.1	0.3	0.0	2.8	0.3
52	0.2	0.1	0.1	0.0	4.9	0.2	0.5	0.0	0.2	0.0	2.1	0.3
55	0.2	0.0	0.1	0.1	3.9	0.2	0.5	0.1	0.4	0.0	2.1	0.5
60	0.1	0.0	0.0	0.0	5.3	0.0	0.4	0.0	0.2	0.1	0.6	0.3
96	0.2	0.0	0.2	0.1	1.2	0.2	0.3	0.1	0.1	0.0	0.7	0.2
97	0.3	0.0	0.1	0.0	6.9	0.2	0.1	0.1	0.0	0.0	0.4	0.1
99	0.1	0.0	0.0	0.0	2.4	0.0	0.1	0.0	0.1	0.0	0.9	0.1
100	0.4	0.1	0.4	0.1	0.1	0.4	0.1	0.0	0.2	0.1	1.0	0.2
106	0.2	0.0	0.2	0.1	0.9	0.2	0.1	0.0	0.1	0.0	0.9	0.1
108	0.1	0.0	0.1	0.0	2.6	0.1	0.5	0.0	0.3	0.0	3.4	0.4
112	0.2	0.0	0.0	0.0	6.5	0.1	0.2	0.0	0.3	0.3	0.6	0.2
117	0.1	0.0	0.0	0.0	3.6	0.1	0.1	0.0	0.1	0.0	1.0	0.1
128	0.1	0.0	0.1	0.0	2.7	0.1	0.1	0.0	0.1	0.0	2.2	0.1
137	0.1	0.0	0.0	0.1	0.2	0.0	0.4	0.0	0.2	0.0	1.2	0.3
138	0.1	0.0	0.1	0.0	1.3	0.1	0.2	0.0	0.1	0.0	2.1	0.2
141	0.1	0.0	0.1	0.1	1.0	0.1	0.3	0.0	0.0	0.0	0.2	0.2
142	0.1	0.0	0.1	0.0	2.2	0.1	0.4	0.1	0.1	0.0	1.1	0.2
143	0.1	0.0	0.1	0.1	1.1	0.1	0.4	0.0	0.1	0.0	1.4	0.3
153	0.1	0.0	0.0	0.1	2.8	0.1	0.4	0.0	0.2	0.0	1.3	0.3
154	0.1	0.0	0.0	0.0	4.2	0.0	0.3	0.1	0.1	0.0	0.5	0.2
155	0.1	0.0	0.1	0.0	1.7	0.1	0.5	0.0	0.5	0.1	2.2	0.5
159	0.3	0.0	0.0	0.0	52.8	0.1	0.6	0.1	0.3	0.0	2.0	0.4
160	0.1	0.0	0.1	0.0	0.2	0.1	0.5	0.0	0.3	0.1	1.3	0.4
162	0.2	0.0	0.0	0.0	30.8	0.1	0.1	0.0	0.1	0.0	0.9	0.1
163	0.2	0.0	0.0	0.0	22.4	0.1	0.6	0.1	0.4	0.1	1.1	0.5
164	0.1	0.0	0.1	0.0	7.5	0.1	0.3	0.0	0.2	0.0	2.1	0.3
167	0.1	0.0	0.0	0.0	13.3	0.1	0.2	0.1	0.1	0.0	0.9	0.2
168	0.2	0.0	0.0	0.0	8.3	0.1	0.2	0.1	0.1	0.0	0.8	0.2
171	0.2	0.0	0.0	0.1	4.7	0.1	0.5	0.1	0.3	0.0	1.4	0.4
172	0.2	0.0	0.3	0.1	1.6	0.3	0.5	0.1	0.4	0.1	1.8	0.5
180	0.2	0.0	0.2	0.0	4.4	0.2	0.5	0.0	0.4	0.0	2.5	0.4
181	0.2	0.0	0.2	0.1	0.1	0.2	0.5	0.1	0.6	0.1	2.1	0.5
182	0.2	0.0	0.2	0.0	0.9	0.2	0.5	0.1	0.4	0.0	2.2	0.5
183	0.2	0.0	0.1	0.0	6.4	0.1	0.3	0.0	0.2	0.1	0.7	0.3
184	0.1	0.0	0.0	0.0	9.4	0.1	0.6	0.3	0.1	0.0	0.1	0.4
186	0.1	0.0	0.1	0.1	0.6	0.1	0.4	0.0	0.1	0.0	0.5	0.2
187	0.1	0.0	0.0	0.0	2.9	0.1	0.1	0.0	0.1	0.0	0.6	0.1
188	0.1	0.0	0.0	0.0	1.7	0.1	0.3	0.0	0.2	0.0	1.3	0.2
189	0.1	0.0	0.1	0.0	1.5	0.1	0.2	0.0	0.2	0.0	2.1	0.2
190	0.1	0.0	0.1	0.0	4.5	0.1	0.1	0.0	0.1	0.0	1.3	0.1
192	0.2	0.0	0.0	0.0	28.9	0.1	0.3	0.0	0.1	0.0	1.3	0.2
193	0.2	0.0	0.0	0.0	16.2	0.1	0.5	0.0	0.1	0.0	1.7	0.3
194	0.1	0.0	0.1	0.0	0.2	0.1	0.5	0.1	0.1	0.0	1.0	0.3
195	0.3	0.0	0.2	0.0	2.8	0.2	0.3	0.0	0.2	0.0	2.8	0.2
196	0.2	0.1	0.2	0.0	0.3	0.2	0.3	0.0	0.1	0.0	1.2	0.2

PA	*E. col* binding						*S.* Typhimurium binding					
	Array 1		Array 2		Array 1 vs Array 2		Array 3		Array 4		Array 3 vs Array 4	
	Mean	SD	Mean	SD	t-Student	AVG	Mean	SD	Mean	SD	t-Student	AVG
197	0.1	0.0	0.4	0.1	9.3	0.3	0.1	0.0	0.1	0.0	1.1	0.1
199	0.1	0.0	0.1	0.0	1.7	0.1	0.3	0.1	0.1	0.1	0.3	0.2
201	0.1	0.0	0.1	0.0	3.4	0.1	0.0	0.0	0.1	0.0	1.1	0.1
214	0.2	0.0	0.1	0.0	29.4	0.1	0.3	0.0	0.3	0.0	2.1	0.3
215	0.1	0.0	0.1	0.0	11.1	0.1	0.3	0.0	0.2	0.0	1.3	0.3
216	0.0	0.0	0.1	0.0	1.0	0.1	0.3	0.0	0.3	0.2	0.7	0.3
218	0.0	0.0	0.1	0.0	4.0	0.1	0.1	0.1	0.2	0.1	0.6	0.2
228	0.1	0.0	0.1	0.1	0.1	0.1	0.3	0.0	0.2	0.0	1.2	0.3
229	0.1	0.0	0.0	0.0	6.8	0.1	0.4	0.0	0.1	0.0	0.5	0.2
230	0.1	0.0	0.0	0.0	8.3	0.0	0.2	0.1	0.1	0.0	0.6	0.1
231	0.1	0.0	0.0	0.0	5.5	0.0	0.1	0.0	0.2	0.2	0.6	0.1
232	0.2	0.0	0.1	0.0	8.0	0.1	0.3	0.0	0.2	0.0	2.2	0.3
233	0.0	0.0	0.0	0.0	2.4	0.0	0.2	0.0	0.2	0.2	0.3	0.2
234	0.1	0.0	0.0	0.0	2.9	0.0	0.2	0.0	0.1	0.0	1.0	0.2
235	0.0	0.0	0.0	0.0	4.5	0.0	0.0	0.0	0.0	0.0	0.8	0.0
236	0.0	0.0	0.0	0.0	0.9	0.0	0.0	0.0	0.0	0.0	0.3	0.0
242	0.1	0.0	0.0	0.0	8.7	0.0	0.1	0.0	0.1	0.0	0.8	0.1
251	0.2	0.0	0.0	0.0	9.8	0.1	0.1	0.0	0.1	0.0	0.9	0.1
255	0.1	0.0	0.1	0.0	1.5	0.1	0.2	0.0	0.1	0.0	0.3	0.2
258	0.1	0.0	0.1	0.0	1.7	0.1	0.3	0.1	0.1	0.0	0.5	0.2
264	0.1	0.0	0.1	0.0	0.6	0.1	0.2	0.1	0.1	0.0	0.4	0.1
267	0.2	0.0	0.1	0.0	7.0	0.1	0.2	0.0	0.1	0.0	1.2	0.1
273	0.2	0.0	0.0	0.0	5.7	0.1	0.2	0.0	0.1	0.0	1.3	0.1
279	0.1	0.0	0.1	0.0	0.8	0.1	0.1	0.0	0.1	0.0	0.9	0.1
280	0.1	0.0	0.1	0.1	1.6	0.1	0.1	0.0	0.1	0.0	0.7	0.1
281	0.1	0.0	0.0	0.0	6.0	0.1	0.1	0.0	0.1	0.0	0.8	0.1
285	0.2	0.0	0.1	0.0	3.5	0.1	0.4	0.0	0.2	0.0	1.6	0.3
291	0.1	0.0	0.1	0.1	1.1	0.1	0.2	0.1	0.1	0.0	0.8	0.2
296	0.2	0.0	0.8	0.0	25.2	0.5	0.3	0.1	0.4	0.0	2.9	0.4
306	0.1	0.0	0.1	0.0	0.4	0.1	0.0	0.0	0.0	0.0	0.6	0.0
307	0.2	0.0	0.1	0.0	6.1	0.1	0.4	0.0	0.1	0.0	1.3	0.2
309	0.1	0.0	0.2	0.1	2.4	0.2	0.0	0.0	0.1	0.0	0.7	0.1
313	0.5	0.0	0.4	0.0	4.7	0.4	0.2	0.0	0.2	0.1	0.9	0.2
316	0.9	0.1	0.6	0.1	3.9	0.8	0.1	0.0	0.1	0.1	0.3	0.1
317	0.6	0.2	0.6	0.1	0.7	0.6	0.1	0.0	0.1	0.0	0.8	0.1
318	0.5	0.0	0.3	0.0	4.8	0.4	0.2	0.1	0.1	0.0	0.4	0.1
321	0.2	0.0	0.2	0.1	1.0	0.2	0.0	0.0	0.0	0.0	0.8	0.0
322	0.1	0.0	0.2	0.0	2.6	0.2	0.0	0.0	0.0	0.1	0.1	0.0
323	0.1	0.1	0.2	0.0	4.2	0.2	0.0	0.0	0.0	0.0	0.4	0.0
324	0.0	0.0	0.0	0.0	2.3	0.0	0.0	0.0	0.1	0.1	0.4	0.0
325	0.0	0.0	0.3	0.1	6.3	0.2	0.0	0.0	0.0	0.0	0.6	0.0
326	0.1	0.0	0.1	0.0	0.1	0.1	0.1	0.0	0.0	0.0	0.4	0.0
327	0.0	0.0	0.2	0.1	3.2	0.1	0.0	0.0	0.0	0.0	0.5	0.0
329	0.1	0.0	0.3	0.1	8.5	0.2	0.1	0.0	0.0	0.0	0.2	0.1
330	0.1	0.1	0.6	0.1	9.5	0.4	0.0	0.0	0.0	0.0	1.3	0.0
331	0.4	0.2	0.7	0.2	2.7	0.6	0.1	0.0	0.0	0.0	0.7	0.0
332	0.2	0.2	0.4	0.1	2.5	0.3	0.1	0.0	0.1	0.0	1.3	0.1
336	0.1	0.0	0.3	0.1	6.0	0.2	0.0	0.0	0.0	0.0	0.4	0.0
337	0.4	0.2	0.6	0.0	2.5	0.5	0.0	0.0	0.0	0.0	1.1	0.0
338	0.4	0.0	0.6	0.1	5.8	0.5	0.0	0.0	0.0	0.0	0.7	0.0
339	0.2	0.0	0.2	0.1	1.4	0.2	0.1	0.0	0.1	0.0	0.6	0.1
340	0.2	0.0	0.2	0.1	0.0	0.2	0.1	0.0	0.1	0.0	2.0	0.1
341	0.3	0.1	0.2	0.0	2.0	0.2	0.2	0.0	0.1	0.0	0.5	0.1
345	0.2	0.1	0.3	0.0	0.9	0.3	0.1	0.0	0.2	0.1	1.0	0.2
346	0.1	0.0	0.2	0.0	8.3	0.1	0.1	0.1	0.1	0.0	0.9	0.1
348	0.1	0.0	0.2	0.0	6.7	0.2	0.2	0.1	0.1	0.0	0.8	0.1
349	0.4	0.0	0.4	0.1	0.2	0.4	0.1	0.0	0.1	0.0	0.9	0.1
357	0.1	0.0	0.1	0.0	3.7	0.1	0.1	0.0	0.0	0.0	0.5	0.1
358	0.1	0.0	0.0	0.0	7.1	0.1	0.1	0.0	0.1	0.0	0.7	0.1
360	0.1	0.0	0.2	0.0	3.7	0.1	0.1	0.0	0.1	0.0	1.1	0.1
361	0.1	0.0	0.2	0.0	5.1	0.2	0.1	0.2	0.1	0.0	0.6	0.1
363	0.3	0.0	0.2	0.1	1.8	0.2	0.2	0.1	0.1	0.0	1.1	0.1
364	0.2	0.0	0.3	0.0	0.8	0.2	0.2	0.0	0.2	0.0	2.3	0.2
369	0.1	0.0	0.0	0.0	7.6	0.1	0.2	0.0	0.0	0.0	0.3	0.1
372	0.2	0.0	0.0	0.0	23.6	0.1	0.6	0.0	0.3	0.1	1.0	0.4
414	0.0	0.0	0.2	0.0	28.4	0.1	0.2	0.0	0.3	0.0	1.8	0.2

PA	*E. col* binding						*S.* Typhimurium binding					
	Array 1		Array 2		Array 1 vs Array 2		Array 3		Array 4		Array 3 vs Array 4	
	Mean	SD	Mean	SD	t-Student	AVG	Mean	SD	Mean	SD	t-Student	AVG
415	0.2	0.0	0.1	0.0	3.7	0.1	0.2	0.0	0.2	0.0	1.1	0.2
416	0.7	0.1	0.6	0.1	2.2	0.7	0.1	0.0	0.0	0.0	0.6	0.1
417	0.1	0.0	0.1	0.0	7.0	0.1	0.1	0.0	0.1	0.0	1.4	0.1
418	0.2	0.0	0.1	0.0	5.6	0.1	0.3	0.3	0.2	0.0	0.7	0.2
419	0.2	0.0	0.1	0.1	4.9	0.2	0.2	0.0	0.1	0.0	1.0	0.2
420	0.2	0.1	0.3	0.0	4.1	0.3	0.2	0.0	0.2	0.0	1.6	0.2
421	0.1	0.0	0.2	0.0	0.2	0.2	0.5	0.0	0.3	0.0	2.0	0.4
422	0.0	0.0	0.1	0.1	2.0	0.1	0.0	0.0	0.0	0.0	0.7	0.0
423	0.1	0.0	0.1	0.1	0.4	0.1	0.1	0.0	0.1	0.0	0.4	0.1
426	0.1	0.0	0.2	0.0	8.2	0.1	0.0	0.0	0.0	0.0	0.6	0.0
428	0.1	0.0	0.2	0.0	4.7	0.2	0.1	0.0	0.1	0.0	0.4	0.1
429	0.2	0.0	0.1	0.0	1.9	0.1	0.1	0.0	0.2	0.0	2.2	0.1
430	0.3	0.1	0.3	0.0	1.4	0.3	0.2	0.0	0.2	0.0	1.2	0.2
431	0.2	0.0	0.1	0.1	3.5	0.2	0.2	0.1	0.1	0.0	1.4	0.2
432	0.2	0.1	0.5	0.1	5.6	0.3	0.2	0.0	0.3	0.1	1.6	0.2
433	0.0	0.0	0.1	0.1	1.3	0.1	0.1	0.0	0.1	0.0	0.8	0.1
434	0.2	0.0	0.0	0.1	4.2	0.1	0.4	0.1	0.1	0.0	0.7	0.2
436	0.2	0.1	0.1	0.0	2.2	0.1	0.0	0.0	0.0	0.0	0.7	0.0
437	0.2	0.0	0.1	0.0	31.6	0.1	0.2	0.0	0.1	0.0	1.3	0.2
440	0.6	0.0	0.2	0.1	7.8	0.4	0.1	0.1	0.0	0.0	0.4	0.1
443	0.1	0.0	0.1	0.0	7.3	0.1	0.3	0.1	0.1	0.0	1.0	0.2
444	0.3	0.0	0.0	0.0	47.0	0.2	0.1	0.0	0.1	0.0	0.8	0.1
445	0.2	0.0	0.0	0.0	37.1	0.1	0.3	0.0	0.1	0.0	0.9	0.2
450	0.2	0.0	0.3	0.1	1.1	0.2	0.1	0.0	0.2	0.0	2.6	0.2
452	0.0	0.0	0.1	0.0	10.3	0.1	0.2	0.3	0.1	0.0	0.3	0.1
453	0.1	0.0	0.1	0.1	0.4	0.1	0.3	0.0	0.1	0.0	2.3	0.2
458	0.2	0.0	0.1	0.0	2.9	0.2	0.1	0.0	0.1	0.0	0.4	0.1
459	0.2	0.0	0.2	0.0	0.5	0.2	0.2	0.0	0.2	0.0	1.9	0.2
460	0.4	0.0	0.3	0.0	6.4	0.4	0.2	0.1	0.2	0.0	2.2	0.2
465	0.1	0.0	0.1	0.0	2.1	0.1	0.1	0.0	0.1	0.0	0.9	0.1
467	0.2	0.0	0.1	0.0	8.2	0.1	0.4	0.0	0.1	0.1	0.3	0.3
468	0.4	0.0	0.3	0.0	7.2	0.3	0.2	0.0	0.3	0.1	1.3	0.3
469	0.2	0.0	0.1	0.0	9.5	0.1	0.3	0.0	0.3	0.0	2.1	0.3
470	0.2	0.0	0.1	0.0	2.7	0.2	0.1	0.0	0.1	0.0	0.7	0.1
474	0.2	0.0	0.0	0.0	12.0	0.1	0.4	0.0	0.1	0.0	0.2	0.2
475	0.1	0.0	0.0	0.0	2.5	0.1	0.1	0.0	0.0	0.0	0.4	0.0
476	0.2	0.0	0.1	0.0	4.7	0.2	0.2	0.3	0.2	0.1	0.4	0.2
477	0.2	0.0	0.0	0.0	72.1	0.1	0.3	0.0	0.2	0.1	0.5	0.2
481	0.1	0.0	0.0	0.0	5.6	0.0	0.2	0.1	0.1	0.0	0.4	0.1
485	0.1	0.0	0.0	0.0	3.5	0.0	0.4	0.0	0.2	0.0	1.3	0.3
493	0.1	0.0	0.0	0.0	3.2	0.1	0.2	0.0	0.1	0.0	0.5	0.1
496	0.4	0.0	0.1	0.0	8.5	0.2	0.1	0.0	0.1	0.0	0.6	0.1
497	0.1	0.0	0.1	0.1	2.2	0.1	0.1	0.0	0.1	0.0	0.7	0.1
500	0.1	0.0	0.1	0.0	1.2	0.1	0.1	0.0	0.1	0.0	0.7	0.1
504	0.7	0.0	0.4	0.0	12.4	0.5	0.2	0.0	0.1	0.0	0.8	0.1
507	0.2	0.0	0.1	0.0	9.6	0.1	0.1	0.0	0.1	0.0	3.3	0.1
508	0.3	0.1	0.2	0.0	1.6	0.3	0.2	0.0	0.1	0.0	0.5	0.1
509	0.3	0.0	0.1	0.0	6.1	0.2	0.2	0.0	0.2	0.0	1.7	0.2
510	0.2	0.1	0.2	0.0	0.4	0.2	0.2	0.0	0.1	0.2	0.0	0.1
511	0.1	0.0	0.2	0.1	2.9	0.2	0.1	0.0	0.1	0.0	1.1	0.1
512	0.5	0.0	0.1	0.0	19.3	0.3	0.1	0.1	0.1	0.0	1.7	0.1
514	0.3	0.1	0.2	0.1	2.7	0.2	0.1	0.0	0.1	0.0	0.5	0.1
515	0.1	0.0	0.1	0.0	0.4	0.1	0.1	0.0	0.1	0.0	1.7	0.1
517	0.2	0.0	0.1	0.0	7.2	0.2	0.5	0.0	0.2	0.0	1.9	0.4
518	0.1	0.0	0.1	0.0	9.5	0.1	0.2	0.1	0.1	0.0	1.7	0.1
519	0.2	0.0	0.2	0.0	0.7	0.2	0.2	0.1	0.1	0.0	0.9	0.2
520	0.2	0.0	0.2	0.0	3.7	0.2	0.1	0.0	0.1	0.0	2.1	0.1
522	0.0	0.0	0.1	0.1	2.0	0.1	0.1	0.0	0.1	0.0	1.5	0.1
523	0.1	0.0	0.2	0.0	1.6	0.1	0.0	0.0	0.0	0.0	0.5	0.0
pg7	0.2	0.0	0.0	0.0	14.1	0.1	0.4	0.1	0.1	0.0	1.6	0.2
pg4	0.1	0.0	0.1	0.0	0.2	0.1	0.3	0.0	0.0	0.0	0.1	0.1
pg15	0.1	0.0	0.0	0.1	6.4	0.1	0.2	0.1	0.0	0.0	0.7	0.1
pg3	0.1	0.0	0.1	0.0	0.3	0.1	0.3	0.0	0.2	0.0	1.2	0.2
pg5	0.1	0.0	0.1	0.0	0.2	0.1	0.4	0.1	0.1	0.0	0.3	0.3
pg1	0.3	0.0	0.0	0.0	18.6	0.1	0.1	0.0	0.1	0.0	1.1	0.1
pg10	0.2	0.0	0.1	0.0	13.4	0.1	0.3	0.0	0.2	0.0	3.2	0.3

PA	*E. col* binding						*S.* Typhimurium binding					
	Array 1		Array 2		Array 1 vs Array 2		Array 3		Array 4		Array 3 vs Array 4	
	Mean	SD	Mean	SD	t-Student	AVG	Mean	SD	Mean	SD	t-Student	AVG
pg11	0.1	0.0	0.0	0.0	5.4	0.0	0.3	0.0	0.1	0.0	0.9	0.2
pg16	0.2	0.0	0.0	0.0	19.6	0.1	0.5	0.0	0.3	0.1	1.2	0.4
pg8	0.2	0.0	0.0	0.0	15.6	0.1	0.6	0.1	0.2	0.1	0.6	0.4
pg3	0.2	0.0	0.1	0.0	12.4	0.1	0.2	0.0	0.1	0.0	0.9	0.1
pg14	0.1	0.0	0.0	0.0	29.8	0.1	0.4	0.1	0.1	0.0	0.4	0.3
pg9	0.2	0.0	0.1	0.0	11.0	0.1	0.4	0.1	0.3	0.0	1.6	0.4
pg19	0.1	0.0	0.1	0.0	3.5	0.1	0.1	0.0	0.1	0.0	1.2	0.1
pg6	0.1	0.0	0.2	0.1	1.9	0.2	0.2	0.1	0.1	0.0	0.9	0.1
pg12	0.1	0.0	0.1	0.0	2.4	0.1	0.3	0.0	0.0	0.0	0.3	0.2
pg13	0.1	0.0	0.1	0.0	1.0	0.1	0.5	0.0	0.1	0.0	2.3	0.3
pg17	0.1	0.0	0.2	0.2	1.4	0.1	0.5	0.1	0.4	0.1	1.0	0.5

Results for *E. coli* and *S.* Typhimurium-polyurethane binding analysis. The fluorescence intensities were normalised by dividing the whole set of the highest fluorescence value examined per polymer microarray. Mean: Mean normalised fluorescence intensity; SD: Standard deviation.

PU	*E. coli* binding						*S.* Typhimurium binding					
	Array 1		Array 2		Array 1 vs Array 2		Array 3		Array 4		Array 3 vs Array 4	
	Mean	SD	Mean	SD	t-Student	AVG	Mean	SD	Mean	SD	t-Student	AVG
1	0.09	0.02	0.04	0.00	6.03	0.06	0.27	0.040	0.07	0.079	0.09	0.17
2	0.08	0.01	0.05	0.02	2.61	0.06	0.20	0.016	0.06	0.022	0.38	0.13
3	0.06	0.02	0.24	0.08	4.65	0.15	0.27	0.042	0.20	0.025	1.49	0.24
4	0.07	0.01	0.06	0.01	1.47	0.07	0.29	0.026	0.04	0.019	0.15	0.17
5	0.11	0.01	0.12	0.07	0.42	0.12	0.11	0.008	0.19	0.018	1.83	0.15
7	0.10	0.02	0.02	0.02	6.05	0.06	0.11	0.008	0.09	0.012	1.12	0.10
8	0.29	0.02	0.18	0.04	4.58	0.24	0.08	0.030	0.17	0.005	3.30	0.13
10	0.36	0.03	0.13	0.01	17.38	0.24	0.30	0.056	0.32	0.039	1.92	0.31
12	0.09	0.00	0.07	0.02	2.88	0.08	0.25	0.046	0.16	0.033	0.97	0.20
13	0.13	0.01	0.11	0.04	1.39	0.12	0.35	0.010	0.18	0.017	1.63	0.27
14	0.04	0.00	0.12	0.03	5.47	0.08	0.48	0.055	0.19	0.018	1.43	0.33
18	0.12	0.02	0.22	0.06	3.27	0.17	0.44	0.056	0.31	0.034	1.89	0.38
19	0.09	0.02	0.02	0.01	5.45	0.06	0.43	0.098	0.11	0.007	1.08	0.27
20	0.13	0.03	0.02	0.03	4.70	0.07	0.22	0.102	0.11	0.014	0.95	0.17
24	0.09	0.01	0.04	0.01	6.06	0.07	0.32	0.029	0.22	0.032	1.40	0.27
25	0.14	0.02	0.08	0.02	4.46	0.11	0.40	0.045	0.23	0.011	2.56	0.31
28	0.16	0.04	0.26	0.03	4.19	0.21	0.50	0.038	0.28	0.034	1.62	0.39
29	0.23	0.01	0.02	0.02	22.02	0.12	0.29	0.059	0.12	0.007	1.49	0.20
33	0.12	0.04	0.02	0.01	4.84	0.07	0.52	0.056	0.18	0.008	2.04	0.35
35	0.11	0.01	0.01	0.00	32.87	0.06	0.27	0.067	0.11	0.019	0.79	0.19
37	0.16	0.01	0.04	0.03	7.49	0.10	0.58	0.044	0.14	0.022	0.71	0.36
39	0.30	0.03	0.17	0.04	4.66	0.23	0.64	0.145	0.49	0.049	2.21	0.56
41	0.14	0.03	0.10	0.00	3.13	0.12	0.50	0.020	0.30	0.008	4.10	0.40
46	0.14	0.02	0.13	0.01	1.10	0.14	0.56	0.010	0.19	0.036	0.84	0.38
48	0.16	0.02	0.15	0.04	0.15	0.15	0.20	0.031	0.21	0.031	1.50	0.21
49	0.06	0.01	0.03	0.00	5.63	0.04	0.13	0.016	0.16	0.074	0.67	0.14
53	0.12	0.01	0.02	0.01	11.59	0.07	0.36	0.043	0.14	0.034	0.71	0.25
63	0.11	0.00	0.14	0.02	3.87	0.12	0.25	0.032	0.21	0.064	0.93	0.23
65	0.10	0.02	0.10	0.01	0.50	0.10	0.41	0.134	0.16	0.011	1.24	0.28
67	0.08	0.01	0.02	0.04	3.07	0.05	0.17	0.006	0.09	0.011	1.06	0.13
69	0.20	0.04	0.02	0.01	9.34	0.11	0.16	0.017	0.13	0.020	1.18	0.15
73	0.08	0.01	0.08	0.05	0.03	0.08	0.28	0.023	0.20	0.042	1.07	0.24
77	0.08	0.02	0.19	0.01	7.43	0.14	0.29	0.016	0.07	0.012	0.56	0.18
79	0.13	0.03	0.22	0.09	1.84	0.18	0.37	0.050	0.18	0.046	0.78	0.28
81	0.14	0.01	0.24	0.01	14.74	0.19	0.26	0.017	0.32	0.010	4.19	0.29
83	0.13	0.01	0.04	0.01	10.38	0.09	0.08	0.007	0.12	0.018	1.14	0.10
85	0.21	0.00	0.06	0.00	70.97	0.14	0.25	0.043	0.15	0.024	1.09	0.20
87	0.18	0.01	0.07	0.03	6.28	0.13	0.18	0.018	0.31	0.039	2.02	0.25
89	0.10	0.01	0.07	0.01	5.72	0.09	0.33	0.031	0.26	0.034	1.63	0.29
92	0.08	0.00	0.26	0.06	5.75	0.17	0.73	0.013	0.57	0.054	2.74	0.65
93	0.15	0.03	0.13	0.04	1.03	0.14	0.38	0.023	0.14	0.033	0.75	0.26
94	0.13	0.02	0.08	0.01	5.16	0.10	0.10	0.065	0.09	0.004	1.58	0.09
95	0.33	0.01	0.42	0.02	8.12	0.37	0.34	0.024	0.39	0.011	4.80	0.36
96	0.13	0.03	0.19	0.02	3.04	0.16	0.41	0.075	0.11	0.003	1.54	0.26
97	0.25	0.01	0.34	0.07	2.56	0.30	0.25	0.034	0.27	0.005	4.91	0.26
98	0.17	0.01	0.05	0.01	21.49	0.11	0.23	0.015	0.35	0.029	2.66	0.29
99	0.19	0.01	0.02	0.10	3.27	0.11	0.38	0.033	0.18	0.010	2.13	0.28
100	0.16	0.00	0.09	0.01	10.43	0.12	0.31	0.039	0.14	0.329	0.05	0.23
101	0.17	0.00	0.08	0.01	21.78	0.13	0.35	0.010	0.29	0.009	3.98	0.32
102	0.12	0.04	0.07	0.02	2.40	0.10	0.25	0.049	0.21	0.019	1.82	0.23
103	0.22	0.02	0.34	0.02	8.38	0.28	0.19	0.031	0.16	0.007	2.31	0.17
104	0.28	0.03	0.28	0.11	0.12	0.28	0.64	0.038	0.37	0.046	1.80	0.51
105	0.18	0.02	0.24	0.03	3.63	0.21	0.21	0.029	0.25	0.020	2.30	0.23
106	0.24	0.03	0.19	0.03	2.15	0.21	0.14	0.012	0.16	0.013	1.83	0.15
107	0.13	0.01	0.15	0.02	2.70	0.14	0.46	0.059	0.29	0.048	1.41	0.37
108	0.17	0.01	0.10	0.04	3.55	0.13	0.20	0.057	0.15	0.024	1.14	0.17
110	0.11	0.02	0.05	0.01	5.21	0.08	0.43	0.037	0.13	0.015	1.07	0.28
111	0.47	0.13	0.42	0.03	0.65	0.44	0.34	0.025	0.45	0.047	2.59	0.40
112	0.25	0.03	0.18	0.01	4.03	0.21	0.44	0.065	0.45	0.074	1.88	0.44
114	0.17	0.00	0.14	0.02	3.04	0.16	0.33	0.023	0.28	0.032	1.85	0.31

PU	*E. coli* binding						*S.* Typhimurium binding					
	Array 1		Array 2		Array 1 vs Array 2		Array 3		Array 4		Array 3 vs Array 4	
	Mean	SD	Mean	SD	t-Student	AVG	Mean	SD	Mean	SD	t-Student	AVG
115	0.17	0.01	0.13	0.01	6.92	0.15	0.35	0.010	0.25	0.047	1.29	0.30
116	0.23	0.02	0.13	0.02	6.97	0.18	0.40	0.040	0.53	0.041	3.28	0.47
117	0.26	0.03	0.19	0.05	2.17	0.22	0.44	0.074	0.40	0.009	4.77	0.42
118	0.59	0.14	0.25	0.02	4.81	0.42	0.45	0.031	0.19	0.024	1.27	0.32
119	0.18	0.04	0.27	0.09	1.92	0.23	0.56	0.020	0.33	0.022	2.56	0.45
120	0.23	0.02	0.30	0.02	4.92	0.27	0.74	0.046	0.52	0.047	2.63	0.63
121	0.21	0.02	0.13	0.06	2.46	0.17	0.37	0.010	0.37	0.053	1.92	0.37
122	0.07	0.02	0.04	0.00	2.62	0.06	0.26	0.050	0.07	0.024	0.39	0.17
123	0.06	0.01	0.04	0.01	1.74	0.05	0.17	0.026	0.20	0.007	3.12	0.18
124	0.14	0.03	0.01	0.01	7.85	0.08	0.30	0.123	0.10	0.006	0.90	0.20
125	0.19	0.01	0.03	0.02	12.90	0.11	0.45	0.015	0.21	0.028	1.31	0.33
126	0.31	0.04	0.25	0.02	2.76	0.28	0.92	0.041	0.88	0.096	3.08	0.90
127	0.21	0.02	0.22	0.02	0.29	0.21	0.40	0.012	0.38	0.073	1.59	0.39
128	0.12	0.01	0.10	0.02	2.10	0.11	0.19	0.035	0.22	0.021	1.90	0.20
129	0.15	0.02	0.12	0.02	1.79	0.14	0.09	0.027	0.08	0.013	0.92	0.09
130	0.06	0.00	0.14	0.03	5.29	0.10	0.31	0.012	0.22	0.009	2.99	0.27
131	0.07	0.02	0.09	0.02	1.27	0.08	0.20	0.039	0.14	0.011	1.59	0.17
132	0.20	0.03	0.49	0.08	6.57	0.34	0.17	0.069	0.42	0.044	2.57	0.29
133	0.63	0.16	0.50	0.05	1.52	0.56	0.29	0.043	0.19	0.019	1.57	0.24
134	0.15	0.02	0.45	0.04	13.67	0.30	0.16	0.069	0.13	0.010	1.55	0.15
135	0.21	0.01	0.15	0.01	7.20	0.18	0.19	0.008	0.20	0.013	2.34	0.19
136	0.18	0.03	0.28	0.02	5.49	0.23	0.27	0.042	0.32	0.054	1.67	0.30
137	0.43	0.05	0.40	0.08	0.70	0.42	0.42	0.033	0.39	0.043	2.25	0.41
138	0.33	0.07	0.24	0.03	2.38	0.29	0.52	0.054	0.44	0.027	3.18	0.48
139	0.18	0.03	0.14	0.04	1.66	0.16	0.44	0.032	0.37	0.042	2.07	0.41
140	0.05	0.01	0.09	0.01	4.13	0.07	0.60	0.089	0.28	0.048	1.12	0.44
141	0.05	0.01	0.12	0.02	6.04	0.08	0.45	0.021	0.10	0.012	0.87	0.28
143	0.15	0.02	0.14	0.03	0.07	0.15	0.54	0.035	0.22	0.012	2.26	0.38
144	0.16	0.01	0.04	0.01	14.73	0.10	0.36	0.039	0.11	0.005	1.67	0.23
145	0.13	0.01	0.02	0.01	16.03	0.07	0.27	0.080	0.14	0.026	0.85	0.20
146	0.26	0.05	0.26	0.06	0.04	0.26	0.20	0.009	0.23	0.013	2.65	0.22
147	0.09	0.02	0.14	0.03	3.10	0.12	0.14	0.025	0.10	0.013	1.11	0.12
148	0.09	0.01	0.02	0.04	3.71	0.06	0.36	0.025	0.24	0.049	1.16	0.30
149	0.16	0.01	0.17	0.02	0.38	0.17	0.40	0.026	0.35	0.025	2.71	0.38
150	0.11	0.02	0.26	0.20	1.44	0.19	0.13	0.035	0.08	0.006	1.30	0.11
151	0.49	0.20	0.65	0.16	1.19	0.57	0.23	0.028	0.13	0.012	1.46	0.18
152	0.16	0.03	0.10	0.01	3.48	0.13	0.30	0.045	0.11	0.010	1.19	0.21
153	0.34	0.05	0.40	0.11	1.06	0.37	0.21	0.026	0.19	0.063	0.85	0.20
154	0.12	0.01	0.06	0.03	4.31	0.09	0.20	0.040	0.16	0.029	1.07	0.18
156	0.14	0.01	0.17	0.16	0.38	0.15	0.34	0.045	0.08	0.024	0.35	0.21
157	0.19	0.04	0.18	0.02	0.89	0.19	0.29	0.041	0.13	0.012	1.38	0.21
158	0.21	0.02	0.35	0.08	3.44	0.28	0.09	0.011	0.11	0.015	1.15	0.10
159	0.22	0.01	0.17	0.02	4.09	0.19	0.47	0.066	0.42	0.055	2.02	0.45
161	0.16	0.07	0.53	0.04	9.25	0.35	0.05	0.005	0.05	0.006	0.84	0.05
162	0.40	0.15	0.39	0.04	0.18	0.39	0.07	0.010	0.06	0.005	1.04	0.06
163	0.25	0.02	0.11	0.02	10.62	0.18	0.60	0.034	0.37	0.028	2.49	0.49
164	0.69	0.11	0.41	0.02	5.18	0.55	0.22	0.065	0.32	0.028	2.39	0.27
165	0.11	0.01	0.31	0.07	6.05	0.21	0.06	0.010	0.07	0.006	1.18	0.06
166	0.10	0.00	0.02	0.00	32.74	0.06	0.39	0.032	0.11	0.024	0.64	0.25
167	0.14	0.01	0.05	0.02	7.34	0.09	0.44	0.047	0.20	0.016	1.71	0.32
170	0.13	0.06	0.20	0.06	1.77	0.16	0.51	0.062	0.15	0.071	0.30	0.33
171	0.39	0.19	0.90	0.10	4.75	0.65	0.55	0.095	0.33	0.085	0.99	0.44
172	0.20	0.02	0.18	0.01	2.25	0.19	0.27	0.056	0.26	0.022	2.10	0.27
173	0.11	0.01	0.07	0.01	4.46	0.09	0.31	0.025	0.09	0.015	0.76	0.20
174	0.36	0.22	0.50	0.09	1.17	0.43	0.18	0.028	0.20	0.007	3.19	0.19
175	0.15	0.04	0.10	0.03	2.35	0.13	0.42	0.047	0.15	0.018	1.18	0.29
178	0.21	0.02	0.05	0.01	13.59	0.13	0.61	0.072	0.33	0.029	1.99	0.47
179	0.12	0.00	0.12	0.02	0.73	0.12	0.39	0.108	0.25	0.042	1.22	0.32
180	0.26	0.02	0.05	0.02	15.49	0.15	0.38	0.113	0.10	0.040	0.28	0.24
181	0.07	0.00	0.05	0.03	1.29	0.06	0.12	0.013	0.06	0.012	0.61	0.09
182	0.13	0.01	0.08	0.01	6.63	0.11	0.28	0.033	0.18	0.031	1.13	0.23
183	0.39	0.10	0.61	0.04	4.12	0.50	0.19	0.013	0.15	0.013	1.67	0.17
184	0.04	0.01	0.09	0.01	5.15	0.06	0.35	0.026	0.07	0.006	0.82	0.21
185	0.34	0.05	0.52	0.07	4.28	0.43	0.31	0.046	0.38	0.052	1.99	0.34
186	0.22	0.05	0.65	0.18	4.46	0.44	0.21	0.062	0.21	0.047	1.13	0.21
187	0.17	0.01	0.02	0.03	10.15	0.09	0.55	0.277	0.26	0.279	0.12	0.41

PU	*E. coli* binding						*S.* Typhimurium binding					
	Array 1		Array 2		Array 1 vs Array 2		Array 3		Array 4		Array 3 vs Array 4	
	Mean	SD	Mean	SD	t-Student	AVG	Mean	SD	Mean	SD	t-Student	AVG
188	0.17	0.00	0.08	0.04	4.27	0.12	0.17	0.041	0.22	0.003	4.87	0.20
189	0.17	0.00	0.09	0.01	14.24	0.13	0.35	0.023	0.28	0.035	1.80	0.32
191	0.28	0.04	0.27	0.04	0.31	0.27	0.52	0.044	0.36	0.040	1.98	0.44
192	0.39	0.04	0.06	0.02	14.79	0.22	0.52	0.092	0.15	0.054	0.38	0.34
194	0.12	0.06	0.09	0.02	1.12	0.11	0.31	0.044	0.23	0.081	0.81	0.27
195	0.19	0.03	0.15	0.01	1.99	0.17	0.41	0.099	0.22	0.024	1.45	0.31
196	0.08	0.02	0.14	0.01	5.24	0.11	0.62	0.036	0.12	0.020	0.60	0.37
197	0.18	0.03	0.23	0.02	2.70	0.20	0.56	0.017	0.29	0.016	2.69	0.42
199	0.21	0.04	0.01	0.00	11.19	0.11	0.41	0.107	0.12	0.005	1.17	0.26
200	0.15	0.02	0.05	0.02	7.18	0.10	0.48	0.041	0.11	0.011	1.00	0.30
201	0.16	0.03	0.06	0.02	6.80	0.11	0.49	0.061	0.32	0.052	1.49	0.41
202	0.11	0.01	0.01	0.01	14.99	0.06	0.10	0.033	0.07	0.001	2.18	0.09
203	0.18	0.01	0.14	0.01	4.89	0.16	0.13	0.020	0.19	0.005	3.81	0.16
205	0.09	0.01	0.07	0.01	1.71	0.08	0.20	0.020	0.11	0.005	1.97	0.16
207	0.15	0.02	0.09	0.02	5.74	0.12	0.40	0.004	0.15	0.032	0.81	0.28
208	0.21	0.02	0.16	0.05	1.46	0.18	0.30	0.049	0.63	0.098	2.54	0.47
210	0.19	0.01	0.08	0.04	5.60	0.14	0.37	0.065	0.16	0.022	1.05	0.26
212	0.10	0.01	0.20	0.03	5.49	0.15	0.26	0.030	0.19	0.014	2.01	0.23
215	0.16	0.01	0.24	0.07	2.36	0.20	0.26	0.031	0.14	0.047	0.64	0.20
216	0.19	0.01	0.20	0.02	1.68	0.20	0.29	0.052	0.26	0.016	2.56	0.28
217	0.13	0.01	0.75	0.11	10.87	0.44	0.08	0.002	0.14	0.013	1.69	0.11
218	0.21	0.00	0.12	0.02	6.79	0.17	0.45	0.022	0.17	0.014	1.60	0.31
219	0.23	0.04	0.20	0.04	1.05	0.21	0.44	0.067	0.58	0.058	2.91	0.51
220	0.30	0.03	0.35	0.04	2.05	0.33	0.32	0.078	0.43	0.047	2.38	0.37
222	0.11	0.05	0.71	0.14	7.86	0.41	0.63	0.054	0.64	0.107	2.11	0.64
223	0.19	0.02	0.50	0.13	4.84	0.34	0.15	0.075	0.11	0.009	1.25	0.13
224	0.15	0.02	0.18	0.03	1.64	0.17	0.49	0.034	0.16	0.009	1.77	0.32
225	0.07	0.01	0.17	0.03	5.62	0.12	0.31	0.029	0.21	0.036	1.26	0.26
226	0.20	0.03	0.51	0.06	9.86	0.36	0.36	0.150	0.17	0.016	1.11	0.26
227	0.25	0.03	0.05	0.01	11.71	0.15	0.17	0.016	0.34	0.023	3.00	0.25
228	0.06	0.01	0.06	0.02	0.19	0.06	0.35	0.058	0.12	0.028	0.60	0.23
229	0.09	0.01	0.02	0.01	7.44	0.06	0.28	0.063	0.07	0.027	0.34	0.17
233	0.05	0.01	0.08	0.02	2.39	0.06	0.34	0.032	0.12	0.003	2.36	0.23
234	0.08	0.01	0.02	0.01	9.38	0.05	0.07	0.017	0.08	0.020	0.70	0.07
235	0.20	0.01	-0.10	0.02	32.78	0.05	0.06	0.011	0.09	0.004	1.85	0.07
236	0.08	0.02	0.08	0.05	0.12	0.08	0.68	0.352	0.08	0.027	0.31	0.38
239	0.07	0.01	0.15	0.02	8.18	0.11	0.12	0.008	0.10	0.011	1.18	0.11
241	0.10	0.03	0.04	0.03	2.55	0.07	0.37	0.020	0.27	0.044	1.43	0.32
244	0.14	0.02	0.06	0.01	8.02	0.10	0.34	0.338	0.28	0.014	1.12	0.31
247	0.09	0.01	0.35	0.04	11.93	0.22	0.13	0.035	0.12	0.006	1.90	0.12
250	0.14	0.01	0.10	0.02	4.16	0.12	0.35	0.029	0.14	0.041	0.62	0.24
253	0.15	0.02	0.07	0.02	5.73	0.11	0.29	0.049	0.17	0.086	0.54	0.23
254	0.09	0.02	0.05	0.03	2.57	0.07	0.39	0.034	0.28	0.052	1.30	0.33
255	0.16	0.02	0.04	0.01	10.24	0.10	0.18	0.054	0.15	0.012	1.62	0.17
257	0.36	0.03	0.23	0.02	6.51	0.29	0.29	0.019	0.36	0.030	2.63	0.32
264	0.13	0.01	0.08	0.00	7.95	0.11	0.21	0.053	0.15	0.036	0.92	0.18
273	0.23	0.02	0.13	0.04	4.43	0.18	0.57	0.025	0.29	0.018	2.45	0.43
277	0.19	0.01	0.12	0.06	2.45	0.16	0.38	0.021	0.34	0.037	2.13	0.36
273	0.23	0.02	0.13	0.04	4.43	0.18	0.57	0.03	0.29	0.02	2.45	0.43
277	0.19	0.01	0.12	0.06	2.45	0.16	0.38	0.02	0.34	0.04	2.13	0.36

Results for *C. jejuni*, *C. perfringens*, *C. difficile*, *S. mutans* and two clinical bacterial cocaktails-polyacrylate binding analysis. The fluorescence intensities were normalised by dividing the whole set of the highest fluorescence value examined per polymer microarray. Mean: Mean normalised fluorescence intensity; SD: Standard deviation.

PA	*C. jejuni* 11168		*C. jejuni* CH4		*C. perfringens*		*C. difficile*		*S. mutans*		Clinical 1		Clinical 2	
	Mean	SD	Mean	SD	Mean	SD	Mean	SD	Mean	SD	Mean	SD	Mean	SD
3	0.14	0.004	0.00	0.002	0.09	0.036	0.01	0.002	0.12	0.022	0.01	0.004	0.06	0.059
11	0.10	0.019	0.01	0.007	0.07	0.034	0.01	0.005	0.08	0.009	0.03	0.004	0.09	0.021
12	0.14	0.012	0.01	0.004	0.03	0.008	0.01	0.002	0.06	0.006	0.03	0.004	0.06	0.017
13	0.01	0.003	0.02	0.002	0.01	0.007	0.00	0.001	0.02	0.001	0.01	0.001	0.03	0.004
14	0.01	0.005	0.01	0.003	0.01	0.014	0.00	0.001	0.03	0.004	0.01	0.002	0.09	0.022
17	0.02	0.008	0.01	0.002	0.02	0.009	0.00	0.001	0.10	0.006	0.01	0.001	0.10	0.018
18	0.04	0.007	0.01	0.005	0.02	0.012	0.01	0.001	0.09	0.011	0.01	0.003	0.18	0.031
19	0.23	0.015	0.02	0.002	0.04	0.012	0.00	0.001	0.12	0.006	0.02	0.002	0.03	0.060
20	0.12	0.004	0.01	0.001	0.05	0.010	0.00	0.001	0.05	0.006	0.03	0.003	0.05	0.011
21	0.18	0.018	0.03	0.006	0.05	0.029	0.01	0.002	0.06	0.005	0.04	0.004	0.05	0.020
22	0.13	0.011	0.01	0.002	0.02	0.005	0.00	0.001	0.06	0.022	0.01	0.002	0.03	0.006
23	0.11	0.035	0.01	0.002	0.03	0.016	0.00	0.001	0.05	0.010	0.01	0.002	0.03	0.011
25	0.12	0.025	0.00	0.001	0.07	0.018	0.00	0.003	0.05	0.008	0.01	0.003	0.05	0.029
26	0.10	0.050	0.03	0.007	-0.05	0.157	0.00	0.001	0.08	0.015	0.02	0.003	0.14	0.015
27	0.20	0.074	0.04	0.009	0.09	0.029	0.01	0.003	0.15	0.021	0.05	0.005	0.24	0.069
37	0.13	0.034	0.01	0.003	0.09	0.016	0.01	0.004	0.09	0.019	0.01	0.002	0.04	0.020
40	0.27	0.014	-0.01	0.003	0.28	0.043	0.00	0.003	0.29	0.016	0.02	0.002	0.06	0.027
43	0.28	0.014	0.00	0.003	0.05	0.020	0.00	0.002	0.15	0.059	0.03	0.003	0.13	0.019
44	0.20	0.014	0.02	0.007	0.01	0.010	0.00	0.002	0.12	0.019	0.02	0.007	0.04	0.008
46	0.32	0.010	0.04	0.008	0.16	0.010	0.01	0.004	0.11	0.013	0.03	0.004	0.19	0.016
50	0.08	0.016	0.00	0.001	0.05	0.012	0.00	0.000	0.04	0.012	0.00	0.001	0.02	0.005
55	0.27	0.048	0.03	0.004	0.07	0.028	0.04	0.003	0.08	0.006	0.09	0.016	0.11	0.010
56	0.44	0.022	0.03	0.004	0.09	0.022	0.02	0.001	0.06	0.004	0.04	0.005	0.11	0.010
56	0.10	0.012	0.07	0.004	0.10	0.025	0.07	0.007	0.13	0.018	0.14	0.006	0.03	0.015
57	0.53	0.027	0.07	0.006	0.12	0.022	0.18	0.109	0.08	0.004	0.26	0.010	0.21	0.029
58	0.47	0.010	0.04	0.005	0.07	0.016	0.08	0.005	0.12	0.016	0.10	0.006	0.11	0.038
59	0.83	0.032	0.16	0.011	0.17	0.021	0.07	0.005	0.20	0.016	0.18	0.008	0.48	0.021
60	0.29	0.029	0.02	0.008	0.04	0.028	0.01	0.001	0.17	0.017	0.04	0.003	0.12	0.015
100	0.08	0.021	0.05	0.037	0.09	0.030	0.07	0.006	0.17	0.002	0.06	0.021	0.10	0.029
102	0.21	0.030	0.03	0.013	0.06	0.041	0.01	0.003	0.12	0.009	0.02	0.001	0.10	0.042
104	0.04	0.020	0.01	0.004	0.07	0.016	0.10	0.007	0.44	0.013	0.03	0.003	0.06	0.026
105	0.02	0.004	0.00	0.001	0.04	0.004	0.00	0.000	0.01	0.002	0.00	0.001	0.01	0.008
106	0.29	0.042	0.00	0.005	0.00	0.003	0.00	0.002	0.14	0.022	0.01	0.003	0.06	0.012
112	0.06	0.025	0.08	0.088	0.10	0.025	0.02	0.003	0.33	0.018	0.02	0.002	0.13	0.030
113	0.16	0.005	0.02	0.002	0.20	0.051	0.02	0.002	0.50	0.014	0.02	0.003	0.03	0.052
117	0.23	0.030	0.02	0.012	0.04	0.007	0.00	0.002	0.13	0.017	0.04	0.005	0.04	0.014
119	0.28	0.049	0.02	0.007	0.10	0.018	0.01	0.002	0.21	0.065	0.05	0.014	0.10	0.017
120	0.01	0.005	0.00	0.002	0.03	0.007	0.00	0.001	0.02	0.005	0.00	0.001	0.18	0.205
128	0.01	0.010	0.01	0.003	0.05	0.013	0.00	0.001	0.22	0.005	0.02	0.004	-0.03	0.071
131	0.02	0.009	0.25	0.011	0.01	0.020	0.00	0.001	0.04	0.004	0.00	0.001	0.06	0.007
132	0.15	0.026	0.02	0.006	0.08	0.018	0.01	0.006	0.15	0.015	0.02	0.001	0.06	0.032
133	0.01	0.003	0.07	0.088	0.04	0.011	0.00	0.002	0.02	0.002	0.02	0.002	0.05	0.082
134	0.04	0.033	-0.02	0.005	0.13	0.026	-0.01	0.002	0.35	0.024	0.03	0.003	0.08	0.012
135	0.07	0.028	0.09	0.116	0.04	0.020	0.00	0.001	0.03	0.006	0.00	0.002	0.03	0.024
136	0.16	0.016	0.04	0.008	0.08	0.017	0.01	0.002	0.07	0.011	0.06	0.006	0.06	0.017
137	0.13	0.026	0.03	0.029	0.04	0.007	0.01	0.001	0.04	0.013	0.01	0.003	0.04	0.027
138	0.13	0.015	0.01	0.005	0.02	0.004	0.00	0.002	0.06	0.005	0.02	0.002	0.04	0.018
139	0.19	0.030	0.02	0.007	0.11	0.025	0.01	0.001	0.11	0.008	0.02	0.004	0.09	0.013
140	0.23	0.064	0.04	0.003	0.13	0.094	0.01	0.012	0.20	0.017	0.11	0.019	0.22	0.039
141	0.16	0.029	0.01	0.002	0.08	0.070	0.01	0.003	0.09	0.006	0.03	0.003	0.06	0.005
142	0.30	0.023	0.03	0.004	0.10	0.021	0.00	0.002	0.13	0.019	0.03	0.001	0.04	0.033
143	0.19	0.029	0.01	0.003	0.04	0.020	0.00	0.002	0.15	0.011	0.03	0.006	0.05	0.013
153	0.14	0.012	0.01	0.003	0.08	0.061	0.00	0.002	0.13	0.013	0.04	0.004	0.04	0.009
154	0.13	0.008	0.00	0.003	0.05	0.017	0.00	0.002	0.07	0.005	0.02	0.002	0.02	0.013
155	0.06	0.021	0.01	0.009	0.13	0.067	0.04	0.003	0.22	0.034	0.02	0.002	0.04	0.005
159	0.16	0.010	-0.01	0.005	0.23	0.043	0.00	0.001	0.29	0.013	0.03	0.003	0.06	0.067
160	0.16	0.040	0.00	0.001	0.05	0.016	0.00	0.001	0.14	0.023	0.01	0.001	0.04	0.014
162	0.17	0.019	0.01	0.011	0.02	0.018	0.00	0.000	0.08	0.004	0.02	0.003	0.06	0.010
163	0.10	0.013	0.02	0.011	0.02	0.013	0.00	0.001	0.05	0.003	0.02	0.006	0.04	0.005
164	0.13	0.053	0.10	0.164	0.09	0.021	0.00	0.002	0.07	0.021	0.01	0.002	0.01	0.010

PA	*C. jejuni* 11168		*C. jejuni* CH4		*C. perfringens*		*C. difficile*		*S. mutans*		Clinical 1		Clinical 2	
	Mean	SD	Mean	SD	Mean	SD	Mean	SD	Mean	SD	Mean	SD	Mean	SD
167	0.13	0.022	0.01	0.003	0.43	0.014	0.23	0.015	0.84	0.037	0.03	0.003	0.30	0.052
168	0.05	0.009	0.01	0.005	0.06	0.014	0.00	0.001	0.03	0.008	0.02	0.002	0.01	0.005
171	0.07	0.017	0.05	0.012	0.06	0.030	0.01	0.003	0.02	0.008	0.01	0.002	0.07	0.068
172	0.17	0.014	0.01	0.002	0.12	0.025	0.01	0.001	0.15	0.007	0.02	0.002	0.09	0.017
175	0.24	0.058	-0.01	0.004	0.31	0.110	0.04	0.002	0.65	0.056	0.03	0.003	0.11	0.037
177	0.10	0.022	0.00	0.001	0.07	0.016	0.00	0.000	0.04	0.008	0.01	0.001	0.02	0.007
178	0.16	0.024	0.00	0.002	0.01	0.005	0.00	0.000	0.08	0.007	0.01	0.003	0.03	0.010
179	0.08	0.008	0.01	0.003	0.01	0.002	0.00	0.001	0.05	0.006	0.00	0.002	0.02	0.002
180	0.06	0.016	0.01	0.003	0.10	0.021	0.00	0.002	0.07	0.010	0.01	0.002	0.02	0.004
181	0.24	0.040	0.01	0.003	0.14	0.079	0.01	0.002	0.63	0.074	0.02	0.002	0.02	0.020
182	0.03	0.004	0.00	0.001	0.01	0.006	0.00	0.001	0.23	0.018	0.01	0.001	0.01	0.005
183	0.14	0.029	0.00	0.002	0.04	0.018	0.00	0.001	0.06	0.003	0.01	0.002	0.02	0.012
184	0.13	0.026	0.02	0.023	0.04	0.012	0.00	0.001	0.04	0.001	0.01	0.005	0.02	0.012
185	0.14	0.012	0.00	0.004	0.04	0.020	0.00	0.000	0.14	0.027	0.01	0.001	0.01	0.039
185	0.12	0.028	0.00	0.002	0.03	0.012	0.00	0.002	0.04	0.004	0.01	0.002	0.03	0.015
186	0.20	0.024	0.03	0.016	0.06	0.018	0.00	0.004	0.22	0.016	0.03	0.004	0.08	0.120
187	0.00	0.002	0.02	0.013	0.02	0.004	0.00	0.001	0.06	0.005	0.00	0.002	0.02	0.047
188	0.07	0.018	-0.02	0.008	0.01	0.023	-0.01	0.002	0.38	0.014	0.01	0.002	0.04	0.042
189	0.09	0.011	0.01	0.002	0.02	0.005	0.00	0.002	0.04	0.004	0.01	0.001	0.05	0.017
190	0.17	0.013	0.02	0.004	0.06	0.018	0.01	0.002	0.14	0.005	0.02	0.002	0.09	0.006
191	0.01	0.003	0.10	0.168	0.03	0.005	0.00	0.000	0.01	0.003	0.01	0.000	0.03	0.005
192	0.22	0.012	0.01	0.005	0.05	0.018	0.00	0.001	0.13	0.026	0.03	0.001	0.14	0.053
193	0.24	0.024	0.01	0.003	0.13	0.013	0.00	0.002	0.16	0.020	0.01	0.003	0.16	0.024
194	0.24	0.030	0.02	0.008	0.00	0.006	0.00	0.001	0.12	0.009	0.03	0.008	0.13	0.035
196	0.02	0.015	0.01	0.002	0.06	0.014	0.00	0.001	0.06	0.009	0.01	0.002	0.03	0.036
197	0.03	0.014	0.01	0.002	0.05	0.013	0.00	0.002	0.10	0.006	0.01	0.002	0.07	0.033
198	0.13	0.019	0.01	0.001	0.07	0.016	0.03	0.002	0.04	0.008	0.29	0.024	0.06	0.020
199	1.00	0.060	0.50	0.024	0.01	0.005	0.38	0.022	0.20	0.017	0.00	0.002	0.55	0.049
201	0.25	0.022	0.01	0.003	0.10	0.022	0.06	0.005	0.09	0.019	0.44	0.011	0.05	0.017
204	0.14	0.009	0.01	0.001	0.11	0.022	0.07	0.004	0.06	0.007	1.00	0.037	0.06	0.013
207	0.04	0.007	0.50	0.037	0.01	0.017	0.00	0.001	0.09	0.008	0.01	0.001	0.04	0.021
208	0.08	0.020	0.06	0.020	0.09	0.019	0.03	0.008	0.05	0.008	0.03	0.009	0.05	0.004
210	0.30	0.023	0.22	0.011	1.00	0.160	1.00	0.039	1.00	0.024	0.77	0.021	0.45	0.028
214	0.18	0.010	0.05	0.046	0.10	0.040	0.00	0.001	0.11	0.005	0.01	0.002	0.05	0.020
215	0.30	0.026	0.03	0.010	0.08	0.038	0.00	0.000	0.15	0.024	0.01	0.002	0.07	0.021
216	0.54	0.043	0.03	0.010	0.03	0.007	0.01	0.003	0.12	0.005	0.02	0.002	0.14	0.016
218	0.16	0.013	0.07	0.009	0.03	0.046	0.00	0.003	0.15	0.017	0.02	0.004	0.09	0.146
222	0.33	0.024	0.05	0.021	0.09	0.028	0.02	0.003	0.15	0.011	0.04	0.002	0.07	0.021
223	0.21	0.059	0.02	0.027	0.05	0.008	0.00	0.001	0.07	0.009	0.02	0.005	0.05	0.058
306	0.00	0.003	0.01	0.007	-0.01	0.005	0.00	0.004	0.00	0.001	0.00	0.000	-0.03	0.045
307	0.09	0.019	0.03	0.006	0.07	0.037	0.00	0.000	0.04	0.009	0.01	0.002	0.01	0.004
309	0.01	0.002	0.01	0.008	0.02	0.006	0.00	0.001	0.02	0.008	0.01	0.002	0.01	0.002
315	0.04	0.007	0.01	0.001	0.03	0.006	0.00	0.001	0.03	0.002	0.00	0.001	0.02	0.011
316	0.02	0.006	0.01	0.003	0.01	0.002	0.00	0.001	0.03	0.005	0.01	0.002	0.01	0.006
318	0.04	0.017	0.06	0.003	0.04	0.010	0.01	0.004	0.02	0.001	0.02	0.002	0.10	0.093
323	0.03	0.035	0.01	0.002	0.04	0.010	0.02	0.002	0.07	0.016	0.01	0.001	0.12	0.024
324	0.03	0.018	0.02	0.019	0.08	0.018	0.00	0.002	0.09	0.007	0.01	0.002	0.12	0.097
325	0.03	0.009	0.01	0.001	0.08	0.019	0.02	0.003	0.11	0.018	0.00	0.001	0.24	0.017
326	0.03	0.015	0.01	0.002	0.10	0.039	0.01	0.003	0.09	0.010	0.00	0.001	0.16	0.041
327	0.02	0.011	-0.01	0.011	0.06	0.025	-0.01	0.001	0.13	0.019	0.00	0.002	0.10	0.010
329	0.08	0.003	-0.01	0.006	0.05	0.015	0.00	0.001	0.11	0.007	0.01	0.003	0.15	0.128
330	0.10	0.004	0.01	0.004	0.03	0.005	0.01	0.001	0.08	0.022	0.02	0.003	0.02	0.004
331	0.13	0.015	0.02	0.008	0.04	0.014	0.01	0.002	0.12	0.020	0.04	0.004	0.03	0.018
332	0.07	0.025	0.02	0.002	0.03	0.016	0.00	0.001	0.10	0.025	0.06	0.003	0.03	0.008
336	0.02	0.004	0.00	0.006	0.01	0.006	0.00	0.001	0.06	0.022	0.00	0.001	0.03	0.003
337	0.01	0.005	0.00	0.001	0.02	0.003	0.00	0.000	0.02	0.004	0.01	0.004	0.02	0.004
338	0.01	0.002	0.00	0.004	0.04	0.005	0.00	0.001	0.03	0.002	0.02	0.007	0.03	0.013
357	0.05	0.008	0.02	0.002	0.07	0.013	0.03	0.005	0.09	0.017	0.02	0.002	0.13	0.017
358	0.02	0.005	0.01	0.002	0.06	0.021	0.01	0.002	0.18	0.011	0.00	0.001	0.08	0.063
359	0.07	0.031	0.14	0.178	0.20	0.017	0.11	0.031	0.91	0.036	0.10	0.014	0.80	0.177
360	0.03	0.006	0.02	0.003	0.05	0.007	0.02	0.001	0.07	0.004	0.01	0.003	0.05	0.012
361	-0.01	0.003	0.00	0.003	0.05	0.009	0.00	0.002	0.11	0.027	0.00	0.001	0.03	0.010
363	0.02	0.006	0.01	0.001	0.04	0.005	0.03	0.001	0.10	0.009	0.06	0.004	0.08	0.014
364	0.01	0.001	0.00	0.001	0.03	0.006	0.00	0.001	0.07	0.019	0.01	0.001	0.02	0.006
369	0.03	0.008	0.00	0.001	0.03	0.017	0.00	0.001	0.06	0.007	0.02	0.002	0.02	0.008
372	0.11	0.008	0.01	0.014	0.06	0.017	0.00	0.002	0.09	0.033	0.00	0.002	0.09	0.053

PA	*C. jejuni* 11168		*C. jejuni* CH4		*C. perfringens*		*C. difficile*		*S. mutans*		Clinical 1		Clinical 2	
	Mean	SD	Mean	SD	Mean	SD	Mean	SD	Mean	SD	Mean	SD	Mean	SD
375	0.05	0.012	0.08	0.110	0.04	0.010	0.00	0.001	0.02	0.003	0.00	0.000	0.01	0.007
387	0.10	0.016	0.02	0.006	0.10	0.015	0.01	0.002	0.08	0.025	0.01	0.002	0.03	0.023
389	0.06	0.022	0.35	0.378	0.07	0.048	0.00	0.001	0.06	0.011	0.00	0.002	0.02	0.018
390	0.03	0.017	0.02	0.004	-0.01	0.015	0.00	0.001	0.04	0.013	0.00	0.002	0.01	0.009
393	0.07	0.016	0.04	0.011	0.07	0.012	0.02	0.004	0.10	0.020	0.03	0.004	0.07	0.021
394	0.01	0.007	0.02	0.012	0.03	0.010	0.00	0.003	0.09	0.020	0.01	0.002	0.07	0.133
395	0.02	0.009	0.02	0.003	0.01	0.005	0.02	0.004	0.25	0.012	0.02	0.002	0.07	0.013
396	0.02	0.010	0.01	0.002	0.02	0.033	0.00	0.000	0.10	0.021	0.00	0.004	0.02	0.017
397	0.06	0.002	0.00	0.009	0.02	0.011	0.00	0.001	0.05	0.007	0.01	0.004	0.02	0.020
398	0.07	0.019	0.00	0.003	0.05	0.014	0.00	0.002	0.15	0.014	0.00	0.001	0.08	0.014
399	0.00	0.009	0.00	0.015	0.03	0.013	0.00	0.000	0.07	0.007	0.01	0.004	0.07	0.024
400	0.01	0.008	0.01	0.003	0.05	0.012	0.00	0.001	0.08	0.017	0.01	0.004	0.04	0.007
401	0.04	0.030	0.00	0.005	0.03	0.007	0.00	0.002	0.07	0.003	0.02	0.007	0.07	0.009
406	0.11	0.016	0.00	0.005	0.07	0.042	0.00	0.001	0.07	0.005	0.01	0.001	0.09	0.065
411	0.17	0.048	0.06	0.010	0.12	0.023	0.08	0.008	0.26	0.018	0.11	0.022	0.04	0.015
412	0.11	0.012	0.00	0.001	0.10	0.033	0.00	0.001	0.10	0.007	0.02	0.001	0.07	0.021
413	0.13	0.036	0.01	0.009	0.07	0.059	0.00	0.001	0.09	0.010	0.01	0.002	0.08	0.063
414	0.00	0.002	0.00	0.001	0.07	0.020	0.00	0.001	0.05	0.003	0.00	0.001	0.02	0.007
415	0.08	0.010	0.01	0.010	0.05	0.008	0.00	0.001	0.11	0.022	0.02	0.002	0.15	0.096
416	0.03	0.007	0.01	0.002	0.27	0.048	0.03	0.005	0.32	0.016	0.03	0.002	0.10	0.009
417	0.15	0.017	0.02	0.004	0.03	0.013	0.01	0.002	0.08	0.005	0.01	0.001	0.11	0.058
418	0.17	0.020	0.02	0.007	0.02	0.003	0.00	0.002	0.09	0.024	0.02	0.002	0.06	0.015
419	0.17	0.019	0.02	0.003	0.09	0.016	0.02	0.001	0.13	0.024	0.03	0.001	0.10	0.078
420	0.07	0.009	0.01	0.002	0.06	0.016	0.00	0.001	0.21	0.021	0.01	0.001	0.06	0.012
421	0.09	0.015	0.02	0.002	0.04	0.006	0.01	0.000	0.08	0.018	0.01	0.001	0.07	0.020
423	0.03	0.025	0.00	0.005	0.08	0.025	0.00	0.002	0.12	0.019	0.01	0.005	0.12	0.066
426	0.05	0.009	0.00	0.005	0.11	0.047	0.00	0.001	0.12	0.008	0.01	0.003	0.07	0.013
427	0.13	0.015	0.01	0.018	0.07	0.025	0.01	0.002	0.15	0.006	0.01	0.003	0.03	0.015
428	0.07	0.032	0.00	0.018	0.15	0.029	0.00	0.002	0.12	0.019	0.01	0.004	0.09	0.030
429	0.05	0.006	0.02	0.003	0.04	0.014	0.01	0.001	0.10	0.007	0.03	0.005	0.12	0.064
430	0.03	0.006	0.02	0.004	0.04	0.011	0.01	0.002	0.11	0.009	0.04	0.004	0.05	0.005
431	0.20	0.021	0.03	0.005	0.06	0.019	0.00	0.002	0.11	0.015	0.04	0.005	0.08	0.037
432	0.03	0.006	0.01	0.006	0.10	0.030	0.02	0.003	0.26	0.023	0.03	0.003	0.06	0.017
434	0.05	0.010	0.00	0.002	0.01	0.004	0.00	0.001	0.03	0.002	0.00	0.003	0.06	0.027
435	0.12	0.034	0.02	0.009	0.03	0.008	0.01	0.003	0.06	0.007	0.01	0.001	0.05	0.014
437	0.13	0.017	0.00	0.004	0.03	0.009	0.00	0.002	0.08	0.020	0.01	0.001	0.06	0.015
442	0.04	0.010	0.10	0.112	0.05	0.019	0.00	0.001	0.04	0.004	0.00	0.001	0.01	0.006
443	0.01	0.009	0.07	0.116	0.03	0.009	0.00	0.002	0.08	0.014	0.01	0.003	0.06	0.019
444	0.05	0.010	0.03	0.009	0.06	0.007	0.00	0.005	0.10	0.031	0.01	0.001	0.05	0.023
446	0.02	0.012	0.01	0.007	0.06	0.010	0.01	0.002	0.08	0.012	0.01	0.002	0.11	0.077
449	0.04	0.006	0.02	0.010	0.06	0.016	0.00	0.002	0.05	0.007	0.01	0.003	0.02	0.097
450	0.02	0.055	0.01	0.003	0.12	0.014	0.00	0.002	0.20	0.025	0.03	0.010	0.17	0.030
452	0.03	0.011	0.00	0.005	0.06	0.006	0.00	0.001	0.12	0.008	0.01	0.001	0.06	0.034
453	0.12	0.019	0.01	0.008	0.04	0.017	0.00	0.000	0.04	0.004	0.02	0.001	0.04	0.009
458	0.11	0.006	0.01	0.005	0.27	0.084	0.01	0.002	0.24	0.021	0.02	0.003	0.08	0.138
459	0.02	0.002	0.02	0.003	0.04	0.013	0.01	0.002	0.10	0.021	0.02	0.003	0.05	0.009
460	0.04	0.006	0.01	0.002	0.06	0.010	0.00	0.001	0.09	0.004	0.01	0.001	0.04	0.018
462	0.00	0.005	0.00	0.001	0.04	0.007	0.01	0.004	0.06	0.022	0.01	0.003	0.01	0.005
465	0.02	0.006	0.02	0.005	0.02	0.003	0.00	0.001	0.02	0.003	0.01	0.002	0.04	0.022
467	0.04	0.008	0.02	0.003	0.03	0.014	0.00	0.002	0.04	0.006	0.00	0.002	0.05	0.007
468	0.01	0.016	0.00	0.003	0.04	0.012	0.00	0.001	0.07	0.020	0.00	0.002	0.03	0.010
469	0.09	0.009	0.02	0.020	0.05	0.024	0.00	0.004	0.07	0.009	0.01	0.001	0.08	0.010
470	0.00	0.005	0.00	0.003	0.13	0.018	0.03	0.005	0.17	0.018	0.03	0.005	0.03	0.008
474	0.07	0.013	0.01	0.001	0.10	0.031	0.01	0.001	0.14	0.017	0.02	0.003	0.03	0.006
475	0.02	0.013	0.00	0.001	0.03	0.010	0.00	0.001	0.02	0.002	0.00	0.001	0.01	0.004
476	0.01	0.003	0.01	0.004	0.06	0.012	0.00	0.002	0.04	0.005	0.02	0.003	0.02	0.008
477	0.11	0.017	0.01	0.006	0.03	0.006	0.00	0.001	0.05	0.018	0.02	0.002	0.06	0.030
481	0.08	0.012	0.02	0.008	0.03	0.004	0.00	0.000	0.05	0.002	0.01	0.001	0.06	0.015
485	0.10	0.028	0.01	0.002	0.01	0.005	0.00	0.001	0.10	0.006	0.03	0.001	0.10	0.039
493	0.07	0.016	0.03	0.010	0.16	0.046	0.00	0.002	0.10	0.014	0.01	0.001	0.10	0.078
496	0.03	0.005	0.00	0.002	0.10	0.015	0.00	0.001	0.07	0.005	0.03	0.004	0.05	0.006
497	0.15	0.010	0.01	0.012	0.06	0.027	0.00	0.001	0.08	0.023	0.02	0.006	0.08	0.012
499	0.06	0.011	0.02	0.042	0.02	0.013	0.00	0.001	0.04	0.006	0.01	0.003	0.02	0.011
500	0.08	0.019	0.01	0.005	0.09	0.049	0.00	0.001	0.15	0.024	0.02	0.002	0.06	0.008
504	0.03	0.012	0.01	0.003	0.07	0.014	0.01	0.002	0.08	0.009	0.02	0.003	0.03	0.007
507	0.18	0.013	0.03	0.005	0.02	0.004	0.00	0.001	0.12	0.018	0.03	0.003	0.10	0.090

PA	*C. jejuni* 11168		*C. jejuni* CH4		*C. perfringens*		*C. difficile*		*S. mutans*		Clinical 1		Clinical 2	
	Mean	SD	Mean	SD	Mean	SD	Mean	SD	Mean	SD	Mean	SD	Mean	SD
508	0.08	0.016	0.02	0.004	0.07	0.021	0.00	0.000	0.13	0.021	0.02	0.002	0.01	0.095
509	0.08	0.008	0.01	0.003	0.06	0.009	0.00	0.001	0.06	0.008	0.01	0.003	0.04	0.007
511	0.04	0.012	0.02	0.002	0.04	0.023	0.00	0.001	0.07	0.018	0.00	0.001	0.07	0.027
512	0.01	0.003	0.00	0.003	0.12	0.019	0.01	0.002	0.21	0.037	0.01	0.002	0.05	0.014
513	0.02	0.005	0.00	0.001	0.03	0.007	0.00	0.000	0.02	0.003	0.01	0.002	0.03	0.010
514	0.02	0.017	0.01	0.002	0.13	0.043	0.02	0.002	0.21	0.005	0.02	0.001	0.04	0.019
515	0.03	0.005	0.01	0.001	0.02	0.003	0.00	0.001	0.01	0.001	0.01	0.001	0.03	0.005
517	0.10	0.013	0.02	0.004	0.06	0.015	0.01	0.002	0.04	0.005	0.03	0.003	0.04	0.024
518	0.04	0.004	0.01	0.004	0.04	0.014	0.01	0.003	0.05	0.003	0.02	0.002	0.08	0.024
519	0.12	0.035	0.02	0.007	0.14	0.017	0.02	0.002	0.20	0.009	0.04	0.007	0.09	0.027
520	0.02	0.008	0.00	0.004	0.05	0.010	0.00	0.002	0.18	0.011	0.01	0.001	0.08	0.029
522	0.00	0.002	0.00	0.002	0.03	0.014	0.00	0.002	0.22	0.090	0.01	0.001	0.03	0.014
523	0.14	0.014	0.02	0.006	0.11	0.015	0.02	0.005	0.17	0.012	0.03	0.003	0.07	0.010
528	0.01	0.004	0.01	0.003	0.06	0.006	0.01	0.002	0.18	0.015	0.01	0.003	0.03	0.004

Results for *C. jejuni*, *C. perfringens*, *C. difficile*, *S. mutans* and two clinical bacterial cocaktails-polyurethane binding analysis. The fluorescence intensities were normalised by dividing the whole set of the highest fluorescence value examined per polymer microarray. Mean: Mean normalised fluorescence intensity; SD: Standard deviation.

PU	*C. jejuni* 11168		*C. jejuni* CH4		*C. perfringens*		*C. difficile*		*S. mutans*		Clinical 1		Clinical 2	
	Mean	SD	Mean	SD	Mean	SD	Mean	SD	Mean	SD	Mean	SD	Mean	SD
1	0.04	0.020	0.04	0.003	0.03	0.016	0.00	0.001	0.01	0.003	0.00	0.002	0.01	0.002
2	0.07	0.017	0.00	0.001	0.06	0.022	0.00	0.001	0.02	0.013	0.01	0.003	0.01	0.009
3	0.09	0.018	0.02	0.029	0.08	0.006	0.00	0.001	0.04	0.004	0.01	0.001	0.01	0.006
4	0.09	0.023	0.02	0.035	0.03	0.023	0.00	0.002	0.04	0.007	0.01	0.003	0.03	0.124
5	0.01	0.005	0.08	0.006	0.01	0.003	0.00	0.001	0.01	0.001	0.00	0.001	0.01	0.005
7	0.05	0.013	0.02	0.006	0.03	0.007	0.00	0.000	0.01	0.002	0.00	0.001	0.00	0.004
8	0.08	0.008	0.09	0.126	0.04	0.019	0.00	0.001	0.04	0.006	0.01	0.002	0.02	0.068
10	0.03	0.010	0.00	0.005	0.01	0.005	0.00	0.002	0.02	0.004	0.01	0.004	0.00	0.000
12	0.07	0.010	0.01	0.005	0.10	0.028	0.00	0.001	0.11	0.004	0.02	0.002	0.03	0.009
13	0.13	0.009	0.00	0.001	0.06	0.007	0.00	0.001	0.14	0.018	0.01	0.001	0.06	0.024
14	0.12	0.008	0.00	0.005	0.07	0.020	0.00	0.001	0.13	0.006	0.01	0.001	0.03	0.013
16	0.01	0.005	0.00	0.005	0.01	0.002	0.01	0.005	0.01	0.002	0.02	0.007	0.00	0.006
17	0.09	0.030	0.01	0.018	0.08	0.032	0.02	0.034	0.14	0.027	0.01	0.002	0.13	0.040
18	0.15	0.069	0.04	0.005	0.16	0.057	0.01	0.006	0.24	0.016	0.06	0.010	0.22	0.057
19	0.08	0.017	0.01	0.002	0.03	0.022	0.01	0.002	0.10	0.021	0.01	0.002	0.02	0.019
20	0.04	0.006	0.00	0.002	0.01	0.009	0.00	0.002	0.03	0.002	0.00	0.003	0.01	0.009
22	0.08	0.007	0.00	0.002	0.02	0.011	0.00	0.003	0.04	0.016	0.00	0.001	-0.01	0.055
23	0.11	0.011	0.00	0.001	0.06	0.013	0.00	0.001	0.04	0.015	0.01	0.005	-0.02	0.059
24	0.05	0.015	0.00	0.002	0.05	0.016	0.00	0.001	0.04	0.011	0.01	0.004	0.01	0.006
25	0.14	0.025	0.00	0.003	0.07	0.014	0.01	0.005	0.12	0.008	0.03	0.005	0.05	0.017
25	0.12	0.008	0.00	0.010	0.05	0.012	0.00	0.002	0.04	0.006	0.01	0.000	0.01	0.005
27	0.16	0.015	0.01	0.008	0.03	0.008	0.00	0.002	0.07	0.005	0.02	0.002	0.04	0.004
28	0.14	0.005	0.00	0.002	-0.05	0.180	0.00	0.002	0.10	0.008	0.00	0.001	0.03	0.008
29	0.18	0.014	0.01	0.013	0.06	0.035	0.00	0.001	0.13	0.037	0.02	0.005	0.04	0.426
33	0.04	0.010	0.00	0.002	0.01	0.005	0.00	0.001	0.06	0.015	0.01	0.002	0.05	0.007
35	0.10	0.009	0.00	0.004	0.01	0.003	0.00	0.001	0.05	0.009	0.01	0.002	0.05	0.045
39	0.10	0.015	0.01	0.002	0.03	0.004	0.00	0.000	0.08	0.005	0.01	0.002	0.03	0.034
41	0.16	0.048	0.00	0.002	0.13	0.023	0.00	0.001	0.14	0.019	0.02	0.002	0.06	0.007
46	0.08	0.039	0.00	0.011	0.07	0.019	0.01	0.001	0.11	0.006	0.01	0.002	0.29	0.068
48	0.13	0.016	0.06	0.072	0.07	0.057	0.01	0.002	0.09	0.010	0.02	0.004	0.03	0.029
53	0.23	0.021	0.02	0.007	0.02	0.002	0.00	0.001	0.15	0.026	0.02	0.002	0.08	0.047
61	0.00	0.002	0.00	0.001	0.01	0.004	0.00	0.001	0.03	0.010	0.00	0.003	0.04	0.076
63	0.05	0.007	0.01	0.006	0.07	0.022	0.00	0.001	0.03	0.006	0.01	0.002	0.04	0.046
67	0.15	0.017	0.17	0.292	0.08	0.022	0.01	0.001	0.07	0.013	0.01	0.002	0.03	0.016
69	0.16	0.010	0.02	0.011	0.10	0.029	0.01	0.003	0.16	0.020	0.02	0.001	0.10	0.016
69	0.09	0.010	0.01	0.003	0.01	0.005	0.00	0.001	0.05	0.004	0.01	0.002	0.03	0.009
71	0.16	0.045	0.01	0.004	0.03	0.030	0.00	0.005	0.11	0.007	0.02	0.004	0.03	0.016
73	0.07	0.014	0.00	0.003	0.05	0.017	0.00	0.000	0.06	0.018	0.01	0.001	-0.03	0.080
77	0.11	0.019	-0.01	0.002	0.10	0.024	0.00	0.001	0.04	0.018	0.00	0.003	0.02	0.007
77	0.10	0.024	0.00	0.001	0.05	0.020	0.00	0.001	0.09	0.012	0.01	0.002	0.22	0.378
79	0.11	0.012	0.02	0.028	0.07	0.033	0.00	0.002	0.05	0.003	0.02	0.003	0.05	0.014
81	0.17	0.010	0.03	0.031	0.04	0.012	0.01	0.002	0.09	0.009	0.02	0.002	0.06	0.008
83	0.00	0.001	0.00	0.002	0.03	0.008	0.00	0.001	0.02	0.002	0.00	0.001	0.01	0.007
85	0.02	0.004	0.02	0.011	0.08	0.008	0.01	0.003	0.06	0.006	0.02	0.002	0.06	0.011
87	0.07	0.011	0.00	0.004	0.10	0.023	0.01	0.003	0.03	0.001	0.01	0.002	0.02	0.068
89	0.51	0.093	0.25	0.041	0.14	0.015	0.08	0.023	0.21	0.006	0.19	0.012	0.82	0.038
92	0.08	0.017	0.00	0.009	0.03	0.012	0.00	0.001	0.11	0.025	0.00	0.001	0.03	0.031
93	0.14	0.012	0.03	0.010	0.22	0.064	0.01	0.003	0.15	0.008	0.02	0.002	0.06	0.018
94	0.16	0.008	0.01	0.002	0.09	0.047	0.00	0.002	0.14	0.015	0.01	0.001	0.04	0.008
95	0.13	0.018	0.01	0.005	0.08	0.030	0.02	0.003	0.11	0.004	0.03	0.005	0.10	0.092
96	0.07	0.015	0.03	0.037	0.02	0.004	0.00	0.001	0.04	0.003	0.01	0.004	0.02	0.009
97	0.14	0.018	0.01	0.004	0.02	0.008	0.00	0.001	0.05	0.003	0.01	0.004	0.03	0.010
98	0.18	0.015	0.01	0.003	0.00	0.002	0.01	0.001	0.09	0.017	0.01	0.001	0.04	0.013
99	0.22	0.028	0.01	0.009	0.02	0.007	0.00	0.002	0.09	0.018	0.02	0.003	0.06	0.004
100	0.07	0.008	0.00	0.011	0.04	0.005	0.00	0.000	0.05	0.003	0.02	0.003	0.04	0.009
101	0.02	0.014	-0.04	0.015	0.04	0.013	-0.02	0.002	0.09	0.009	-0.03	0.001	0.07	0.043
102	0.11	0.024	0.02	0.012	0.07	0.026	0.01	0.001	0.13	0.024	0.01	0.001	0.12	0.058
103	0.18	0.028	0.04	0.004	0.16	0.052	0.02	0.005	0.13	0.006	0.03	0.004	0.07	0.038
104	0.11	0.020	0.01	0.002	0.03	0.014	0.00	0.001	0.07	0.004	0.01	0.002	0.03	0.012
105	0.09	0.015	0.01	0.003	0.24	0.037	0.00	0.002	0.16	0.024	0.01	0.003	-0.06	0.241

PU	*C. jejuni* 11168		*C. jejuni* CH4		*C. perfringens*		*C. difficile*		*S. mutans*		Clinical 1		Clinical 2	
	Mean	SD	Mean	SD	Mean	SD	Mean	SD	Mean	SD	Mean	SD	Mean	SD
108	0.14	0.016	0.01	0.004	0.02	0.007	0.00	0.001	0.07	0.004	0.02	0.002	0.04	0.004
110	0.20	0.019	0.01	0.005	0.01	0.004	0.00	0.001	0.11	0.016	0.02	0.002	0.05	0.019
112	0.14	0.033	0.01	0.005	0.01	0.008	0.00	0.001	0.11	0.021	0.03	0.007	0.02	0.005
115	0.07	0.016	0.01	0.005	0.06	0.015	0.00	0.001	0.06	0.003	0.01	0.002	0.06	0.067
116	0.13	0.006	0.01	0.004	0.07	0.029	0.01	0.003	0.06	0.008	0.02	0.004	0.06	0.015
117	0.20	0.008	0.02	0.008	0.09	0.037	0.00	0.003	0.06	0.004	0.02	0.003	0.02	0.004
118	0.21	0.026	0.02	0.009	0.19	0.100	0.02	0.003	0.23	0.024	0.05	0.006	0.20	0.118
119	0.22	0.018	0.02	0.003	0.03	0.010	0.01	0.002	0.12	0.009	0.04	0.003	0.12	0.139
120	0.13	0.009	0.02	0.003	0.06	0.039	0.01	0.001	0.04	0.003	0.03	0.002	0.09	0.015
121	0.16	0.026	0.03	0.005	0.03	0.013	0.00	0.001	0.11	0.012	0.03	0.002	0.09	0.015
122	0.24	0.031	0.00	0.008	0.03	0.033	0.00	0.002	0.14	0.030	0.03	0.003	0.05	0.023
123	0.06	0.022	0.03	0.046	0.04	0.025	0.00	0.001	0.02	0.008	0.00	0.002	0.03	0.029
124	0.10	0.026	-0.06	0.101	0.07	0.054	-0.01	0.007	0.06	0.012	0.00	0.001	0.01	0.014
126	0.13	0.027	0.04	0.019	0.06	0.030	0.02	0.005	0.07	0.010	0.02	0.005	0.08	0.090
128	0.12	0.020	0.02	0.007	0.06	0.019	0.00	0.001	0.05	0.010	0.01	0.005	0.06	0.139
129	0.03	0.009	0.03	0.003	0.03	0.010	0.00	0.000	0.01	0.004	0.01	0.003	0.02	0.007
130	0.06	0.011	0.02	0.003	0.02	0.030	0.00	0.001	0.03	0.004	0.01	0.003	0.03	0.057
131	0.03	0.007	0.01	0.004	0.02	0.026	0.00	0.001	0.02	0.003	0.29	0.175	0.04	0.055
132	0.13	0.022	0.00	0.014	0.11	0.015	0.01	0.001	0.14	0.010	0.01	0.002	0.02	0.018
134	0.12	0.007	0.00	0.001	0.07	0.018	0.01	0.001	0.12	0.004	0.01	0.000	0.08	0.109
135	0.17	0.015	0.04	0.004	0.19	0.068	0.01	0.002	0.13	0.017	0.07	0.004	0.24	0.017
137	0.17	0.009	0.02	0.002	0.07	0.016	0.02	0.003	0.19	0.016	0.05	0.005	0.10	0.019
138	0.16	0.014	0.03	0.002	0.08	0.014	0.02	0.001	0.10	0.004	0.05	0.002	0.09	0.019
139	0.08	0.006	0.01	0.002	0.05	0.008	0.00	0.003	0.04	0.002	0.01	0.003	0.02	0.012
140	0.03	0.008	0.01	0.010	0.07	0.012	0.00	0.002	0.03	0.003	0.01	0.004	0.03	0.009
141	0.04	0.010	0.01	0.005	0.05	0.005	0.00	0.001	0.06	0.008	0.01	0.004	0.04	0.024
142	0.26	0.014	0.05	0.011	0.19	0.010	0.05	0.002	0.12	0.010	0.05	0.002	0.16	0.029
143	0.11	0.008	0.01	0.002	0.07	0.010	0.00	0.002	0.13	0.011	0.02	0.001	0.06	0.014
144	0.12	0.022	0.05	0.052	0.17	0.118	0.01	0.005	0.09	0.006	0.02	0.005	0.10	0.036
145	0.09	0.018	0.01	0.003	0.06	0.039	0.01	0.002	0.08	0.021	0.02	0.005	0.00	0.061
148	0.20	0.016	0.01	0.009	0.04	0.007	0.01	0.001	0.10	0.011	0.04	0.006	0.08	0.017
149	0.19	0.029	0.02	0.004	0.03	0.006	0.01	0.001	0.10	0.017	0.04	0.006	0.07	0.007
151	0.05	0.013	0.01	0.005	0.06	0.017	0.00	0.000	0.13	0.016	0.01	0.002	0.03	0.019
152	0.06	0.014	0.01	0.003	0.05	0.008	0.00	0.001	0.07	0.018	0.03	0.003	0.02	0.007
153	0.11	0.011	0.01	0.002	0.11	0.013	0.00	0.001	0.16	0.009	0.03	0.003	0.10	0.027
154	0.28	0.034	0.02	0.003	0.08	0.040	0.03	0.004	0.15	0.017	0.09	0.007	0.15	0.023
156	0.09	0.013	0.02	0.006	0.03	0.009	0.00	0.002	0.09	0.015	0.00	0.001	0.05	0.014
159	0.12	0.021	0.01	0.005	0.02	0.005	0.00	0.001	0.08	0.005	0.02	0.004	0.05	0.009
161	0.06	0.008	0.03	0.005	0.01	0.012	0.00	0.001	0.03	0.004	0.01	0.007	0.06	0.080
162	0.06	0.008	0.05	0.071	0.06	0.016	0.00	0.001	0.05	0.005	0.01	0.002	0.15	0.173
163	0.11	0.015	0.03	0.007	0.18	0.045	0.01	0.003	0.08	0.023	0.02	0.001	0.06	0.017
164	0.09	0.020	0.02	0.006	0.04	0.017	0.00	0.003	0.09	0.014	0.03	0.007	0.09	0.123
166	0.21	0.011	0.07	0.098	0.02	0.004	0.00	0.001	0.14	0.009	0.04	0.005	0.03	0.015
168	0.10	0.009	0.01	0.002	0.05	0.004	0.00	0.002	0.05	0.005	0.02	0.002	0.11	0.014
171	0.10	0.010	0.01	0.012	0.08	0.025	0.00	0.001	0.07	0.019	0.02	0.002	0.04	0.013
172	0.14	0.028	0.01	0.019	0.10	0.020	0.00	0.001	0.16	0.018	0.01	0.002	0.09	0.019
173	0.05	0.004	0.00	0.001	0.06	0.012	0.00	0.001	0.07	0.019	0.01	0.001	0.02	0.011
174	0.16	0.013	0.02	0.005	0.09	0.027	0.01	0.003	0.07	0.012	0.02	0.002	0.03	0.012
175	0.13	0.013	0.00	0.002	0.03	0.010	0.01	0.002	0.08	0.009	0.02	0.002	-0.03	0.188
178	0.02	0.010	0.00	0.004	0.03	0.013	0.00	0.002	0.04	0.004	0.00	0.001	0.07	0.069
179	0.01	0.003	0.01	0.003	0.01	0.001	0.00	0.003	0.03	0.004	0.00	0.001	0.01	0.005
181	0.09	0.013	0.01	0.006	0.10	0.031	0.01	0.004	0.04	0.004	0.02	0.003	0.05	0.056
183	0.12	0.010	0.00	0.003	0.10	0.033	0.03	0.044	0.11	0.010	0.02	0.004	0.00	0.022
184	0.14	0.007	0.01	0.007	0.07	0.026	0.01	0.001	0.15	0.019	0.01	0.002	0.04	0.007
185	0.18	0.014	0.01	0.003	0.09	0.017	0.01	0.002	0.14	0.028	0.02	0.002	0.06	0.020
187	0.15	0.013	0.03	0.005	0.10	0.031	0.00	0.002	0.17	0.010	0.02	0.002	0.04	0.009
188	0.25	0.016	0.03	0.008	0.06	0.022	0.00	0.001	0.11	0.020	0.04	0.008	0.13	0.068
189	0.12	0.024	0.03	0.018	0.22	0.074	0.00	0.002	0.05	0.003	0.01	0.005	0.04	0.011
190	0.17	0.024	0.00	0.004	0.17	0.056	0.01	0.002	0.14	0.018	0.05	0.008	0.04	0.063
191	0.02	0.005	0.02	0.004	0.01	0.007	0.00	0.004	0.03	0.001	0.01	0.002	0.12	0.052
192	0.08	0.016	0.03	0.041	0.06	0.012	0.00	0.001	0.07	0.006	0.02	0.003	0.01	0.004
196	0.14	0.012	0.02	0.004	0.11	0.043	0.00	0.001	0.12	0.012	0.01	0.002	0.09	0.068
197	0.18	0.026	0.02	0.010	0.08	0.038	0.00	0.001	0.10	0.017	0.02	0.002	0.07	0.034
199	0.18	0.023	0.02	0.002	0.02	0.016	0.00	0.001	0.10	0.017	0.02	0.005	0.02	0.042
201	0.13	0.014	0.01	0.006	0.03	0.009	0.00	0.001	0.11	0.006	0.03	0.008	0.03	0.017
202	0.11	0.011	0.00	0.002	0.10	0.014	0.00	0.002	0.15	0.009	0.01	0.001	0.06	0.056

PU	*C. jejuni* 11168		*C. jejuni* CH4		*C. perfringens*		*C. difficile*		*S. mutans*		Clinical 1		Clinical 2	
	Mean	SD	Mean	SD	Mean	SD	Mean	SD	Mean	SD	Mean	SD	Mean	SD
203	0.24	0.005	0.02	0.007	0.09	0.005	0.03	0.007	0.09	0.008	0.04	0.003	0.04	0.065
204	0.19	0.011	0.01	0.003	0.17	0.056	0.03	0.003	0.11	0.028	0.03	0.003	0.05	0.020
205	0.14	0.009	0.02	0.002	0.02	0.006	0.00	0.001	0.01	0.003	0.01	0.005	0.05	0.026
205	0.05	0.016	0.05	0.082	0.01	0.005	0.00	0.004	0.05	0.003	0.01	0.003	0.02	0.016
207	0.12	0.014	0.00	0.009	0.07	0.020	0.00	0.003	0.11	0.004	0.02	0.004	0.13	0.135
208	0.28	0.023	0.06	0.011	0.11	0.024	0.03	0.002	0.15	0.021	0.07	0.009	0.05	0.022
210	0.17	0.035	0.00	0.015	0.12	0.078	0.00	0.002	0.18	0.007	0.03	0.004	0.09	0.011
212	0.21	0.021	0.02	0.003	0.05	0.015	0.01	0.003	0.15	0.006	0.03	0.006	0.10	0.017
214	0.21	0.029	0.02	0.008	0.12	0.025	0.01	0.001	0.09	0.009	0.02	0.003	0.05	0.011
215	0.07	0.027	0.00	0.002	0.07	0.017	0.00	0.003	0.08	0.014	0.02	0.003	0.04	0.016
216	0.11	0.024	0.00	0.005	0.09	0.016	0.00	0.001	0.08	0.009	0.01	0.003	0.02	0.013
217	0.23	0.060	0.09	0.080	0.20	0.062	0.02	0.011	0.22	0.014	0.04	0.005	0.11	0.010
218	0.11	0.018	0.01	0.005	0.06	0.036	0.00	0.001	0.05	0.004	0.02	0.007	0.03	0.074
219	0.13	0.045	0.01	0.011	0.15	0.048	0.01	0.003	0.15	0.027	0.02	0.005	0.22	0.052
220	0.05	0.005	0.02	0.008	0.05	0.006	0.01	0.001	0.05	0.001	0.01	0.002	0.02	0.007
221	0.21	0.019	0.02	0.003	0.20	0.042	0.02	0.005	0.21	0.010	0.05	0.018	0.10	0.057
222	0.16	0.031	0.01	0.003	0.05	0.011	0.00	0.002	0.06	0.005	0.03	0.006	0.03	0.012
223	0.14	0.013	0.01	0.001	0.02	0.006	0.00	0.001	0.08	0.012	0.02	0.002	0.03	0.030
224	0.28	0.028	0.02	0.005	0.07	0.031	0.00	0.003	0.13	0.013	0.02	0.003	0.07	0.004
225	0.23	0.016	0.02	0.006	0.01	0.006	0.00	0.001	0.15	0.010	0.03	0.004	0.02	0.009
226	0.13	0.016	0.01	0.005	0.10	0.037	0.01	0.003	0.05	0.007	0.02	0.001	0.04	0.046
227	0.06	0.020	0.01	0.006	0.04	0.013	0.00	0.001	0.02	0.001	0.01	0.002	0.01	0.009
228	0.12	0.028	0.04	0.050	0.07	0.022	0.00	0.001	0.07	0.012	0.00	0.002	-0.03	0.054
229	0.09	0.025	0.00	0.003	0.02	0.025	0.00	0.001	0.03	0.006	0.01	0.004	0.05	0.134
230	0.10	0.012	0.01	0.002	0.04	0.016	0.00	0.001	0.05	0.004	0.02	0.002	0.03	0.012
233	0.11	0.011	0.03	0.018	0.01	0.005	0.00	0.001	0.07	0.006	0.02	0.002	0.04	0.020
234	0.17	0.022	0.00	0.003	0.04	0.173	0.00	0.002	0.18	0.019	0.02	0.002	0.08	0.007
235	0.12	0.011	0.02	0.002	0.01	0.005	0.00	0.001	0.13	0.018	0.03	0.004	0.18	0.071
236	0.21	0.020	0.01	0.007	0.08	0.080	0.00	0.002	0.17	0.009	0.03	0.001	0.05	0.012
239	0.13	0.020	0.01	0.010	0.04	0.010	0.00	0.001	0.06	0.040	0.01	0.001	-0.04	0.092
241	0.11	0.010	0.02	0.008	0.22	0.128	0.00	0.002	0.19	0.017	0.02	0.003	0.05	0.028
242	0.09	0.020	0.01	0.005	0.01	0.014	0.00	0.001	0.03	0.003	0.01	0.002	0.05	0.040
244	0.12	0.028	0.01	0.001	0.02	0.006	0.00	0.001	0.10	0.014	0.01	0.001	0.07	0.020
245	0.19	0.024	0.01	0.003	0.10	0.012	0.01	0.003	0.13	0.009	0.05	0.004	0.06	0.022
246	0.23	0.055	0.03	0.005	0.05	0.011	0.01	0.001	0.09	0.003	0.02	0.007	0.07	0.040
247	0.21	0.059	0.02	0.005	0.13	0.044	0.01	0.003	0.11	0.009	0.07	0.018	0.05	0.009
250	0.18	0.013	0.01	0.003	0.12	0.033	0.03	0.004	0.11	0.004	0.01	0.001	0.08	0.020
253	0.13	0.011	0.01	0.003	0.06	0.044	0.00	0.001	0.09	0.019	0.01	0.001	0.06	0.010
254	0.20	0.011	0.03	0.035	0.14	0.109	0.01	0.001	0.15	0.019	0.02	0.003	0.09	0.028
256	0.18	0.005	0.04	0.003	0.19	0.043	0.02	0.001	0.15	0.008	0.04	0.001	0.09	0.018
257	0.21	0.034	0.01	0.006	0.03	0.016	0.00	0.001	0.07	0.003	0.02	0.002	0.05	0.019
259	0.11	0.012	0.01	0.001	0.07	0.029	0.01	0.002	0.10	0.008	0.01	0.004	0.06	0.011
264	0.07	0.010	0.05	0.008	0.13	0.045	0.00	0.001	0.11	0.010	0.01	0.003	0.09	0.047
269	0.11	0.013	0.02	0.002	0.07	0.042	0.00	0.002	0.06	0.002	0.01	0.006	0.03	0.019

Oocyst-polyacrylate binding analysis (average from 3 spots of same polymer). Mean: Mean number of oocysts; SD: Standard deviation.

PA	Number of oocysts (per polymer spot)		PA	Number of oocysts (per polymer spot)	
	Mean	SD		Mean	SD
1	1	0.5	63	26	7.1
2	4	2.1	98	87	6.9
3	3	1.7	99	7	3.1
4	1	0.5	100	20	7.7
5	1	0.0	101	90	14.3
6	1	0.5	102	8	0.5
7	4	1.7	103	33	18.3
8	1	0.0	104	65	27.8
9	2	1.9	105	11	5.7
10	1	0.0	106	8	4.1
11	1	0.5	107	71	44.9
12	2	1.9	108	3	1.6
13	4	1.2	109	24	6.4
14	1	0.5	110	6	1.4
15	2	0.9	111	30	14.4
16	1	0.5	113	6	5.0
17	2	0.9	114	13	1.2
19	2	1.2	115	72	9.7
20	2	0.0	116	34	16.1
21	3	2.4	117	31	6.9
22	2	0.5	118	2	1.4
23	1	0.0	119	6	0.9
24	1	0.5	120	3	2.1
25	2	0.8	121	39	14.6
26	2	0.8	122	23	5.4
27	1	0.5	123	9	2.4
28	1	0.0	124	3	1.2
29	1	0.0	125	17	18.7
30	3	2.6	126	20	3.7
31	2	0.5	127	14	1.4
32	2	0.9	128	38	2.9
33	1	0.0	129	2	1.4
34	1	0.0	130	8	3.4
35	3	0.0	131	1	0.5
36	2	1.9	132	9	6.2
37	2	0.8	133	12	5.9
38	1	0.0	134	5	2.1
39	1	0.5	135	7	2.9
40	2	0.9	136	14	4.6
41	3	0.9	137	3	1.2
42	1	0.0	138	16	5.9
43	2	0.8	139	11	3.4
44	2	0.9	140	4	2.1
45	1	0.0	142	5	2.2
46	4	1.6	143	8	4.5
47	7	4.9	150	8	0.9
48	3	1.7	152	20	12.5
49	5	2.1	153	12	10.5
50	1	0.5	154	47	9.5
51	1	0.5	155	1	0.0
52	2	1.9	156	8	7.1
53	3	1.7	157	8	9.4
54	3	2.8	158	7	4.3
55	1	0.5	159	1	0.0
56	1	0.5	160	1	0.0
57	1	0.5	161	18	22.6
58	2	0.8	162	1	0.0
59	7	2.5	163	1	0.0
60	1	0.0	164	1	0.5
61	1	0.0	165	58	4.5
62	2	0.5	167	49	27.4

PA	Number of oocysts (per polymer spot)		PA	Number of oocysts (per polymer spot)	
	Mean	SD		Mean	SD
168	12	3.3	236	9	2.2
169	1	0.5	237	1	0.0
170	2	1.4	238	2	0.8
172	1	0.0	240	8	2.9
173	2	0.9	241	22	5.8
174	3	0.8	242	74	12.4
175	10	2.4	243	11	1.7
176	3	0.0	244	16	7.4
177	2	0.9	245	2	1.4
178	1	0.0	246	43	13.9
179	1	0.5	247	33	3.3
180	1	0.0	248	53	9.7
181	1	0.0	249	6	0.5
182	25	6.6	250	33	2.9
182	2	0.5	251	4	2.1
184	4	1.7	252	10	0.8
185	1	0.5	253	31	11.4
186	1	0.0	254	20	2.6
187	1	0.0	255	13	1.2
188	7	6.8	256	15	6.2
189	9	5.9	257	36	1.6
190	1	0.5	258	5	1.2
191	2	0.9	259	13	3.7
192	2	0.9	260	3	0.5
193	3	1.7	261	7	6.9
194	8	4.5	262	32	8.6
195	2	0.9	264	25	6.7
196	2	0.8	265	7	3.8
197	6	3.1	266	27	5.7
198	7	4.1	267	16	4.0
199	1	0.0	268	22	4.9
200	3	0.8	270	12	12.4
201	2	0.5	271	1	0.0
202	1	0.0	273	16	4.7
203	7	7.8	274	24	6.8
204	3	2.4	276	17	9.0
205	1	0.0	277	1	0.0
206	2	0.5	279	8	1.7
207	2	1.2	280	3	1.7
208	2	0.5	281	20	3.9
209	2	0.8	285	2	0.8
210	1	0.0	291	7	4.3
213	2	0.8	296	167	40.3
214	3	1.7	303	15	4.6
215	1	0.0	304	10	5.4
216	4	1.2	305	2	0.8
218	2	0.5	306	2	0.9
219	8	8.5	309	27	11.9
220	1	0.5	315	1	0.0
221	4	3.4	316	4	1.6
222	1	0.5	318	19	14.4
223	2	0.8	319	6	3.7
224	3	3.3	320	2	0.9
225	3	1.9	321	21	7.9
226	5	1.7	322	14	5.9
227	3	0.8	323	17	2.6
228	1	0.0	324	1	0.0
229	20	6.6	327	1	0.0
230	3	2.8	329	18	17.2
231	1	0.0	330	3	2.6
232	3	0.9	331	1	0.0
233	43	13.2	332	2	1.9
234	2	1.9	335	8	5.4
235	2	0.5	336	9	2.9

PA	Number of oocysts (per polymer spot)		PA	Number of oocysts (per polymer spot)	
	Mean	SD		Mean	SD
337	2	1.2	423	32	6.7
338	1	0.0	424	22	22.4
339	3	0.9	425	27	5.2
348	1	0.5	426	45	24.1
354	1	0.5	427	35	4.5
355	6	2.4	428	22	4.2
357	1	0.0	429	19	1.7
358	13	9.0	430	43	11.3
360	2	1.2	431	13	1.6
361	5	2.1	432	40	15.6
363	6	2.2	433	6	2.4
364	78	65.7	434	5	3.3
365	69	88.2	435	20	11.6
366	1	0.5	436	47	2.8
367	7	1.2	437	9	8.2
368	43	13.1	442	7	2.5
369	16	3.7	443	42	3.1
370	11	6.2	444	10	8.5
372	6	1.4	445	79	18.9
373	15	5.4	446	16	4.0
374	4	3.6	447	47	16.5
375	2	0.5	448	5	2.8
375	1	0.5	449	12	3.6
376	8	4.6	450	27	3.6
377	51	8.7	451	20	7.6
378	1	0.0	452	34	20.5
381	2	1.9	453	7	4.0
384	2	0.5	454	31	11.7
385	5	2.2	455	62	9.4
386	17	8.6	457	11	1.9
387	2	1.9	458	13	6.5
388	2	0.8	459	28	5.1
389	17	3.3	460	43	17.6
390	4	2.2	461	8	4.2
391	3	3.3	462	33	8.3
392	8	4.0	463	20	3.6
393	13	5.0	464	52	10.2
394	18	10.9	465	25	6.2
395	10	7.0	467	1	0.0
396	6	3.1	468	25	16.4
397	8	0.0	469	4	2.4
398	14	3.3	470	24	7.6
400	5	3.3	474	4	1.2
401	65	41.3	475	8	3.7
402	3	0.9	476	61	10.4
403	2	0.0	477	9	1.9
404	4	1.9	478	1	0.0
405	6	1.4	480	15	4.6
406	2	0.9	481	9	4.6
407	12	2.5	482	4	1.7
408	4	2.6	483	1	0.0
410	7	4.5	484	15	6.2
411	8	4.5	485	1	0.5
412	9	5.6	486	17	7.1
413	49	14.1	488	7	4.5
414	57	14.7	489	3	1.7
415	12	3.7	490	2	0.8
416	91	18.5	491	3	2.2
417	15	5.8	492	13	5.7
418	13	9.5	493	3	1.7
419	22	2.9	495	2	0.5
420	55	19.7	496	40	17.9
421	29	11.1	497	1	0.0
422	24	4.5	498	10	11.3

PA	Number of oocysts (per polymer spot)		PA	Number of oocysts (per polymer spot)	
	Mean	SD		Mean	SD
499	2	0.5	535	10	7.1
500	2	1.9	536	26	1.7
501	1	0.0	537	6	5.0
502	8	0.9	538	52	35.6
504	10	7.1	539	50	14.1
507	2	0.9	540	2	0.5
508	61	23.7	541	4	3.1
509	3	2.6	542	2	0.9
510	1	0.5	543	58	40.7
511	8	1.2	544	72	8.1
512	96	12.3	545	12	4.1
514	3	1.2	546	11	10.8
515	1	0.5	547	40	29.9
517	3	2.8	548	49	11.1
518	1	0.0	549	3	0.8
519	1	0.0	550	30	6.8
520	2	0.8	551	18	4.2
522	8	1.2	552	27	7.7
523	4	1.2	553	4	2.9
524	16	2.1	554	2	0.9
525	1	0.0	555	17	3.1
526	13	3.4	556	20	1.7
527	87	13.2	557	12	6.5
528	150	48.6	558	2	1.4
529	23	6.5	559	45	1.6
530	31	4.2	560	30	14.9
531	107	28.0	561	50	14.7
532	5	4.5	563	20	2.2
533	1	0.0	564	9	3.3
534	6	4.1	565	2	0.9

Oocyst-polyurethane binding analysis (average from 3 spots of same polymer). Mean: Mean number of oocysts; SD: Standard deviation.

PU	Number of oocysts (per polymer spot)		PU	Number of oocysts (per polymer spot)	
	Mean	SD		Mean	SD
1	16	10.0	106	1	0.5
2	35	2.9	107	3	0.5
3	29	15.8	108	1	0.0
4	13	1.9	110	3	1.9
5	6	4.5	111	1	0.0
6	11	8.2	112	2	0.5
7	11	1.7	114	1	0.0
8	3	1.7	116	3	1.6
9	12	2.6	117	2	0.5
10	3	1.7	118	10	0.8
11	7	2.1	119	7	2.2
12	6	2.6	120	1	0.0
13	13	6.8	121	2	0.8
14	11	3.9	122	15	4.9
15	11	4.9	123	1	0.0
16	1	0.0	124	2	0.9
17	8	9.4	125	5	3.6
18	14	9.0	126	4	1.9
19	5	3.3	127	14	5.4
20	12	2.5	128	1	0.5
21	2	1.9	129	7	1.2
22	1	0.0	130	2	1.9
23	4	1.7	131	6	4.6
24	4	2.5	132	1	0.0
25	7	1.2	133	3	1.7
26	14	9.2	134	6	3.7
27	15	9.0	135	3	2.8
28	63	14.6	136	4	0.9
29	8	5.2	137	1	0.0
33	16	5.3	138	1	0.5
35	21	7.0	139	12	3.7
37	30	14.4	140	2	0.9
39	3	2.6	141	4	1.4
41	5	5.0	142	14	5.0
48	26	5.7	143	9	1.7
53	25	8.2	144	1	0.5
61	2	0.9	145	1	0.5
65	16	13.6	146	35	14.2
67	12	8.2	147	18	6.9
69	50	20.8	148	1	0.5
71	21	10.4	149	6	3.4
73	1	0.5	150	17	1.9
77	1	0.0	151	9	1.2
79	9	1.7	152	6	3.9
81	11	1.9	153	9	4.2
83	1	0.0	154	7	0.5
85	1	0.0	156	6	0.5
91	1	0.0	157	5	2.9
92	1	0.0	158	2	1.4
93	18	8.3	159	22	6.2
94	3	2.4	161	16	2.2
95	4	3.6	162	10	2.5
96	1	0.0	163	11	4.6
97	7	7.8	164	29	5.9
98	4	2.2	165	5	0.8
99	2	0.8	166	9	1.4
100	1	0.0	167	32	5.9
102	2	0.5	168	14	2.5
103	1	0.5	169	11	2.4
104	2	0.0	171	12	2.9
105	2	1.2	172	22	15.9

PU	Number of oocysts (per polymer spot)		PU	Number of oocysts (per polymer spot)	
	Mean	SD		Mean	SD
173	10	11.3	223	3	1.7
174	13	3.7	224	9	4.8
175	4	2.8	225	1	0.0
176	14	14.2	226	1	0.0
178	17	2.1	227	7	2.5
179	19	7.4	228	14	8.6
181	6	4.1	229	3	0.9
183	23	5.9	230	1	0.0
184	10	2.9	233	1	0.0
185	16	5.0	234	22	4.2
186	14	2.2	235	4	1.9
187	2	0.9	236	16	10.7
188	5	0.5	238	16	11.2
189	8	1.9	239	1	0.5
190	1	0.0	241	2	1.4
191	2	0.5	242	5	3.1
192	5	0.5	244	2	0.9
196	22	14.4	245	3	2.2
197	1	0.5	246	1	0.0
199	2	0.9	247	1	0.0
201	4	1.7	249	2	1.4
202	1	0.5	250	1	0.5
203	19	10.2	252	7	5.8
204	5	0.9	253	1	0.0
205	7	3.6	254	1	0.0
206	18	14.6	255	1	0.5
207	1	0.5	256	10	2.5
208	13	4.9	257	3	0.5
210	15	3.7	259	1	0.5
212	14	11.1	260	19	2.5
213	1	0.0	263	21	8.0
214	3	0.5	264	15	3.3
215	25	16.4	269	9	3.3
216	4	4.7	271	32	4.9
217	9	4.7	275	10	2.5
218	14	9.8	276	16	8.2
219	1	0.0	277	8	5.4
220	18	3.8	278	1	0.0
221	9	1.2	39DE	4	0.8
222	9	10.8	49DE	7	1.6

Cyst-polyacrylate binding analysis (average from 3 spots of same polymer). Mean: Mean number of cysts; SD: Standard deviation.

PA	Number of cysts (per polymer spot)		PA	Number of cysts (per polymer spot)	
	Mean	SD		Mean	SD
1	9	3.3	63	1	0.0
2	1	0.0	98	67	7.8
3	6	2.1	99	3	1.6
4	3	1.7	100	142	6.6
5	3	2.1	101	151	16.2
6	5	2.4	102	4	1.9
7	22	23.4	103	29	13.5
8	5	1.2	104	131	25.9
9	4	3.8	105	3	0.8
10	7	5.9	106	6	2.1
11	5	4.3	107	59	42.0
12	1	0.0	108	3	2.4
13	13	5.9	109	5	4.8
14	6	3.1	110	2	0.8
15	2	0.8	111	7	1.7
16	1	0.5	113	62	26.0
17	10	2.9	114	6	2.9
19	3	3.3	115	27	36.3
20	3	2.2	116	39	53.5
21	1	0.0	117	30	13.5
22	3	1.4	118	28	27.7
23	2	0.9	119	1	0.0
24	1	0.0	120	2	1.4
25	1	0.5	121	12	15.3
26	6	1.7	122	43	6.1
27	1	0.5	123	72	43.6
28	5	1.4	124	1	0.0
29	1	0.5	125	67	59.5
30	5	1.7	126	7	0.9
31	1	0.0	127	17	0.9
32	1	0.0	128	31	5.4
33	1	0.0	129	1	0.0
34	4	1.7	130	1	0.0
35	1	0.0	131	1	0.0
36	1	0.0	132	1	0.5
37	1	0.5	133	1	0.0
38	8	9.7	134	5	0.9
39	1	0.0	135	1	0.0
40	1	0.0	136	2	0.8
41	1	0.0	137	1	0.0
42	3	1.6	138	1	0.0
43	1	0.0	139	1	0.5
44	2	1.9	140	1	0.0
45	1	0.0	142	1	0.0
46	2	0.9	143	1	0.0
47	3	0.5	150	17	22.2
48	1	0.0	152	58	38.0
49	1	0.0	153	1	0.0
50	4	0.8	154	2	0.9
51	1	0.5	155	75	53.7
52	1	0.0	156	1	0.0
53	1	0.5	157	1	0.0
54	6	0.8	158	1	0.0
55	1	0.0	159	1	0.0
56	1	0.0	160	1	0.0
57	1	0.0	161	3	1.7
58	1	0.0	162	26	34.4
59	3	0.9	163	1	0.5
60	1	0.5	164	1	0.5
61	2	0.5	165	77	60.0
62	2	1.4	167	64	45.1

PA	Number of cysts (per polymer spot)		PA	Number of cysts (per polymer spot)	
	Mean	SD		Mean	SD
168	2	0.9	235	4	2.1
169	15	8.7	236	45	29.9
170	6	3.6	237	72	50.4
170	11	6.9	238	3	1.7
172	4	2.1	240	2	1.4
173	10	6.2	241	18	23.8
174	13	5.0	242	29	36.3
175	18	12.1	243	4	2.2
176	2	1.4	244	1	0.0
177	12	16.0	245	7	4.2
178	9	4.2	246	5	2.4
179	4	1.2	247	9	4.1
180	1	0.5	248	55	0.9
181	39	10.6	249	3	0.5
182	3	1.6	250	7	2.9
182	18	3.3	251	4	2.9
184	10	10.2	252	3	1.2
185	15	3.6	253	15	9.9
186	3	1.2	254	9	5.7
187	7	5.3	255	2	0.8
188	2	1.4	256	2	1.2
189	5	5.4	257	5	0.8
190	8	6.1	258	2	1.9
191	1	0.0	259	8	8.1
192	1	0.5	260	1	0.0
193	8	5.0	261	5	3.3
194	2	0.8	262	8	2.9
195	2	1.4	264	4	2.1
196	1	0.5	265	3	1.2
197	21	8.2	266	52	33.7
198	39	43.4	267	6	4.6
199	2	0.9	268	56	35.0
200	22	28.5	270	3	2.4
201	4	1.2	271	1	0.0
202	1	0.5	273	1	0.0
203	1	0.0	274	2	0.5
204	1	0.0	276	6	3.9
205	3	1.7	277	1	0.0
206	1	0.0	279	2	1.4
207	2	0.5	280	39	25.9
208	1	0.0	281	1	0.0
209	4	2.5	285	4	2.9
210	2	1.9	291	3	2.4
213	4	2.5	296	117	16.1
214	2	0.5	303	2	0.9
215	2	0.8	304	1	0.5
216	22	15.7	305	1	0.5
218	13	8.5	306	1	0.0
219	1	0.0	309	1	0.0
220	2	0.8	315	2	0.9
221	2	1.2	316	1	0.0
222	1	0.0	318	1	0.0
223	1	0.5	319	1	0.0
224	2	0.5	320	46	63.2
225	1	0.5	321	26	29.0
226	1	0.0	322	3	2.6
227	1	0.0	323	1	0.0
228	1	0.0	324	3	0.5
229	6	2.6	327	5	2.1
230	3	1.7	329	2	1.9
231	2	0.9	330	1	0.5
232	2	1.9	331	2	1.4
233	5	2.2	332	19	12.6
234	1	0.0	335	1	0.0

PA	Number of cysts (per polymer spot)		PA	Number of cysts (per polymer spot)	
	Mean	SD		Mean	SD
336	40	53.3	419	3	0.9
337	16	5.3	420	16	0.8
338	9	2.1	421	2	0.5
339	1	0.5	422	29	16.2
340	4	4.2	423	6	4.1
341	39	5.9	424	20	4.9
342	26	3.4	425	2	1.2
345	42	46.0	426	11	14.6
348	3	1.7	427	24	9.0
354	35	4.5	428	10	11.6
355	19	9.8	429	1	0.0
357	4	2.2	430	34	41.0
358	37	14.1	431	5	3.1
360	8	0.5	432	31	42.2
361	8	5.1	433	1	0.0
363	1	0.0	434	6	3.3
364	25	14.2	435	12	1.4
365	95	66.4	436	6	4.3
366	2	1.4	437	2	0.8
367	16	20.7	442	1	0.0
368	21	2.4	443	58	5.7
369	11	5.4	444	3	2.4
370	5	2.1	445	80	7.7
372	23	14.8	446	14	3.8
373	33	34.1	447	69	5.9
374	3	1.2	448	1	0.0
375	3	2.2	449	2	0.8
376	18	8.6	450	64	3.6
377	66	37.0	451	4	1.2
378	15	11.3	452	18	12.0
381	1	0.5	453	8	6.9
384	4	3.1	454	21	13.0
385	2	0.9	455	30	41.5
386	6	4.6	457	3	1.4
387	1	0.5	458	39	20.5
388	9	10.6	459	14	17.2
389	13	3.7	460	100	32.3
390	12	4.0	461	16	9.1
391	7	7.3	462	57	26.2
392	35	6.5	463	36	23.6
393	17	3.6	464	88	61.4
394	7	3.7	465	1	0.0
395	89	5.9	467	2	0.8
396	3	1.4	468	24	16.9
397	16	4.5	469	1	0.5
398	35	5.3	470	27	37.2
400	22	15.0	474	40	19.2
401	92	20.9	475	66	89.8
402	1	0.5	476	59	40.2
403	1	0.0	477	1	0.5
404	1	0.0	478	15	10.1
405	3	1.6	480	117	41.2
406	2	1.9	481	2	0.9
407	10	12.0	482	4	4.0
408	4	2.2	483	2	0.5
410	1	0.0	484	79	12.2
411	1	0.0	485	1	0.0
412	1	0.5	486	12	15.6
413	2	0.0	488	100	35.3
414	53	2.2	489	19	9.1
415	10	1.7	490	35	45.1
416	131	17.0	491	25	33.0
417	3	2.2	492	56	42.9
418	2	0.8	493	80	7.1

PA	Number of cysts (per polymer spot)		PA	Number of cysts (per polymer spot)	
	Mean	SD		Mean	SD
495	67	25.5	533	4	1.7
496	87	33.6	534	45	7.3
497	7	0.8	535	93	3.4
498	53	36.9	536	119	30.0
499	7	8.5	537	1	0.0
500	56	35.2	538	89	60.4
501	11	4.0	539	114	13.2
502	77	25.2	540	6	4.5
504	57	37.5	541	4	2.2
507	3	3.3	542	2	0.9
508	31	23.0	543	166	18.8
509	35	20.5	544	59	9.6
510	14	9.5	545	1	0.0
511	14	4.2	546	5	2.2
512	51	18.1	547	39	2.6
514	19	15.1	548	54	15.1
515	9	8.7	549	1	0.0
517	19	3.3	550	4	1.7
518	31	15.5	551	14	8.6
519	11	7.5	552	4	2.9
520	7	9.0	553	1	0.0
522	9	6.2	554	4	2.9
523	4	1.7	555	21	13.4
524	5	1.6	556	1	0.0
525	1	0.0	557	3	1.4
526	87	47.8	558	1	0.0
527	139	58.1	559	29	5.1
528	34	43.6	560	5	5.4
529	49	48.3	561	6	1.4
530	59	43.4	563	2	1.4
531	107	34.4	564	10	3.3
532	59	41.7	565	3	1.7

Cyst-polyurethane binding analysis (average from 3 spots of same polymer). Mean: Mean number of cysts; SD: Standard deviation.

PU	Number of cysts (per polymer spot)		PU	Number of cysts (per polymer spot)	
	Mean	SD		Mean	SD
1	4	3.8	106	3	2.4
2	1	0.0	107	26	7.9
3	2	0.5	108	5	3.3
4	1	0.5	110	6	5.7
5	2	1.9	111	4	0.8
6	9	4.5	112	16	9.2
7	4	3.4	114	6	2.4
8	1	0.0	116	3	1.4
9	8	9.2	117	14	4.9
10	3	1.9	118	3	3.3
11	2	1.4	119	5	3.3
12	1	0.5	120	1	0.5
13	1	0.0	121	13	9.3
14	1	0.0	122	8	3.7
15	2	0.8	123	2	0.9
16	1	0.5	124	1	0.0
17	1	0.5	125	2	0.5
18	1	0.5	126	5	5.2
19	2	1.4	127	1	0.0
20	1	0.0	128	3	2.4
21	1	0.0	129	17	2.4
22	1	0.0	130	1	0.0
23	1	0.0	131	1	0.5
24	1	0.5	132	1	0.0
25	1	0.0	133	3	0.5
26	4	4.2	134	24	1.2
27	2	1.4	135	2	0.9
28	1	0.5	136	32	18.4
29	1	0.5	137	2	1.2
33	1	0.0	138	1	0.0
35	1	0.0	139	1	0.0
37	1	0.0	140	2	0.9
39	1	0.0	141	6	2.9
41	1	0.0	142	9	5.9
48	1	0.5	143	4	2.9
53	1	0.0	144	7	6.6
61	1	0.0	145	4	1.2
65	1	0.5	146	10	1.6
67	2	1.9	147	2	1.9
69	4	2.4	148	6	3.9
71	1	0.0	149	8	1.7
73	1	0.0	150	9	5.4
77	1	0.0	151	2	0.9
79	1	0.0	152	1	0.0
81	2	0.8	153	9	6.6
83	2	0.8	154	3	1.7
85	3	1.2	156	1	0.5
91	1	0.5	157	1	0.0
92	4	2.6	158	7	4.9
93	3	2.4	159	13	4.9
94	1	0.0	161	4	3.4
95	2	1.4	162	2	0.8
96	2	1.4	163	10	5.0
97	1	0.5	164	6	2.6
98	3	1.7	165	2	0.5
99	7	2.2	166	3	0.5
100	4	2.1	167	3	0.8
102	8	6.2	168	2	1.9
103	12	6.8	169	1	0.0
104	38	48.1	171	1	0.0
105	28	38.2	172	3	1.2

PU	Number of cysts (per polymer spot)		PU	Number of cysts (per polymer spot)	
	Mean	SD		Mean	SD
173	6	7.1	223	2	0.9
174	6	5.0	224	1	0.0
175	1	0.0	225	1	0.0
176	68	43.9	226	1	0.5
178	1	0.5	227	2	1.9
179	2	0.5	228	1	0.0
181	21	12.2	229	3	1.2
183	30	18.1	230	1	0.0
184	3	1.2	233	1	0.0
185	1	0.0	234	4	1.4
186	1	0.0	235	1	0.0
187	2	1.4	236	1	0.0
188	2	0.9	238	1	0.5
189	2	0.9	239	1	0.0
190	1	0.5	241	11	7.3
191	1	0.0	242	1	0.0
192	1	0.0	244	1	0.5
196	2	0.5	245	4	3.1
197	2	0.8	246	2	1.9
199	1	0.5	247	1	0.5
201	1	0.0	249	1	0.5
202	1	0.0	250	23	2.6
203	2	0.5	252	1	0.0
204	1	0.0	253	3	1.7
205	1	0.5	254	1	0.5
206	1	0.0	255	5	2.9
207	1	0.0	256	2	1.4
208	1	0.0	257	1	0.5
210	1	0.5	259	1	0.0
212	1	0.0	260	12	9.1
213	1	0.5	263	9	4.5
214	2	0.9	264	2	0.5
215	1	0.0	269	1	0.5
216	1	0.5	271	49	4.2
217	1	0.0	275	2	0.9
218	5	2.6	276	4	2.2
219	7	1.7	277	1	0.0
220	1	0.5	278	1	0.0
221	1	0.0	39DE	2	0.8
222	1	0.0	49DE	1	0.0

Appendix IV: Patents and Publications

(12) INTERNATIONAL APPLICATION PUBLISHED UNDER THE PATENT COOPERATION TREATY (PCT)

(19) World Intellectual Property Organization
International Bureau

(43) International Publication Date
22 March 2012 (22.03.2012)

PCT

(10) International Publication Number
WO 2012/035302 A1

(51) International Patent Classification:
C09D 175/08 (2006.01) *A01N 33/04* (2006.01)
C09D 133/14 (2006.01) *A61L 26/00* (2006.01)
C09D 5/14 (2006.01) *A01N 37/00* (2006.01)
C09D 5/02 (2006.01) *C08J 7/04* (2006.01)

(21) International Application Number:
PCT/GB2011/001354

(22) International Filing Date:
16 September 2011 (16.09.2011)

(25) Filing Language: English

(26) Publication Language: English

(30) Priority Data:
1015492.0 16 September 2010 (16.09.2010) GB

(71) Applicant *(for all designated States except US)*: **THE UNIVERSITY COURT OF THE UNIVERSITY OF EDINBURGH** [GB/GB]; Old College, South Bridge, Edinburgh, EH8 9YL (GB).

(72) Inventors; and
(75) Inventors/Applicants *(for US only)*: **BRADLEY, Mark** [GB/GB]; School of Chemistry, c/o University of Edinburgh, West Mains Road, Joseph Black Building, Edinburgh, EH9 3JJ (GB). **GALLAGHER, Maurice, Patrick** [GB/GB]; Riverbank House, 35A Newmills Road, Dalkeith, Midlothian, EH22 1 ET (GB). **PERNAGALLO, Salvatore** [IT/GB]; 27/9 Blair Street, Edinburgh EH1 1QR (GB). **WU, Mei** [CN/GB]; School of Chemistry, c/o University of Edinburgh, West Mains Road, Joseph Black Building, Edinburgh, EH9 3JJ (GB).

(74) Agents: **NAISMITH, Robert, Stewart** et al.; Marks & Clerk LLP, Aurora, 120 Bothwell Street, Glasgow, G2 7JS (GB).

(81) Designated States *(unless otherwise indicated, for every kind of national protection available)*: AE, AG, AL, AM, AO, AT, AU, AZ, BA, BB, BG, BH, BR, BW, BY, BZ, CA, CH, CL, CN, CO, CR, CU, CZ, DE, DK, DM, DO, DZ, EC, EE, EG, ES, FI, GB, GD, GE, GH, GM, GT, HN, HR, HU, ID, IL, IN, IS, JP, KE, KG, KM, KN, KP, KR, KZ, LA, LC, LK, LR, LS, LT, LU, LY, MA, MD, ME, MG, MK, MN, MW, MX, MY, MZ, NA, NG, NI, NO, NZ, OM, PE, PG, PH, PL, PT, QA, RO, RS, RU, RW, SC, SD, SE, SG, SK, SL, SM, ST, SV, SY, TH, TJ, TM, TN, TR, TT, TZ, UA, UG, US, UZ, VC, VN, ZA, ZM, ZW.

(84) Designated States *(unless otherwise indicated, for every kind of regional protection available)*: ARIPO (BW, GH, GM, KE, LR, LS, MW, MZ, NA, SD, SL, SZ, TZ, UG, ZM, ZW), Eurasian (AM, AZ, BY, KG, KZ, MD, RU, TJ, TM), European (AL, AT, BE, BG, CH, CY, CZ, DE, DK, EE, ES, FI, FR, GB, GR, HR, HU, IE, IS, IT, LT, LU, LV, MC, MK, MT, NL, NO, PL, PT, RO, RS, SE, SI, SK,

[Continued on next page]

WO 2012/035302 A1

(54) Title: BINDING AND NON-BINDING POLYMERS

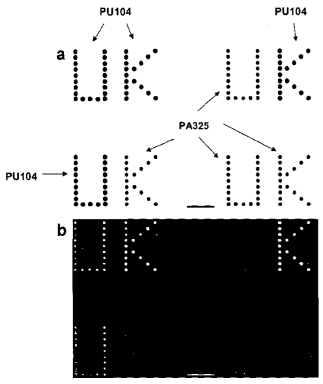

Fig. 1

(57) Abstract: Polyacrylate and polyurethane polymers that are selected to have either; surface properties that allow microorganisms, in particular bacteria, to bind to the surface; or have surface properties that are repellent to the binding of microorganisms are described. Products comprising, consisting of or coated with the polymers are also described. The polyacrylate polymers include polyacrylates that are non-binding or selectively binding to microorganisms and have a methacrylate or acrylate containing polymer backbone that is provided with pendant tertiary amine groups.

View Online / Journal Homepage / Table of Contents for this issue
Dynamic Article Links

Journal of Materials Chemistry

Cite this: *J. Mater. Chem.*, 2011, **21**, 96

www.rsc.org/materials

PAPER

Colonising new frontiers—microarrays reveal biofilm modulating polymers†

Salvatore Pernagallo,‡[a] Mei Wu,‡[a] Maurice P. Gallagher[b] and Mark Bradley*[a]

Received 22nd June 2010, Accepted 2nd September 2010
DOI: 10.1039/c0jm01987a

Polymer microarrays provide an innovative approach to identify materials with novel bacterial binding or repellent properties which could subsequently be used in a variety of practical applications. Here, we report a polymer microarray screen of hundreds of synthetic polymers to identify those which either selectively capture the major food-borne pathogen, *Salmonella enterica* serovar Typhimurium (*S.* Typhimurium), or prevent its binding. A parallel study with a lab strain of *Escherichia coli* (*E. coli*) is also reported; revealing polymers which either display a common binding activity or which exhibit species discrimination. Moreover, substrates were also uncovered which showed no binding of either organism, even when cultured at high density. The correlation between polymer structure and microbial-modulating behaviour was analysed further, while SEM analysis allowed visualization of the detailed interactions between surface and bacteria. Such polymers offer many new opportunities for bacterial enrichment or surface repulsion, in cleaning materials, as surface coatings for use in the food production industry or as a "bacterial scavenger" resin.

1 Introduction

It is well known that bacterial cell surface charge, cell density, and the presence of a variety of microbially produced compounds such as exopolysaccharides are determinant factors in the adhesion process, but other physicochemical features such as pH, temperature, composition of growth media and surface conditioning factors are also known to affect surface attachment.[1] In order to control bacterial attachment, there is a need for materials which result in specific bacterial sequestration or repulsion. These materials when discovered could underpin wide-ranging applications in hygiene and bio-fouling and offering for example a means for the rapid isolation of hospital pathogens, or minimisation of surface contamination through the development of microbe repelling surfaces. They could also provide opportunities for innovative intervention approaches, such as the selective reduction of pathogen loads *via* animal feeds. Other possible application could be the selective capture of bacteria, spores or viruses on cleaning materials used in clinical, industrial and domestic environments. Minimising attachment and colonisation could be benefit in areas, ranging from artificial implants to packaging for food preparation.

Polymer microarrays have become established as a method to identify polymers that can enrich, manipulate or modulate a variety of adherent or suspended mammalian cell types, including stem cells for regenerative medicine or tissue engineering applications.[2–10] In the present study, we assessed the value of the polymer-based microarray platform to identify novel materials which could be used for the rapid and selective capture of major food-borne pathogens or materials capable of limiting or preventing bacterial adhesion onto surfaces.

For the purposes of this study we focused on the adhesion of the food-borne pathogenic bacterium *Salmonella enterica* serovar Typhimurium (strain SL1344),[11] which is a serious pathogen of clinical and veterinary importance[12] globally and is also a substantial problem in the food industry, and the commensal bacterium *Escherichia coli* (strain W3110).[13]

2 Experimental

2.1 Chemicals and materials

All chemicals were of analytical grade and used as received without further purification. Silane-prep glass slides, tetracycline, sodium cacodylate trihydrate and all the monomers used were from Sigma-Aldrich. Phosphate buffered saline (PBS) tablet was from Oxoid. GeneFrames were from Thermo Scientific, and 2.5% (w/v) glutaraldehyde and 1% (w/v) osmium tetroxide were from Electron Microscopy Sciences. The

[a]*School of Chemistry, EaStCHEM, University of Edinburgh, King's Buildings, West Mains Road, Edinburgh, EH9 3JJ, UK. E-mail: mark.bradley@ed.ac.uk; Fax: +44 (0)1316506453*
[b]*School of Biological Sciences, University of Edinburgh, Mayfield Road, Edinburgh, EH9 3JR, UK*

† Electronic supplementary information (ESI) available: Fig S1 LaVision Bio Analyzer 4F/4S BioTech quantification. Fig. S2 Brightfield and fluorescent microscopy imaging of *S.* Typhimurium binding (Pathfinder™, IMSTAR). Fig. S3 Automated counting of *S.* Typhimurium binding. Table S1 Polyacrylates for *S.* Typhimurium strong/poor binding. Table S2 Polyurethanes showing *S.* Typhimurium binding. Table S3 Polyacrylate series with poor *S.* Typhimurium binding. Fig S4 Fluorescent microscopy image of *S.* Typhimurium-GFP binding on a 5 × 5 spot polymer microarray. See DOI: 10.1039/c0jm01987a

‡ These authors contributed equally to this work.

rectangular four-well plates were from Nunc. Gridded glass coverslips were from CELL-VU.

2.2 Polymer microarray fabrication

Polymer microarrays were prepared as previously reported.[7,14]

2.3 Culture of bacteria

S. Typhimurium and *E. coli* transformed with pHC60 (referred to as *S.* Typhimurium-GFP and *E. coli*-GFP)[15,16] were grown overnight with aeration at 37 °C or 30 °C respectively in Luria-Bertani (LB) broth containing tetracycline (10 μg mL^{-1}). Cultures were collected by centrifugation, washed with fresh LB broth and diluted tenfold to a final concentration of approximately (2×10^8 CFU mL^{-1}) for microarray binding studies.

2.4 Bacterial binding

Either *S.* Typhimurium-GFP or *E. coli*-GFP was added to polymer microarrays (in duplicate) in a four-well plate and incubated overnight (except where stated) at room temperature. Subsequently, the polymer microarray slides were washed robustly three times with PBS, rinsed in deionised water, and dried with a stream of air. A GeneFrame and a coverslip (1.9 × 6.0 cm, AB-0630) were then applied to each slide and cleaned with 70% ethanol. Polymer microarrays were analysed using a LaVision BioAnalyzer 4F/4S scanner with a FITC filter. Bacterial adhesion was evaluated *via* integration of the fluorescence intensity after background correction (see ESI, Fig. S1†). The average and standard deviation for sets of four identical polymer features were determined, with the reproducibility between two identical microarrays evaluated by a Student's *t*-test. Polymers with *p*-values <0.001 and 6 degrees of freedom were considered statistically significant.

2.5 Fluorescence-based high-content imaging

High-content imaging was carried out using an automated fluorescent microscope with an XYZ stage running Pathfinder™ (IMSTAR) that allowed the capture of single images for each polymer spot. Bacteria were imaged with both brightfield and fluorescein channels with a ×20 objective (see ESI, Fig. S2†).

2.6 SEM analysis

Bacteria on the polymer samples were washed (×2) with 0.1 M cacodylate buffer (pH 7.4) and then fixed with 2.5% (w/v) glutaraldehyde in 0.1 M cacodylate buffer (pH 7.4) for 2 h. Samples were post-fixed with 1% (w/v) osmium tetroxide for 1 h at room temperature, dehydrated stepwise with ethanol (50, 70, 90 and 100% (v/v)), critical point dried in CO_2 and gold coated by sputtering. The samples were examined with a Philips XL30CP Scanning Electron Microscope.

2.7 Coverslip scale-up

Polymers were spin-coated onto grided glass coverslips (DRM 800) and incubated with *S.* Typhimurium-GFP and imaged *via* SEM. The numbers of bacteria in randomly selected sub-squares (four for each coverslip) were counted with Image-Pro Plus 4.5 (©2001 Media Cybernetics) (see ESI, Fig. S3†).[17] Reproducibility was determined by calculating the average and the standard deviation for the four identical sub-squares.

3 Results and discussion

3.1 Analysis of bacteria attachment

Analysis was enabled by the expression of Green Fluorescent Protein (GFP)[15] within the bacteria, allowing detection of bacterial binding on a polymer microarray of 370 polyurethanes (PUs) and polyacrylates (PAs).[14]

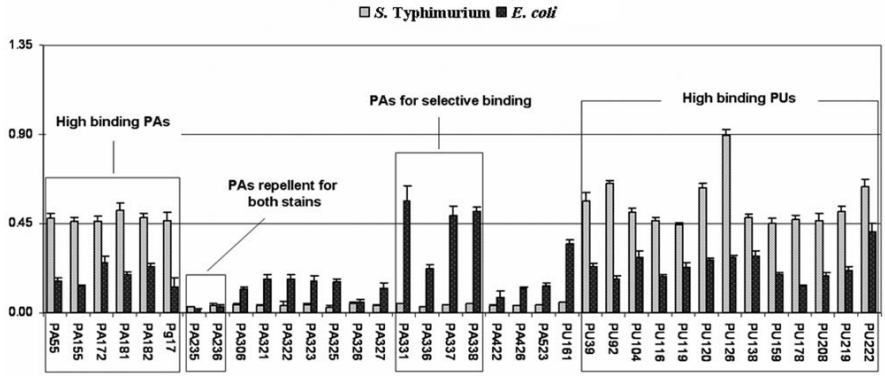

Fig. 1 Analysis of *S.* Typhimurium and *E. coli* binding on the polymer microarrays. PA and PU library members showing strong/poor *S.* Typhimurium and/or *E. coli* binding. Binding is expressed as background corrected mean fluorescent intensity with error bars representing the standard deviation. *X*-axis: polymer code. *Y*-axis: fluorescent intensity in arbitrary units (au).

Analysis revealed six PAs and thirteen PUs which showed strong binding of *S.* Typhimurium (Fig. 1). *E. coli* affinity was weaker in general, but varied with the particular polymer.

Four of the six high binding PAs (155, 172, 181 and 182) (Fig. 1) contained the monomer 2-hydroxyethylmethacrylate (HEMA) (see ESI, Table S1†) and of those four, two (PA181 and 182) contained the monomer 1-vinylimidazo (VI) within monomer ratio: 70/30 and 50/50, respectively (Table 1).

On the other hand, polymer structure analysis of the PUs revealed that the diols polybutylene glycol (PTMG) and

Table 1 Structure of the strong binding PAs and PUs

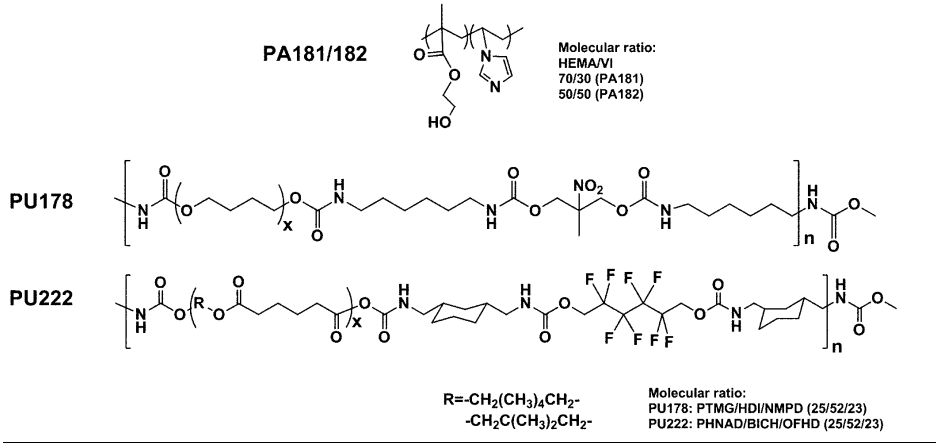

Table 2 Scheme of the poor binding polymer functionalisation and structure of the selected poor binding PAs

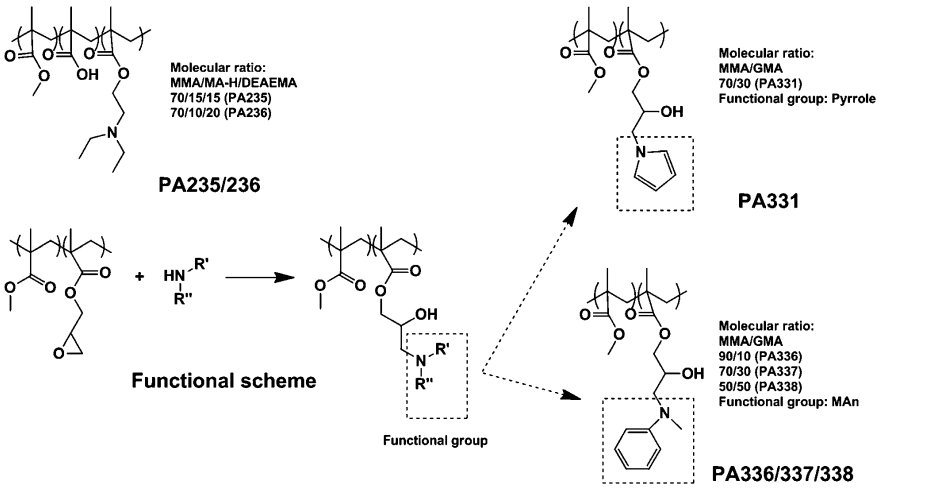

polypropylene glycol (PPG) were common in ten of the thirteen "hit" polymers (see ESI, Table S2†). Thus, for example, polymer PU222 showed good-binding of *S.* Typhimurium and *E. coli*, whereas there was a substantial difference between the binding of *S.* Typhimurium and *E. coli* on polymer PU178 (Table 1).

Sixteen PAs showed substantial inhibition of *S.* Typhimurium adhesion (Fig. 1), with thirteen containing the monomer methyl methacrylate (MMA), and with eleven of these also containing the derivatisable monomer glycidyl methacrylate (GMA) (Table 2 (functional scheme) and ESI: Tables S1† (poor binding polymers) and S3† (different functionalisations)).

PA235 and PA236, which were composed of methyl methacrylate (MMA), methacrylic acid (MA-H) and 2-(diethylamino)ethyl methacrylate (DEAEMA), were highly successful in preventing adhesion of both *S.* Typhimurium and *E. coli* (Table 2). Polymers PA331, PA337 and PA338 selectively bound *E. coli*, but did not bind *S.* Typhimurium, with PA337 and PA338 differing only in the molar ratios of the relevant monomers (MMA and GMA): 70/30 (PA337) and 50/50 (PA338) (Table 2). The related polymer PA336 (90/10) showed a similar trend, but with slightly less selectivity (Table 2). This suggested the importance of GMA functionalisation with *N*-methylaniline (MAn) in making this group of polymers selective for *E. coli* (see also ESI, Table S3†).

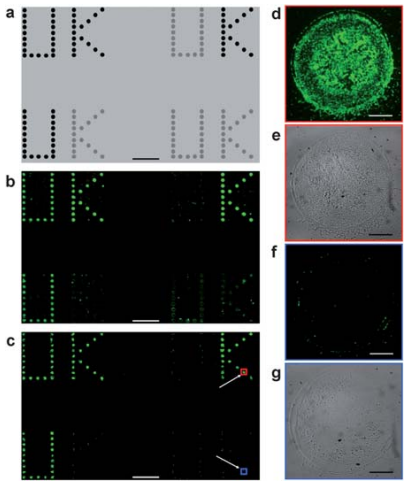

Fig. 2 *S.* Typhimurium attachment/repulsion: (a) array design with the binding polymer PU104 (in black) and the poor binding polymer PA325 (in grey); (b) BioAnalyzer scanning of the array using a fluorescein filter; (c) fluorescent microscopy imaging (×20 objective). Scale bar = 4 mm. Arrows indicate fluorescent and brightfield microscopy images of S. Typhimurium grown on representative polymer spots: (d) fluorescein channel and (e) brightfield of PU104; (f) fluorescein channel and (g) brightfield of PA325. Scale bar = 100 μm.

3.2 Reproducibility

Following the initial analysis of the entire library (in duplicate and with eight copies of each polymer), several polymers which resulted in the strongest or poorest binding of *S.* Typhimurium were re-printed and re-examined with each polymer printed in

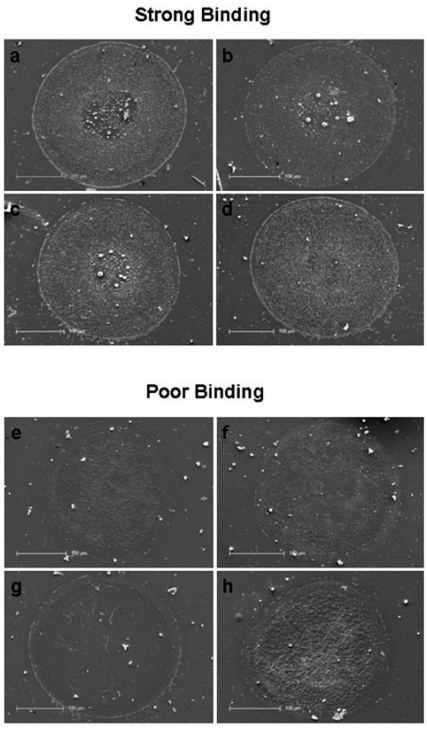

Fig. 3 SEM images of *S.* Typhimurium strong/poor binding on selected polymer spots. Strong binding: (a) PU104; (b) PU126; (c) PU120; and (d) PA155. Poor binding: (e) PA426; (f) PA422; (g) PA325; and (h) PA235. Scale bar = 100 μm.

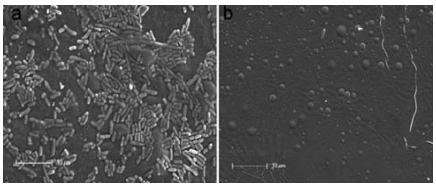

Fig. 4 High magnification SEM images of *S.* Typhimurium binding/non-binding on selected polymers: (a) PA155 and (b) PA325. Scale bar = 10 μm.

a 5 × 5 pattern. Of the four good polymers examined (PU104, PA155, PU120, and PU126), each showed consistent cellular attachment, whilst the four poor binding polymers (PA325, PA422, PA426, and PA235) confirmed their "anti-bacterial" binding properties (see ESI, Fig. S4†).

3.3 Impact of time on attachment

It would clearly be advantageous for a polymer to be able to bind bacteria in a rapid time frame. Therefore, to test the rapidity of *S.* Typhimurium binding, an array with the letters 'UK' was fabricated using high and low binding polymers (PU104 and PA325, respectively), and *S.* Typhimurium incubated on the array for four hours.

As can be seen in Fig. 2, a uniform binding pattern was observed with PU104, with little binding observed on polymer PA325.

S. Typhimurium binding on several selected polymers which resulted (PU104, PA155, PU120, PU126, PA325, PA422, PA426 and PA235) was assessed with particular attention paid to the binding characteristics and polymer spot morphology (Fig. 3).

Bacteria appeared firmly attached and closely packed on PA155, aligning along their longitudinal axis. Small micro-colonies were observed on the strong-binding polymer surface (Fig. 4a). In contrast, non-binding polymers (PA325) showed little attachment and no evidence for early biofilm formation, implicating these polymers as potential new materials for anti-bacterial surface coatings (Fig. 4b).

3.4 Scale-up analysis

In order to see if the selected polymers could be scaled-up and, to find whether those polymers could be used in practical applications, PA155 and PA325 were spin-coated onto glass coverslips, which were formed of a central square (1 × 1 mm) subdivided in one hundred squares (100 × 100 μm). These coated coverslips, and uncoated coverslips (as a control), were incubated with *S.* Typhimurium-GFP as previously reported (Section 3.1) and imaged *via* SEM (Fig. 5a–c). The number of bacteria on randomly selected subsquares on the coverslips were counted to give the number of bacteria per mm^2 (Fig. 5d). The analysis of binding on both coated and uncoated coverslips confirmed the expected results. *S.* Typhimurium attached onto polymer PA155 with a 7-fold increase in binding compared to an uncoated coverslip, whereas the number of *S.* Typhimurium on the anti-binding polymer PA325 was twenty times less than the glass control (Fig. 5d).

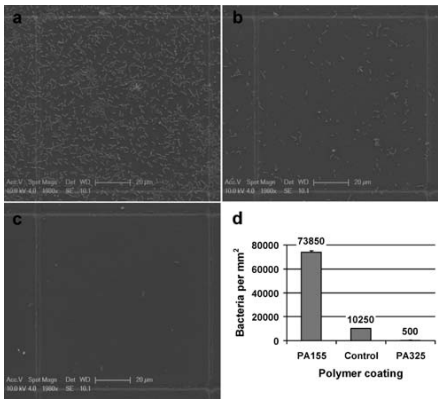

Fig. 5 SEM images and analysis of the *S.* Typhimurium binding on the selected polymer coated coverslips: (a) PA155 (strong binding); (b) control (no-polymer coated) and (c) PA325 (non-binding). Scale bar: 20 μm. (d) The average number of bacteria (*S.* Typhimurium) per mm^2 on PA155 (strong binding) and PA325 (non-binding) coated coverslips ($n = 4$).

4 Conclusion

Polymer microarrays were successfully used for the identification of polymers which bound either *S.* Typhimurium and/or *E. coli* or prevented their colonisation of surfaces, with fluorescence imaging that allowed the rapid, parallel, and comprehensive, evaluation of bacterial adhesion on 370 polymers. Binding and non-binding surfaces were shown to be highly dependent on both the chemical structures and properties of the polymers, and were sufficient to allow discrimination between adhesive properties of different bacterial genera. For the strongest binding polymers SEM revealed the formation of early biofilm-like micro-colonies, where cells were longitudinally aligned and closely packed, whereas a number of polymers were also identified which clearly prevented bacterial attachment, even at very high cell densities. Identified polymers are now being developed as coating materials to help reduce hospital endotracheal tube infections as well as in *Campylobacter jejuni* and *Clostridium difficile* infections.

Acknowledgements

We thank Edinburgh University and the China Scholarship Council (MW) for funding.

References

1 H. Morisaki and H. Tabuchi, *Colloids Surf., B*, 2009, **74**, 51–55.
2 D. G. Anderson, S. Levenberg and R. Langer, *Nat. Biotechnol.*, 2004, **22**, 863–866.
3 D. G. Anderson, D. Putnam, E. B. Lavik, T. A. Mahmood and R. Langer, *Biomaterials*, 2005, **26**, 4892–4897.
4 A. L. Hook, D. G. Anderson, R. Langer, P. Williams, M. C. Davies and M. R. Alexander, *Biomaterials*, 2010, **31**, 187–198.
5 A. L. Hook, H. Thissen and N. H. Voelcker, *Biomacromolecules*, 2009, **10**, 573–579.
6 S. E. How, B. Yingyongnarongkul, M. A. Fara, J. J. Diaz-Mochon, S. Mitto and M. Bradley, *Comb. Chem. High Throughput Screening*, 2004, **7**, 423–430.
7 G. Tourniaire, J. Collins, S. Campbell, H. Mizomoto, S. Ogawa, J.-F. Thaburet and M. Bradley, *Chem. Commun.*, 2006, 2118–2120.
8 R. Zhang, A. Liberski, F. Khan, J. J. Diaz-Mochon and M. Bradley, *Chem. Commun.*, 2008, 1317–1319.
9 (*a*) S. Pernagallo, A. Unciti-Broceta, J. J. Diaz-Mochon and M. Bradley, *Biomed. Mater. (Bristol, U. K.)*, 2008, **3**, 034112; (*b*) A. Liberski, R. Zhang and M. Bradley, *Chem. Commun.*, 2009, 334–336.
10 F. Khan, R. S. Tare, J. M. Kanczler, R. O. C. Oreffo and M. Bradley, *Biomaterials*, 2010, **31**, 2216–2228.
11 S. K. Hoiseth and B. A. Stocker, *Nature*, 1981, **291**, 238–239.
12 B. Coburn, G. A. Grassl and B. B. Finlay, *Immunol. Cell Biol.*, 2007, **85**, 112–118.

13 M. Riley, T. Abe, M. B. Arnaud, M. K. Berlyn, F. R. Blattner, R. R. Chaudhuri, J. D. Glasner, T. Horiuchi, I. M. Keseler, T. Kosuge, H. Mori, N. T. Perna, G. Plunkett III, K. E. Rudd, M. H. Serres, G. H. Thomas, N. R. Thomson, D. Wishart and B. L. Wanner, *Nucleic Acids Res.*, 2006, **34**, 1–9.
14 (*a*) S. Pernagallo, J. J. Diaz-Mochon and M. Bradley, *Lab Chip*, 2009, **9**, 397–403; (*b*) H. Mizomoto, PhD thesis, University of Southampton, Southampton, 2004; (*c*) J. F. O. Thaburet, H. Mizomoto and M. Bradley, *Macromol. Rapid Commun.*, 2004, **25**, 366–370; (*d*) A. Unciti-Broceta, J. J. Diaz-Mochon, H. Mizomoto and M. Bradley, *J. Comb. Chem.*, 2008, **10**, 179–184.
15 R. Heim, A. B. Cubitt and R. Y. Tsien, *Nature*, 1995, **373**, 663–664.
16 H. P. Cheng and G. C. Walker, *J. Bacteriol.*, 1998, **180**, 5183–5191.
17 A. J. Jose, L. S. Wong, J. Merrington and M. Bradley, *Ind. Eng. Chem. Res.*, 2005, **44**, 8659–8662.

WATER RESEARCH 46 (2012) 1715–1722

Available online at www.sciencedirect.com

SciVerse ScienceDirect

journal homepage: www.elsevier.com/locate/watres

Targeting *Cryptosporidium parvum* capture

Mei Wu [a], *Helen Bridle* [b,*], *Mark Bradley* [a,*]

[a] School of Chemistry, University of Edinburgh, West Mains Road, Edinburgh EH9 3JJ, United Kingdom
[b] Institute for Infrastructure and Environment, School of Engineering, The University of Edinburgh, Edinburgh EH9 3JL, United Kingdom

ARTICLE INFO

Article history:
Received 25 July 2011
Received in revised form
29 November 2011
Accepted 18 December 2011
Available online 27 December 2011

Keywords:
Polymer microarray
Waterborne protozoan
Cryptosporidium parvum
Protozoan–polymer interaction
Parasite removal

ABSTRACT

Polymer microarrays offer a high-throughput approach to the screening and assessment of a large number of polymeric materials. Here, we report the first study of protozoan–polymer interactions using a microarray approach. Specifically, from screening hundreds of synthetic polymers, we identified materials that either trap the waterborne protozoan parasite, *Cryptosporidium parvum*, or prevent its adhesion, both of which have major practical applications. Comparison of array results revealed differences in the adhesion characteristics of viable and non-viable *C. parvum* oocysts. Material properties, including polymer composition, wettability and surface chemistry, allowed correlation of binding and identification of structure function relationships. Understanding *C. parvum* binding interactions could assist in improved water treatment processes and the identified polymers could find applications in sensor and filter materials.

1. Introduction

Contamination of water by *Cryptosporidium parvum* (*C. parvum*) protozoa is a serious global issue. *C. parvum* is ubiquitous in the environment, resistant to the standard chlorination disinfection procedures and has a low infectious dose (Snelling et al., 2007; Casemore et al., 2001; Smith and Nichols, 2010). Ingestion of *C. parvum* oocysts causes cryptosporidiosis, for which there is no safe and effective treatment (Davies and Chalmers, 2009). In developing countries, it is estimated that 250–500 million cases occur each year, playing a significant role in high childhood mortality and morbidity. In developed countries, numerous outbreaks associated with contamination of drinking water have been reported, one of the most serious being in Milawaukee in 1993 (Mackenzie et al., 1994), and several recent cases in the UK (Davies and Chalmers, 2009), Australia (Ng et al., 2010) and in 2010, Sweden (Smittskyddsinstitutet, 2011).

Understanding the behaviour and fate of *C. parvum* in water treatment systems is essential to assess risk at existing plants and appropriately design future systems (Tufenkji et al., 2006; Dai et al., 2004). Although it is known that the nature of the coagulation pretreatment is very important for the efficiency of the subsequent water treatment processes, the exact adhesion and removal mechanisms have not been elucidated (Tufenkji et al., 2006; Gao and Chorover, 2009). Few field studies of *C. parvum* in water treatment systems have been undertaken, due to limitations in assay techniques for determining a mass balance for oocysts and lack of understanding of the mechanisms of interaction with chemicals or surfaces within the process (Tufenkji et al., 2006). Instead, laboratory studies have concentrated on the adhesion characteristics, to a range of materials, and measurement of interaction forces.

Numerous factors influence the oocyst–surface interaction including oocyst treatment (*e.g.* formalin or heat treatment to inactivate oocysts or proteinase K to digest surface macromolecules), nature of the surface (charge and hydrophobicity) and solution conditions (*e.g.* presence of divalent ions or high ionic strength) (Tufenkji et al., 2006; Dai et al.,

* *Corresponding authors.*
E-mail addresses: h.bridle@ed.ac.uk (H. Bridle), mark.bradley@ed.ac.uk (M. Bradley).
0043-1354/$ – see front matter
doi:10.1016/j.watres.2011.12.041

2004; Kuznar and Elimelech, 2004; Janjaroen et al., 2010; Searcy et al., 2005; Walker, 1999). However these previous studies have demonstrated some deviation from the predicted theory developed by: Derjaguin and Landau; Verwey and Overbeek (DLVO). The attachment efficiency was generally low, even at high ionic strengths, where DLVO theory predicts no energy barrier to adhesion. These results have been explained by the presence of a fluffy glycoprotein layer (Liu et al., 2010) extending approximately 115 nm from the oocyst wall (Byrd and Walz, 2007). This brush-like arrangement of macromolecules contributes "electrosteric" repulsion preventing oocyst adhesion to surfaces.

While various studies of *C. parvum* adhesion have been undertaken, with materials ranging from metal oxides (Walker, 1999), quartz (Kuznar and Elimelech, 2004; Liu et al., 2010), silanes (Byrd and Walz, 2007), natural organic matter (Janjaroen et al., 2010), biofilms (Searcy et al., 2006), clays and natural suspended sediments (Searcy et al., 2005), little work, apart from a paper by Dai et al. have investigated polymeric materials (Dai et al., 2004). Understanding the adhesion of *C. parvum* to polymers would be highly useful for numerous reasons: firstly, the membranes employed in filtration methods of water treatment, and monitoring, are made out of polymeric materials; secondly, polymers could easily be used as coatings in water treatment systems or sensing applications; thirdly, it is easy to systematically vary polymer properties to facilitate studies to elucidate structure–activity relationships.

Polymer microarrays provide a rapid format to enable the screening of a large number of polymers (How et al., 2004; Tourniaire et al., 2006; Diaz-Mochon et al., 2007). Such arrays have been applied to determine which materials can enrich, manipulate or modulate a variety of cell types, including human embryonic cells (Anderson et al., 2004; Hay et al., 2009, 2011), human skeletal progenitor cells (Tare et al., 2009; Khan et al., 2010), human renal tubular epithelial cells (Tourniaire et al., 2006) and mouse bone marrow dendritic cells (Mant et al., 2006), suspension cells (Pernagallo et al., 2008) and bacteria (Pernagallo et al., 2011). However, polymer microarrays have not previously been applied to investigate protozoan, or more specifically *C. parvum*, deposition.

In this study 652 polymers were screened to determine which materials would enhance or limit *C. parvum* adhesion, investigating the role of viability on surface interactions as well as the influence of hydrophobicity, surface roughness and polymer composition to develop our understanding of *C. parvum* interactions with surfaces.

2. Materials and methods

2.1. Synthesis of polymers

Polymer libraries were synthesised via radical polymerization on a mmol scale as previously reported (Mizomoto, 2004; Thaburet et al., 2004).

2.2. Chemicals and materials

All chemicals were of analytical grade and used as received without further purification. Sodium cacodylate trihydrate and all the monomers used were from Sigma–Aldrich. 2.5% (w/v) glutaraldehyde and 1% (w/v) osmium tetroxide were from Electron Microscopy Sciences. The rectangular four-well plates were from Nunc. Silane-prep glass slides were from Sigma–Aldrich and glass coverslips were from VWR. GeneFrames were from Thermo Scientific.

2.3. Polymer microarray fabrication

Polymer microarrays were fabricated with polyurethane (PU) and polyacrylate (PA) by contact printing (QArraymini, Genetix, UK) with a 32 aQu solid pins (K2785, Genetix) using 1% w/v polymer solutions in N-methylpyrrolidone (NMP) on microscope slides. The printing conditions used were 5 stamps per spot, with a 200 ms inking timing and a 100 ms stamping time on amino-alkylsilane treated glass slides (Sigma–Aldrich, UK), previously coated with agarose Type I-B (Sigma–Aldrich, UK) (Tourniaire et al., 2006). Typical spot diameters were 300–320 μm. Two types of array were used: the initial array contained 2016 polymer spots (triplicate of 652 polymers, including 468 polyacrylates and 164 polyurethanes); the subsequent hit array contained a selection of the 34 of the best and worst polymers.

2.4. Scanning for C. parvum oocyst interactions

C. parvum oocysts (Creative Science, Moredun, UK) were diluted in sterilised water to a count of 1.66×10^5 oocysts per ml. When required, heat treatment of the samples for 5 min at 70 °C was performed, using a Trechne Dri-Heat heating block, to obtain non-viable oocysts. Polymer microarrays were sterilised by exposure under UV light for 15 min and freshly prepared 6 ml aliquots (1 million oocysts per experiment) were added to a polymer microarray in a four-well plate. The slides were incubated with oocysts on a plate shaker at 20–50 rpm for 3 h at room temperature. Subsequently, the slides were rinsed with sterilised water and either fluorescently stained or prepared for SEM analysis.

2.5. Scale up

Polymers were spin-coated onto circular glass coverslips (13 mm in diameter), incubated with *C. parvum* (1.66×10^5 oocysts per ml in sterilised water) and imaged via brightfield and fluorescent microscopy as well as scanning electron microscopy (SEM).

2.6. Fluorescent staining of C. parvum oocysts

The standard *C. parvum* staining protocol (EPA1623) was adapted for the larger array area. After the slide was rinsed and air dried, 1 ml of methanol (MeOH) was added to the slide and allowed to air dry; 2 ml of 4′,6-diamidino-2-phenylindole (DAPI) (1 μg/ml) was applied to the slide for 1 min followed by a sterilised water rinse; finally, 2 ml of Crypto-a-glo was added to the slide (1–2 h) before rinsing in sterilised water and being left to air dry. A GeneFrame and a coverslip (1.9 × 6.0 cm, AB-0630) were then applied to each slide and cleaned with 70% ethanol. Image capture of the polymer microarray was performed via a Nikon 50i fluorescence microscope (20×

objective) with an automated X–Y–Z stage, using the IMSTAR Pathfinder™ software package (IMSTAR S.A., Paris, France).

2.7. Scanning electron microscopy

Array slides, or the coated substrates, were washed (×2) with 0.1 M cacodylate buffer (pH 7.4) and then fixed with 2.5% (w/v) glutaraldehyde in 0.1 M cacodylate buffer (pH 7.4) for 2 h. Samples were post-fixed with 1% (w/v) osmium tetroxide for 1 h at room temperature, dehydrated stepwise with ethanol (50, 70, 90 and 100% (v/v)), critical point dried in CO_2 and gold coated by sputtering. The samples were examined with a Philips XL30CP Scanning Electron Microscope at an accelerating voltage of 20 kV.

2.8. Atomic force microscopy

An atomic force microscope (AFM) (DimensionV Nanoscope, VEECO) was used to scan the polymer surface within an area 10 μm × 10 μm. The scan rate ranged from 1.32 Hz to 1.60 Hz,

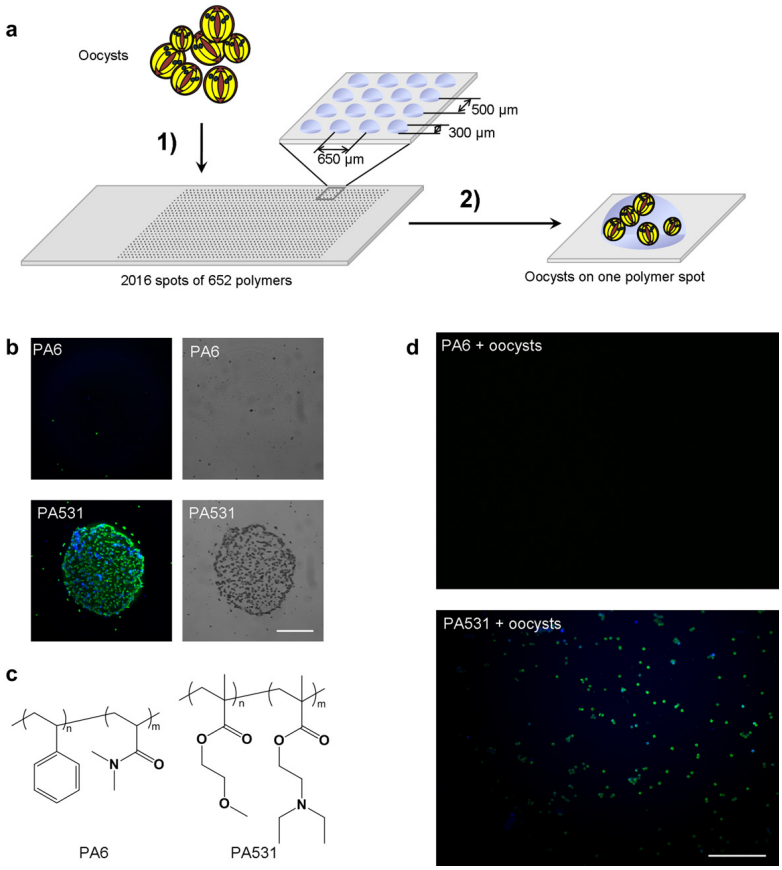

Fig. 1 – Array screening for *C. parvum* oocyst binding. (a). Oocysts (1 million) were incubated for 3 h on the polymer microarray. Adhesion to the polymers was analysed by high-content imaging ($n = 3$). (b) Images of the polymer features binding viable *C. parvum* with oocysts stained with Crypto-a-glo (green fluorescence), and DAPI (blue fluorescence). Fluorescent (left) and phase contrast (right) images of one polymer feature selected from a poor binding polymer (PA6) and a strongly binding polymer (PA531). (c) Chemical structures for the two polymers. (d) Viable oocysts on the polymer surface of PA6 and PA531 coated coverslips. Scale bars are 100 μm in (b) and (d). (For interpretation of the references to colour in this figure legend, the reader is referred to the web version of this article.)

and the height values of the surface were obtained with a resolution of 512 × 512 pixels in the scanned region. The root mean square (RMS) of all the spots in the hit array were calculated (by averaging over three 9 μm^2 areas) through the NanoScope analysis software (VEECO version 1.20). The RMS average of height deviations were taken from the mean image data plane, expressed as:

$$R_q = \sqrt{\frac{\sum (Z_i)^2}{N}}$$

where Z_i is the current Z value, and N is the number of points within the box cursor.

3. Results and discussion

The principle of high-throughput polymer array screening is illustrated in Fig. 1a. Briefly, pre-synthesised and characterised polymers were printed onto a glass slide, which was subsequently exposed to *C. parvum* oocysts. Following staining of the slides, automated screening was performed to capture images for each polymer with automatic counting of the number of oocysts per polymer feature.

The initial microarray of 652 polymers showed considerable differences in binding affinities between different polymers (see Fig. S1). There were also differences in the interaction behaviour of viable (untreated) (Fig. S1) and non-viable (heat-treated) (Fig. S2) oocysts. From these initial experiments, 34 polymers were selected for further investigation, to increase our understanding of how polymer material properties influence oocysts adherence, and these were re-printed in quintuplicate to give so-called "hit-arrays". This included those polymers which promoted strong interaction (PA480, PA528 and PA531); those which prevented adhesion (PAs 1, 2, 3, 4, 5 and 6, and a group of polyurethanes) and those which demonstrated some selectivity between viable and non-viable oocysts (PA113, PA152, PA365 and PA464).

The results show that PA531 most successfully bound *C. parvum* oocysts whereas PA6 acted to prevent binding and therefore, these two polymers were selected for investigation on larger surfaces in order to confirm suitability for practical applications. These polymers (chemical structures are shown in Fig. 1c) were re-synthesised and spin-coated onto individual glass surfaces and exposed to oocysts. Fig. 1d shows that polymer performance was maintained on the larger scale; with numerous oocysts observed adhered to the PA531 coated surface in contrast to no oocysts on the surface of PA6.

Scanning electron microscopy (SEM) was utilised to study the binding of both viable and non-viable oocysts on these selected polymers (Fig. 2 and Fig. S3). SEM images of the large scale substrates coated with PA531 and PA6 were consistent with the polymer microarray results and fluorescent images of the coated surfaces (Fig. 1d and Fig. S3g, h, i and j).

The morphologies of viable (Fig. 2c) oocysts on PA531 exhibited the expected oocyst features, with shape, size and presence of a central suture all in agreement with previous SEM studies of *C. parvum* oocysts (Poitras et al., 2009). Occasionally differences in morphology were observed, with a higher proportion of non-viable oocysts having undergone excystation and release of their sporozoites (Figs. 2d and S3c).

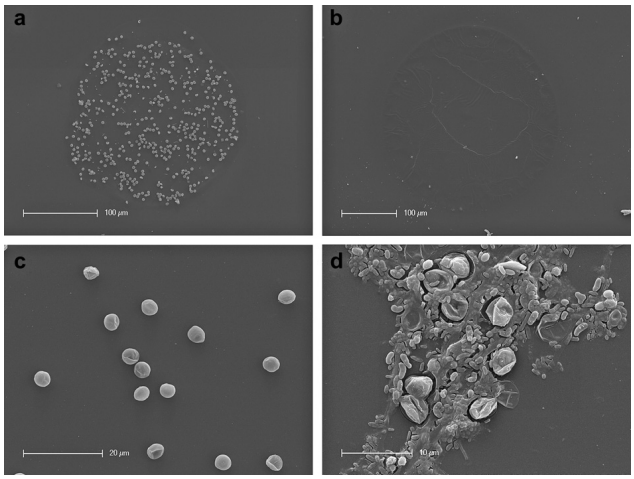

Fig. 2 – SEM images of viable/non-viable oocysts binding on selected polymers. (a) Viable cell attachment on the strong binding polymer PA531; (b) Negligible viable cell attachment on the poor binding polymer PA6; (c) Morphology of viable oocyst attachment on PA531 coated glass surface. (d) A proportion of non-viable cells adhering to the surface, with some having undergone excystation expelling their internal sporozoites. Scale bars are shown in (a)–(d).

3.1. C. parvum *characteristics*

On the hit array, some polymers, such as PA531, PA528 and PA480, showed high binding for both viable and non-viable oocysts (Fig. S4). Additionally polymers such as PA1, PA2, PA3, PA4, PA5 and PA6 completely prevented viable and non-viable oocyst adhesion (Figs. S4 and S5). However, in general, notable differences in adhesion characteristics were observed in the results for viable and non-viable oocysts (Fig. S6). PA113 and PA531 were the top two polymers for adhesion of non-viable oocysts, while PA528 and PA364 demonstrated highest affinity binding for viable oocysts, perhaps indicative of different mechanisms, and relative strengths, of interactions. The polymers PA104 and PA504 demonstrated the highest selectivity in favouring of binding viable oocysts given that the ratio of viable oocysts to non-viable oocysts bound greater than 20 as opposed to an average of 4.5 for the selected hit polymer library (Fig. S6). However, these two polymers were poor enhancers of oocyst adhesion and are therefore unlikely to be of use in discriminating between viable and non-viable oocysts.

A lower number of oocysts per polymer spot for the non-viable oocysts was observed, contradicting prior work which suggests that heat treatment of oocysts enables better adhesion via alteration/removal of surface glycoproteins (Gao and Chorover, 2009; Byrd and Walz, 2007). However, the influence of viability on oocysts adhesion has not previously been studied for polymer materials. Possibly, for polymer materials, the interaction is dominated by forces, such as hydrogen bonding and Lewis acid base interactions (Grasso et al., 2002), and non-viable oocysts, with a reduced proportion of surface glycoproteins, are thus less able to interact with polymer surfaces. Comparison of the structures (Fig. 1c) of PA531 (strong interaction) and PA6 (inhibition of adhesion) supports this argument. PA531 comprises of MEMA (Methoxyethyl methacrylate) and DEAEMA (2-(Diethylamino) ethyl methacrylate) (Figs. 1c and 3e) which contain several groups capable of participating in hydrogen bonding and ionic interactions, whereas PA6 is composed of styrene and DMAA (N,N-Dimethyl acrylate) (Figs. 1c and 3e) and as such has a reduced capacity for these interactions. Analysis of the polymer microarray results aimed to investigate relationships between binding and factors, such as oocyst viability (discussed above), as well as material properties, such as hydrophobicity, surface roughness and polymer composition, which are well-known to influence cellular, bacterial and protozoan adhesion (Dai et al., 2004; Liu et al., 2010; Yang et al., 2010; Bazaka et al., 2011). These relationships are visualised in Figs. 3 and 4.

3.2. *Wettability analysis*

Wettability is one of the most important properties utilised in the area of polymeric analysis, and is used as a measurement of the hydrophobicity/hydrophilicity of materials. The Bradley group developed the first high-throughput method to evaluate hydrophobicity/hydrophilicity (Mizomoto, 2004; Thaburet et al., 2004). Importantly, this measurement is dynamic as water contact angle (WCA) varies with time (see Table S1, and Fig. 3, for the WCA of the polymers used in this study). Previous studies by Dai et al. reported that hydrophobicity was not the most important factor for *C. parvum* adhesion (Dai et al., 2004). This work suggested that other factors, such as surface charge and polymer composition, were probably more important. As Fig. 3a shows, the eight best-binding polymer spots all had a WCA between 60° and 72° (Table S1), suggesting that this range of WCAs is optimal for oocyst binding. Furthermore, it appears from Fig. 3a, that extremes of hydrophobicity or hydrophilicity have a negative influence on oocyst attachment. The previously identified poor binding polymers, PA1-6 exhibited high WCAs as do the PUs 91, 223 and 226. Poor adhesion was also seen with the other polyurethanes, which exhibited the lowest WCAs, such as PU230 and PU239. However, fitting of the data demonstrated no correlation between oocyst adherence and WCA. This lack of correlation is supported by the observation that many poor-binding polymers also had WCAs, in the so-called optimal binding range, between 60° and 72° (Fig. 3a, Table S1). Additionally, PA113, noted for its strong interaction with *C. parvum* oocysts, had a low contact angle, comparable to PA1 and 6

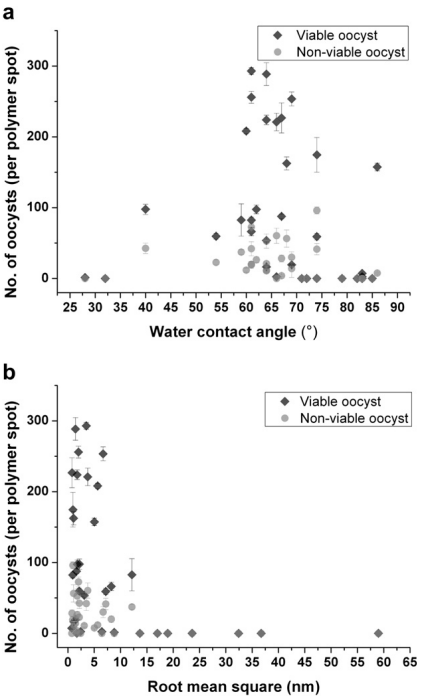

Fig. 3 – Correlation between *C. parvum* oocysts adherence and polymer surface properties of hit polymers. (a) Viable/non-viable oocysts adherence per polymer spot ($n = 5$) and polymer contact angle. (b) Viable/non-viable oocysts adherence per polymer spot ($n = 5$) compared to surface roughness (root mean square).

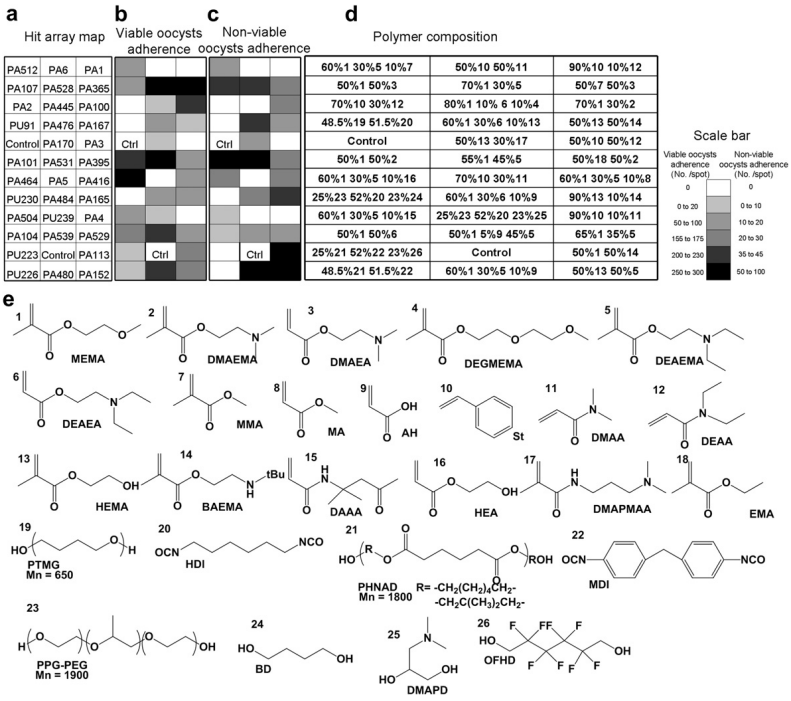

Fig. 4 – Mapping the binding behaviour of viable and non-viable *C. parvum* oocysts. (a) Location map of the 34 selected polymers. (b)/(c) Viable/non-viable oocysts adherence on the arrays. (d) Composition of the polymers, with the monomer shown in (e).

(Fig. 3a, Table S1). Therefore, our results support the assertion by Dai et al. that hydrophobicity is not an important factor controlling the adhesion of *C. parvum*.

3.3. *Surface roughness analysis*

Atomic force microscopy (AFM) was employed to investigate the influence of the surface roughness on *C. parvum* adherence (Fig. 3b). The root mean square (RMS) surface roughness value ranged from 0.01 to 59.0 nm and did not correlate with the WCA (Fig. S8, Table S1). The RMS of strongly binding polymers such as PA531, PA528 and PA480 are 2.02 nm, 3.50 nm and 1.75 nm respectively, suggesting that low surface roughness may assist *C. parvum* oocysts attachment. Likewise, those polymers with the highest RMS showed lowest binding of *C. parvum* oocysts; for example, the inhibitory polyacrylates, PA1 (32.4 nm), PA2 (23.6 nm), PA3 (36.7 nm), PA4 (19.0 nm), and PA5 (16.7 nm) as well as PU230 (59.0 nm) and PU91 (17.0 nm). Fitting of linear, logarithmic and polynomial trend lines, to a plot of oocyst adherence (both viable and non-viable) against RMS, all generated low R^2 values (of 0.17 or less) (data not shown) indicating a lack of correlation between the surface roughness and *C. parvum* adhesion. However, Fig. 3b suggests that for polymers with RMS values greater than 17 nm, *C. parvum* interactions are inhibited. Interestingly, the surface roughness of oocysts is between 5 and 20 nm over micron-sized areas (Tufenkji et al., 2006; Considine et al., 2001). Since for bacterial attachment it is known that irregularities that conform to the size of the bacteria increases the adhesion due to maximising bacteria-surface contact area (Bazaka et al., 2011; Whitehead et al., 2005) perhaps for *C. parvum* a similar surface roughness for oocysts promotes attachment.

3.4. *Polymer composition*

Analysis of Fig. 4 shows clearly that specific chemical compositions inhibit binding and includes polymers containing styrene and DMAA (N,N-Dimethyl acrylate) or DEAA (N,N-Diethyl acrylate), while three out of four of those polymers which had the highest adherence of viable oocysts contained MEMA with DEAEMA or MEMA with DMAEMA (2-(Dimethylamino) ethyl methacrylate). We suggested that hydrogen

bonding and acid–base interactions could play an important role in controlling surface adhesion of oocysts to polymers. The presence of MEMA and HEMA (2-Hydroxyethyl methacrylate), which have several sites to act as either hydrogen bond acceptors or donors, were found in many of the polymers selected for further analysis, supports this theory.

While knowledge relating to the exact composition of, and glycoprotein structures within, the oocyst wall is limited, the 5 nm outer layer is believed to consist of acidic glycoproteins (Kuznar and Elimelech, 2006) and the ability of oocyst surfaces to form hydrogen bonds has been noted (Karaman et al., 1999). Additionally, the presence of carboxylates and phosphates has been suggested by the fitted pKa value of 2.5 found by Karaman et al. Our hypothesis is that hydrogen bonding, and acid–base interactions, play a key role in explaining the interaction of oocysts with polymer surfaces, and have more significant impact upon adhesion than hydrophobicity or surface roughness.

A key component of PA531 is DEAEMA, which has a reported pK_a of 8.4 (van de Wetering et al., 1998) which means that it will be protonated at all physiologically relevant pH's. This will thus ion-pair with the carboxylate/phosphate rich oocyst wall. The same argument holds for PA101 and PA480. The poor binding of PA1-6 can be rationalised by the non-charged nature of styrene and the acrylamides, DMAA and DEAA. Likewise, the PUs have no formal positive charge.

4. Conclusion

In summary, we have demonstrated the first protozoan–polymer microarray screening study. From the analysis of over 652 polymers, materials were identified which binding or prevent the binding of the waterborne, protozoan parasite *C. parvum*. Results from the initial array were confirmed on a hit array, containing the best and worst performing polymers, and on larger polymer coated substrates. Additionally, differences were observed between the adhesion characteristics of viable and non-viable oocysts.

Comparison of the results with the physical properties of the polymers indicated that neither wettability or surface roughness of the polymers were important factors controlling the adhesion of *C. parvum* oocysts. However, the polymer composition was critical in determining oocyst–polymer interactions. The presence of certain monomers, *e.g.* DEAEMA or DMAEMA with MEMA, were associated with enhanced binding whereas other monomers, *e.g.* styrene and DEAA or DMAA, in the polymers appeared to prevent adhesion. This was explained by ion-pair interactions between the polymer surfaces and the oocyst wall.

Future work is necessary to investigate the kinetics of adhesion, the influence of different solution conditions and the adhesion behaviour of different species and also to explore potential applications, such as in filters or sensor materials.

Author contributions

MW and HB contributed equally to this work. All authors co-wrote this paper.

Acknowledgements

We thank the University of Edinburgh, the China Scholarship Council (MW) and the Royal Academy of Engineering/EPSRC (HB) for funding. We thank Oleg Nerushev for AFM technical support.

Appendix. Supplementary data

Supplementary data related to this article can be found online at doi:10.1016/j.watres.2011.12.041.

REFERENCES

Anderson, D.G., Levenberg, S., Langer, R., 2004. Nanoliter-scale synthesis of arrayed biomaterials and application to human embryonic stem cells. Nature Biotechnology 22 (7), 863–866.

Bazaka, K., Jacob, M.V., Crawford, R.J., Ivanova, E.P., 2011. Plasma-assisted surface modification of organic biopolymers to prevent bacterial attachment. Acta Biomaterialia 7, 2015–2028.

Byrd, T.L., Walz, J.Y., 2007. Investigation of the interaction force between *Cryptosporidium parvum* oocysts and solid surfaces. Langmuir 23, 7475–7483.

Casemore, D.P., Hoyle, B., Tynan, P., Smith, M.S., 2001. In: Smith, M., Thompson, K.C. (Eds.), Cryptosporidium: The Analytical Challenge. Royal Soc Chemistry, Cambridge, pp. 73–83.

Considine, R.F., Drummond, C.J., Dixon, D.R., 2001. Force of interaction between a biocolloid and an inorganic oxide: complexity of surface deformation, roughness, and brushlike behavior. Langmuir 17 (20), 6325–6335.

Dai, X., Boll, J., Hayes, M.E., Aston, D.E., 2004. Adhesion of *Cryptosporidium parvum* and *Giardia lamblia* to solid surfaces: the role of surface charge and hydrophobicity. Colloids and Surfaces B 34, 259–263.

Davies, A.P., Chalmers, R.M., 2009. Cryptosporidiosis. British Medical Journal 339, b4168.

Diaz-Mochon, J.J., Tourniaire, G., Bradley, M., 2007. Microarray platforms for enzymatic and cell-based assays. Chemical Society Reviews 36 (3), 449–457.

Gao, X., Chorover, J., 2009. In-situ monitoring of *Cryptosporidium parvum* oocyst surface adhesion using ATR-FTIR spectroscopy. Colloids and Surfaces B 71, 169–176.

Grasso, D., Subramaniam, K., Butkus, M., Strevett, K., Bergendahl, J., 2002. A review of non-DLVO interactions in environmental colloidal systems. Reviews in Environmental Science and Biotechnology 1, 17–38.

Hay, D.C., Pernagallo, S., Diaz-Mochon, J., Schrader, J., Fletcher, J., Dalgetty, D., Medine, C., Black, J.R., Thompson, A.I., Hannoun, Z., Newsome, P.N., Forbes, S.J., Ross, J.A., Bradley, M., Iredale, J.P., 2009. A simple polyurethane matrix promotes hepatic endoderm viability and inducible drug metabolism: implications for drug toxicology testing and the design of liver support devices. Hepatology 50 (6), LB1.

Hay, D.C., Pernagallo, S., Diaz-Mochon, J.J., Medine, C.N., Greenhough, S., Hannoun, Z., Schrader, J., Black, J.R., Fletcher, J., Dalgetty, D., Thompson, A.I., Newsome, P.N., Forbes, S.J., Ross, J.A., Bradley, M., redale, J.P., 2011. Unbiased screening of polymer libraries to define novel substrates for functional hepatocytes with inducible drug metabolism. Stem Cell Research 6 (2), 92–102.

How, S.E., Yingyongnarongkul, B., Fara, M.A., Diaz-Mochon, J.J., Mittoo, S., Bradley, M., 2004. Polyplexes and lipoplexes for mammalian gene delivery: from traditional to microarray screening. Combinatorial Chemistry and High Throughput Screening 7 (5), 423–430.

Janjaroen, D., Liu, Y., Kuhlenschmidt, M.S., Kuhlenschmidt, T.B., Nguyen, T.H., 2010. Role of divalent cations on deposition of *Cryptosporidium parvum* oocysts on natural organic matter surfaces. Environmental Science and Technology 44, 4519–4524.

Karaman, M.E., Pashley, R.M., Bustamante, H., Shanker, S.R., 1999. Microelectrophoresis of *Cryptosporidium parvum* oocysts in aqueous solutions of inorganic and surfactant cations. Colloids and Surfaces A 146, 217–225.

Khan, F., Tare, R.S., Kanczler, J.M., Oreffo, R.O.C., Bradley, M., 2010. Strategies for cell manipulation and skeletal tissue engineering using high-throughput polymer blend formulation and microarray techniques. Biomaterials 31 (8), 2216–2228.

Kuznar, Z.A., Elimelech, M., 2004. Adhesion kinetics of viable *Cryptosporidium parvum* oocysts to quartz surfaces. Environmental Science and Technology 38, 6839–6845.

Kuznar, Z.A., Elimelech, M., 2006. Cryptosporidium oocyst surface macromolecules significantly hinder oocyst attachment. Environmental Science and Technology 40, 1837–1842.

Liu, Y., Kuhlenschmidt, M.S., Kuhlenschmidt, T.B., Nguyen, T.H., 2010. Composition and conformation of *Cryptosporidium parvum* oocyst wall surface macromolecules and their effect on adhesion kinetics of oocysts on quartz surface. Biomacromolecules 11, 2109–2115.

Mackenzie, W.R., Hoxie, N.J., Proctor, M.E., Gradus, M.S., Blair, K.A., Peterson, D.E., Kazmierczak, J.J., Addiss, D.G., Fox, K.R., Rose, J.B., Davis, J.P., 1994. A massive outbreak in milwaukee of Cryptosporidium infection transmitted through the public water supply. New England Journal of Medicine 331 (3), 161–167.

Mant, A., Tourniaire, G., Diaz-Mochon, J.J., Elliott, T.J., Williams, A.P., Bradley, M., 2006. Polymer microarrays: identification of substrates for phagocytosis assays. Biomaterials 27 (30), 5299–5306.

Mizomoto, H., 2004. The Synthesis and Screening of Polymer Libraries Using a High Throughput Approach. Thesis in School of Chemistry, University of Southampton.

Ng, J.S.Y., Pingault, N., Gibbs, R., Koehler, A., Ryan, U., 2010. Molecular characterisation of Cryptosporidium outbreaks in western and South Australia. Experimental Parasitology 125 (4), 325–328.

Pernagallo, S., Unciti-Broceta, A., Diaz-Mochon, J.J., Bradley, M., 2008. Deciphering cellular morphology and biocompatibility using polymer microarrays. Biomedical Materials 3 (3), 034112.

Pernagallo, S., Wu, M., Gallagher, M.P., Bradley, M., 2011. Colonising new frontiers-microarrays reveal biofilm modulating polymers. Journal of Material Chemistry 21 (1), 96–101.

Poitras, C., Fatisson, J., Tufenkji, N., 2009. Real-time microgravimetric quantification of *Cryptosporidium parvum* in the presence of potential interferents. Water Research 43 (10), 2631–2638.

Searcy, K.E., Packman, A.I., Atwill, E.R., Harter, T., 2005. Association of *Cryptosporidium parvum* with suspended particles: impact on oocyst sedimentation. Applied and Environmental Microbiology 71 (2), 1072–1078.

Searcy, K.E., Packman, A.I., Atwill, E.R., Harter, T., 2006. Capture and retention of *Cryptosporidium parvum* oocysts by *Pseudomonas aeruginosa* biofilms. Applied and Environmental Microbiology 72 (9), 6242–6247.

Smith, H.V., Nichols, R.A.B., 2010. Cryptosporidium: detection in water and food. Experimental Parasitology 124 (1), 61–79.

Smittskyddsinstitutet (SMI), 2011. Smittskyddsinstitutets arbete med det vattenburna utbrottet av Cryptosporidium i Östersund (in Swedish), news archive SMI.

Snelling, W.J., Xiao, L., Ortega-Pierres, G., Lowery, C.J., Moore, J.E., Rao, J.R., Smyth, S., Millar, B.C., Rooney, P.J., Matsuda, M., Kenny, F., Xu, J., Dooley, J.S., 2007. Cryptosporidiosis in developing countries. Journal of Infection in Developing Countries 1 (3), 242–256.

Tare, R.S., Khan, F., Tourniaire, G., Morgan, S.M., Bradley, M., Oreffo, R.O.C., 2009. A microarray approach to the identification of polyurethanes for the isolation of human skeletal progenitor cells and augmentation of skeletal cell growth. Biomaterials 30 (6), 1045–1055.

Thaburet, J.F.O., Mizomoto, H., Bradley, M., 2004. High-throughput evaluation of the wettability of polymer libraries. Macromolecular Rapid Communications 25 (1), 366–370.

Tourniaire, G., Collins, J., Campbell, S., Mizomoto, H., Ogawa, S., Thaburet, J.F., Bradley, M., 2006. Polymer microarrays for cellular adhesion. Chemical Communications (20), 2118–2120.

Tufenkji, N., Dixon, D.R., Considine, R., Drummond, C.J., 2006. Multi-scale cryptosporidium/sand interactions in water treatment. Water Research 40, 3315–3331.

van de Wetering, P., Zuidam, N.J., van Steenbergen, M.J., van der Houwen, O., Underberg, W.J.M., Hennink, W.E., 1998. A mechanistic study of the hydrolytic stability of poly(2-(dimethylamino)ethyl methacrylate). Macromolecules 31 (23), 8063–8068.

Walker, M.J., 1999. Sorption of *Cryptosporidium parvum* oocysts in aqueous solution to metal oxide and hydrophobic substrates. Environmental Science and Technology 33, 3134–3139.

Whitehead, K.A., Colligon, J., Verran, J., 2005. Retention of microbial cells in substratum surface features of micrometer and sub-micrometer dimensions. Colloids and Surfaces B 41 (2–3), 129–138.

Yang, J., Mei, Y., Hook, A.L., Taylor, M., Urquhart, A.J., Bogatyrev, S.R., Langer, R., Anderson, D.G., Davies, M.C., Alexander, M.R., 2010. Polymer surface functionalities that control human embryoid body cell adhesion revealed by high throughput surface characterization of combinatorial material microarrays. Biomaterials 31 (34), 8827–8838.

Environmental Science & Technology

Article

pubs.acs.org/est

Analysis of *Giardia lamblia* Interactions with Polymer Surfaces Using a Microarray Approach

Harry Pickering,[†,‡] Mei Wu,[§,‡] Mark Bradley,[*,§] and Helen Bridle[*,†]

[†]Institute for Infrastructure and Environment, School of Engineering, University of Edinburgh, Edinburgh, EH9 3JL, United Kingdom
[§]School of Chemistry, University of Edinburgh, Edinburgh, EH9 3JJ, United Kingdom

Supporting Information

ABSTRACT: The interaction of the waterborne protozoan parasite, *Giardia lamblia*, with polymeric materials was investigated by microarray screening of 652 polymers. Polymers were identified which either bound *G. lamblia* cysts or prevented their binding. Correlation of material properties such as wettability and surface roughness with cyst attachment revealed no influence of these factors upon *Giardia* adhesion. However, the study of polymer composition allowed the correlation of binding and generation of polymer structure function relationships; glycol and aromatic functionalities appeared to prevent adhesion, whereas secondary amine groups promoted adhesion, in agreement with previous literature. A significant reduction in attachment was observed following both cyst treatments with proteinase K and performing experiments at extremes of pH (2 and 12). It is suggested that proteinase K removes the proteins needed for specific surface interactions, whereas extremes of pH influence either protonation of the polymer or the surface charge of the cysts. The mechanism by which the protozoa attach to polymeric surfaces is proposed to be through ion−pair interactions. Improved understanding of *G. lamblia* surface interactions could assist in predicting transport and fate behavior in the environment and contribute to better design of water treatment processes, while the polymers identified in this work could find use in sensor applications and membrane filtration.

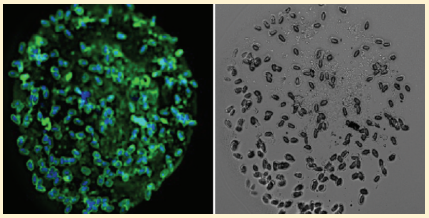

INTRODUCTION

The protozoan parasite *Giardia lamblia* (*G. lamblia*), which has a low infectious dose (1−10 cysts), contaminates water supplies across the globe and causes giardiasis.[1] Treatment of giardiasis varies depending on the patient, as does the effectiveness of different drugs, whose side effects are common.[2] Prevalence of *G. lamblia* is around 20−30% in the developing world,[3] with up to 100% of children acquiring the infection before the age of 3.[2] In the developed world, where water treatment is better and more widespread prevalence is lower but outbreaks do occur. In 1985 there were particularly serious cases in both the United Kingdom[4] and the United States.[5] In the United States *G. lamblia* was one of the most common intestinal protozoan infections in 2001.[6] In 2004, over 1000 cases were reported in Norway, resulting from leaking sewage and ineffective water treatment.[7] This pathogen causes a major problem in the water industry as it is resistant to disinfection by chlorine treatment[8] and can also pass with up to 30% efficiency through advanced membrane filters.[9]

The majority of studies investigating *G. lamblia* interactions with surfaces have focused on the postingestion trophozoite stage and its attachment through an adhesive disk.[10] There has been limited investigation of the cyst stage, where the adhesive disk is internalized and fragmented.[10] Cyst interaction with polymeric materials, as previously investigated in a paper by Dai et al.,[11] is very important in the control of waterborne giardiasis. Since polymers are utilized in production of membrane filters for water treatment and monitoring, pathogen-specific coatings could help to improve the performance of these methods.[9] Furthermore, the relative simplicity with which polymeric material properties can be modified provides an easy method to gain insight into structure−activity relationships with respect to parasite/material interactions. Improved knowledge of *G. lamblia* interactions could assist in the design of improved water treatment processes.

The screening of a large number of polymers can be achieved rapidly through the use of polymer microarrays.[12−14] Such arrays have been applied to determine which materials can enrich, manipulate, or modulate a variety of cell types, including human embryonic cells[15,16] human skeletal progenitor cells,[17,18] human renal tubular epithelial cells,[12] mouse bone marrow dendritic cells,[19] suspension cells,[20] bacteria,[21] and most recently the waterborne, protozoan pathogen, *Cryptosporidium*.[22] In this paper the focus was on the study of another problematic waterborne protozoan pathogen, *G. lamblia*. This

Received: October 20, 2011
Revised: January 13, 2012
Accepted: January 13, 2012
Published: February 2, 2012

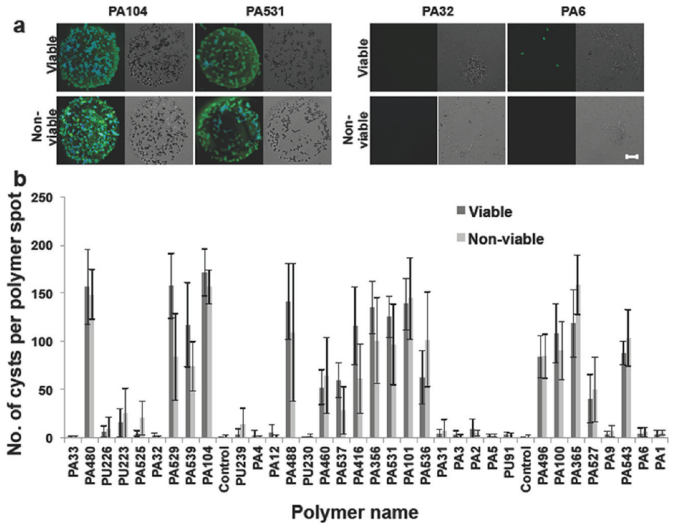

Figure 1. Microarray screening of selected polymers for *G. lamblia* cyst binding. (a) Images of the cysts stained with Giardia-a-glo (green) and DAPI (blue) bound to polymer spots. Fluorescent (left) and phase contrast (right) images of selected polymers are shown; two strong binding polymers (PA104 and PA531) and two poor binding polymers (PA6 and PA32). Scale bar = 100 μm. (b) Chart comparing the results of hit arrays with viable (dark gray) and nonviable cysts (light gray), showing strong correlation between them.

approach allowed for investigation of the mechanisms by which the protozoa attaches to polymer. Six hundred fifty two polymers were screened to determine which materials have positive or negative effects on *G. lamblia* adhesion. The effect of viability on surface interactions as well as the impact of certain polymeric properties such as hydrophobicity, surface roughness, presence of specific monomers, and relative number of ester moieties was investigated. In addition, the influence of both pH and proteinase K on *G. lamblia* interactions with surfaces was studied. Such improved understanding is likely to contribute to better design of water treatment processes for this pathogen, and the polymers identified in this paper may find applications in coatings for membrane filters or even in the development of sensing technology.

MATERIALS AND METHODS

Chemicals and Materials. All chemicals were of analytical grade and used as received without further purification. Sodium cacodylate trihydrate and all monomers used were from Sigma-Aldrich. Two and a half percent (w/v) glutaraldehyde and 1% (w/v) osmium tetroxide were from Electron Microscopy Sciences. Rectangular 4-well plates and 24-well plates were from Nunc. Silane-prep glass slides were from Sigma-Aldrich, and glass coverslips were from VWR. GeneFrames were from Thermo Scientific.

Polymer Microarray Fabrication. Polymer microarrays were fabricated as previously reported (see Supporting Information for further details).

Scanning for Cyst Interactions. *G. lamblia* cysts were obtained from Waterborne Inc., USA (catalog number P101). The cysts were the human isolate H-3, passed through gerbils. *G. lamblia* cysts were diluted in sterilized water to a concentration of 1.66×10^5 cysts/mL. When required, heat treatment of the samples for 5 min at 70 °C was performed[23] using a Trechne Dri-Heat heating block to obtain nonviable cysts, confirmed by staining with propidium iodide (Figure S1, Supporting Information). Polymer microarrays were sterilized by exposure under UV light for 15 min, and freshly prepared 6 mL aliquots (1 million cysts per experiment) were added to the polymer microarray. The slides were incubated with cysts on a plate shaker at 20 rpm for 3 h at 25 °C. Subsequently, the slides were rinsed with sterilized water and fluorescently stained using an adapted version of the standard EPA1623 protocol.[24]

Scale Up. Polymers were spin coated onto glass coverslips (13 mm in diameter), incubated with *G. lamblia* (0.833×10^5 cysts/mL in sterilized water) in 24-well plates, and imaged via fluorescence microscopy and scanning electron microscopy (SEM).

Fluorescent Staining of Cysts. The standard *G. lamblia* staining protocol (EPA1623) was adapted for the larger array area. Slides were rinsed and air dried; 1 mL of MeOH was added and allowed to air dry; 4 mL of a solution of DAPI (1 μg/mL) was applied for 1 min followed by a sterilized water rinse; finally, 2 mL of Giardia-a-glo, a fluorescein-labeled mouse monoclonal antibody made to a cyst wall antigenic site (at EPA1623 concentration) (Waterborne Inc., USA), was added (25 min) before rinsing in sterilized water and being left to air dry. A GeneFrame and a coverslip (1.9 × 6.0 cm, AB-0630) were then applied to each slide, and the external surface of the slide construct was cleaned with 70% ethanol. Image capture

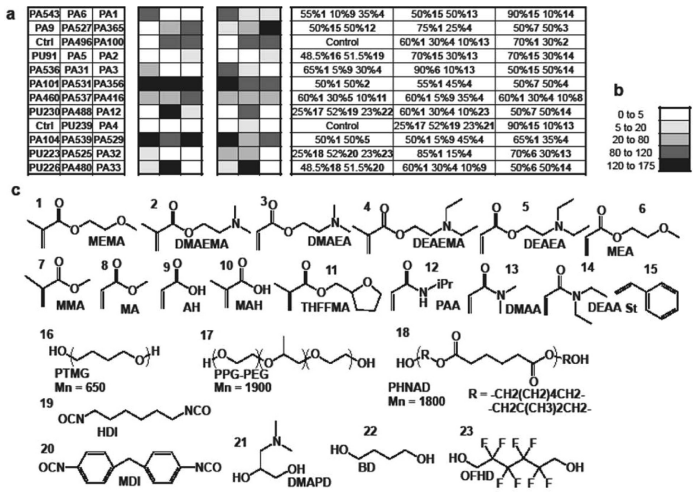

Figure 2. Analysis of microarray results and polymer structures. (a) (Left to right) Polymer identity, binding of viable and nonviable cysts, and polymer composition. (b) Bars relating color intensity to cyst binding. (c) Chemical structures of the monomers.

from the polymer microarray was performed via a Nikon 50i fluorescence microscope (20× objective) with an automated *X-Y-Z* stage, using the IMSTAR Pathfinder software package (IMSTAR S.A., Paris, France).

Scanning Electron Microscopy. Coated substrates, were washed (×2) with 0.1 M cacodylate buffer (pH 7.4) and then fixed with 2.5% (w/v) glutaraldehyde in 0.1 M cacodylate buffer (pH 7.4) for 2 h. Samples were postfixed with 1% (w/v) osmium tetroxide for 1 h at room temperature, dehydrated stepwise with ethanol (50%, 70%, 90%, and 100% (v/v)), critical point dried in CO_2, and gold coated by sputtering. Samples were examined with a Philips XL30CP Scanning Electron Microscope.

Wettability/Surface Roughness. Wettability was measured using the high-throughput method developed by Bradley.[25,28] Surface roughness was quantified using atomic force microscopy (AFM). Images were taken over a 100 μm^2 area of the polymer surfaces using a DimensionV Nanoscope (VEECO). The scan rate ranged from 1.32 to 1.60 Hz, and the height values of the surface were obtained with a resolution of 512 × 512 pixels in the scanned region. The root mean square of the features in the hit array were calculated by averaging over three 9 μm^2 areas through the NanoScope analysis software (VEECO version 1.20).

For the *G. lamblia* surface roughness measurement, the sample was prepared by overnight incubation of cysts on a PA104-coated coverslip (13 mm in diameter), followed by fixing in 1% glutaraldehyde and air drying. AFM was performed with a contact cantilever in air at a scan rate of 0.788 Hz, and the roughness was determined over a scan area of 36 nm^2.

Proteinase K Treatment. One million cysts of *G. lamblia* were incubated at 37 °C on a plate shaker for 3 h with a solution containing 9 mg/mL proteinase k, 1 M Tris buffer, and 10 mM $CaCl_2$. Subsequently, the solution was centrifuged for 5 min at 12 000*g*. The supernatant was removed, the pellet was resuspended in 1 mL of distilled water, and this solution was centrifuged for a further 5 min. The supernatant was again removed, the pellet was resuspended in 5 mL of sterilized water, and the solution was examined using the protocol described for the 'hit' arrays.

Influence of pH. One molar hydrochloric acid and 1 M sodium hydroxide were used to prepare pH 2 and 12 aqueous solutions, respectively, and 5.2 mL of the acidified/basified solution was added to 800 μL of *G. lamblia* to give a cyst concentration of 1.66 × 10^5 cysts/mL; these were then examined using the protocol described for the 'hit' arrays.

RESULTS

The 652 polymers examined in the initial microarray showed significant differences in their parasite binding ability (Figure S2, Supporting Information). From these results 34 polymers were selected to undergo more detailed investigation to understand how their properties influence cyst adherence. Six copies of each selected polymer were printed on a microscope slide to form 'hit arrays'. The polymers chosen were a mix of those which promoted strong adhesion (PA104, PA531, and PA480), those which prevented binding (PAs 1−6, PA32, PA33, and a group of polyurethanes), and those which showed some selection between viable and nonviable cysts (PA356, PA496, and PA527).

The results from these 'hit array' experiments (Figures 1, 2 and S3, Supporting Information) agreed with those of the initial array. Fluorescent images of the complete 'hit' arrays, with one image per polymer, can be seen in Figure S3, Supporting Information. Figure S4, Supporting Information, demonstrates the good correlation between the binding of both viable and nonviable parasites. These results confirmed PA104, PA531, and PA480 as the best binding polymers while highlighting PA6

and PA32 as polymers which prevented binding. These polymers were selected for further investigation on larger surfaces to demonstrate appropriateness for practical applications. The chosen polymers were resynthesized and spin coated onto glass surfaces, followed by exposure to cysts. Large-scale polymer performance was as expected (Figures S5–S7, Supporting Information) with PA6 and PA32 preventing cyst adhesion and PA531, PA480, and PA104 promoting strong binding, showing the robustness of the screen.

SEM imaging (Figures S5 and S6, Supporting Information) demonstrated the features expected of *G. lamblia* cysts, with their shape and sizes being consistent with results from previous studies.[27] They also highlighted the differences between viable and nonviable cysts, with the walls being generally rougher and thicker in the latter.[28]

Next, the influence of wettability and surface roughness on adhesion was considered. (Figure 3, Table S1, Supporting Information). Initially it appeared as though overall high hydrophobicity or hydrophilicity (outside 50–70°) seemed to prevent cyst adhesion, as did high rms values (greater than 10 nm). This is illustrated by polymers, such as PA5 (83°; 13.67 nm) and PA32 (17°; 10 nm). Additionally, the strong binding polymers, PA480 and PA531, had wettability values within the range 60–65° and rms values of 2 nm or below. However, fitting of the results demonstrated no correlation between wettability or surface roughness on cyst adhesion.

To further understand the cysts surface interactions, viable cysts were treated with proteinase K to remove proteins from the outer layers of the cyst wall before analysis on a 'hit' array. The results showed that binding was severely limited for all polymers, with the number of cysts bound reduced by 70% compared to the untreated cysts (Figure 4). Changes in morphology were also observed, with cysts appearing rounded with slightly thicker outer walls.

Examining the 'hit' arrays at acid (pH 2) and base (pH 12) systems as opposed to the neutral system (pH 7), used in the standard arrays, made little difference to the repellant polymers while significantly reducing the adhesive capacity of the strong binding polymers. Polymers demonstrating poor binding (less than 10 cysts per spot) in the previous 'hit' arrays showed little change. For those polymers previously shown to support adhesion the numbers of bound cysts was significantly reduced, with the average reduction, for the binding polymers, being 94% at pH 2 and 80% at pH 12 (Figure 5).

DISCUSSION

In this work, comparison of the adhesion results with polymer properties, such as wettability, surface roughness, and polymer composition, was undertaken to elucidate which factors control cyst–polymer surface interactions. Previous literature on cellular/microbial attachment to polymer surfaces has identified structure–property relationships, noting that hydrophilic, electroneutral surfaces which contain hydrogen-bond (H-bond) acceptors but not H-bond donors resist adhesion. These factors prevent protein adhesion, which mediates cellular attachment, by binding a layer of water to the surface which acts as a steric or energetic barrier to adhesion.[29] It is not clear whether these factors will influence protozoan attachment, which will not proceed via protein adhesion since protozoa do not secrete proteins nor will proteins be present in the water samples used in the experiments reported here.

For both wettability and surface roughness no correlation was observed, though extremes of hydrophobicity/hydrophilicity and surface roughness were generally associated with poor adhesion. In terms of polymer composition, the presence of aromatic monomers (such as styrene), amide groups (in, e.g., dimethylacrylamide (DMAA) and diethylacrylamide (DEAA)) and glycol moieties (most PU monomers) appeared to prevent adhesion. In contrast, secondary amine functionalities were linked with good adhesion. Methylethylene methacrylate (MEMA) and methyl methacrylate (MMA) copolymerized with amine monomers, such as 2-(dimethylamino) ethyl methacrylate (DEAEMA) and 2-(dimethylamino) ethyl acrylate (DEAEA), were also identified as monomers which enhance adhesion. Certain monomers appear to be capable of participating in specific chemical reactions with the outer wall of the cysts, suggested to be ion–pair interactions between

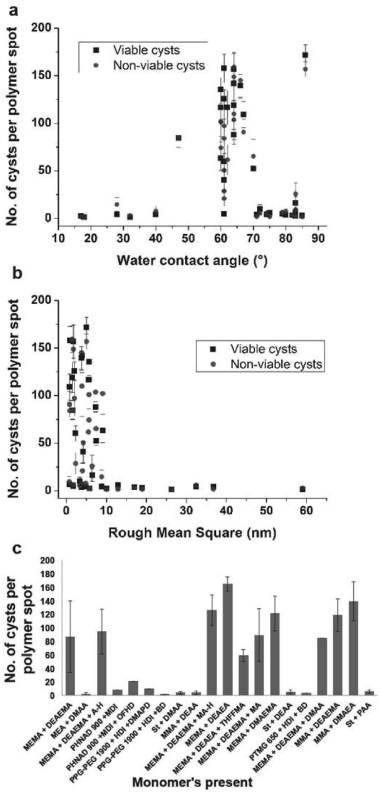

Figure 3. Correlation between *G. lamblia* cyst binding and polymer surface properties and composition. (a) Viable (square) and nonviable (circle) cyst binding versus contact angle. (b) Viable (square) and nonviable (circle) cyst binding versus surface roughness (root mean square). (c) Cyst binding in relation to monomeric composition of the polymers.

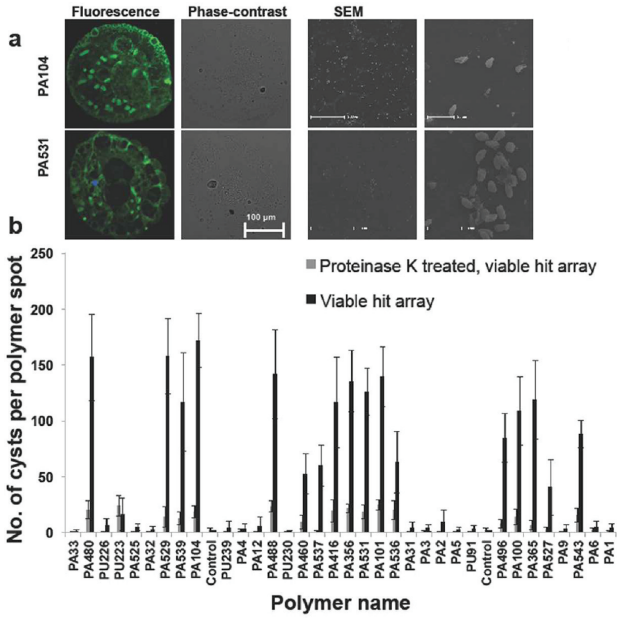

Figure 4. Proteinase K treated hit array. (a) Images of the cysts stained with Giardia-a-glo (green) and DAPI (blue) bound to polymer spots. Fluorescent (left) and phase contrast (right) images of selected polymers are shown; two strong binding polymers (PA104 and PA531) and two poor binding polymers (PA6 and PA32). (b) Chart comparing binding of viable cysts in the hit arrays before (dark gray) and after (light gray) proteinase K treatment.

protonated amines and negatively charged groups on the cyst wall. These interactions do not occur following particular cyst treatments.

***G. lamblia* Characteristics.** The culmination of the lifecycle of *G. lamblia* in its host is the release of thick-walled cysts, which are resistant to a wide range of environmental stresses. The wall consists of a fibrillar extracellular matrix, lined by a double inner membrane and an outer filamentous wall.[30] This outer wall is around 300 nm thick and is the most important aspect when considering the adhesive abilities of the cysts.

The outer wall is composed of around 43% carbohydrates,[31] 86% of which is a novel β-(1−3)-*N*-acetyl-D-galactosamine homopolymer.[32] The novel galactosamine forms curled fibrils, which bind to cyst wall proteins via internal lectin domains. Binding to these proteins compresses the homopolymers into the narrow, mesh-like structure in fully formed cyst walls.[33]

Most previous studies of *G. lamblia* surface interactions have focused on the postingestion trophozoite stage with the aim of understanding host susceptibility and the process of infection. Relatively little work[34] has considered the cyst stage, which is evidently more important in environmental analysis, for example, to understand the transport and fate of cysts in the environment, to predict and explain the performance of water treatment technologies, and to design novel materials for membranes and filters.

Cyst Viability. Specific polymers, such as PA531 and PA104, showed high binding, regardless of the viability of the cysts. There were also a considerable number of polymers, such as PA1−6, which effectively prevented binding of both viable and nonviable cysts. Overall, the viability of the cysts had a low impact upon whether binding to the polymer surfaces was observed, as supported by an R^2 value of 0.607 (initial arrays) and an R^2 value of 0.857 ('hit' arrays) (Figure S4, Supporting Information) between viable and nonviable cyst adhesion, showing that viability is not a significant factor in the adhesion characteristics of *G. lamblia* cysts.

The absence of any viability influence on *G. lamblia* adhesion contrasts with results from a previous paper which investigated the binding of another waterborne protozoan pathogen, *Cryptosporidium parvum* (*C. parvum*).[22] In this case, viable oocysts were shown to bind significantly more than nonviable oocysts. This finding was attributed to denaturation (in the heat treatment to render oocysts nonviable) of the surface glycoproteins which normally extend into solution[11,35] and mediate specific chemical interactions with polymer materials. There are differences in both the chemical composition and the structure of *C. parvum* and *G. lamblia* and in the latter the cyst walls form a filamentous mesh-like structure.[33] Previous

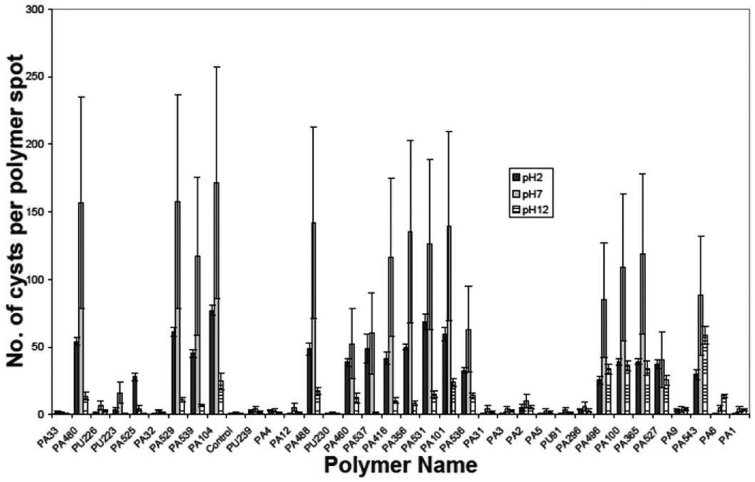

Figure 5. Effects of pH on *G. lamblia* cyst binding. Chart of viable cyst binding at pH 2 (black), 7 (light gray), and 12 (cross-hatched).

differences in adhesion characteristics for these two pathogens have been observed,[11] though the influence of viability was not investigated.

Hydrophobicity/Wettability. Wettability is a crucial property for analysis of polymers, with dynamic water contact angles (WCA) (this being a measurement after contact on a surface for few minutes rather than immediate, static measurements, which fail to simulate biological relevance) being the most common values used to quantify hydrophobicity. Previous work has demonstrated that hydrophobic forces dominate surface charge when considering *G. lamblia* interactions,[11] and although correlation between hydrophobicity and polymer binding was expected, none was observed. However, Figure 3 did show that the majority of the polymers with significant binding had a WCA between 60° and 65°. The WCAs of two of the best binding polymers, PA531 and PA480, were 61° and 64°, respectively. Values of wettability, outside of this range, generally indicated poor adhesion; for example, PA32, PA33, and PU230, which all prevented cyst adhesion, had low WCAs (17°, 18°, and 32°, respectively), PA6, PA4, and PU91, which also prevented adhesion, had high WCAs (79°, 85°, and 82°, respectively) (Table S1, Supporting Information). This is in direct contrast with the previous work by Dai et al., who observed that *G. lamblia* cysts demonstrated the strongest adhesion to hydrophobic (WCA 95°) fluorosiloxane-coated glass beads and considerable interaction with cationic polymer-coated beads (WCA 45°), whereas aminosiloxane-coated beads (WCA 70°) prevented adhesion.[11] Thus, from the experimental results it is concluded that the wettability/hydrophobicity of a polymer material is not a property which successfully predicts the degree of *G. lamblia* cyst interaction; other factors must play an important role.

Surface Roughness. Atomic force microscopy (AFM) was employed to investigate the influence of the surface roughness on *G. lamblia* adherence (Figure 3b). For each polymer surface, analysis was taken over a 100 μm^2 area and the root mean square (rms) surface roughness was determined from an average of three random positions. The rms ranged from 0.01 to 59.0 nm and did not correlate with the WCA (Figure S8 and Table S1, Supporting Information).

Similar to the wettability analysis, surface roughness also demonstrated no clear correlation with cyst adhesion (Figure 3). PA6, PA32, and PU230, which were selected for preventing adhesion, had rms values of 1.71, 10.01, and 59 nm, respectively, while PA104, PA480, and PA531, the strongest binding polymers, had rms values of 5.02, 1.75, and 2.02 nm, respectively. However, it is clear from Figure 3b that high values of rms, specifically those greater than 10 nm, appear to prevent adhesion. None of the polymers with rms values of over 10 nm had more than 10 cysts bound, including polymers such as PA1 and PA3−5 and a number of polyurethanes. This suggests that while surface roughness is not well correlated with cyst adhesion, high rms values are likely to limit binding ability.

For bacterial attachment it is known that irregularities that conform to the size of the bacteria increases adhesion due to maximizing bacteria−surface contact area.[36,37] If this hypothesis was correct for *G. lamblia*, it would imply that the surface roughness of cysts is likely to be on the order of 1−10 nm (the rms value above which no adhesion was observed for *G. lamblia*). However, AFM measurement of *G. lamblia* cysts was carried out by binding *G. lamblia* cysts on PA104-coated surface and gave a surface roughness of 53 nm, higher than all of the hit polymers except PU230 (Figure S9 and Table S1, Supporting Information).

Polymer Composition. In a previous paper investigating *C. parvum* adhesion to polymer microarrays we proposed that the interactions between oocysts and polymers were dominated by specific protein−polymer interactions, in particular ion−pair formation between carboxylate/phosphate groups on the oocyst wall and protonated amine groups in the polymers.[22]

Several of the polymers in the *G. lamblia* hit array were identical or very similar to those selected for the *C. parvum* hit array both for polymers which promoted and those which prevented adhesion. This suggests that perhaps similar mechanisms control the adhesion of these two protozoan pathogens and some similarity between the composition of the oocyst and cyst outer walls. To investigate the relationship between chemical composition of the polymers and cyst adhesion, the monomeric composition was mapped against the results of the 'hit' array (Figure 2).

Comparison of Figures 1 and 2 indicated that inhibition of cyst binding was strongest in polyacrylates containing DMAA, DEAA, or styrene as well as selected polyurethanes. Monomers promoting strong binding were more variable; however, the presence of DMAEMA, DEAEMA, DMAEA, or DEAEA was very common among the best performing polymers, such as PA104, PA480, and PA531.

Next, the nature of different functional groups present in the polymers was considered. For cellular adhesion it has been reported that glycol functionalities act in a preventative manner.[38,39] This is normally attributed to the protein-repellent nature of these moieties; for the majority of cell types adhesion is considered to occur via initial protein adsorption, which subsequently mediates cellular adhesion. For the protozoan experiments reported here prior protein interaction with the surface is not thought to be a possible mechanism of adhesion given that the experiments are performed in water and the cysts do not secrete proteins. However, the repellent nature of glycol functionalities is still consistent with our results, since none of the polyurethanes containing monomers with glycols exhibited strong interactions with cysts. In this case, the known poor likelihood of protein interaction with glycol moieties could apply to the cyst surface proteins, thus limiting any interactions between these polymers and the cyst outer wall.

A recent paper by Yang et al. reported that aromatic functionalities were correlated with low cell adhesion, whereas amine and ester moieties were found to promote cellular adhesion.[38] The monomer most associated with low *G. lamblia* adhesion in the hit arrays was styrene, in agreement with the above finding that aromatic functionalities prevent adhesion. To investigate whether ester moieties correlate with adhesion for protozoan cysts, the concentration of ester moieties was plotted against the number of cysts per polymer spot (Figure S10, Supporting Information). Poor correlation was observed (R^2 values of 0.43 or less depending upon the type of fit), and the average ester concentrations are well above the values exhibited by the polymers studied by Yang et al.[38] In terms of amine functionalities the monomers DMAEA, DEAEA, DMAEMA, and DEAEMA, present in the 'hit' array in polymers also containing MEMA and MMA, all contain secondary amine groups and are associated with high levels of cyst adhesion. Previous work has also shown that these monomers promote leuco binding.[25] For cyst adhesion, the hypothesis is that at physiological pH values the amines will be protonated and thus ion pair with the cyst wall. DMAA and DEAA contain amide groups and are present in polymers which prevent adhesion. Since amide groups will not protonated at physiologically relevant pH this explains the lack of interaction with *G. lamblia*.

Thus, it is concluded that glycol and aromatic and amide functional groups act to prevent adhesion whereas amine groups promote adhesion. This is in agreement with previous cellular/microbial attachment literature. However, the mechanism is not via prior protein attachment, as discussed above, but direct interaction of cyst wall proteins with the surface.

Proteinase K Treatment. Proteinase K has previously been employed to study the nature of surface macromolecules of *C. parvum*[40] and *Giardia*[32] as well as alter the adhesion characteristics of *C. parvum*. Adhesion of *C. parvum* to quartz surfaces was improved after proteinase K treatment.[35] However, the 'hit' array exposed to *G. lamblia*, which had been previously treated with proteinase K, showed severely reduced binding (Figures 4 and S11, Supporting Information), although polymers which normally promoted strong adhesion, such as PA104 and PA480, still bound the highest number of cysts. Proteinase K removes any proteins stretching out from the cyst and also contributes to degradation of those involved in the mesh-like outer wall. SEM images (Figure 4) illustrate changes in cyst morphology, e.g., wall thickening, as expected; Chatterjee et al.[33] previously reported that removal of the cyst wall proteins decompresses the galactosamine fibrils, thus thickening the cyst wall. The reduction in adhesive ability suggests that the cyst wall proteins that bind the galactosamine fibrils play a crucial role in surface interactions. This supports the theory that protein-specific interactions with polymers control adhesion of cysts to these surfaces.

pH. Analysis of cyst adhesion at different pH values (pH 2 and 12) showed an overall reduction in binding (Figures 5 and S12, Supporting Information). Those polymers with weak adhesion at pH 7 did not exhibit significantly different results at extremes of pH, whereas those which had strong adhesion at pH 7 showed severe reductions in binding at both pH 2 and 12. In the previous discussion, analysis of polymer composition and proteinase K treatment on cyst adhesion both suggested that ion−pair interactions play a key role in controlling the binding of *G. lamblia* to polymer surfaces. At pH 2, below the isoelectric point for *G. lamblia*,[41] the cyst wall will be mainly positively charged and therefore will not react with the protonated amines. At pH 12, while the cyst wall will be negative, the amines will be unprotonated and again no interactions will occur. Thus, performing experiments at different pH values significantly worsened the adhesive capacity of *G. lamblia* cysts to the polymers.

■ ASSOCIATED CONTENT

Supporting Information

Extensive figures showing initial array results, images of the whole 'hit' array, and extra analysis graphs; table of all 'hit' array results. This material is available free of charge via the Internet at http://pubs.acs.org.

■ AUTHOR INFORMATION

Corresponding Author

*Phone: +44 131 650 5814 (H.B.); +44 131 650 4820 (M.B.). E-mail: h.bridle@ed.ac.uk (H.B.); mark.bradley@ed.ac.uk (M.B.).

Author Contributions

‡These authors contributed equally to this work.

Notes

The authors declare no competing financial interests.

■ ACKNOWLEDGMENTS

We thank the University of Edinburgh, the China Scholarship Council (M.W.), and the Royal Academy of Engineering/EPSRC (H.B.) for funding. We thank Oleg Nerushev for AFM

technical support. H.B. and M.B. came up with the concept/idea. All authors cowrote this paper.

REFERENCES

(1) Caccio, S. M.; Thompson, R. C.; McLauchlin, J.; Smith, H. V. Unravelling Cryptosporidium and Giardia epidemiology. *Trends Parasitol* **2005**, *21*, 430−7.
(2) Heresi, G. P.; Murphy, J. R.; Cleary, T. G. Giardiasis. *Semin. Pediatric Infectious Dis.* **2000**, *11*, 189−95.
(3) Farthing, M. J. G. In *Giardia: From molecules to disease*; Thompson, R. C. A., Reynoldson, J. A., Lymbery, A. J., Eds.; CABI Publishing: Wallingford, 1994; pp 15−37.
(4) Jephcott, A. E.; Begg, N. T.; Baker, I. A. Outbreak of giardiasis associated with mains water in the United Kingdom. *Lancet* **1986**, *29* (1), 730−2.
(5) Kent, G. P.; et al. Epidemic giardiasis caused by a contaminated public water supply. *Am. J. Public Health* **1988**, *78*, 139−43.
(6) Lebwohl, B.; Deckelbaum, R. J.; Green, P. H. R. Giardiasis. *Gastrointestinal Endosc.* **2003**, *57*, 906−13.
(7) Nygard, K.; et al. A large community outbreak of waterborne giardiasis-delayed detection in a non-endemic urban area. *BMC Public Health* **2006**, *6*, 141.
(8) Owen, R. L. The ultrastructural basis of Giardia function. *Trans. R. Soc. Tropical Med. Hyg.* **1980**, *74*, 429−433.
(9) Falk, C. C.; Karanis, P.; Schoenen, D.; Seitz, H. M. Bench scale experiments for the evaluation of a membrane filtration method for the recovery efficiency of Giardia and Cryptosporidium from water. *Water Res.* **1998**, *32*, 565−8.
(10) Palm, D.; et al. Developmental changes in the adhesive disk during Giardia differentiation. *Mol. Biochem. Parasitol.* **2005**, *141*, 199−207.
(11) Dai, X.; Boll, J.; Hayes, M. E.; Aston, D. E. Adhesion of Cryptosporidium parvum and Giardia lamblia to solid surfaces: the role of surface charge and hydrophobicity. *Colloids Surf., B* **2004**, *34*, 259−263.
(12) Tourniaire, G.; et al. Polymer microarrays for cellular adhesion. *Chem. Commun.* **2006**, 2118−2120.
(13) How, S. E.; et al. Polyplexes and lipoplexes for mammalian gene delivery: From traditional to microarray screening. *Comb. Chem. High Throughput Screening* **2004**, *7*, 423−430.
(14) Diaz-Mochon, J. J.; Tourniaire, G.; Bradley, M. Microarray platforms for enzymatic and cell-based assays. *Chem. Soc. Rev.* **2007**, *36*, 449−457.
(15) Anderson, D. G.; Levenberg, S.; Langer, R. Nanoliter-scale synthesis of arrayed biomaterials and application to human embryonic stem cells. *Nat. Biotechnol.* **2004**, *22*, 863−866.
(16) Hay, D. C.; et al. Unbiased screening of polymer libraries to define novel substrates for functional hepatocytes with inducible drug metabolism. *Stem Cell Res.* **2011**, *6*, 92−102.
(17) Tare, R. S.; et al. A microarray approach to the identification of polyurethanes for the isolation of human skeletal progenitor cells and augmentation of skeletal cell growth. *Biomaterials* **2009**, *30*, 1045−55.
(18) Khan, F.; Tare, R. S.; Kanczler, J. M.; Oreffo, R. O. C.; Bradley, M. Strategies for cell manipulation and skeletal tissue engineering using high-throughput polymer blend formulation and microarray techniques. *Biomaterials* **2010**, *31*, 2216−28.
(19) Mant, A.; et al. Polymer microarrays: Identification of substrates for phagocytosis assays. *Biomaterials* **2006**, *27*, 5299−306.
(20) Pernagallo, S.; Unciti-Broceta, A.; Diaz-Mochon, J. J.; Bradley, M. Deciphering cellular morphology and biocompatibility using polymer microarrays. *Biomed. Mater.* **2008**, *3*, 034112.
(21) Pernagallo, S.; Wu, M.; Gallagher, M. P.; Bradley, M. Colonising new frontiers-microarrays reveal biofilm modulating polymers. *J Mater Chem* **2011**, *21*, 96−101.
(22) Wu, M.; Bridle, H.; Bradley, M. Targeting Cryptosporidium capture. *Water Res.* **2011**, DOI: (http://dx.doi.org/10.1016/j.watres.2011.12.041).
(23) Ongerth, J. E.; Johnson, R. L.; MacDonald, S. C.; Frost, F.; Stibbs, H. H. Backcountry Water Treatment to Prevent Giardiasis. *Am. J. Public Health* **1989**, *79*, 1633−1637.
(24) (United States Environmental Protection Agency, 2005.
(25) Mizomoto, H. School of Chemistry, University of Southampton, Southampton, 2004.
(26) Thaburet, J. F. O.; Mizomoto, H.; Bradley, M. High-throughput evaluation of the wettability of polymer libraries. *Macromol. Rapid Commun.* **2004**, *25*, 366−370.
(27) Deng, M. Y.; Cliver, D. O. Degradation of Giardia lambia cysts in mixed human and swine wates. *Appl. Environ. Microbiol.* **1992**, *58*, 2368−2374.
(28) Schupp, D. G.; Erlandsen, S. L. Determination of Giardia muris Cyst Viability by Differential Interference Contrast, Phase, or Brightfield Microscopy. *J. Parasitol.* **1987**, *73*, 723−729.
(29) Elimelech, M.; Phillip, W. A. The Furture of Seawater Desalination: Energy, Technology and the Environment. *Science* **2011**, *333*, 712−717.
(30) Reiner, D. S. Cell Cycle and Differentiation in Giardia Lamblia. Ph.D. Thesis, Department of Microbiology, Tumor, and Cell Biology, Karolinska Institutet, Stockholm, 2008.
(31) Manning, P.; Erlandsen, S. L.; Jarroll, E. L. Carbohydrate and amino acid analyses of Giardia muris cysts. *J. Protozool.* **1992**, *39*, 290−296.
(32) Gerwig, G. J.; et al. The Giardia intestinalis filamentous cyst wall contains a novel beta(1−3)-N-acetyl-D-galactosamine polymer: a structural and conformational study. *Glycobiology* **2002**, *12*, 499−505.
(33) Chatterjee, A.et al.Giardia cyst wall protein 1 is a lectin that binds to curled fibrils of the GalNAc homopolymer. *PLoS Pathogens 6* (**2010**).
(34) Dai, X.; Boll, J. Evaluation of attachment of Cryptosporidium parvum and Giardia lamblia to soil particles. *J. Environ. Quality* **2003**, *32*, 296−304.
(35) Kuznar, Z. A.; Elimelech, M. Cryptosporidium oocyst surface macromolecules significantly hinder oocyst attachment. *Environ. Sci. Technol.* **2006**, *40*, 1837−1842.
(36) Whitehead, K. A.; Colligon, J.; Verran, J. Retention of microbial cells in substratum surface features of micrometer and sub-micrometer dimensions. *Colloids Surf., B* **2005**, *41*, 129−138.
(37) Bazaka, K.; Jacob, M. V.; Crawford, R. J.; Ivanova, E. P. Plasma-assisted surface modification of organic biopolymers to prevent bacterial attachment. *Acta Biomater.* **2011**, *7*, 2015−2028.
(38) Yang, J.; et al. Polymer surface functionalities that control human embryoid body cell adhesion revealed by high throughput surface characterization of combinatorial material microarrays. *Biomaterials* **2010**, *31*, 8827−8838.
(39) Cima, L. G. Polymer substrates for controlled biological interactions. *J. Cell. Biochem.* **1994**, *56*, 155−61.
(40) Liu, Y.; Kuhlenschmidt, M. S.; Kuhlenschmidt, T. B.; Nguyen, T. H. Composition and Conformation of Cryptosporidium parvum Oocyst Wall Surface Macromolecules and Their Effect on Adhesion Kinetics of Oocysts on Quartz Surface. *Biomacromolecules* **2010**, *11*, 2109−2115.
(41) Hsu, B.-M.; Huang, C. Influence of ionic strength and pH on hydrophobicity and zeta potential of Giardia and Cryptosporidium. *Colloids Surf., A* **2002**, *201*, 201−206.

Appendix V: Oral Presentations

- Bradley group presentation, 27th November 2008, Edinburgh (UK)
- School research seminar, 2nd December 2008, Edinburgh (UK)
- Bradley group presentation, 28th May 2009, Edinburgh (UK)
- Bradley group presentation, 4th February 2010, Edinburgh (UK)
- School research seminar, 9th June 2010, Edinburgh (UK)
- Second year viva presentation, 30th August 2010, Edinburgh (UK)
- Bradley group presentation, 14th October 2010, Edinburgh (UK)
- 6th International Workshop on Combinatorial Materials Science and Technology, 26th-29th October 2010, Hokkaido Rusutsu (Japan)
- Polymer Chemistry Conference 2010, 19th-22nd November 2010, Puerto Morelos (Mexico)
- Final year presentation, 8th April 2011, Firbush (UK).
- Bradley group presentation, 15th September 2011, Edinburgh (UK)

Appendix VI: Posters

- Postgraduate meeting, 4th April 2010, Firbush (UK)

Colonising New Frontiers - Microarrays Reveal Biofilm Modulating Polymers

Mei Wu[a], Salvatore Pernagallo[a], Maurice P. Gallagher[b] and Mark Bradley[a]

[a]School of Chemistry, University of Edinburgh, West Mains Road, Edinburgh, EH9 3JJ, U.K.
[b]School of Biological Sciences, University of Edinburgh, Mayfield Road, Edinburgh, EH9 3JR, U.K.
Email: m.wu-4@sms.ed.ac.uk

Overview

Polymer libraries provide an innovative approach to identifying surface modulating materials for clinical, industrial or food production use. Here, we use polymer microarrays to identify materials which selectively promote or prevent capture of the food-borne pathogen, *S.* typhimurium and *E. coli*, and display either polymer structure-based species discrimination or common binding. Such polymers offer novel potential for bacterial enrichment or surface repulsion, in cleaning materials, feed additives or surface coatings.

Methods

-Polymer Microarray Fabrication-

Stage 1- Solutions
Polymers were dissolved at 1% w/v in N-methyl pyrrolidinone (NMP). The solutions were placed into a 384-well polypropylene microplate prior to printing.

Stage 2- Printing
The robot used was the Qarray mini® (Genetix Ltd; UK).The solutions were deposited by contact printing using 150 mm solid pins (Fig. 1). The nature of the substrates were adapted to the different screenings in order to obtain the lowest background and most uniform spots. [1]

Stage 3- Drying
Once printed, the solvent was removed by drying under vacuum at 40 °C overnight, to give a microarray over 2000 spots per slide.

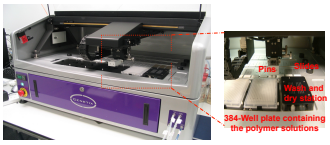

Fig.1 Arrayer: *Qarray mini* (Genetix Ltd, UK)

-Bacterial Culture-

Salmonella enterica serovar typhimurium (*S.* typhimurium SL1344) and *Escherichia coli* (*E. coli* W3110) transformed with pHC60 (referred to as S. typhimurium-GFP and *E. coli*-GFP)[2] were grown overnight with aeration at 37 °C or 30 °C respectively in Luria-Bertani (LB) broth containing tetracycline (10 μg ml^{-1}). Cultures were collected by centrifugation, washed with fresh LB broth and diluted for microarray binding studies (Fig. 2).

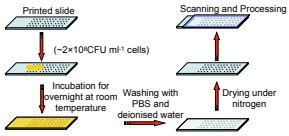

Fig. 2 Scheme of polymer microarray for bacteria culture

-Microarray Screening-

Polymer microarrays were analysed using a LaVision BioAnalyzer 4F/4S scanner with a fluorescein filter. High-Content Imaging was carried out using Imstar OSA / HCS Scanner that allowed the capture of single images for each polymer spot with both bright-field and fluorescein channels with a ×20 objective (Fig. 3).

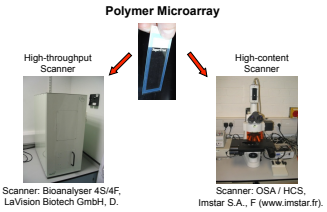

Fig. 3 High-throughput scanner and high-content scanner

-Scale Up-

Selected polymers were spin-coated onto grided glass coverslips (CELL-VU DRM 800) and incubated with *S.* typhimurium GFP and imaged *via* SEM. The numbers of bacteria in randomly selected sub-squares (four for each coverslip) were counted with Image-Pro Plus 4.5 (Fig. 4). [3]

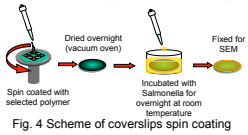

Fig. 4 Scheme of coverslips spin coating

Results

-Polymer Microarray Analysis-

Analysis was enabled by the expression of Green Fluorescent Protein (GFP) within the bacteria, allowing detection of bacterial binding on a polymer microarray of 370 polyurethanes and polyacrylates (Fig. 5). Following the initial analysis of the entire library, several polymers which resulted in the strongest or poorest binding of *S.* typhimurium were re-printed and re-examined.

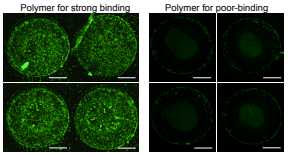

Fig. 5 Examples of *S.* typhimurium strong and poor binding polymers. Scale bar = 100 μm.

-Binding Efficiency Test-

To test the rapidity of *S.* typhimurium binding, an array with the letters 'UK' was fabricated using strong and poor binding polymers and *S.* typhimurium incubated on the array for four hours (Fig. 6).

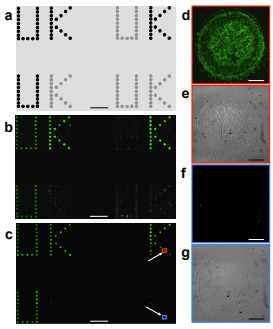

Fig. 6 *S.* typhimurium attachment/repulsion: (a) array design with the binding polymer (in black) and the poor binding polymer (in grey); (b) Bio Analyzer scanning of the array using a fluorescein filter; (c) fluorescent microscopy imaging (×20 objective). Scale bar = 4 mm. Arrows indicate (d-g) (d) fluorescein channel and (e) brightfield of binding polymer; (f) fluorescein channel and (g) bright-field of the poor binding polymer. Scale bar = 100 μm.

-SEM Analysis of Strong/Poor Binding Polymers-

Strong/Poor binding polymer spots and their spin-coated onto CELL–VU coverslips were analysed, and the average number of bacteria per coverslip was measured, with uncoated coverslips used as controls. *S.* typhimurium attached onto strong polymer displaying a 7-fold increase in binding compared to an uncoated coverslip, whereas the number of *S.* typhimurium on the poor-binding polymer was twenty times less than the glass control (Fig. 7). [3]

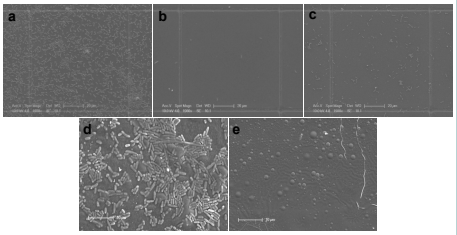

Fig. 7 Scanning electron microscopy (SEM) images and analysis of the *S.* typhimurium binding on the selected polymer coated coverslips. (a) strong binding; (b) poor binding; (c) Control (no-polymer coated). Scale bar = 20 μm. The biofilm on surfaces of the strong binding and poor binding polymers were shown on (d) and (e) respectively. Scale bar= 10 μm.

Conclusion

Polymer microarrays were successfully used for the identification of polymers which bound either *S.* typhimurium and/or *E. coli* or prevented their colonisation of surfaces, with fluorescence imaging allowed the rapid, parallel, and comprehensive, evaluation of bacterial adhesion on 370 polymers. Identified polymers are now being developed as coating materials to help reduce hospital endotracheal tube infections as well as in *Campylobacter jejuni* and *Clostridium difficile* infections.[3]

Reference

1. Tourniaire, G et al. *Chem. Commum* **20**, 2118-2120, 2009
2. Cheng, H.P. & Walker, G.C. *J Bacteriol* **180**, 5183-5191 (1998).
3. Pernagallo, S., Wu, M., Gallagher, M.P. & Bradley, M. *Chem. Commum*, submitted

Acknowledgement

We thank Edinburgh University and the China Scholarship Council (MW) for funding.